

Some pages of this thesis may have been removed for copyright restrictions.

If you have discovered material in Aston Research Explorer which is unlawful e.g. breaches copyright, (either yours or that of a third party) or any other law, including but not limited to those relating to patent, trademark, confidentiality, data protection, obscenity, defamation, libel, then please read our [Takedown policy](#) and contact the service immediately (openaccess@aston.ac.uk)

**GENETIC STUDIES OF Cu-Pb-Zn MINERALISATION IN TRIASSIC
RED BEDS OF WESTERN EUROPE**

by

PATRICIA HELEN NAYLOR

Thesis submitted for the Doctor of Philosophy

at the

University of Aston in Birmingham

September 1988

This copy of the thesis has been supplied on condition that anyone who consults it is understood to recognise that its copyright rests with its author and that no quotation from the thesis and no information derived from it may be published without the author's prior, written consent.

GENETIC STUDIES OF CU-PB-ZN MINERALISATION IN TRIASSIC

RED BEDS OF WESTERN EUROPE

by

Patricia Helen Naylor

Thesis submitted for the Doctor of Philosophy

at the University of Aston in Birmingham.

1988

SUMMARY

Continental red bed sequences are host, on a worldwide scale, to a characteristic style of mineralisation which is dominated by copper, lead, zinc, uranium and vanadium. This study examines the features of sediment-hosted ore deposits in the Permo-Triassic basins of Western Europe, with particular reference to the Cu-Pb-Zn-Ba mineralisation in the Cheshire Basin, northwest England, the Pb-Ba-F deposits of the Inner Moray Firth Basin, northeast Scotland, and the Pb-rich deposits of the Eifel and Oberpfalz regions, West Germany.

The deposits occur primarily but not exclusively in fluvial and aeolian sandstones on the margins of deep, avolcanic sedimentary basins containing red beds, evaporites and occasionally hydrocarbons. The host sediments range in age from Permian to Rhaetian and often contain (or can be inferred to have originally contained) organic matter. Textural studies have shown that early diagenetic quartz overgrowths precede the main episode of sulphide deposition.

Fluid inclusion and sulphur isotope data have significantly constrained the genetic hypotheses for the mineralisation and a model involving the expulsion of diagenetic fluids and basinal brines up the faulted margins of sedimentary basins is favoured. Consideration of the development of these sedimentary basins suggest that ore emplacement occurred during the tectonic stage of basin evolution or during basin inversion in the Tertiary. $\delta^{34}\text{S}$ values for barite in the Cheshire Basin range from 13.8 ‰ to 19.3 ‰ and support the theory that the Upper Triassic evaporites were the principal sulphur source for the mineralisation and provided the means by which mineralising fluids became saline. In contrast, $\delta^{34}\text{S}$ values for barite in the Inner Moray Firth Basin (mean $\delta^{34}\text{S} = +29$ ‰) are not consistent with simple derivation of sulphur from the evaporite horizons in the basin and it is likely that sulphur-rich Jurassic shales supplied the sulphur for the mineralisation at Elgin. Possible sources of sulphur for the mineralisation in West Germany include hydrothermal vein sulphides in the underlying Devonian sediments and evaporites in the overlying Muschelkalk. Textural studies of the deeply buried sandstones in the Cheshire Basin reveal widespread dissolution and replacement of detrital phases and support the theory that red bed diagenetic processes are responsible for the release of metals into pore fluids.

The ore solutions are envisaged as being warm (60-150°C), saline (9-22 wt % equiv NaCl) fluids in which metals were transported as chloride complexes. The distribution of $\delta^{34}\text{S}$ values for sulphides in the Cheshire Basin (-1.8 ‰ to +16 ‰), the Moray Firth Basin (-4.8 ‰ to +27 ‰) and the German Permo-Triassic Basins (-22.2 ‰ to -12.2 ‰) preclude a magmatic source for the sulphides and support the contention that sulphide precipitation is thought to result principally from sulphate reduction processes, although a decrease in temperature of the ore fluid or reaction with carbonates may also be important. Methane is invoked as the principal reducing agent in the Cheshire Basin, whilst terrestrial organic debris and bacterial reduction processes are thought to have played a major part in the genesis of the German ore deposits.

KEY WORDS Permo-Triassic Red beds Mineralisation Diagenesis Sulphur isotopes

Acknowledgements

Thanks are extended to Dr. P. Turner and Professor D.J. Vaughan for supervising the project. Financial support was provided by NERC studentship GT4/85/GS/4 and is gratefully acknowledged.

The British Museum (Natural History) and Dr. C. Stanley in particular are thanked for the provision of certain samples studied in this work. The director and staff of the Institute of Geological Sciences are thanked for providing access to samples and data from the Wilkesley borehole, Cheshire. The British Geological Survey and T. Colman in particular are thanked for providing further samples from the Cheshire Basin. Thanks are due to Mr. P. Sorenson and to the National Trust for allowing access to the Alderley Edge Mines and to members of the Derbyshire Caving Club for supervising the visits. Thanks are extended to Drs. Knapp, Ribbert and Weinelt for supervising fieldwork and access to mine material during a visit to Germany in September 1987.

Electron probe microanalyses were carried out at the University of Manchester under the supervision of T. Hopkins and D. Plant. Sulphur isotope analyses were carried out at SURRC, East Kilbride, where J. Gerc and E. Tweedie provided technical assistance. The stable isotope laboratory at SURRC is supported by NERC grant GR3/5399 and by the Scottish Universities. SEM facilities at Reading University were used by kind permission of Dr. A. Parker and under the supervision of K. Purvis.

Thanks are extended to technical staff at Aston University for their assistance. The thesis benefitted through long discussions with Adrian Boyce and Tony Fallick (SURRC) and Dr. A. Searl, Aston University. The author is indebted to B. Parker and E. Smith for assistance with diagrams.

Finally, I thank my parents and Jim for their support throughout this work.

CONTENTS

PAGE

Title page	1
Summary	2
Acknowledgements	3
Contents	4
List of figures	10
List of tables	13
List of plates	15
CHAPTER 1: INTRODUCTION	17
1.1 Approach and aims of the study	17
1.2 Thesis format	18
References	21
CHAPTER 2 : GENETIC STUDIES OF RED BED MINERALISATION IN THE TRIASSIC OF THE CHESHIRE BASIN, NORTHWEST ENGLAND	22
Abstract	22
2.1 Introduction	23
2.2 Basin evolution	25
2.3 Geological setting of the mineralisation	31
2.4 Ore mineralogy	35
2.5 Fluid inclusion data	41
2.6 Sulphur isotope data	43
2.6.1 Gypsum and anhydrite	43
2.6.2 Barite	44
2.6.3 Sulphides	44
2.7 Discussion	48
2.7.1 Structural control and constraints on timing of the mineralisation	48

2.7.2 Sources of metals and sulphur	50
2.7.3 Transport of metals; nature of the mineralising fluids	52
2.7.4 Mechanism of precipitation of the ores	54
2.8 Concluding remarks	62
References	64

CHAPTER 3 : ASPECTS OF THE DIAGENESIS OF THE SHERWOOD

SANDSTONE AND MERCIA MUDSTONE GROUP SEDIMENTS OF

THE CHESHIRE BASIN	70
Abstract	70
3.1 Introduction	70
3.2 Methodology	73
3.3 Sedimentology and stratigraphy	73
3.4 Burial history of the Cheshire Basin sediments	77
3.5 Petrography of the Sherwood Sandstone Group sandstones	77
3.5.1 Detrital mineralogy	77
3.5.2 Diagenetic history	80
3.6 Petrography of the Mercia Mudstone Group, Wilkesley borehole	92
3.6.1 Detrital mineralogy	92
3.6.2 Diagenetic history	94
3.7 Discussion	98
3.7.1 Eodiagenesis	99
3.7.2 Mesodiagenesis	101
3.7.3 Telodiagenesis	102
3.8 Concluding remarks	103
References	105

CHAPTER 4 : THE DIAGENESIS AND Pb-Ba-F MINERALISATION IN PERMO-TRIASSIC SANDSTONES, INNER MORAY FIRTH BASIN, NORTHEAST SCOTLAND	109
Abstract	109
4.1 Introduction	110
4.2 Evolution of the Inner Moray Firth Basin	113
4.3 Sedimentology of the exposures on the southern basin margin	120
4.4 Petrographic and diagenetic studies	123
4.4.1 Quartz and feldspar	126
4.4.2 Calcite	129
4.4.3 Fluorite	133
4.4.4 Barite	134
4.4.5 Clay mineralogy	137
4.4.6 Porosity	140
4.5 Sulphide mineralisation	141
4.6 Geochemistry	149
4.7 Fluid inclusion studies	149
4.8 Sulphur and oxygen stable isotopes	154
4.8.1 Barite	154
4.8.2 Galena	155
4.8.3 Pyrite	155
4.9. Discussion	159
4.9.1 Tectonic control and timing of the mineralisation	159
4.9.2 Sources of Pb, F, Ba, Si, Fe and S	160
4.9.3 Nature of the mineralising solutions	163
4.9.4 Precipitation mechanisms for the sulphides, barite and fluorite	166
4.10 Concluding remarks	167
References	169

CHAPTER 5 : THE GENESIS OF THE CHERTY ROCK, ELGIN	176
Abstract	176
5.1 Introduction	176
5.2 Geological setting	179
5.3 Field occurrence	180
5.4 Analytical methods	180
5.5 Petrographic studies	183
5.5.1 Description	183
5.5.2 Interpretation	187
5.6 Geochemistry	194
5.7 Carbon and oxygen stable isotope studies	196
5.7.1 Introduction	196
5.7.2 Results	197
5.8 Discussion	199
5.9 Concluding remarks	208
References	210

CHAPTER 6 : ASPECTS OF THE GENESIS OF BASE METAL MINERALISATION

IN THE TRIASSIC OF NORTHWEST EUROPE WITH SPECIAL REFERENCE TO MAUBACH AND MECHERNICH Pb DEPOSITS	216
Abstract	216
6.1. Introduction	216
6.2 Maubach and Mechernich	221
6.2.1 Geological setting	221
6.2.2 Sedimentology of the Middle Buntsandstein in the Eifel	224
6.2.3 Petrographic and diagenetic studies	232
6.2.4 Ore Mineralogy	238
6.2.5 Sulphur isotope studies	244
6.2.6 Discussion	246
6.2.6.1 Timing of mineralisation	250

6.2.6.2 Sources of metals and sulphur	251
6.2.6.3 Precipitation mechanisms and genetic models	252
6.3 Oberpfalz deposits, Bavaria	254
6.3.1 Geological setting	254
6.3.2 Petrographic and diagenetic studies	257
6.3.3 Sulphide ores	258
6.3.4 Discussion	261
6.4 Switzerland	263
6.5 Concluding remarks	263
References	266
CHAPTER 7 : CONCLUSIONS	271
7.1 Introduction	271
7.2 Review of similar European deposits	271
7.3. Comparison of the characteristics of the deposits	280
7.3.1 Associated metals	280
7.3.2 Host lithology and regional stratigraphic succession	281
7.3.3 Sulphide paragenesis	283
7.3.4 Tectonic setting	284
7.3.5 Association with evaporites	285
7.3.6 Association with organic matter and hydrocarbons	285
7.3.7 Association with volcanic activity	286
7.3.8 Timing of ore emplacement	286
7.3.9 Temperature of sulphide deposition	288
7.3.10 Sulphur isotope characteristics	289
7.3.11 Summary	290
7.4 Genetic models	292
7.4.1 Sources of the metals and sulphur	292
7.4.2 The physicochemical characteristics of the mineralising fluids	293
7.4.3 Mechanisms of ore deposition	295

7.5 Suggestions for further research	296
References	298

APPENDIX I : SAMPLE PREPARATION AND ANALYTICAL
TECHNIQUES

1. X-ray fluorescence spectrometry	302
2. X-ray diffraction analysis	302
3. Atomic absorption spectrophotometry	303
4. Electron probe microanalysis	303
5. Sulphur isotope analysis	304
References	305

APPENDIX II : FLUID INCLUSION STUDIES

1. Fluid inclusion wafer preparation	308
2. Calibration of the Linkam TH600 heating-cooling stage	308
References	310

Figure 1.1 Scythian palaeogeographic map of Western Europe showing the location of the study areas	20
Figure 2.1 Geological map of the Cheshire Basin	24
Figure 2.2 Stratigraphical and sedimentological diagram of the Permo-Triassic sediments of the Cheshire Basin	27
Figure 2.3 Sketch section across the northern Cheshire Basin	30
Figure 2.4 Schematic section across the Alderley Edge fault block	32
Figure 2.5A Geological map of the Mid-Cheshire Ridge	
B Schematic section across the orebody at Bickerton	34
Figure 2.6 Paragenetic diagram for sulphides and associated authigenic phases in the Cheshire Basin	36
Figure 2.7 Histogram of homogenisation temperatures for calcite-hosted fluid inclusions at Bickerton	42
Figure 2.8 Histogram of sulphur isotope data	47
Figure 2.9 The distribution of $\delta^{34}\text{S}$ values for H_2S and sulphides generated by the reduction of sulphate	56
Figure 2.10A Summary diagram to show possible origins of the mineralisation in Cheshire	58
B Schematic diagram of the mineralisation at Alderley Edge	58
Figure 2.11 Flow diagram showing possible migration pathways for the mineralising fluids	61
Figure 3.1 Simplified geological map of the Permo-Triassic basins in northwest England	71
Figure 3.2 Geological map of the Cheshire Basin, showing the exposures of the Helsby Sandstone Formation	74
Figure 3.3 Stratigraphical relationship between the Sherwood Sandstone Group and Mercia Mudstone Group sediments of Cheshire	75

Figure 3.4 Mineralogical classification of the Cheshire Basin sandstones	78
Figure 3.5 XRD traces of the < 2 μ m clay fraction of the Cheshire sandstones	90
Figure 3.6 Diagenetic scheme for the Sherwood Sandstone and Mercia Mudstone Group sediments	100
Figure 4.1 Simplified geological map of northeast Scotland and the Moray Firth Basin	111
Figure 4.2A Geological map of the field area showing the distribution of barite and fluorite mineralisation.	116
B A sketch section across the Elgin area	116
Figure 4.3 A schematic section accros the Inner Moray Firth Basin showing the present structural configuration	119
Figure 4.4 Sedimentological log of fluvial sands in the Burghead Sandstone Formation	122
Figure 4.5 Mineralogical classification of the Elgin sandstones	124
Figure 4.6 XRD traces of the < 2 μ m clay fraction of the Elgin sandstones	139
Figure 4.7 Schematic diagram of the diagenetic history of the Inner Moray Firth sediments	143
Figure 4.8 Homogenisation temperatures for quartz-hosted fluid inclusions in the Cherty Rock, Lossiemouth	153
Figure 4.9 Histogram of sulphur isotope data for sulphides and barite	157
Figure 5.1 Tectonic map of the Inner Moray Firth Basin	178
Figure 5.2A Geological map of the Elgin district showing exposures of the Cherty Rock	182
B Sedimentological logs of the Lossiemouth Sandstone Formation and the Cherty Rock	182
Figure 5.3 Textural evolution of the Cherty Rock horizon	185
Figure 5.4 Plot of $\delta^{13}\text{C}$ vs $\delta^{18}\text{O}$ for worldwide calcretes, lacustrine carbonate, marine carbonate and data from the present study	202

Figure 5.5 Carbon isotopic composition of vegetation, soil CO ₂ and atmospheric CO ₂	203
Figure 5.6 Carbon and oxygen isotopic composition of calcite in the Cherty Rock, Mull calcretes and Elgin sandstones	204
Figure 6.1 Location map showing the situation of the Maubach and Mechernich	218
Figure 6.2 Geological map of the Nideggen Trough	220
Figure 6.3A A tectonic map of the Mechernich district	223
B A section across the orebody at Mechernich	223
Figure 6.4 Sedimentological logs of the Middle Buntsandstein sediments, Kallmuther Berg Pit, Mechernich	227
Figure 6.5 A paragenetic diagram for sulphides and gangue phases at Maubach and Mechernich	240
Figure 6.6 Histograms of sulphur isotope data from the Eifel	249
Figure 6.7A Geological map of the Oberpfalz region	256
B Schematic section across the Oberpfalz	256
Figure 7.1 Map showing the location of Triassic and Liassic sediment-hosted ore deposits in France	274
Figure 7.2 Isopach map of the Triassic sediments in the southeast Basin of France	276
Figure 7.3 Section across the Triassic succession in the southeast Basin of France	278
Figure 7.4 Pattern of sulphur isotopes for the Permo-Triassic red bed deposits of Western Europe	291
Figure II 1.1 Calibration curve for the Linkam TH600 heating-cooling stage	312

LIST OF TABLES**PAGE**

Table 2.1 Electron probe microanalyses of sulphides in the Cheshire Basin	37
Table 2.2 Sulphur isotope analyses of evaporites, barite and sulphides in the Cheshire Basin	46
Table 3.1 Point count data, Sherwood Sandstone Group sediments, Cheshire	79
Table 3.2 Electron probe microanalyses of feldspars in the Cheshire sediments	86
Table 3.3 Point count data, Mercia Mudstone Group sediments, Cheshire	93
Table 4.1 Point count data, Elgin sandstones	125
Table 4.2 Electron probe microanalyses of feldspars in the Elgin sandstones	130
Table 4.3 Electron probe microanalyses of sulphides in the Cherty Rock, Lossiemouth	148
Table 4.4 Major element geochemistry of the Elgin Permo-Triassic sandstones	150
Table 4.5 Minor element geochemistry of the Elgin Permo-Triassic sandstones	151
Table 4.6 Sulphur isotope analyses of sulphides and barite, Inner Moray Firth	156
Table 4.7 Oxygen stable isotope analyses of quartz, Cherty Rock, Lossiemouth	158
Table 5.1 Major element geochemistry of the Cherty Rock	195
Table 5.2 Minor element geochemistry of the Cherty Rock	195
Table 5.3 Carbon and oxygen isotope analyses of calcite in the Cherty Rock, Mull calcretes and Elgin sandstones	198
Table 6.1 Electron probe microanalyses of sulphides in the Triassic of Germany	245
Table 6.2 New sulphur isotope analyses of sulphides at Maubach and Mechernich	247
Table 6.3 Mineralisation and sedimentary facies in northern Switzerland	264
Table 7.1 Summary of suggestions for further research	297

Table I1 Accuracy of the semi-quantative X-ray fluorescence data	306
Table I2 Reproducibility of the X-ray fluorescence data	307
Table II1 Data from the calibration of the fluid inclusion stage	311

LIST OF PLATES**PAGE**

Plate 2.1 Tennantite-bornite ores, Gallantry Bank Mine, Bickerton	39
Plate 2.2 Sulphides cementing and replacing detrital silicate grains, Bickerton	39
Plate 3.1 Authigenic K-feldspar and quartz overgrowths, Helsby Sandstone Formation	82
Plate 3.2 Epitaxial K-feldspar overgrowths, Helsby Sandstone Formation, Rawhead	82
Plate 3.3 K-feldspar dissolution textures, Helsby Sandstone Formation, Hawkshead	84
Plate 3.4 Authigenic illite and K-feldspar, Helsby Sandstone Formation, Clive	84
Plate 3.5 Micritic calcite cements, Helsby Sandstone Formation, Alderley Edge	88
Plate 3.6 Barite cements in aeolian sandstones, Helsby Sandstone Formation, Beeston	88
Plate 3.8 Saddle dolomite, Tarporley Siltstone Formation, Wilkesley borehole	97
Plate 3.7 Blocky anhydrite cements, Tarporley Siltstone Formation, Wilkesley borehole	97
Plate 4.1 Well-developed quartz overgrowths, Burghead Sandstone Formation, Burghead	128
Plate 4.2 Authigenic K-feldspar, Hopeman Sandstone Formation, Hopeman	128
Plate 4.3 Calcite nodules in fluvial sands, Burghead Sandstone Formation, Burghead	132
Plate 4.4 Barite mineralisation, Hopeman Sandstone Formation, Covesea	132
Plate 4.5 Nodular calcite cements, Burghead Sandstone Formation, Burghead	136
Plate 4.6 Fluorite cements and authigenic K-feldspar, Hopeman Sandstone Formation, Hopeman	136
Plate 4.7 Pervasive barite cements, Hopeman Sandstone Formation, Hopeman	145
Plate 4.8 Fractured pyrite and marcasite crystals, Cherty Rock, Lossiemouth	145

Plate 4.9 Stockwork of weathered sulphide veins, Hopeman Sandstone Formation, Masonhaugh	147
Plate 4.10 Disseminated galena crystals, Cherty Rock, Lossiemouth	147
Plate 5.1 Original sandstone fabric, Cherty Rock, Inverugie	189
Plate 5.2 Laminar layering in micritic calcite, Cherty Rock, Inverugie	189
Plate 5.3 Calcrete textures; pellets, Cherty Rock, Inverugie	191
Plate 5.4 CL characteristics of spar cements, Cherty Rock, Inverugie	191
Plate 5.5 Complex silica void-fill, Cherty Rock, Lossiemouth	193
Plate 5.6 Calcite relics in microquartz fabric, Cherty Rock, Lossiemouth	193
Plate 6.1 Sedimentary structures in conglomerates, Middle Buntsandstein, Kallmuther Berg	230
Plate 6.2 Sedimentary structures and mineralisation, Middle Buntsandstein, Kallmuther Berg	230
Plate 6.3 Authigenic cements and porosity, Upper Buntsandstein, Kall	234
Plate 6.4 Authigenic cements and porosity, Upper Buntsandstein, Kall	234
Plate 6.5 Authigenic dickite, Middle Buntsandstein, Kallmuther Berg	237
Plate 6.6 Galena cements, Middle Buntsandstein, Kallmuther Berg	237
Plate 6.7 Rhombic dolomite crystals, Middle Buntsandstein, Kallmuther Berg	242
Plate 6.8 Pore-filling galena in Middle Buntsandstein sandstones, Kallmuther Berg	242
Plate 6.9 Dissolution and replacement textures in Muschelkalk sandstones, Parkstein	260
Plate 6.10 Sulphide ores replacing wood cells, Freihung	260

CHAPTER 1

INTRODUCTION

Subsidence of complex rift systems during late Permian and Triassic times in Western and Central Europe heralded the disintegration of the Pangean supercontinent in the Jurassic, Cretaceous and Early Cenozoic (Ziegler 1982). Triassic sediments were deposited in a series of deep, fault-bounded sedimentary basins which are characterised by the lack of associated volcanism. Continental aeolian and fluvial sediments accumulated during the arid depositional regime that prevailed during Permian and Early Triassic times, as a result of the general northward drift of Pangea whereby Western and Central Europe moved into the northern trade wind belt.

Such continental red bed sequences are host worldwide to a characteristic style of mineralisation which is dominated by copper, lead, zinc, uranium and vanadium. This common association has been noted by several authors (eg. Stanton 1972) and suggests that red bed formation and ore deposit formation may be genetically related. This study is primarily concerned with the evaluation of the roles of red bed diagenesis and sedimentary basin evolution in the formation of such ore deposits.

1.1 APPROACH AND AIMS OF THE STUDY

In this study, the nature of sediment-hosted mineralisation in several European Permo-Triassic basins was investigated. The Cu-Pb-Zn mineralisation of the Cheshire Basin, northwest England, the Pb-Fe-rich ores on the margins of the Inner Moray Firth Basin, northeast Scotland and the Pb-bearing sandstones of the Eifel and Oberpfalz regions, West Germany received particular attention. The overall approach was to initially review the sedimentological and tectonic evolution of each sedimentary basin. Detailed textural studies were carried out to establish a sequence of diagenetic events in both the ore-bearing horizons and the adjacent sedimentary sequences. Mineralogical studies using electron probe microanalysis were undertaken to determine minor element concentrations in sulphide phases and to investigate the levels of barium in detrital K-feldspar. Fluid inclusion microthermometry was used to supplement oxygen and sulphur stable isotope analyses, in order to increase the understanding of the nature of the mineralising fluids and to constrain the genetic models for the mineralisation.

1.2 THESIS FORMAT

The thesis is presented as a series of five self-contained papers which make up the five main chapters, a style recently approved by the University of Aston.

The features of the Cu-Pb-Zn-Ba mineralisation in the Cheshire Basin are described in Chapter 2. New mineralogical, sulphur isotope and fluid inclusion data are presented and are used to refine genetic models for the deposits. The origin of the widespread barite mineralisation is discussed in detail.

In Chapter 3, the diagenetic events that occurred in the deeply buried Mercia Mudstone Group sediments of the Wilkesley borehole, Cheshire Basin, are detailed and compared to the diagenetic modifications observed in the shallowly buried Sherwood Sandstone Group sediments at the basin margins. This study provides the opportunity to examine the depth-related diagenetic processes that have operated in the Cheshire Basin. This work complements the investigation described in Chapter 2 and an attempt is made to relate diagenetic events to the processes involved in the formation of ore deposits.

The sedimentological, diagenetic and mineralisation history of the Permo-Triassic sandstones on the southern margin of the Inner Moray Firth Basin is documented in Chapters 4 and 5. Sulphide mineralisation is concentrated in an ancient calcrete horizon and is accompanied by widespread fluorite and barite. New fluid inclusion and sulphur isotope data are presented, followed by a detailed discussion of possible genetic models for the mineralisation.

Chapter 5 outlines the development and early diagenetic history of the carbonate-rich horizon (the Cherty Rock) at Lossiemouth, Inner Moray Firth Basin, which hosts the sulphide mineralisation. New textural evidence, geochemical studies and carbon and oxygen stable isotope analyses have been used to resolve the controversy over the origin of the horizon.

The sandstone-hosted Pb deposits in the Triassic of West Germany are the subject of Chapter 6. It is widely accepted that the accumulation of ores in the Oberpfalz region, northeast Bavaria, occurred during early diagenesis; however, the timing and origin of the deposits in the Eifel Mountains is still disputed. Interpretation of sulphur isotope data for the ores in the Eifel was hampered by the limited information on the development of the associated sedimentary basin, and also by the uncertainty surrounding the relationship of

Figure 1.1. Scythian palaeogeographic map of Western Europe showing the location of the study areas. Abbreviations are as follows: MFB = Moray Firth Basin, SWB = Solway Basin, MNH = Mid-North Sea High, CB = Cheshire Basin, WB = Worcester Basin, SP = Sole Pit Basin, TB = Trier Embayment, OB = Oberpfalz Basin.

Aut

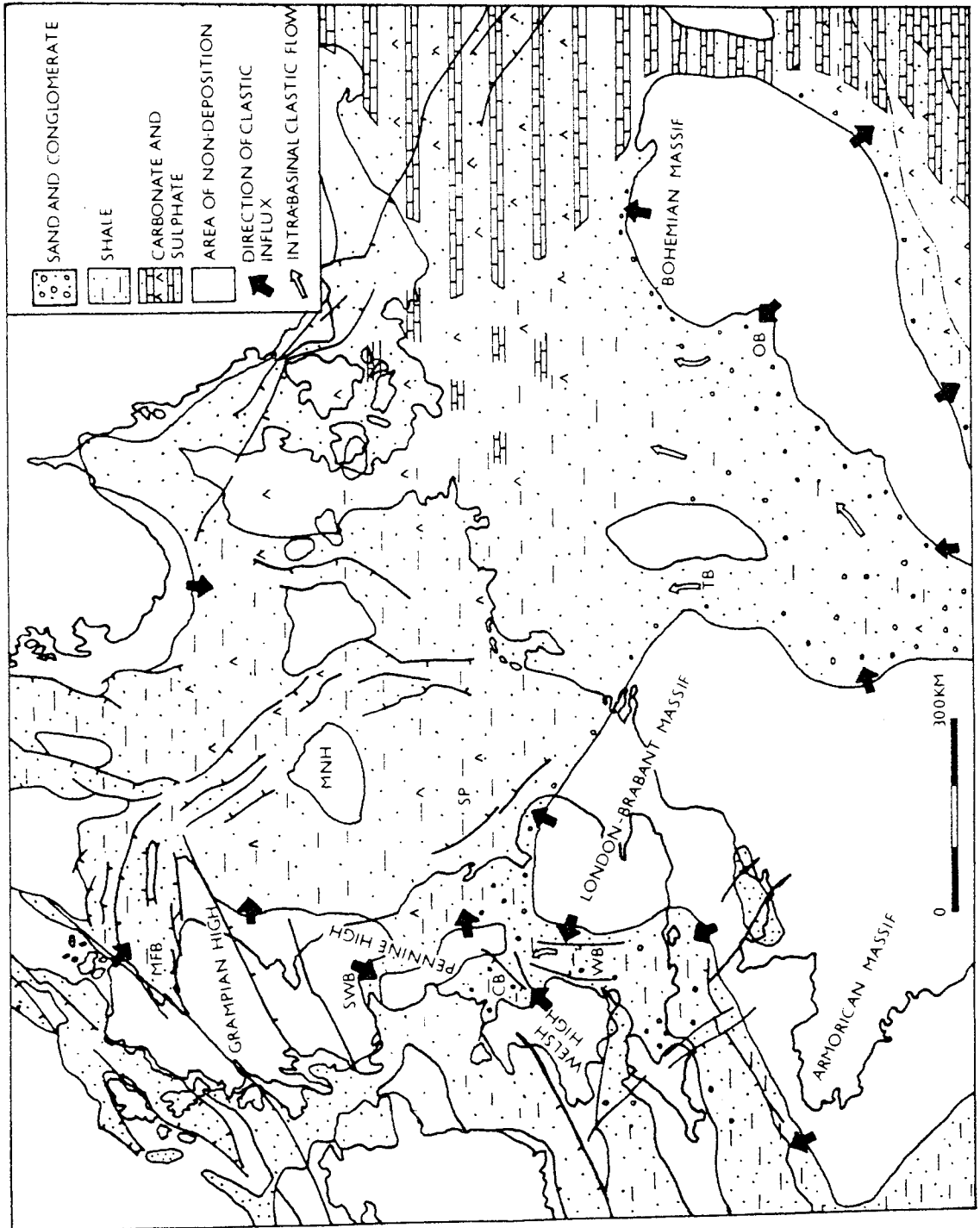
Titl

Av

=

1000
900
800
700
600
500
400
300
200
100
0
-100
-200
-300
-400
-500
-600
-700
-800
-900
-1000

FIGURE 1.1



the deposits to sulphide-bearing veins in the Devonian basement.

In the concluding Chapter (Chapter 7), the salient features of the mineralisation in the European Permo-Triassic basins are noted, with special reference to the deposits studied during the course of this work. Three fundamental questions are considered;

- i) the sources of the metals and sulphur.
- ii) the nature and origin of the mineralising solutions.
- iii) the cause(s) of sulphide deposition.

The ore deposits are considered within a framework of the burial diagenesis of clastic sequences dominated by red beds and of sedimentary basin development. A single genetic model is proposed for the mineralisation, with local variations in basin evolution and sedimentary basin fill accounting for the differences between the deposits. Finally, a critical review of the classification of red bed Cu-Pb-Zn deposits by previous authors is presented and their relationship to Mississippi Valley-type and other sediment-hosted deposits is discussed.

REFERENCES

- STANTON, R.L. 1972. *Ore Petrology*. McGraw-Hill, New York.
- ZIEGLER, P.A. 1982. *Geological Atlas of Western and Central Europe*. Elsevier, Amsterdam.

CHAPTER 2
GENETIC STUDIES OF RED BED MINERALISATION IN THE TRIASSIC
OF THE CHESHIRE BASIN, NORTHWEST ENGLAND

ABSTRACT

The Triassic sediments of the Cheshire Basin are host to a number of small ore deposits of the type characteristic of red beds. The mineralisation comprises Cu and Pb with minor Zn, Ag, Co, V, Ni, As, Sb and Mn, which together with widespread barite mineralisation is closely associated with basin margin faults. The Wilmslow Sandstone Formation is cemented by authigenic quartz overgrowths enclosing iron sulphides, that predate the main sulphide cements of tennantite, bornite and sulpharsenides. Studies on late calcite-hosted fluid inclusions show homogenisation temperatures ranging between 60-70°C (regarded as the minimum temperature of mineralisation) and salinities of 9-22 wt% equivalent NaCl (mean = 17 wt%), indicating that the mineralising fluids were warm and saline. Consideration of the basin history suggests that fluid temperatures in the Permo-Triassic sequence may have reached 150°C at the time of mineralisation. New data significantly constrain the genetic hypotheses for the deposits, refuting a magmatic origin. A basin brine expulsion model is favoured. The sulphur isotope data from the barite mineralisation (mean $\delta^{34}\text{S} = +17\text{‰}$) suggest that the bulk of the barite sulphur was derived directly from the Upper Triassic evaporites (mean $\delta^{34}\text{S} = +19\text{‰}$), whilst the distribution of $\delta^{34}\text{S}$ values for sulphides (-1.8‰ to +16.2‰) is consistent with ultimate derivation of sulphur from the evaporites by closed system reduction of a sulphate-bearing brine. It seems likely that the reducing agent was organic material derived from the underlying Coal Measures, but it is uncertain at present whether the principal mechanism was thermochemical or bacterial reduction. The pattern of sulphide $\delta^{34}\text{S}$ favours the former process.

2.1 INTRODUCTION

The Cheshire Basin (north-west England, see Fig. 2.1) is a deep, fault-bounded, 'graben-like' structure containing up to 4.5 km of Permo-Triassic sediments (Chadwick

1985). These sediments are underlain by Carboniferous strata in the north and by Pre-Cambrian volcanics and sediments in the south (Thompson 1983). The basin is approximately 100 km north-south and up to 50 km east-west and is bounded on its eastern margin by the Wem-Red Rock fault system (Fig. 2.1). The faults of this system have a N.N.E. inherited Charnoid trend and have dominated the evolution of the Cheshire Basin. Syn-depositional movements on the Wem-Red Rock system during the Permo-Triassic had a significant effect on subsidence and sedimentation rates within the basin, and crustal uplift and erosion during the Tertiary were a direct result of reactivation of the same faults (Chadwick 1985).

The Permo-Triassic basin fill comprises a variable sequence of continental clastics of fluvial, aeolian and marginal marine origin. The Chester Pebble Beds lie unconformably on Permian sediments (Steel & Thompson 1983) and are coarse, texturally mature conglomerates which mark the base of the Sherwood Sandstone Group (see Fig. 2.2). The Chester Pebble Beds are themselves overlain by predominantly fluvial sediments of the Wilmslow and Helsby Sandstone Formations, although the latter has important aeolian intercalations (Thompson 1970). Upper Triassic sediments of the Mercia Mudstone Group include lacustrine sediments and thick (600 m) evaporite facies deposited in shallow, hypersaline basins (Arthurton 1980).

The fluvial and aeolian sediments of the Wilmslow and Helsby Sandstone Formations (see Figs. 2.2 and 2.3) are host to number of ore deposits of the type termed U-V-Cu sandstone deposits by Stanton (1972) and by Craig & Vaughan (1981) and sometimes referred to in short as ' red-bed copper deposits'. The mineralisation comprises Cu and Pb as sulphides together with a variety of hydrated and oxygenated species, with minor amounts of Zn, Ag, Co, V, Ni, As, Sb and Mn. The ores are concentrated along the basin margin faults and as cements in the sandstones down-dip from the faults. At Alderley Edge, in the north-east of the basin, lead and zinc sulphides are found in and adjacent to fault zones, whereas copper minerals are more widespread (Carlson 1979). Cobalt, nickel and iron sulphides occur as cements within the Wilmslow Sandstone Formation on the western margin of the Cheshire Basin. They impregnate sandstones adjacent to the Bickerton-Bulkeley fault and are found in economic quantities at Gallantry Bank

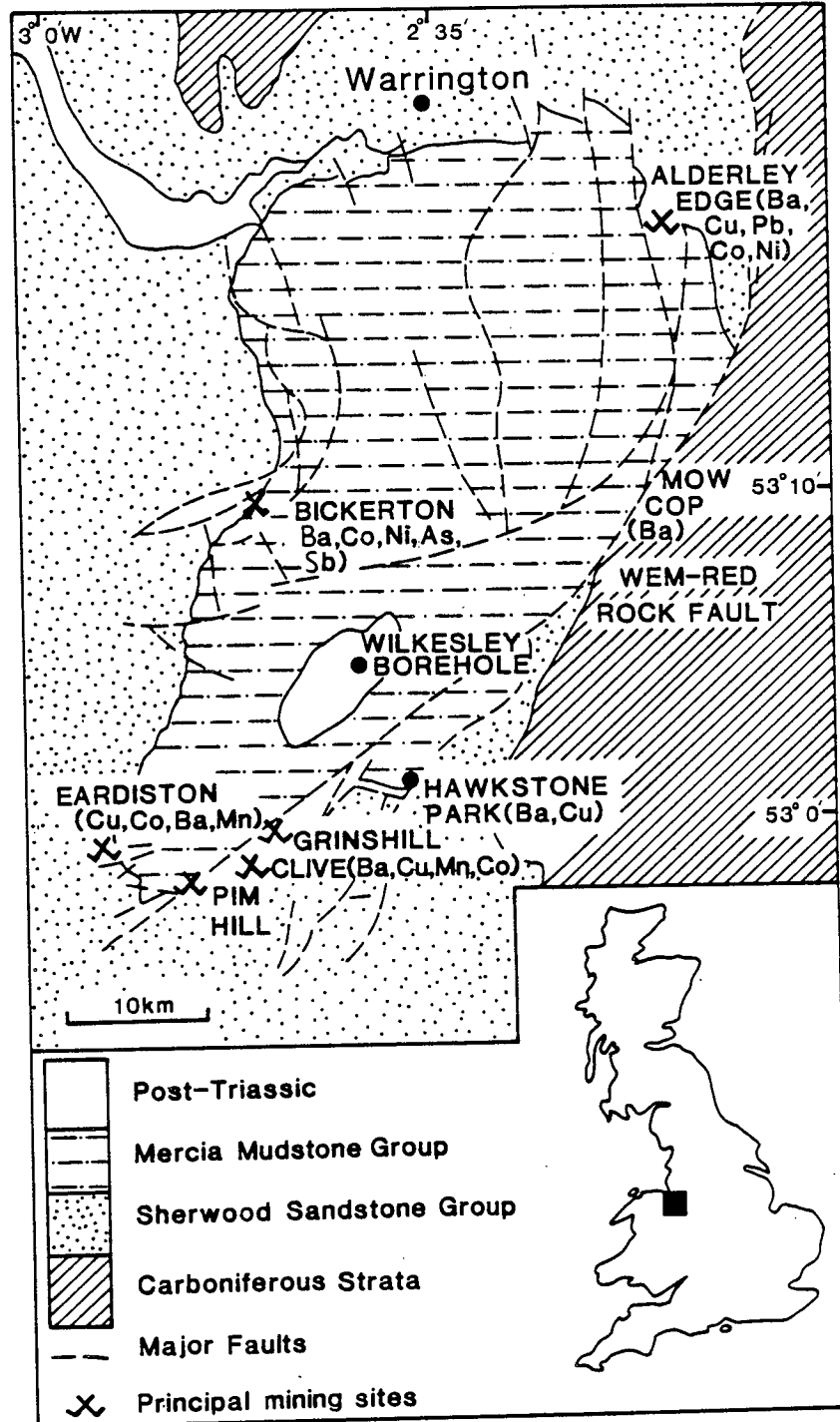


Figure 2.1. Geological map of the Cheshire Basin showing the NNW trend of the major faults and the mineralisation which is associated with the basin margins. Principle sampling locations are shown together with the position of the Wilkesley Borehole.

(Carlon 1981).

Barite is widespread near the base of the Helsby Sandstone Formation, and in the upper part of the Wilmslow Sandstone Formation around the basin margins (Carlon 1975). There appears to be no facies control on the several generations of barite which are concentrated in the interbedded aeolian and fluvial units. Fault control on barite distribution is shown by the increase in concentration of barite near the faults and the similar orientation of barite veins compared to adjacent faults (Carlon 1975).

In the present work, detailed mineralogical studies have been undertaken of the ores at Gallantry Bank, Bickerton, to complement a similar study at Alderley Edge (Iker & Vaughan 1982). Some preliminary fluid inclusion studies have also been undertaken on material from Bickerton and Alderley Edge, and a sulphur isotope study of evaporites, barite, and sulphides in the Cheshire Basin has been carried out. The main sampling sites for the isotope study were Alderley Edge, Bickerton and Hawkstone Park (Fig. 2.1). The purpose of the investigation was to elucidate the genesis of the primary sulphides and the barite mineralisation within the basin.

2.2 BASIN EVOLUTION

The sediment infill of the Cheshire Basin is of Permian to Lower Jurassic age (see Figs 2.2 and 2.3) and is up to 4.5 km thick in the south-east, suggesting that greater subsidence occurred in this basin than in any of the other onshore British Permo-Triassic basins. An extensional regime in the early Permian interval is believed to have initiated major faults which were to form the basin margins, most notably those of the Wem-Red Rock fault system in the east (Chadwick 1985). Subsidence related to this fault movement heralded the beginning of basin formation and of infilling by early Permian sediments, the distribution of which is thought to have been controlled by N-S faults parallel to the Wem-Red Rock faults (Whittaker 1985). Basal Permian breccias deposited as alluvial fans lie unconformably on the folded strata of the Coal Measures and are themselves overlain by the mainly aeolian Collyhurst Sandstone (Fig. 2.2). The Manchester Marls (Figs. 2.2 and 2.3) represent a brief marine transgression in the Mid-Permian, their distribution and the increased thickness of the Permian sediments in the north indicates a depocentre towards the north or north-east of the basin at this time (Whittaker 1985).

Figure 2.2. Schematic log of the Permo-Triassic sediments within the Cheshire Basin (after Thompson 1983). The continental sediments deposited during fault controlled subsidence in the Permian and early Triassic gave way to marls and evaporites of the Mercia Mudstone Group which were deposited in shallow marine environments.

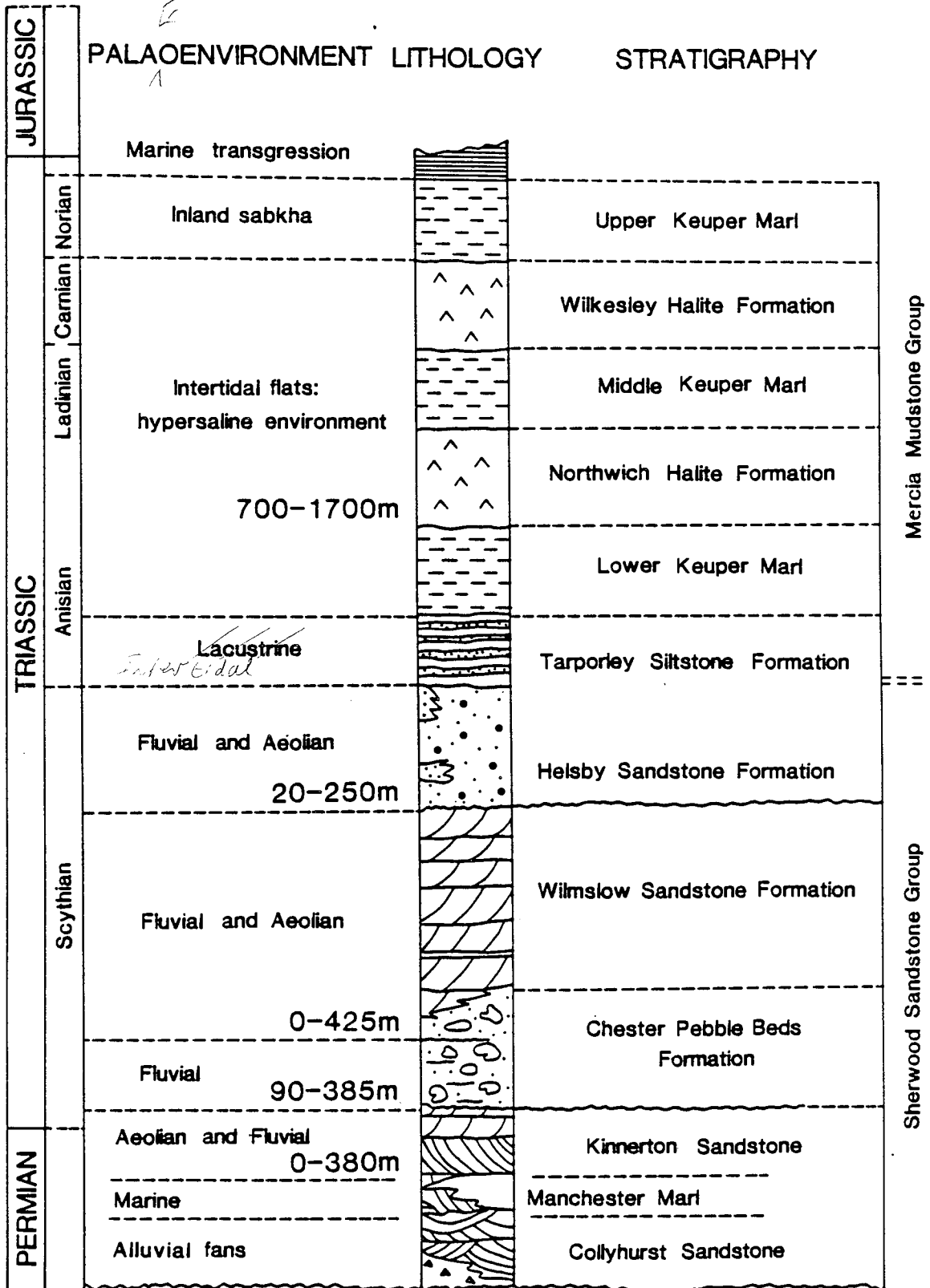
Aut

Titl

Av

=

FIGURE 2.2



Basin development was initiated in the early Triassic, when subsidence related to movements on the faults on the eastern margins of the Worcester and Cheshire Basins, led to a connection between them and to the evolution of a drainage system with rivers sourced in the Variscan foreland (Whittaker 1985). The Lower Triassic sediments of Cheshire, in the form of the Sherwood Sandstone Group, comprise a series of conglomerates, coarse sandstones and mudstones. The Chester Pebble Beds Formation represents material deposited in an alluvial fan / braided river system (Steel & Thompson 1983). The finer sediments of the Wilmslow and Helsby Sandstone Formations represent alluvial deposits of low sinuosity stream channels (Audley-Charles 1970). Minor aeolian dunes are present in the Helsby Sandstone Formation (Thompson 1969). The majority of the Lower Triassic clastic sediments originated from a Variscan source area in northern France with minor local input, as in the case of some of the Alderley Edge conglomerates which consist of material originating from the Pennine block to the east.

The Tarporley Siltstone Formation consists of fine- grained sands and silts deposited in inter-tidal conditions (Ireland et al. 1978). It is overlain by a thick succession of evaporites and mudstones deposited on wide inter-tidal flats which were repeatedly isolated from the sea by tectonic movements and/or sea level changes. This resulted in hypersaline conditions necessary to precipitate considerable thicknesses (up to 600 m) of evaporites, comprising halite along with more minor sulphates. The Northwich and Wilkesley Halite Formations consist of individual units of halite up to 40m thick, which are separated by dolomite and sulphate-rich silty clays (Tucker & Tucker 1981). Between the halite formations (and above and below them) are thick mudstone and siltstone formations containing sulphate nodules and veins (Arthurton 1980). The laminated facies described by Arthurton (1980) contains abundant anhydrite and gypsum nodules, with gypsum veins making up 5-10 % of the whole rock. Anhydrite nodules are also common in the more massive blocky facies which is cut by displacive veins of gypsum and anhydrite. Active normal faulting continued during the deposition of the Mercia Mudstone Group and micro-structures in the halite show that there was continued contemporaneous movement along Carboniferous basement faults (Tucker & Tucker 1981).

By the end of the Triassic, it is estimated that up to 4.5 km thickness of Permo- Triassic

Figure 2.3. Sketch section across the Northern Cheshire Basin to show the stratigraphic position of the mineralisation at Alderley Edge and the regional extent of the Tarporley Siltstone Formation above the Helsby Sandstone Formation (data in part from Thompson (1970) and Ebbenn (1981)).

Aut

Tit'

Av

=

sediments may have accumulated in the basin centre (Whittaker 1985). Apart from an outlier of Liassic rocks, Jurassic sediments in the Cheshire Basin have now been removed by erosion but in the adjoining Worcester Basin, over 500 m of Lower Jurassic strata are present. Other Permo-Triassic basins such as Cardigan Bay (west Wales) are known to have Tertiary sediment fill, but in the case of the Irish Sea Basin this was lost due to basin inversion and erosion. In the latter case, vitrinite reflectance studies have suggested maximum burial depths to have been up to 2 km greater than at the present day (Colter 1978). The evolution of the Cheshire Basin is thought to have been similar to the Irish Sea Basin in that reactivation of previously extensional faults, culminating in Miocene times caused preferential uplift and erosion of up to 2 km of post Triassic sedimentary cover. Some of the later faulting postdated minor dyke emplacement in the southern part of the basin (Poole & Whiteman 1966). These dykes have been radiometrically dated at 50 ± 13 m.y. old (Fitch et al. 1969).

2.3 GEOLOGICAL SETTING OF THE MINERALISATION

The geological setting of the mineralisation in the Cheshire Basin is well documented in the literature. In one of the first descriptions, Murchison (1839) referred to the ores at Pim Hill, Eardiston and Hawkstone Park (Fig. 2.1) in the southern part of the basin. The mineralisation around Bickerton and Eardiston was further described by Hull (1869), Wedd et al. (1929) and Poole & Whiteman (1966). An early but thorough account of the mineralisation in the Cheshire Basin is given in Dewey & Eastwood (1925).

The best known and documented area of mineralisation is at Alderley Edge (Fig. 2.4) where Cu ores and associated Ag and Co were mined (Carlson 1979). Descriptions of the geological setting and mineralisation at Alderley Edge are given by Dewey & Eastwood (1925), Taylor et al. (1963), Warrington (1965), Carlson (1979) and Ixer & Vaughan (1982).

Mineralisation is found on the west side of the basin in the Wilmslow Sandstone Formation and at the base of the Helsby Sandstone Formation of the Mid-Cheshire Ridge. The ridge rises 250 m O.D. above the Cheshire Plain near Tarporley and is bounded by NNE-SSW trending faults (Fig. 2.5). The Bickerton - Bulkeley fault on the east side of the ridge downthrows approximately 363 m to the east and in the footwall

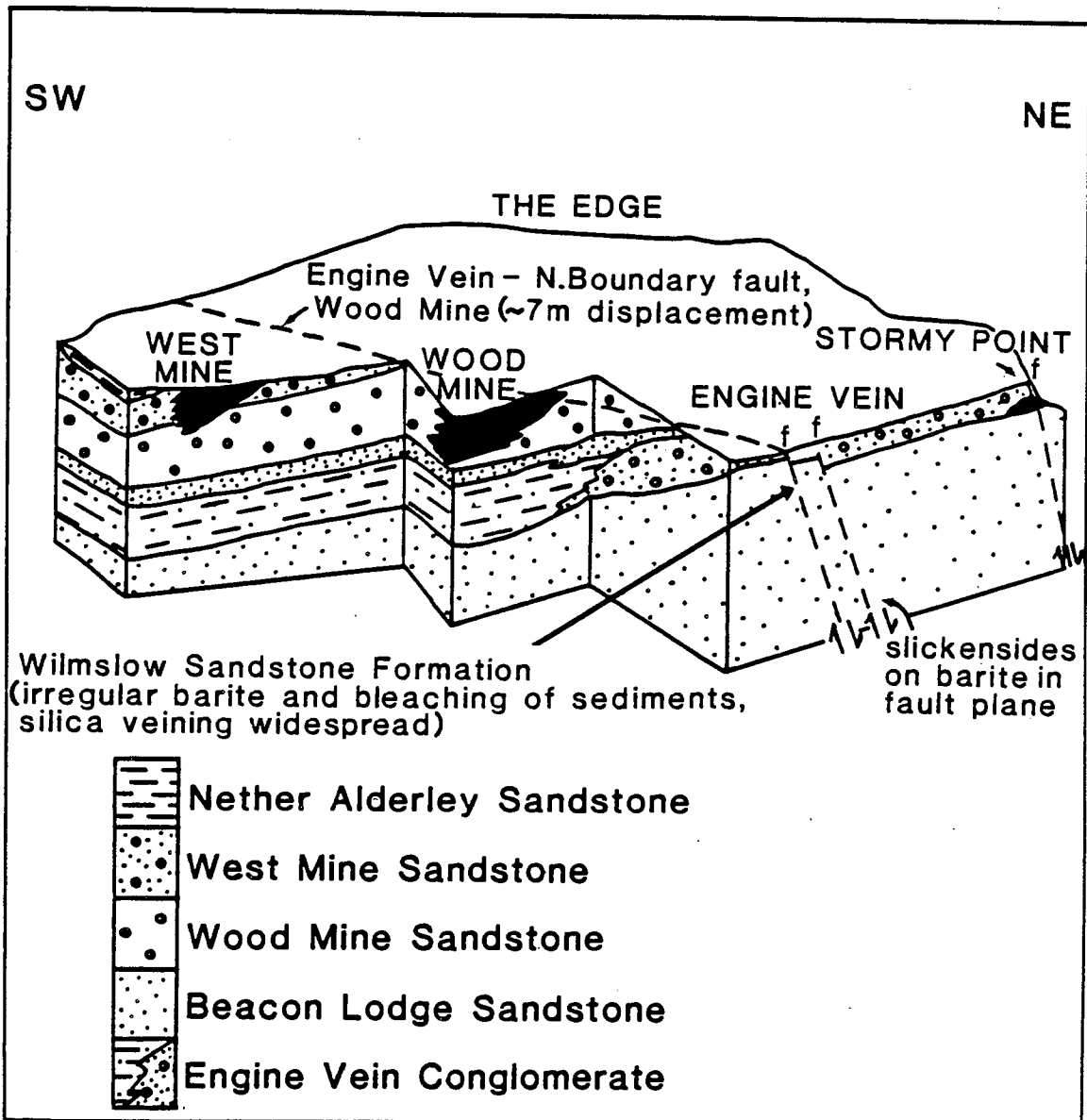


Figure 2.4. Schematic section across the Alderley Edge fault block showing the spatial and stratigraphical distribution of the mineralisation and the main sampling sites of Wood Mine and Engine Vein (adapted from Carlon 1979).

Figure 2.5A. Geological map of the Mid-Cheshire Ridge near Gallantry Bank and Bickerton. The NNE-SSW trending faults bounding the ridge may have a minor strike-slip component. Smaller NW-SE and E-W trending faults have smaller displacements (30-40 m) and divide the ridge into individual horst blocks. Barite is abundant in the porous horizons within the Helsby Sandstone Formation of Burwardsley Hill and Rawhead. Its precipitation is associated with widespread silica dissolution within the sandstones, barite crystals within the fault remain undeformed so that the barite appears to postdate fault movement.

B. Schematic cross-section showing the ore body at Gallantry Bank, Bickerton (after Carlon 1981). Sulphides are found impregnating the sandstones in a narrow zone adjacent to the fault which dips 70-80° to the SE and E and has a large displacement. The impermeable Mercia Mudstone Group and Tarporley Siltstone Formation in the footwall have caused ponding of mineralising fluids within the fault zone. The bleached zone of sandstone adjacent to the fault is a result of the removal of haematite from the sediments previous to or during mineralisation.

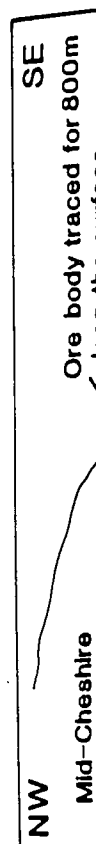
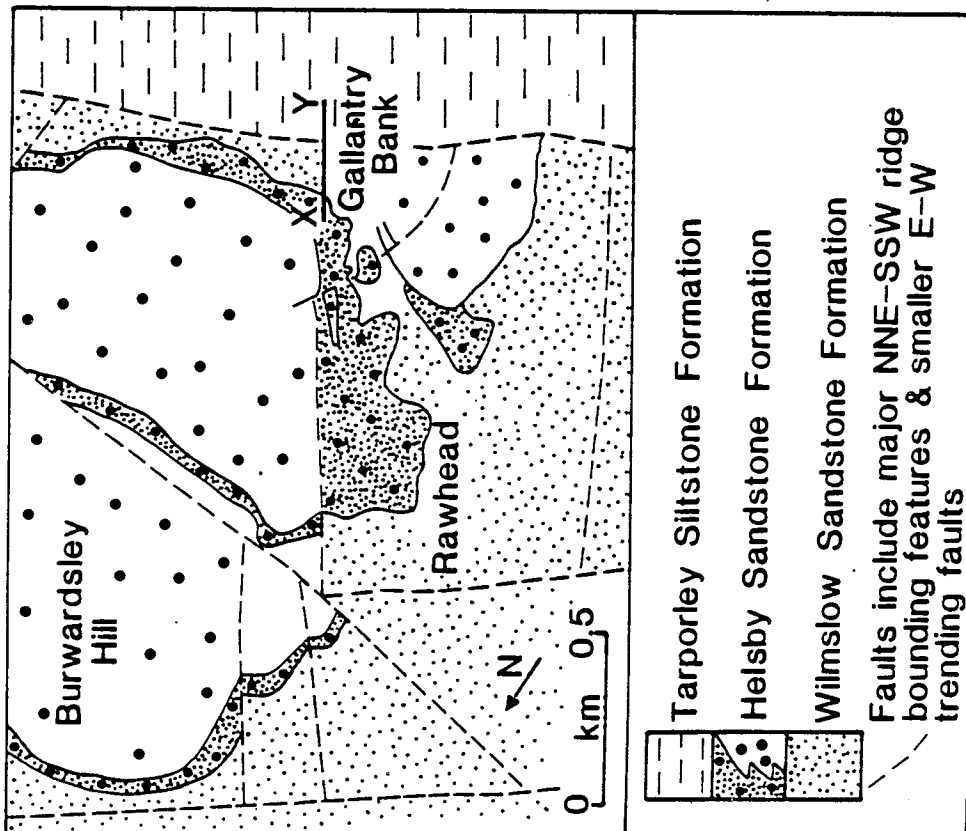
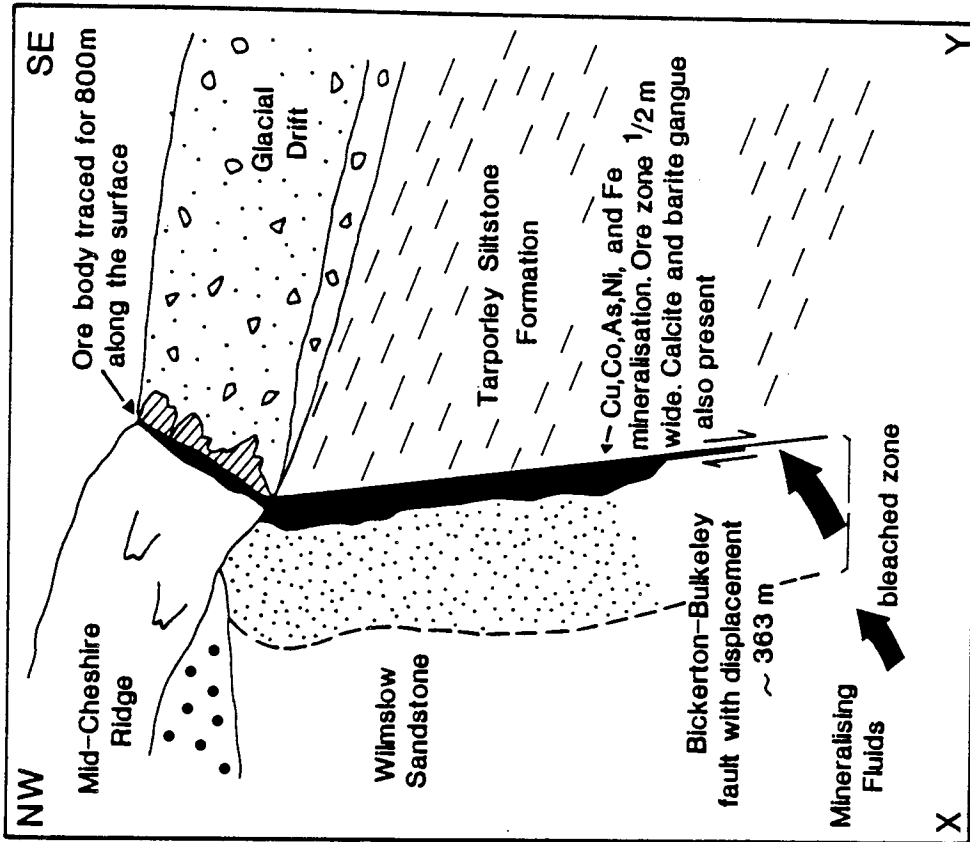


FIGURE 2.5



at Gallantry Bank, Bickerton, is a small orebody hosted by the Wilmslow Sandstone Formation (Fig. 2.5). Barite is also found in the fault zone where it occurs along with a coarse calcite gangue while several generations of barite mineralisation are also found in the overlying Helsby Sandstone Formation. Samples from the orebody at Bickerton were studied in the present work by reflected and transmitted light microscopy and electron probe microanalysis in order to establish the sulphide mineralogy, and to relate the paragenesis to the precipitation of authigenic phases in the host rock.

2.4. ORE MINERALOGY

A detailed mineralogical study of the primary ore minerals at Alderley Edge has revealed a complex paragenetic sequence. Authigenic quartz overgrowths enclose some early sulphides, so that at least the early sulphide precipitation is thought to be closely related to the diagenetic history of the host sandstone (Ixer & Vaughan 1982). The paragenetic diagram in Fig. 2.6 shows early chalcopyrite, pyrite and bravoite to be enclosed within quartz overgrowths and the main sulphide cements to consist primarily of galena, sphalerite and chalcopyrite.

New data obtained in this study from the Bickerton ore zone reveal that the primary ores contain no lead but comprise Cu, Fe, As sulphides with minor Zn, Ni, Co and Sb. Supergene alteration does not appear to be as widespread as at Alderley Edge where there is a complex suite of secondary minerals. As shown in the paragenetic diagram (Fig. 2.6), the earliest sulphides to precipitate at Bickerton were chalcopyrite and bravoite which are totally enclosed within authigenic quartz overgrowths. The sulphides are anhedral and small (~5 µm diameter) and their occurrence within the overgrowths suggests that they were precipitated during the diagenesis of the host sandstones.

The main sulphide cements postdate quartz and feldspar overgrowths. Bravoite and nickeloan pyrite were the first sulphides to be precipitated and occur as euhedral crystals with a mean diameter of 50 µm (Plate 2.1). Some bravoite crystals occur in clusters and most exhibit continuous, multiple zoning parallel to crystal edges similar to that described by Vaughan (1969). The zoning is a result of variations in Ni, Co, Fe and Cu contents where Ni and Co show a sympathetic relationship, antipathetic toward Fe and Cu (see Table 2.1). The bravoite crystals have a pink coloured, nickel-rich core and

Figure 2.6. Paragenetic diagram for the sulphides and authigenic minerals in the ore deposits of Cheshire. (A) Data from the present study of the ore minerals at Bickerton. (B) Relative timing of sulphide precipitation at Alderley Edge for comparative purposes (adapted from Ixer & Vaughan 1982).

Phase	Quartz overgrowth	Main sulphide	Secondary sulphides
A.			
Bravoite	_____	_____	
Pyrite	_____	_____	
Ni-Co-Fe sulpharsenides			_____
Bornite		_____	
Tennantite		_____	
Chalcopyrite	_____	_____	
Covellite			_____
Barite	_____ ?		_____ - ?
Calcite			_____
B.			
Pyrite, bravoite		_____	_____
Ni-Co-Fe sulpharsenides			_____
Marcasite		_____	
Chalcopyrite	_____	_____	
Tetrahedrite		_____	
Sphalerite, galena			_____
Idaite, Covellite, Djurleite			_____
Barite			_____ - ?
Calcite			_____

TABLE 2.1. Electron probe microanalysis data for ore minerals at Bickerton*

Phase	Zn	Cu	Ni	Co	Fe	As	S	Pb	Bi	Ag	Cd	Sb	TOTAL	Calculated formula
Bravoite (Outer Zone)	0.1	2.2	5.0	0.2	39.3	0.8	52.0	0.2	0.2	n.d.	0.1	n.d.	100.0	(Fe _{0.87} Cu _{0.04} Ni _{0.10})S ₂
Bravoite (Inner Zone)	0.1	3.0	10.9	7.2	26.8	0.5	50.7	0.1	0.4	0.1	0.1	n.d.	99.9	(Fe _{0.61} Co _{0.15} Cu _{0.06} Ni _{0.23})S ₂
Bravoite (Outer Zone)	n.d.	2.1	6.8	0.3	38.1	n.d.	52.1	0.2	0.2	n.d.	n.d.	n.d.	99.8	(Fe _{0.84} Cu _{0.04} Ni _{0.14})S ₂
Bravoite (Inner Zone)	n.d.	5.6	13.4	2.3	27.2	n.d.	50.3	0.2	0.3	n.d.	0.2	n.d.	99.5	(Fe _{0.62} Co _{0.05} Cu _{0.11} Ni _{0.29})S ₂
Tennantite	6.0	42.6	0.1	n.d.	2.1	14.6	26.7	0.0	0.1	n.d.	0.2	7.4	99.8	Cu _{10.44} (FeZn) _{2.02} (SbAs) _{3.99} S ₁₃
Tennantite	3.9	42.7	n.d.	0.12	3.3	16.1	27.9	0.2	0.1	0.1	0.3	5.3	100.0	Cu _{9.98} (FeZn) _{1.77} (SbAs) _{3.86} S ₁₃
Bornite	0.1	61.2	0.1	n.d.	11.4	n.d.	26.0	0.1	0.1	0.1	0.2	n.d.	99.3	Cu _{4.74} Fe _{1.01} S ₄
Sulpharsenide	n.d.	2.5	17.2	15.6	1.6	41.6	19.81	n.d.	0.1	n.d.	0.9	0.5	99.8	
Sulpharsenide	n.d.	1.6	15.0	19.7	0.5	44.0	20.1	n.d.	0.1	n.d.	0.4	0.3	101.7	
Chalcopyrite	n.d.	34.8	0.3	0.6	28.8	1.1	33.1	0.1	0.1	n.d.	n.d.	0.1	99.0	Cu _{1.06} Fe _{1.00} S ₂

*All data expressed in weight per cent. Analyses obtained using a Cameca Camebax electron microprobe at an accelerating voltage of 20 k.v. and employing natural and synthetic sulphides as standards.

Plate 2.1 Reflected light micrograph of sulphide ores at Bickerton.

Bravoite (B) is paragenetically early and contains concentric zones in which Co, Ni, Fe and Cu are enriched (see text). Tennantite (pale blue) and bornite (pink) are the main sulphide cements, chalcopyrite 'ex-solution' lamellae are common in bornite. Scale bar = 25 μm .

Plate 2.2 Reflected light micrograph of sulphide ores at Bickerton. Bornite occurs as a cement between the detrital grains but is also seen to replace rounded detrital grains along with pyrite, chalcopyrite and Fe, Ni, Co sulpharsenides. Bornite is altered to covellite along fractures. Scale bar = 200 μm .

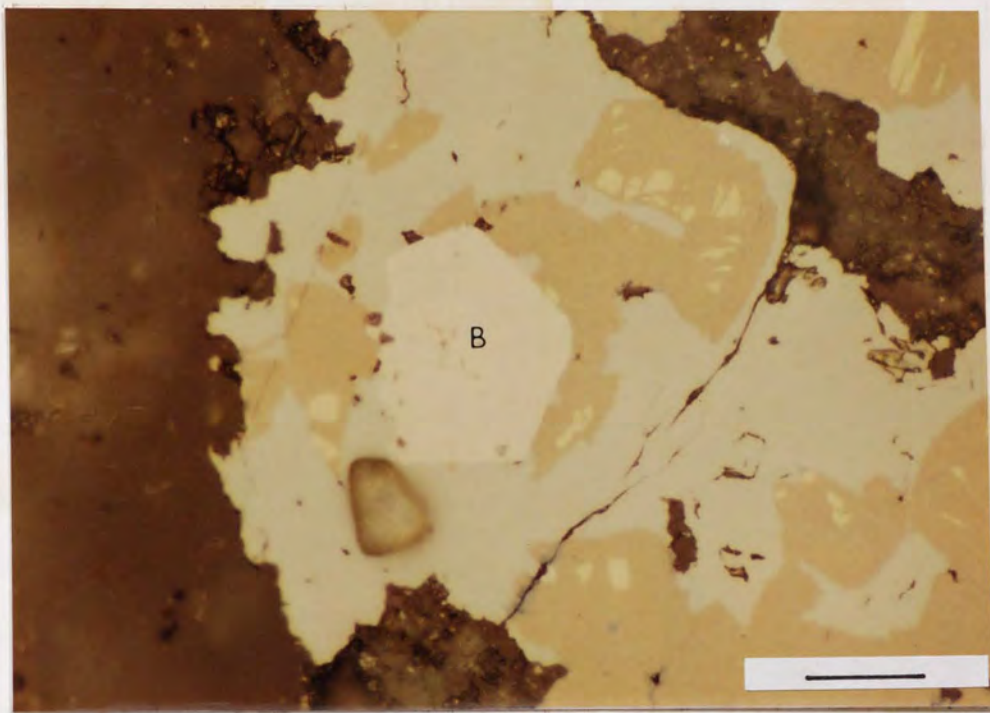
Aut

Tit'

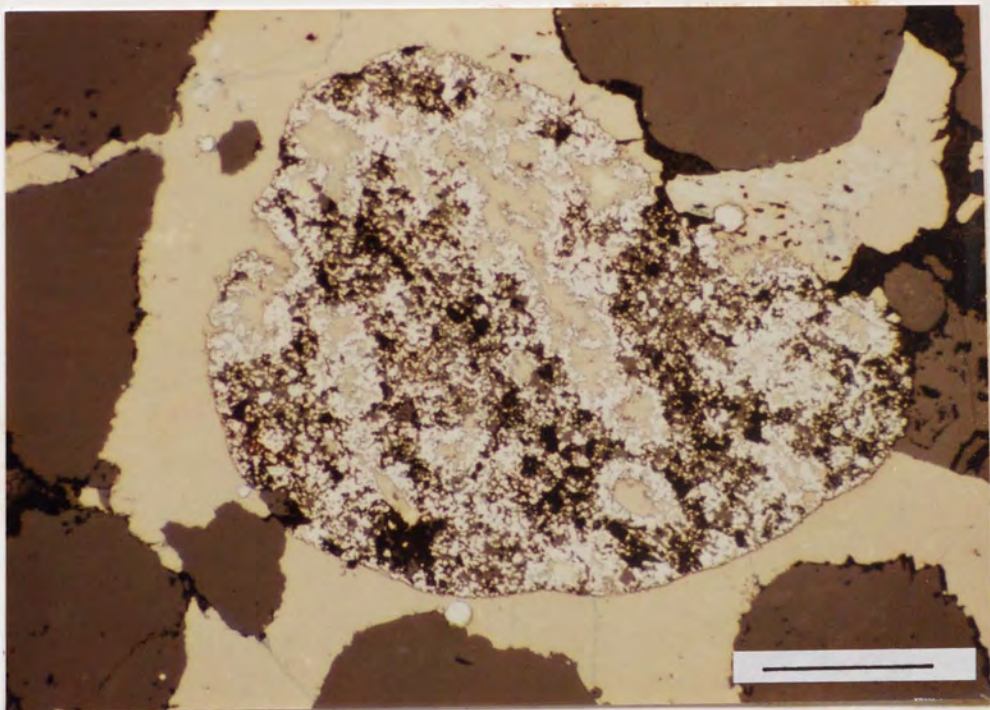
Av

=

c zones in
e (pale blue)
rite
25 μm .



. Bornite
en to replace
Fe, Ni, Co
es. Scale bar



occasionally exhibit overgrowths too small to analyse. A Co, Ni, Fe sulpharsenide (1-2.5 wt% Cu, 15-17 wt% Ni, 15-20 wt% Co and 0.5-1.5 wt% Fe; Table 2.1) occurs next in the paragenesis and has a composition similar to nickeliferous cobaltite although it is slightly enriched in copper, unlike a similar phase described from Alderley Edge by Ixer & Vaughan (1982).

Pyrite crystals that precipitated together with bravoite early in the paragenesis (Fig.2.6) contain significant Ni and Cu. Bravoite, chalcopyrite and the sulpharsenides can be seen to be directly replacing rounded detrital grains (Plate 2.2).

Tennantite and bornite are the most abundant sulphides in the main sulphide cement and are often complexly intergrown. The bornite is stoichiometric (see Table 2.1) unlike the 'sulphur rich' varieties often associated with similar deposits (Craig & Vaughan 1981). The tennantite ($\text{Cu}_{10}(\text{Fe Zn}) (\text{Sb As})_4 \text{S}_{13}$) is a phase that has not been previously recorded from the Cheshire Basin. In places it appears to have been replaced by bornite. Chalcopyrite lamellae are common within bornite and tennantite. Analyses of the chalcopyrite show it to contain up to 1.1 wt % As (Table 1). Covellite is the only secondary copper sulphide present and it occurs as small acicular crystals replacing bornite and tennantite along fractures and cleavage planes. Barite and calcite tend to postdate the precipitation of both the authigenic overgrowths and the sulphide ores.

Barite is widespread in the Mid-Cheshire Ridge sandstones; it is found in both aeolian and fluvial lithofacies, although its distribution is primarily controlled by the faulting (Carlon 1975). Several generations of barite are evident in the Wilmslow and Helsby Sandstone Formations of the Mid-Cheshire Ridge and Hawkstone Park on the southern basin margin. Multiphase precipitation of barite has resulted in the deposition of different forms of barite such as single bladed crystals, barite 'rosettes' and multiple vein systems whose dominant trend is sub-parallel to that of adjacent faults (Carlon1975). Barite has also been recorded at Mow Cop, Grinshill and Eardiston (Fig. 2.1) and is always concentrated at the same stratigraphic horizons around the basin margin.

Copper minerals impregnate the Triassic sandstones elsewhere in the basin and are found along with varying amounts of Co, Mn and Ba at Pim Hill, Eardiston, Clive, Mow Cop, Yorton and Wixhill (Carlon 1981). Because of the absence of sulphides at these

localities, no detailed mineralogical or isotopic studies were undertaken.

2.5 FLUID INCLUSION DATA

Fluid inclusions in the quartz overgrowths, barite and calcite gangue of samples from Bickerton and Alderley Edge were examined under the microscope and those suitable for microthermometry were studied using a Linkam TH600 heating-cooling stage (Shepherd 1981).

Inclusions in the iron sulphide-bearing quartz overgrowths were poorly developed (1-2 μm diameter) and this prevented their use in heating-freezing studies. Inclusions in barite were abundant and filled with a single liquid phase. On cooling to -70°C no visible change occurred within the barite-hosted inclusions indicating that they probably contain low salinity fluids trapped at near-surface temperatures (Roedder 1984). Previous studies (Leach 1980; Kaiser et al. 1987) encountered problems with similar barite-hosted inclusions due to their tendency to behave metastably. Despite this, inclusions in barite from Southeast Missouri were found to contain fluids of low to moderate salinity (0-14 wt % NaCl) and were thought to represent the fluid from which the barite precipitated (Kaiser et al. 1987). The fluids responsible for the deposition of the barite in the Cheshire Basin appear to be similar to those fluids which precipitated barite as a gangue mineral in Mississippi Valley-type ore deposits on the basis of the inclusion types and their behaviour (Leach 1980). However the temperature of barite precipitation in the Cheshire Basin remains unconstrained due to the lack of two phase inclusions.

Liquid and vapour filled inclusions in the late calcite gangue at Bickerton and the late calcite cements at Alderley Edge were used for microthermometric study. Inclusions hosted by calcite are prone to leakage and post-trapping alteration; however, results from this study are encouraging as they are both consistent and geologically reasonable. Fluid inclusions in the calcite from Bickerton range from 2-20 μm in diameter with a mean of 13 μm . The mean depression of freezing point for these inclusions was found to be -13.3°C which corresponds to a salinity of approximately 17 wt % NaCl equivalent (Potter et al. 1978). Homogenisation temperatures obtained for these inclusions range from 56.6 to 79.9°C with a mean of 68.7°C (Fig. 2.7). The few isolated, clearly primary inclusions yielded similar results to those controlled by cleavage direction which were indisputably of

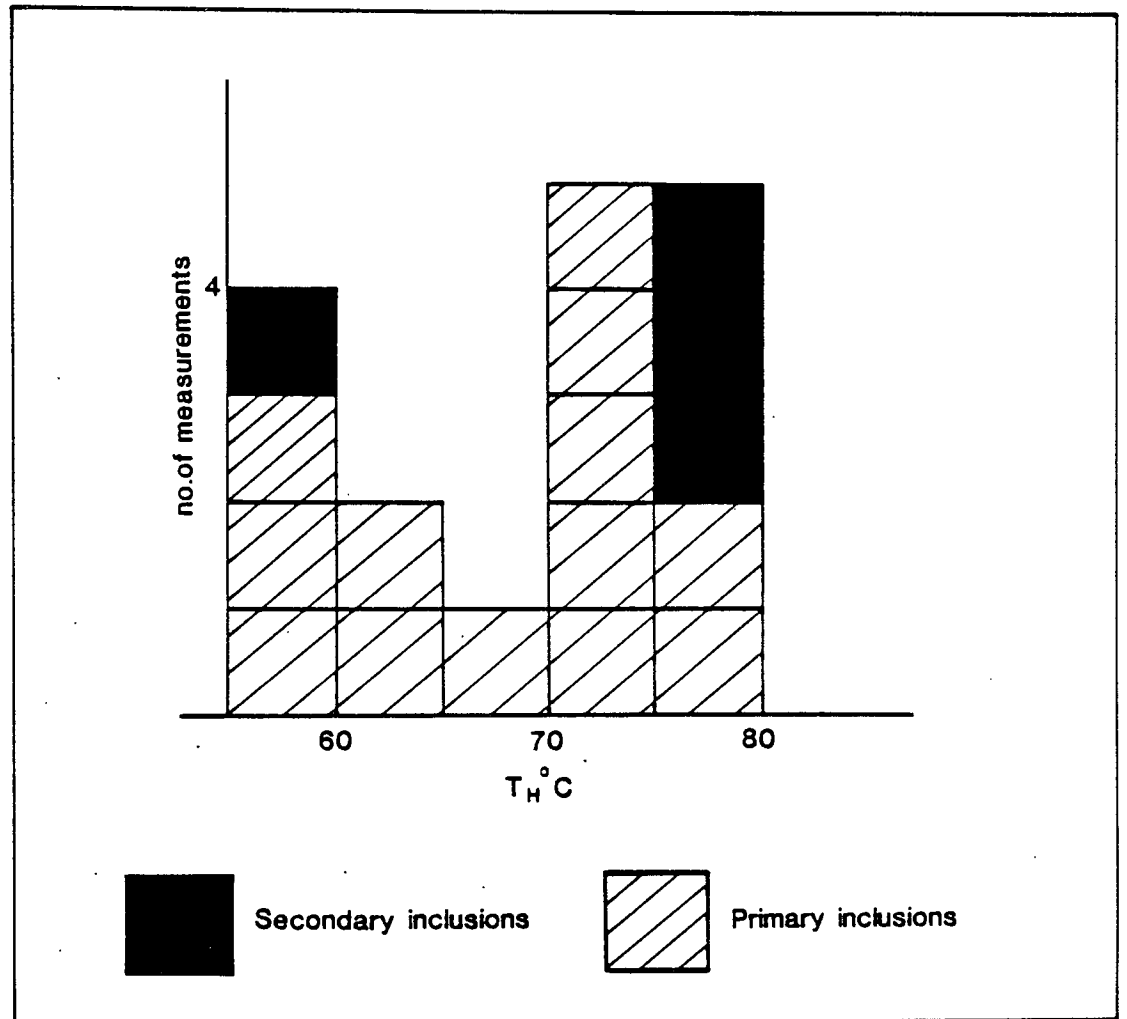


Figure 2.7. Histogram of homogenisation temperatures of fluid inclusions hosted by calcite gangue at Bickerton.

secondary origin, These data indicate that the late aqueous fluids passing up the fault at Bickerton were warm and saline. Studies of inclusions hosted by the late calcite cements at Alderley Edge yielded similar results, with a mean homogenisation temperature of 61.3°C.

2.6 SULPHUR ISOTOPE DATA

Sulphur isotope studies were carried out on sulphate and sulphide minerals in the Cheshire Basin in an attempt to 1) resolve the controversy of the origin of sulphur in the deposits, 2) investigate isotopic constraints on the formation temperatures of sulphide ores and the nature of the mineralising solutions and 3) constrain the mechanism of ore deposition. Sulphate and sulphide samples were collected from abandoned mine workings and surface outcrops. Sulphates from the Middle and Upper Triassic evaporite horizons were also studied using material taken from underground workings and boreholes.

Sample preparation techniques are detailed in Appendix I. The $\delta^{34}\text{S}$ values obtained are given in Table 2.2 and plotted in Fig. 2.7; they are discussed below for each of the major sample types.

2.6.1 GYPSUM AND ANHYDRITE

Three evaporite samples from the Cheshire Basin gave values ranging from +18.4 ‰ to 20.8 ‰. Sample 9799 is an anhydrite from the Lower Mercia Mudstone Group in the Wilkesley Borehole (Pugh 1960), whereas sample 42433 is from the Northwich Halite Formation of northern Cheshire, which is younger. Sample MA1 is gypsum from the laminated facies of the Lower Keuper Marl (Mercia Mudstone Group), north-east Cheshire. Gypsum and anhydrite are enriched in $\delta^{34}\text{S}$ relative to aqueous sulphate by 1.5 ‰ (Thode & Monster 1965), so that barring post-depositional alteration, the $\delta^{34}\text{S}$ values of these ancient evaporites should approximate the $\delta^{34}\text{S}$ value of Middle-Upper Triassic seawater sulphate. Published estimates of $\delta^{34}\text{S}$ values for Triassic marine sulphates range from +15 ‰ to +22 ‰ with a mean of +16.5 ‰ (Claypool et al. 1980) and the close agreement between these and the values from Cheshire indicates that the Cheshire evaporites have a marine source. By contrast, a limited number of sulphates from the Mercia Mudstone Group near Whitchurch, central Cheshire studied by Taylor (1983) gave $\delta^{34}\text{S}$ values of

around +13 ‰ ; these sulphates are thought to have precipitated from continental brines.

2.6.2 BARITE

The $\delta^{34}\text{S}$ ratios obtained for barite from Alderley Edge have a narrow range (+13‰ to +17‰) with a mean value of +16‰. The $\delta^{34}\text{S}$ values for barite are generally heavier (enriched in ^{34}S) than the $\delta^{34}\text{S}$ values for galena and chalcopyrite. The $\delta^{34}\text{S}$ of barite from different stratigraphic horizons, from coarsely crystalline barite on fault planes and from barite cements within the sandstones were not significantly different.

The $\delta^{34}\text{S}$ values for barite in the sandstone of the Mid-Cheshire Ridge and Hawkstone Park ranged from +16.6‰ to +19.3‰ (mean +18.1‰). Barite $\delta^{34}\text{S}$ values are uniform throughout the basin and although they correspond closely to the $\delta^{34}\text{S}$ values of the evaporites in the Mercia Mudstone Group, the evaporites are consistently heavier (Fig. 2.8). The isotopic data indicates that most of the barite sulphur was derived ultimately from the Triassic evaporites.

However, it is obvious from Fig. 2.8 that the $\delta^{34}\text{S}$ values for barite at Alderley Edge are lighter than those obtained for barite at Bickerton and Hawkstone Park. It would appear that whilst the evaporites are the dominant sulphur source, another minor source of sulphur may have been present. Alternatively, the slight discrepancy in the $\delta^{34}\text{S}_{\text{barite}}$ at Alderley Edge may have been caused by different transport and depositional mechanisms operating in the north-eastern part of the basin. At the Mid-Cheshire Ridge and Hawkstone Park, the $\delta^{34}\text{S}_{\text{barite}}$ values are more consistent with simple derivation of sulphate from the evaporites.

2.6.3 SULPHIDES

The $\delta^{34}\text{S}$ values shown in Fig. 2.8 were obtained from galena and chalcopyrite in the main sulphide cement at Alderley Edge and from a sulphide sample of intergrown bornite-tennantite from Bickerton. Galena and sphalerite were too finely intergrown in the Alderley Edge samples to be able to separate out the sphalerite for isotopic analysis.

The $\delta^{34}\text{S}$ values for galena at Alderley Edge range from +1.3‰ to +15‰ with a mean

of +8.2‰. There is no significant stratigraphic or spatial control on the $\delta^{34}\text{S}$ values for galena but there is a significant difference in the isotopic values obtained for different textural varieties of galena at Engine Vein Mine. The galena cementing the sandstones and conglomerate yield a mean $\delta^{34}\text{S}$ value of $5.9\text{‰} \pm 3\text{‰}$ ($n = 6$), in contrast to the galena found in a one metre by half metre 'pod' of massive ore within the Engine Vein fault which has a mean $\delta^{34}\text{S}$ of $14.9 \pm 1\text{‰}$ ($n = 2$). Chalcopyrite samples yielded $\delta^{34}\text{S}$ values ranging from +10.7‰ to +16.2‰ whilst the $\delta^{34}\text{S}$ value obtained for the bornite-tennantite sample from Bickerton was -1.8‰.

The fine intergrowths of chalcopyrite and galena at Alderley Edge prevented their separation for isotopic analysis, hence it was not possible to establish whether these coexisting (though not necessarily coprecipitated) sulphides have achieved isotopic equilibrium. This is considered unlikely as isotopic equilibrium between sulphides is not a common feature of low temperature, red bed-associated deposits (Ohmoto 1986). Furthermore, sulphur isotopic disequilibrium is often associated with sulphide pairs involving chalcopyrite and/or pyrite (Ohmoto 1986).

The isotopic disequilibrium exhibited between the sulphides and barite in these deposits is also common in low temperature ore-forming environments, particularly in cases where the temperature may not have exceeded $\sim 100^\circ\text{C}$. Data from Ohmoto & Lasaga (1982) indicate that in most natural systems at $T \leq 100^\circ\text{C}$ sulphate-sulphide equilibrium is unlikely to be established within a geologically reasonable time period. In contrast to the sulphide $\delta^{34}\text{S}$ values which vary considerably in the Cheshire Basin, $\delta^{34}\text{S}_{\text{barite}}$ values remain relatively constant. Barite deposition is envisaged as a complex process, occurring before, possibly during and after sulphide precipitation. Barite need not represent a separate mineralising event but the more extensive barite mineralisation suggests that sulphate availability was probably greater than sulphide during deposition.

TABLE 2.2. Sulphur Isotope Data from the Cheshire Basin

Sample No	Mineral	Remarks	$\delta^{34}\text{S}^*$
42433	Anhydrite	Northwich Halite Formation, Meadowbank Mine, Winsford	18.6
M.A.I.	Gypsum	Lower Keuper Marl, Manchester Airport	20.8
9799	Anhydrite	Tarporley Siltstone Formation, (1500 m depth) Wilkesley Borehole	18.4
EV1	Barite	Coarse barite, Engine Vein fault, Alderley Edge	16.4
AE8	Barite	Barite in fault, Wood Mine, Alderley Edge	16.6
WM13	Barite	Barite in fault, Wood Mine, Alderley Edge	13.8
AE13	Barite	Barite cement, Wood Mine, Alderley Edge	15.4
WM14	Barite	Barite cement, Wood Mine, Alderley Edge	15.6
AE1	Barite	Barite cement, Middle Fault, Wood Mine, Alderley Edge	15.0
AE9	Barite	Barite cement, N Boundary Fault, Wood Mine, Alderley Edge	16.5
AE21	Barite	Barite cement, Engine Vein Conglomerate, Alderley Edge	17.6
80880AE	Barite	Barite cement, Engine Vein Conglomerate, Alderley Edge	17.3
AE19	Barite	Barite vein in West Mine Sandstone, Alderley Edge	16.2
BEES.1	Barite	Cement in Helsby Sandstone Formation, Beeston Castle	19.3
BEES.2	Barite	Cement in Helsby Sandstone Formation, Beeston Castle	19.2
RAW2	Barite	Cement in Lower Helsby Sandstone Formation, Rawhead	16.6
RAW3	Barite	Cement in Lower Helsby Sandstone Formation, Rawhead	17.6
RAW4	Barite	Cement in Lower Helsby Sandstone Formation, Rawhead	17.9
RAW5	Barite	Cement in Lower Helsby Sandstone Formation, Rawhead	17.6
HAWK1	Barite	Cement in Grinshill Sandstone Formation, Hawkstone Park	17.8
HAWK2	Barite	Cement in Grinshill Sandstone Formation, Hawkstone Park	17.7
GB2	Barite	Barite cement, Wilmslow Sandstone Formation, Bickerton	17.9
R622	Barite	Barite cement, Wilmslow Sandstone Formation, Bickerton	19.1
R622	Bn-Tennantite	Ore impregnation, Wilmslow Sandstone Formation, Bickerton	-1.8
EV3	Galena	Ore impregnation, Engine Vein Conglomerate, Alderley Edge	4.1
EV4	Galena	Ore impregnation, Engine Vein Conglomerate, Alderley Edge	11.5
EV5	Galena	Ore impregnation, Engine Vein Conglomerate, Alderley Edge	5.1
EV6	Galena	Ore impregnation, Engine Vein Conglomerate, Alderley Edge	5.7
AE7	Galena	Ore impregnation, Engine Vein Conglomerate, Alderley Edge	8.0
AE18	Galena	Cement in West Mine Sandstone, Alderley Edge	7.9
AE22	Galena	Massive ore, Engine Vein Fault, Alderley Edge	14.1
AE23	Galena	Massive ore, Engine Vein Fault, Alderley Edge	15.7
80880AE	Galena	Ore impregnation, Engine Vein Conglomerate, Alderley Edge	1.3
SC8	Chalcopyrite	Cement nr. Middle Fault, Wood Mine, Alderley Edge	16.1
SC9	Chalcopyrite	Cement nr. Middle Fault, Wood Mine, Alderley Edge	16.2
P11	Chalcopyrite	Cement nr. S. Boundary Fault, Wood Mine, Alderley Edge	10.7
P12	Chalcopyrite	Cement nr. S. Boundary Fault, Wood Mine, Alderley Edge	11.4

* All sulphur isotope results are expressed as per mil deviation of the $^{34}\text{S}/^{32}\text{S}$ ratio relative to the troilite phase of the Canon Diablo standard.

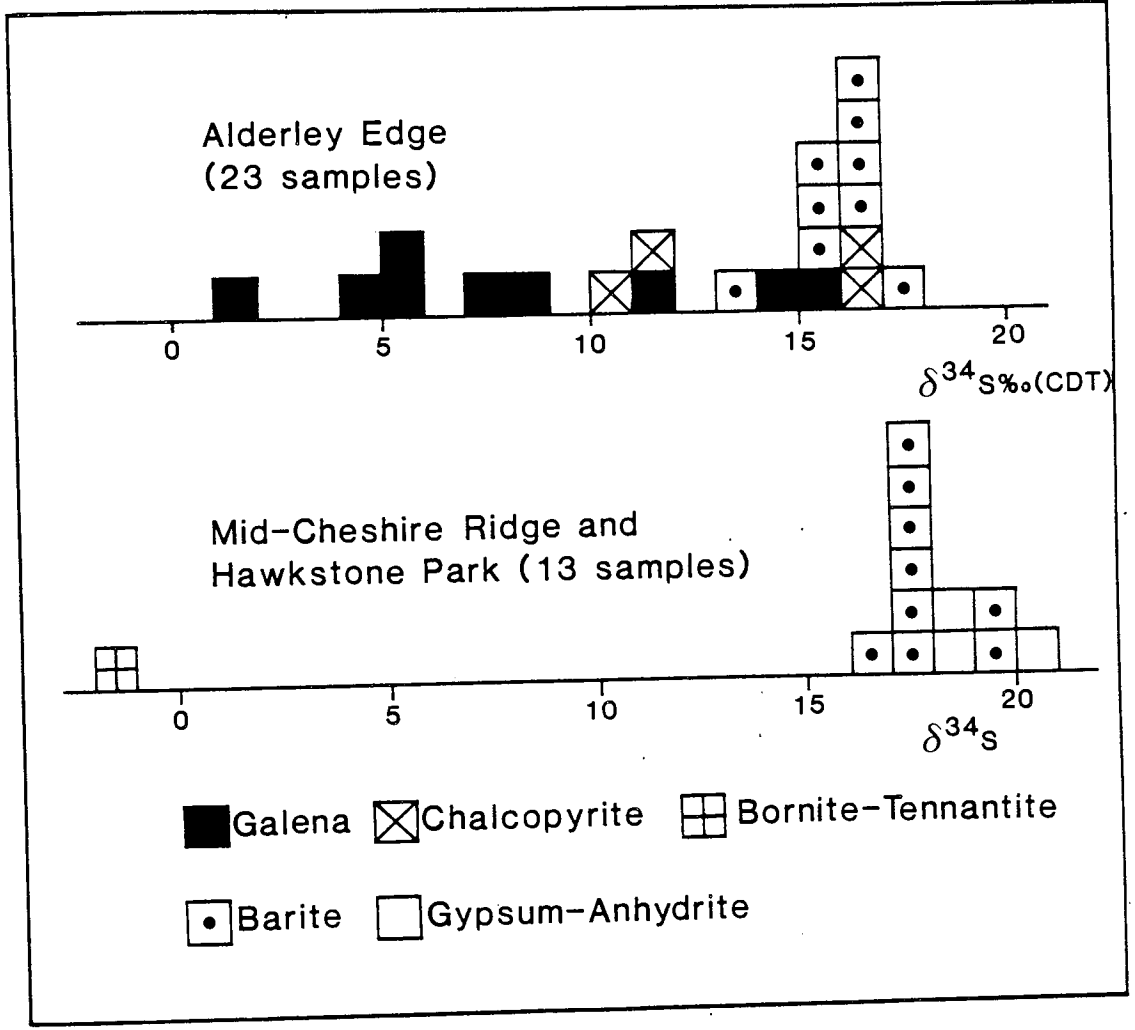


Figure 2.8. Histogram of sulphur isotopic data from the Cheshire Basin.

2.7 DISCUSSION

The origin of the mineralisation in the Cheshire Basin, and at Alderley Edge in particular has received extensive discussion in the literature. Early workers including Hull in the 1860's, and Dewey & Eastwood (1925) favoured the theory that detrital lead and copper sulphides were deposited contemporaneously with the Helsby Sandstone Formation. Dewey and Eastwood (1925) suggested that detrital sulphide grains from an easterly or southerly source were incorporated within the sediments during deposition and were subsequently altered to carbonates and oxides by the action of meteoric water. Subsequently, authors such as Taylor et al. (1963) and Warrington (1965) suggested that the minerals were deposited from fluids introduced long after the deposition of the sandstone. Warrington (1965) summarises the evidence for such epigenetic models where metals were introduced by late, hydrothermal fluids moving up the faults, and proposed that the fluids may have originated from a concealed, acid igneous mass at depth during the Jurassic. A model proposed by King (1968) stressed the importance of precipitation from downward percolating metal-bearing groundwater. A diagenetic origin for the mineralising fluids was discussed by Holmes et al. (1983) who proposed that the diagenesis of the red beds within the basin was responsible for the release of trace metals from detrital minerals into solution. The mineralising fluids were thought to be oxidising basinal brines of moderate salinity.

2.7.1 STRUCTURAL CONTROL AND CONSTRAINTS ON TIMING OF THE MINERALISATION

The spatial distribution of the mineralisation on both a local and a basin-wide scale is controlled by the main tectonic features in the basin. Both the sulphide and sulphate mineralisation are associated with faulted blocks on or around the basin margins. Impersistent mudstone horizons within the Helsby Sandstone Formation appear to have acted as local seals to the fluids responsible for the mineralisation whereas the Tarporley Siltstone Formation provides an important regional seal. Lead and zinc sulphides at Alderley Edge are concentrated in and adjacent to faults, whereas copper minerals are more widespread, possibly due to the remobilisation of primary sulphides. Fault control of the barite mineralisation is seen throughout the basin, particularly at Hawkstone Park where the

veins of barite are parallel to local faults (Carlson 1975). The distribution of the ore deposits around the faulted basin margin suggests that the faults were important channels for ore fluids moving up from within the basin. Movement on these faults was greatest during rapid subsidence in the Triassic and again in the Tertiary when inversion occurred.

The concentration of the mineralisation beneath impermeable horizons at several locations within the basin has been noted by several authors (Carlson 1975, Thompson 1983). Prior to erosion, the Tarporley Siltstone Formation provided a regional seal to the mineralising fluids indicating that the predominant direction of ore-forming fluids was up the basin margin fault systems. In the light of the sulphur isotope data the evaporites of the Mercia Mudstone Group (Upper Triassic) are thought to have been a major source for the barite mineralisation. Due to basin inversion during the Tertiary, the evaporite-bearing Mercia Mudstone Group lies topographically lower than the mineralised horizons in the Sherwood Sandstone Group in the basin margin fault blocks. This is thought to have enabled SO_4^{2-} -bearing fluids passing through, or derived from the Upper Triassic evaporites to ascend the fault systems into structural and lithological traps. This observation is consistent with the general absence of brecciation of the metalliferous ores within the fault zones which suggests that the mineralisation postdates most of the faulting and is therefore Tertiary or younger in age.

The timing of sulphide mineralisation has proved difficult to constrain; limited lead isotope data on galena from Alderley Edge indicate an Upper Triassic age (210 m.y. \pm 60 m.y) for the mineralisation (Moorbath 1962). However, it has become increasingly apparent that model ages based on a single growth curve for lead evolution may be grossly in error (Gustafson & Williams 1981). Thus the model age quoted above must be viewed with caution.

There is no definitive evidence for the timing of mineralisation, but it seems likely from the relationship between faults and mineralisation that, during and after the Tertiary inversion, warm basinal brines were expelled from the sediments within the basin and ascended along faults to be trapped in the porous sandstones beneath the Tarporley Siltstone Formation.

2.7.2 SOURCES OF METALS AND SULPHUR

Possible sources of metals for the Cheshire Basin deposits that have been proposed include detrital sulphides (Dewey & Eastwood 1925), or hydrothermal fluids of magmatic origin (Warrington 1965). A groundwater model was proposed by King (1968) and a diagenetic source discussed by Holmes et al. (1983) who suggested that trace metals were released from detrital minerals during diagenesis of the Permo-Triassic sediments within the basin. Thompson (1983) suggests that metals may also have originated in the black shales of the underlying Coal Measures.

Objections to any theory involving contemporaneous deposition of detrital sulphides with the host sandstones include i) the observation that the ores are closely related to faulting; ii) the absence of a suitable detrital source of metals in areas to the south and east of the Cheshire Basin where the Permo-Triassic sediments were derived and iii) there is no evidence at Alderley Edge of mineralised clasts or detrital sulphides (Ixer & Vaughan 1982); mineralogical data from the present study reveal that detrital sulphides are not present in the Wilmslow Sandstone Formation at Bickerton. Finally, the distal sedimentological setting of the mineralisation would make transportation and continued survival of such material very unlikely.

A source involving hydrothermal fluids of magmatic origin has been invoked by several authors whose evidence is summarised by Warrington (1965). A deeply buried source of such fluids cannot be totally discounted, but appears unlikely in the light of the recent geophysical data (Gale et al. 1984), sulphur isotope and fluid inclusion data from the present study and detailed field observations. Geophysical studies in the basin (Gale et al. 1984) indicate that there is no igneous mass at depth and widespread hydrothermal alteration of the type often associated with the passage of hydrothermal fluids has not been recorded in the Permo-Triassic sediments. Emphasis was placed upon the high Co:Ni ratio in galena as being indicative of a partly magmatic source by Warrington (1965), but this was not confirmed in a more recent study by Ixer & Vaughan (1982). The fault-controlled distribution of the mineralisation is not unequivocal evidence that mineralising fluids had a magmatic source, as the permeable strata and fault zones could also act as passageways to basinal brines and pore fluids derived from deeply buried sediments. Precipitation of ores

from downward percolating groundwater (King 1968) is not supported by the authors' field observations at Alderley Edge, where sulphides are seen to concentrate beneath impermeable mudstone horizons, suggesting that ascending fluids were dominant, during deposition.

A possible sedimentary source of metals is from the dissolution of detrital grains introduced into the basin, notably potassium feldspar and ferromagnesian minerals which, it has been argued, can provide substantial amounts of metals (Holmes et al. 1983). In his study of red-bed diagenesis, Walker (1976) has shown that during burial, ferro-magnesian silicates, feldspars and detrital oxides are often completely dissolved releasing both major and minor elements into solution. Studies of trace metal concentrations in detrital phases have shown that copper contents in pyroxenes may reach 1000 ppm, and potassium feldspar may contain up to 11,000 ppm lead (Wedepohl 1978). Diagenetic studies of the Sherwood Sandstone Group of the Cheshire Basin by Thompson (1983), and Naylor & Turner (in prep) have revealed evidence of substantial alteration and dissolution of potassium feldspar and ferromagnesian minerals similar to that described by Walker (1976). Thus the potential exists to derive metals from detrital minerals during dissolution processes. The black organic-rich shales of the Carboniferous constitute an alternative source of base metals. Black shales are known to be enriched in metals including Pb, Zn, Cu, Ag (Vine & Tourtelot 1970) and have been invoked as the source of metals for the carbonate-hosted 'Mississippi Valley-type' ore deposits by numerous authors since Jackson & Beales (1967).

Possible sulphur sources include the magmatic/hydrothermal source proposed by several authors including Warrington (1965), and the detrital source proposed by earlier authors such as Dewey & Eastwood (1925). The latter hypothesis has been shown to be invalid, from the evidence outlined above, and the sulphur isotope data from the present study do not support a magmatic origin for the sulphur. Ore deposits having a clear magmatic source typically exhibit a narrow range of sulphur isotope values, approximately $0 \pm 4\text{‰}$; Ohmoto & Rye (1979). The sulphur isotope ratios for sulphides from the Cheshire Basin range from -1.8‰ to $+16.2\text{‰}$ and support the geological evidence that the

sulphur was not derived from an ultimately magmatic source (Fig. 2.8).

Potential sedimentary sulphur sources are found in the form of the Carboniferous shales and the evaporites within the Permo-Triassic basin fill. Sulphur isotope data from the present study support the hypothesis that barite was derived directly from solutions passing through, or derived from the gypsum and anhydrite horizons within the Mercia Mudstone Group. Partial dissolution of gypsum and anhydrite with $\delta^{34}\text{S}$ values of +19‰ would produce a fluid with a $\delta^{34}\text{S}$ value of $\sim +17.5\text{‰}$. Thus, a fluid responsible for evaporite dissolution would precipitate barite with a sulphur isotopic value of +17.5‰ because barite incorporates sulphur without significant isotopic fractionation (Kusakabe & Robinson 1977). In addition, preliminary oxygen isotope data were recently obtained by the author from two barite samples from Alderley Edge and Hawkstone Park and gave $\delta^{18}\text{O}$ values (relative to SMOW) of 17.1‰ and 16.5 ‰ respectively. These data also correspond closely to values obtained for $\delta^{18}\text{O}$ of Triassic seawater sulphate (Claypool et al. 1980) and are consistent with the hypothesis that barite was derived from the Triassic evaporites of the Cheshire Basin.)

Almost without exception red-bed copper deposits are hosted by clastic successions that contain evaporites (Gustafson & Williams 1981), this has led to suggestions by several authors that a genetic link exists between evaporites, chloride brines and copper mineralisation (eg. Rose 1976). The sulphur (and oxygen) data presented here emphasise the importance of the evaporites as a source for the barite mineralisation. As further discussed below, the range of $\delta^{34}\text{S}$ values for the sulphides and their distribution relative to the barite values suggests that the evaporites were also the ultimate source of sulphur for the sulphides.

2.7.3 TRANSPORT OF METALS; NATURE OF THE MINERALISING FLUIDS

The geological, mineralogical and stable isotope data outlined above suggest that the metals and sulphur for the Cheshire Basin deposits were derived from a 'sedimentary' source and that, in common with other 'red bed copper deposits' (Gustafson & Williams

1981), the ores were precipitated after deposition of the host rocks by subsurface fluids in equilibrium with the mineral assemblage in the red beds (Rose 1976). Despite the fact that copper solubility is low in oxidising groundwaters of the type that would be in equilibrium with the assemblage in red beds, Rose (1976) has shown that at temperatures as low as 75°C, chloride solutions containing more than 0.01 m Cl (350 ppm) can be effective solvents for copper due to the formation of CuCl_3^{2-} and CuCl complexes. These complexes allow solubilities of 100 ppm in 0.5 m Cl solutions, at intermediate Eh, in the stability field of haematite at neutral pH. In the Cheshire Basin, the evaporites of the Mercia Mudstone Group could have provided the high Cl fluids necessary for the transportation of copper and (possibly of other trace metals).

A modern analogue of the dissolution, transportation and precipitation of trace metals such as Pb, Cu and Zn in a red bed sequence is provided by Lebedev (1972) and Lebedev et al. (1972) in their description of the Cheleken Peninsula (U.S.S.R.) brines. Here, lead, copper and zinc contents of hot (87-98°C) brines derived from red beds were reported, with the lead content of some solutions reaching 77 ppm (mean 2 ppm) and the copper content reaching 15 ppm (mean 2 ppm). Lead was transported as the chloride complexes PbCl_3^- and PbCl_4^{2-} (Lebedev et al. 1971).

Alternatively, the fluids may have originated in the Carboniferous strata where they may have been initially reducing and have evolved into a more oxidised state after migration through a red bed sequence. A recent study by Sverjensky (1987) has indicated that the reaction of a reducing brine with red beds and evaporites can result in its transformation into a more oxidising fluid, capable of transporting Cu, Pb, Zn and sulphate, and of forming sediment-hosted, copper-rich deposits. The presence of evaporites was crucial to the oxidation of basinal fluids and the red beds were shown to be capable of enhancing the oxidised state of the evolved fluids and of probably providing them with copper. Given that the dominant source of dissolved sulphur in these fluids is likely to be leached diagenetic sulphide fixed within Carboniferous sediments, the evolved sulphate would be isotopically lighter than sulphur derived from the Triassic evaporites. Thus, if sulphate derived from oxidation of sulphide were a significant source in the genesis of the Cheshire Basin

deposits, we would expect to observe barite with $\delta^{34}\text{S}$ values considerably lighter than those obtained in the present study. A temperature of 125 °C was used in the calculations by Sverjensky (1987) in order to assess the potential role of warm basinal fluids in the genesis of red-bed hosted copper deposits. Maximum burial depths for Permo-Triassic sediments within the Cheshire Basin were approximately 4.5 km; thus even with a relatively high geothermal gradient ($\sim 35^\circ\text{C}/\text{km}$), fluids circulating near the base of the sedimentary pile may only have reached temperatures of 130-150 °C.

The mineralising fluids are envisaged as being warm, chloride-rich saline solutions in equilibrium with the red bed aquifer units and sulphate facies of the Upper Triassic. Salinity estimates obtained in this study for calcite-hosted inclusions at Bickerton indicate that the late fluids flowing up the fault were saline (17 wt% NaCl equiv.). Chloride brines are envisaged as being responsible for the transport of metals through the red bed sequences. Reduction of a Cu, Pb, Zn, Ba, Cl, SO_4^- bearing fluid at the site of ore deposition, for example, by organic matter would result in the precipitation of sulphides. This reduction process would result in weak acid generation which may have been responsible for the removal of iron oxides from the ore-bearing strata and adjacent sandstone.

2.7.4 MECHANISM OF PRECIPITATION OF THE ORES

The consistency of the sulphur isotope data obtained for the barite and the Triassic evaporites of Cheshire suggest that the mineralising fluids were carrying this evaporite-derived sulphate making it the most likely and dominant source for the barite sulphur. Furthermore, sulphide $\delta^{34}\text{S}$ values range from -1.8 ‰ to 16.2 ‰, the highest value corresponding to the lower values obtained for the barite. Thus, the distribution pattern of $\delta^{34}\text{S}$ values for the sulphides relative to the barite is consistent with a mechanism whereby the sulphide was derived from the sulphate by means of reducing a sulphate-bearing fluid, the initial sulphur isotopic ratio of which was +17‰, in a closed system (Fig. 2.9). Possible sulphate reduction mechanisms include chemical reduction by inorganic material such as Fe^{2+} , bacteriogenic reduction or chemical reduction by organic matter (Ohmoto 1986).

Inorganic reduction of sulphate by iron minerals fixed in the sediment has been shown to be an important mechanism at temperatures above 250-300°C (Mottl 1976). Circulating fluids in the Cheshire Basin are most unlikely to have reached these temperatures as burial of the Permo-Triassic reached a maximum of 4.5 km before the Tertiary. Even allowing for the high geothermal gradients associated with lithospheric extension and thinning, fluids circulating at a depth of 4.5 km may only have reached temperatures of 130-150°C. It is also unlikely that the clean, fluvial and aeolian sands hosting the ores ever contained sufficient quantities of iron minerals to make this type of reduction a significant H₂S source. Thus, both the geological setting and the history of the Cheshire Basin deposits indicate that sulphate reduction by ferrous iron was not significant in the genesis of the sulphide ores.

Bacterial sulphate reduction is thought to be a major mechanism whereby sulphide is produced in a number of sediment-hosted ore deposits (Trudinger et al. 1985). The close association of petroleum and evaporites with caprock sulphur deposits and the presence of sulphate-reducing bacteria in oil-field waters have led several authors including Kyle & Price (1986) to invoke bacteriogenic sulphide as a significant component in associated ores. Bacteriogenic sulphate reduction may have been significant in the genesis of the Cheshire deposits. However, two physiologically limiting factors raise doubts as to the importance of such sulphide in the genesis of the sulphide ores in the Cheshire Basin. Firstly, there is no evidence for a nutrient supply (in the form of organic matter) for the bacteria to metabolise. Trapped methane, such as may have accumulated in the Cheshire Basin (see below), has not yet been proven to be a significant nutrient supply for sulphate reducing bacteria (Postgate 1984). In addition, the proposed mineralisation temperature range of 70-150°C for the Cheshire deposits are considerably higher than those generally accepted for the activities of sulphate-reducing bacteria which typically operate at temperatures lower than 45-50°C (Trudinger et al. 1985). Despite reports of thermophillic species existing up to temperatures of 80°C (Pfennig & Widdell 1982), no sulphate reducing bacteria have been found to metabolise above these temperatures. The observed isotopic differences between the sulphate and sulphide ($\Delta\text{SO}_4\text{-H}_2\text{S} \sim 0$ to 20‰) in the Cheshire Basin are not typical of

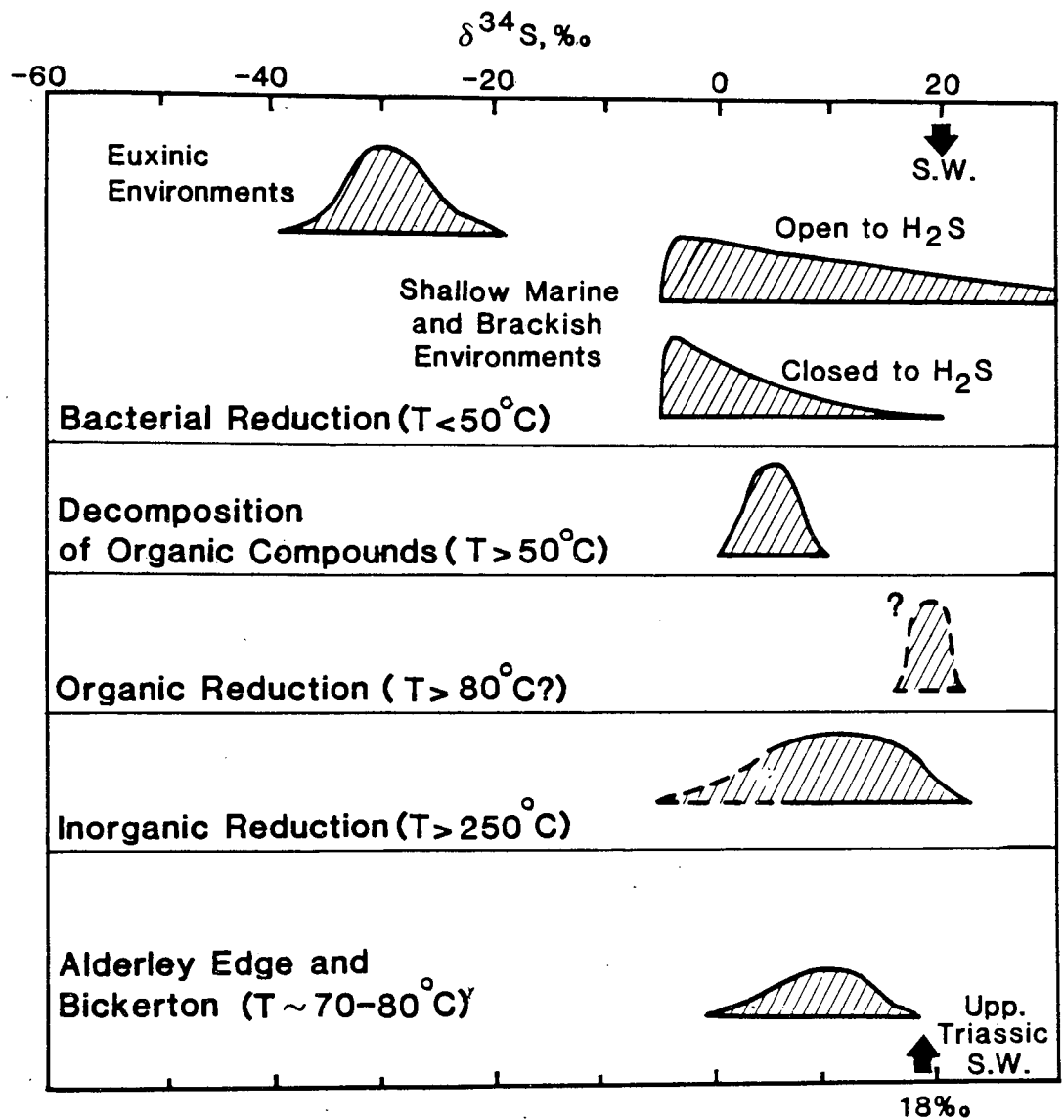


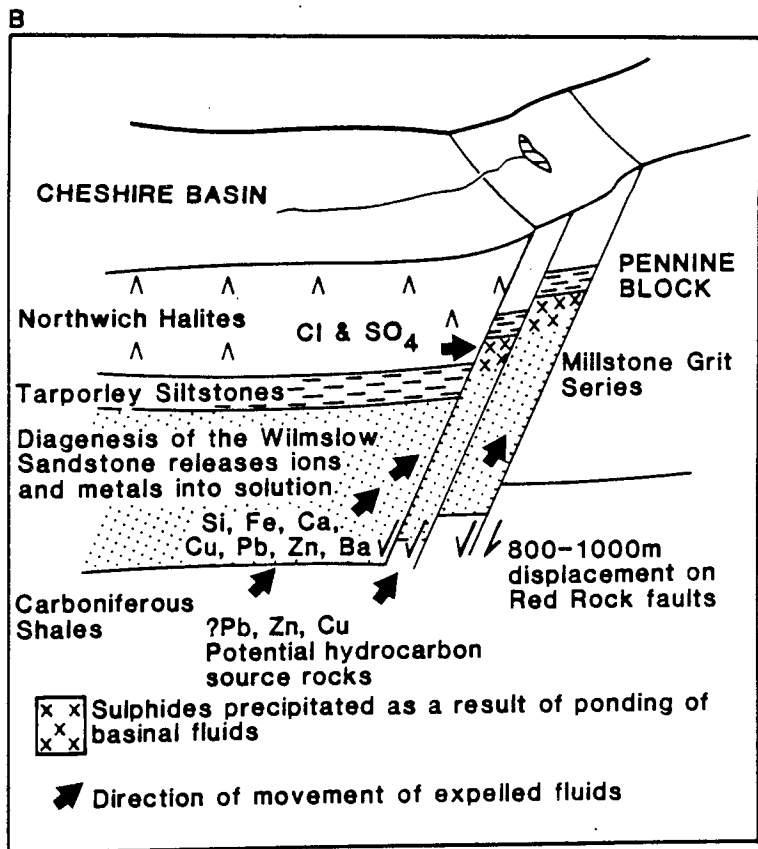
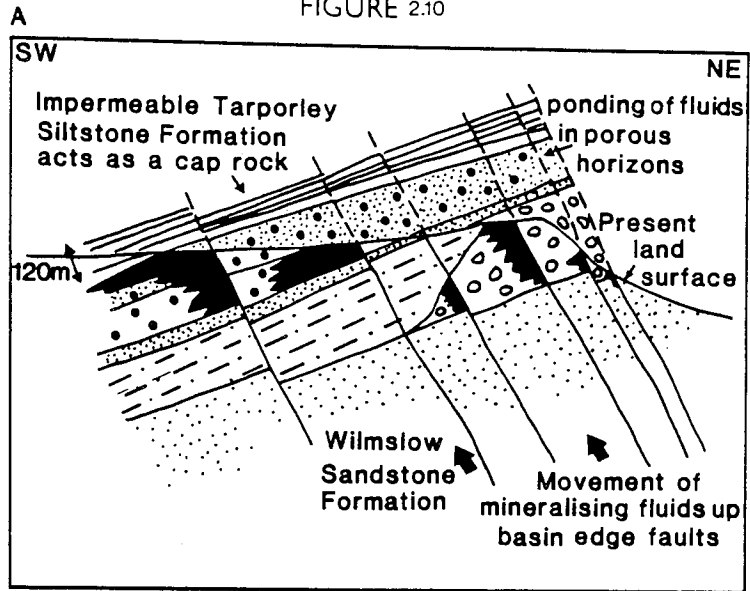
Figure 2.9. The distribution pattern for $\delta^{34}\text{S}$ of H_2S and sulphide when sulphate of initial composition $+20\text{‰}$ is reduced by different mechanisms (after Ohmoto & Rye 1979). The distribution of $\delta^{34}\text{S}$ values obtained from sulphides in the Cheshire Basin is also shown together with the $\delta^{34}\text{S}$ of Upper Triassic seawater sulphate. Mechanisms for producing this spread of values for sulphides in a low temperature red-bed environment are discussed in the text.

Figure 2.10A. A schematic section (not to scale) across Alderley Edge

illustrates the mineralisation prior to exploitation and mining of the deposit (shaded black). Reconstruction of the geological setting of the sandstones below the Tarporley Siltstone Formation emphasises its importance as a seal to the mineralising fluids ascending the faults. The extent of the mineralisation before erosion remains unknown but the present day ore minerals are concentrated down-dip from the faults in the porous sandstone units. Bleaching of the mineralised horizons is a common phenomena as at Bickerton.

B. Summary diagram to show the possible origins of the mineralisation around the margins of the Cheshire Basin. Potential sources of metals and sulphur exist in the underlying Carboniferous and in the basin itself where diagenesis of the Lower Triassic and Upper Permian sandstones may have resulted in the release of trace metals into solution. The traps around the basin margins are topographically higher than the rich Cl^- and SO_4^{2-} source in the form of the evaporites due to basin inversion during the Tertiary.

FIGURE 2.10



bacteriogenic sulphate reduction where Δ has a mean value of 40 ± 20 ‰ reflecting the kinetic isotope effect associated with bacterial sulphate reduction (Ohmoto 1986). Also, the sulphur isotope distribution of closed system bacterial sulphate reduction would typically be asymmetrical with a tight grouping at light values tailing off towards heavier values (see Fig. 2.9). There is an obvious discrepancy between such a pattern and that observed for $\delta^{34}\text{S}$ sulphides-sulphates in the Cheshire Basin. In view of this and the conclusions reached concerning the physiological limitations of the sulphate reducing bacteria, it is suggested that although bacterial sulphate reduction cannot be ruled out, it appears not to have been a significant mechanism of sulphide precipitation in the Cheshire Basin.

The host rocks for the sulphide ores of the Cheshire Basin are fluvial and aeolian sands deposited in a continental setting in which there is no evidence of there having been a significant concentration of organic debris. Thermochemical reduction of sulphate by hydrocarbons has been suggested to be significant for hydrogen sulphide formation and the precipitation of metals in the 'Mississippi Valley-type' ore deposits at Pine Point (Powell & Macqueen 1984) and may have been important in the genesis of the Cheshire Basin deposits. Potential hydrocarbon source rocks of Lower and Upper Carboniferous age are found beneath the Cheshire Basin, but due to the removal of the Mercia Mudstone Group which may have acted as a regional seal (Fig. 2.10), the only traces of hydrocarbons are found on the western margin of the basin at Ashton and Ellesmere Port (Thompson 1983). In the Irish Sea Basin the Triassic sandstones are the reservoir rocks, the Mercia Mudstone Group the cap rock and the Upper Carboniferous Coal Measures the source of methane in the Morecambe Bay Gas Field (Ebborn 1981). In a similar geological setting in the Cheshire Basin, prior to Tertiary inversion and erosion, methane may have been trapped beneath the Mercia Mudstone Group where it could have acted as a reducing agent for the sulphate-bearing fluids. There is no unequivocal experimental evidence of net sulphide production from sulphate reduction by hydrocarbons at temperatures below 200°C (Trudinger et al. 1985). However, studies of the Pine Point ore deposit by Powell & Macqueen (1984) suggest that in the natural environment, this mechanism may be important in the formation of sulphides at temperatures of 75-100°C. Furthermore, Orr

(1977) from his studies on the genesis of H₂S in natural gases, considers thermochemical sulphate reduction unlikely below 80°C, but most likely in the temperature range 120-160°C. Following complete reduction by hydrocarbons, $\delta^{34}\text{S H}_2\text{S}$ is essentially similar to the $\delta^{34}\text{S SO}_4$ of the original sulphate-bearing fluid, while the $\delta^{34}\text{SO}_4$ of the residual fluid increases dramatically (tens of per mille) as complete reduction is approached (Orr 1974; Ohmoto & Rye 1979). On completion of the reduction of the evaporite sulphate, and following the precipitation of sulphides in the Cheshire Basin, erosion may have removed the regional seal in the form of the Mercia Mudstone Group causing any methane present to escape and the remaining sulphides to undergo the supergene alteration now seen.

The narrow range of $\delta^{34}\text{S}_{\text{barite}}$ and the production of sulphide during closed system reduction suggests that barite precipitation was not contemporaneous with sulphide deposition. If this were the case, $\delta^{34}\text{S}$ values for barite are likely to have been particularly high as the system approached complete reduction, a situation suggested by the sulphide $\delta^{34}\text{S}$ values similar to the $\delta^{34}\text{S}_{\text{barite}}$.

This indicates that although the Triassic evaporites are envisaged as the major sulphur source for both sulphides and sulphates; they were deposited at distinct times during the mineralising event. This is wholly supported by the field evidence where barite precipitation is seen to predate and postdate sulphide deposition. In the light of this, it is suggested that SO₄⁻-bearing fluids were abundant at the sites of ore deposition and that in contrast to barite which can precipitate as the result of simple cooling (Holland & Malinin 1979), sulphide deposition was dependent on the availability of a suitable reductant. The discrepancy in $\delta^{34}\text{S}_{\text{galena}}$ values at Alderley Edge can be explained by closed system reduction of sulphate where the galena cements in the sandstone precipitated first as depletion of sulphate continued. The isotopically heavier $\delta^{34}\text{S}$ values for the massive galena in the Engine Vein fault may represent sulphide deposition during the later stages of sulphate reduction. Finally, the isotopically lighter $\delta^{34}\text{S}_{\text{barite}}$ at Alderley Edge (Fig. 2.8) hints at the involvement of a minor, lighter sulphate component which may have been

FIGURE 2.11

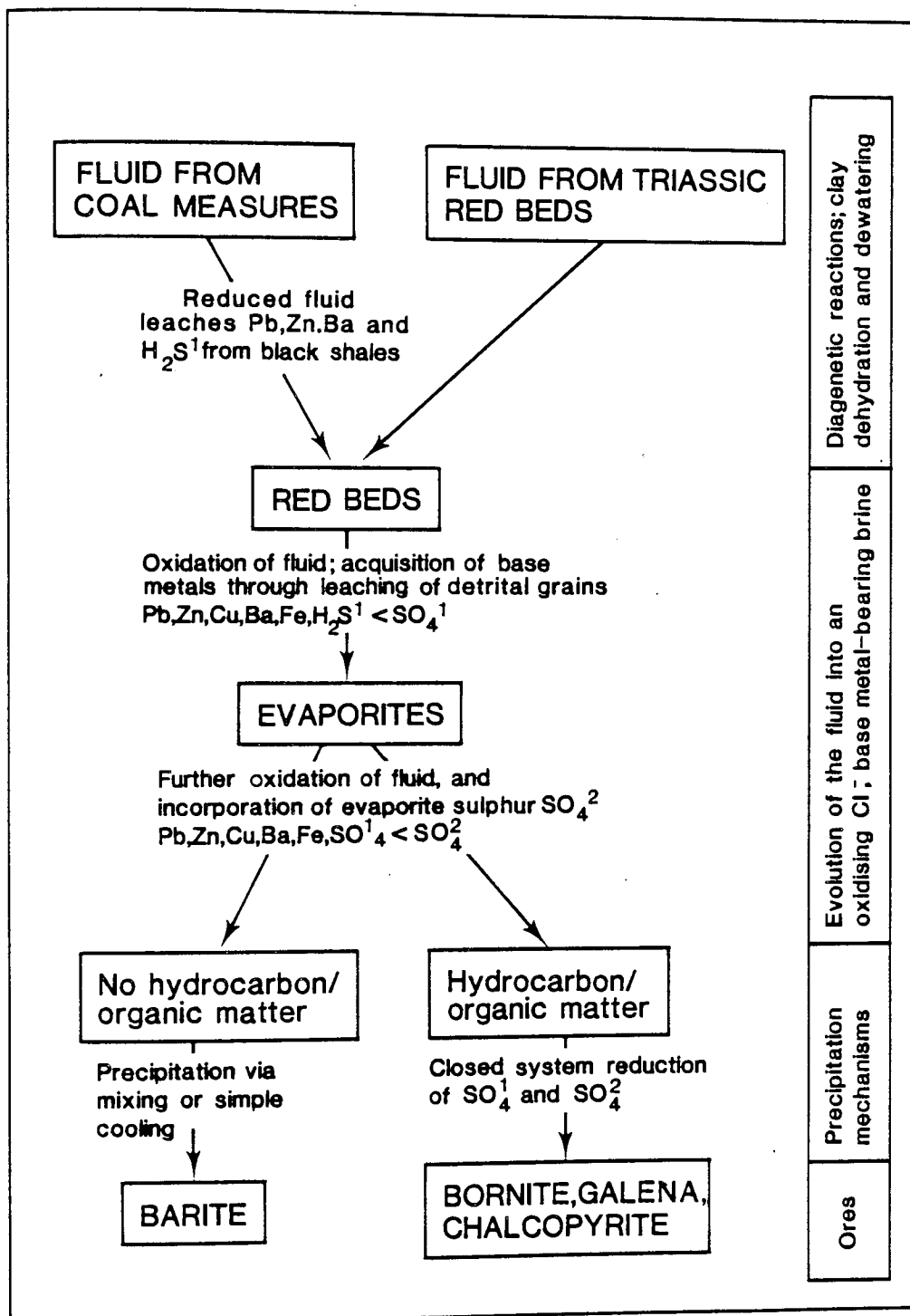


Figure 2.11. Flow diagram showing the possible fluid migration pathways in the Cheshire Basin.

derived through oxidation of reduced sulphide in the underlying Carboniferous strata.

The sulphur isotope data and the geological setting of the Cheshire Basin mineralisation favour two possible closed system sulphate reduction mechanisms where sulphate was derived from the Triassic evaporites. The first involves thermochemical sulphate reduction of a chloride and sulphate-bearing aqueous fluid carrying metals via oxidation of trapped hydrocarbons beneath the impermeable Tarporley Siltstone Formation. Alternatively, bacteriogenic sulphate reduction may have been significant despite the limiting factors of relatively high temperatures for sulphide deposition and the lack of evidence for organic matter at the site of ore deposition. In view of the uncertainty surrounding the temperature of sulphide deposition, neither mechanism can be proven. However, the pattern of $\delta^{34}\text{S}$ sulphide from the Cheshire Basin does not favour the bacterial reduction model.

2.8 CONCLUDING REMARKS

The genesis of the ore deposits within the Cheshire Basin appears to be intimately related to the structural evolution of the basin and the diagenetic reactions within the Permo-Triassic basin fill. The data presented in this study support the hypothesis that the mineralisation is a result of deposition from ore-bearing fluids within structural and lithological traps around the basin margins.

Hydrothermal fluids of magmatic origin can be essentially discounted in the light of the fluid inclusion and stable isotope data from the present study, where a 'sedimentary' source for the metals and sulphur is proposed. The rapid subsidence of the basin during the Triassic led to the deposition of a thick, red-bed evaporite sequence which is thought to be an important potential source of metals, chloride and sulphate for the mineralising fluids (Rose 1976; Sverjensky 1987). An additional sedimentary source exists in the form of fluids derived from the Carboniferous strata beneath the basin (Fig. 2.10). The sulphur isotope data (and the limited sulphate-oxygen data) from the barite mineralisation of the Cheshire Basin are consistent with the hypothesis that the barite sulphur was derived directly from the evaporites within the Mercia Mudstone Group. The $\delta^{34}\text{S}$ values for the sulphides have a range of approximately 18‰, with the heaviest value being

indistinguishable from that of the barite. Thus, it is suggested that the sulphide ores were also derived ultimately from the Triassic evaporites as a result of closed system reduction of sulphate-bearing fluids (Fig. 2.11).

The limited fluid inclusion data from calcite gangue suggest minimum temperatures for ore deposition in the range 65-80°C. Mineralising fluids are thought to have been saline (17 wt% NaCl equivalent), oxidising brines with a near-neutral pH. Taking into account the maximum burial depths of the Permo-Triassic sequence, it seems reasonable to suggest that fluids derived from the Permo-Triassic sediments or originating in the Carboniferous strata may have reached temperatures of 150°C or higher. The exact temperature of the mineralisation remains poorly constrained as a result of the fine-grained nature of the gangue phases in the Cheshire Basin. Metals such as Cu, Pb and Zn are envisaged as having been transported as chloride complexes; Rose (1976) described similar ore-forming fluids associated with other 'red-bed copper deposits'. A recent study by Sverjensky (1987) illustrates that even if the brine were initially reducing, interaction with a thick red bed-evaporite sequence would result in the evolution of the fluid into a more oxidising state capable of transporting Cu, Pb, Zn and sulphate. An indication of the importance of this Carboniferous source may be the contribution of isotopically light sulphate to the barite at Alderley Edge, northeast Cheshire.

Precipitation of the ores is suggested to have occurred as a result of closed system sulphate reduction by bacteriogenic processes or via thermochemical reduction by hydrocarbons. Trapped hydrocarbons may have been responsible for sulphate reduction since the similarity in geological setting between the Cheshire Basin and the Morecambe Bay Gas Field in the Irish Sea Basin indicates that methane may have been available prior to Tertiary erosion of the Mercia Mudstone Group of Cheshire. This process is thought to be more consistent with the pattern of $\delta^{34}\text{S}_{\text{sulphide}}$ values.

REFERENCES

- ARTHURTON, T.D. 1980. Rhythmic sedimentary sequences in the Triassic Keuper Marl (Mercia Mudstone Group) of Cheshire, northwest England. *Geological Journal*, **15**, 43- 58.
- AUDLEY-CHARLES, M.G. 1970. Triassic palaeogeography of the British Isles. *Quarterly Journal of the Geological Society of London*, **126**, 49-89.
- CARLON, C.J. 1975. *The Geology and Geochemistry of some British barite deposits*. Phd. Thesis, University of Manchester.
- CARLON, C.J. 1979. *The Alderley Edge Mines*. J. Sherratt & Son, Altrincham.
- CARLON, C.J. 1981. The Gallantry Bank Copper Mine. *British Mining* no. 16.
- CHADWICK, R.A. 1985. Permian, Mesozoic and Cenozoic structural evolution of England and Wales in relation to the principles of extension and inversion tectonics. In: A. WHITTAKER (ed.) *Atlas of Onshore Sedimentary Basins in England and Wales : Post-Carboniferous Tectonics and Stratigraphy*. Blackie. London.
- CLAYPOOL, G.E., HOLSER, W.T., KAPLAN, I.R., SAKAI, H., & ZAK, I. 1980. The age curves of sulphur and oxygen isotopes and their mutual interpretation. *Chemical Geology*, **28**, 199-260.
- COLTER, V.S. 1978. Exploration for gas in the Irish Sea Basin. *Geologisches en Mijnbouw*, **57**, 503-516.
- CRAIG, J.R. & VAUGHAN, D.J. 1981. *Ore Microscopy and Ore Petrography*. J. Wiley & Sons. Inc. N.York.
- DEWEY, H. & EASTWOOD, T. 1925. Copper ores of the Midlands, Wales, the Lake District and the Isle of Man. *Memoirs of the Geological Survey, Special Report on the Mineral Resources of Great Britain*, **30.**, H.M.S.O.
- EBBERN, J. 1981. The geology of the Morecambe Bay Gas Field. In: ILLING, L.V & HOBSON, G.D (eds) *Petroleum Geology of the Continental Shelf of*

North-West Europe.

- FITCH, F. J., MILLER, J.A., EVANS, A.L., GRASTY, R.L. & MENEISY, M.Y. 1969. Isotopic age determinations on rocks from Wales and the Welsh Borders. In: WOOD, A. (ed.) *Pre-Cambrian and Lower Palaeozoic rocks of Wales*, University of Wales Press.
- GALE, I.N., EVANS, C.J., SMITH, I.F. HOUGHTON, M.T. & BURGESS, W.G. 1984. Investigation of the geothermal potential of the U.K. The Permo-Triassic aquifers of Cheshire and West Lancashire basins. *BGS Geothermal Resources Programme, London*, HMSO for NERC.
- GUSTAFSON, L. B. & WILLIAMS, N. 1981. Sediment-hosted stratiform deposits of copper, lead and zinc. *Economic Geology, 75th Anniversary Volume*, 139-178.
- HOLLAND, H. D. & MALININ, S. D. 1979. The solubility and occurrence of non-ore minerals. In: BARNES, H.L. (ed.) *Geochemistry of Hydrothermal Ore Deposits*, 2nd edition. Wiley & Sons, New York.
- HOLMES, I., CHAMBERS, A.D., IXER, R.A., TURNER, P. & VAUGHAN, D.J. 1983. Diagenetic processes and the mineralization in the Triassic of Central England. *Mineralium Deposita*, **18**, 365-377.
- HULL, E. 1869. Triassic and Permian rocks of the Midland counties of England. *Memoirs of the Geological Survey of Great Britain, London*.
- IRELAND, R.J., POLLARD, J.E., STEEL, R.J. & THOMPSON, D.B. 1978. Intertidal sediments and trace fossils from the Waterstones (Scythian-Anisian?) at Daresbury, Cheshire. *Proceedings of the Yorkshire Geological Society*, **41**, 399-436.
- IXER, R.A. & VAUGHAN, D.J. 1982. The primary ore mineralogy of the Alderley Edge deposit, Cheshire. *Mineralogical Magazine*, **46**, 485-492.
- JACKSON, S.A. & BEALES, F.W. 1967. An aspect of sedimentary basin evolution: the concentration of Mississippi Valley-type ores during late stages of diagenesis. *Bulletin of Canadian Petroleum Geology*,

15, 383-433.

- KAISER, C.J., KELLY, W.C., WAGNER, R.J. & SHANKS, W.C. 1987. Geologic and geochemical controls on mineralisation in the southeast Missouri barite district. *Economic Geology*, **82**, 719-734.
- KING, R.J. 1968. Mineralization. In: SYLVESTER-BRADLEY, P.C. & FORD, D.T. (eds) *The Geology of the East Midlands*. Leicester University Press.
- KUSAKABE, M. & ROBINSON, B.W. 1977. Oxygen and sulphur isotope equilibria in the BaSO₄-HSO₄- H₂O system from 110°C to 350°C and applications. *Geochimica et Cosmochimica Acta*, **41**, 1033-1041.
- KYLE, J.R. & PRICE, P.E. 1986. Metallic sulphide mineralisation in salt dome cap rocks, Gulf Coast, U.S.A. *Transactions of the Institution of Mining and Metallurgy*, **958**, 6-16.
- LEACH, D. L. 1980. Nature of mineralizing fluids in the barite deposits of central and southeast Missouri. *Economic Geology*, **75**, 1168-1180.
- LEBEDEV, L.M. 1972. Minerals of contemporary hydrotherms of Cheleken. *Geochemistry International*, **9**, 485-504.
- LEBEDEV, L.M., BARANOVA, N.N., NIKITANA, I.B. & VERNADSKIY, V.I. 1971. On the forms of lead and zinc in the Cheleken thermal brines. *Geochemistry International*, **8**, 511-516.
- MOORBATH, S. 1962. Lead isotope abundance studies on mineral occurrences in the British Isles. *Philosophical Transactions of the Royal Society of London*, **A245**, 295-360.
- MOTTL, M. 1976. *Chemical exchange between seawater and basalt during hydrothermal alteration of the oceanic crust*. Ph.D Thesis, Harvard University.
- MURCHISON, R.I. 1839. *The Silurian System, founded on geological researches in the counties of Salop, Hereford, Radnor, Montgomery, Caermarthen, Brecon, Pembroke, Monmouth, Gloucester, Worcester, and Stafford*. London.

- NAYLOR, H. & TURNER, P. (in prep.) Aspects of the diagenesis of the Sherwood Sandstone Group and Mercia Mudstone Group sediments in the Cheshire Basin.
- OHMOTO, H. 1986. Stable Isotope Geochemistry of Ore Deposits. In: VALLEY, J.W., TAYLOR, H.P. & O'NEIL, J.R. (eds.) *Stable Isotopes and High Temperature Geological Processes*. Reviews in Mineralogy 16, Mineralogical Society of America.
- OHMOTO, H. & LASAGA, A.C. 1982. Kinetics of reactions between aqueous sulphates and sulphides in hydrothermal systems. *Geochimica et Cosmochimica Acta*, **46**, 1727-1745.
- OHMOTO, H. & RYE, R.O. 1979. Isotopes of sulphur and carbon. In: BARNES, H.L. (ed.). *Geochemistry of Hydrothermal Ore Deposits*, 2nd edition, Wiley & Sons, New York. N. Y.
- ORR, W.L. 1974. Changes in sulphur content and isotopic ratios of sulphur during petroleum maturation- study of Big Horn Basin paleozoic oils. *Bulletin American Association of Petroleum Geologists*, **58**, 2295-2318.
- ORR, W.L. 1977. Geologic and geochemical controls on the distribution of hydrogen sulphide in natural gas. In: CAMPOS, R. & GONI, J. (eds) *Advances in Organic Geochemistry*, 1975. Enadisma, Madrid.
- PFENNIG, N. & WIDDELL, F. 1982. The bacteria of the sulphur cycle. *Philosophical Transactions of the Royal Society of London*, **298B**, 433-441.
- POOLE, T.G. & WHITEMAN, A.J. 1966. Geology of the country around Nantwich and Whitchurch. *Memoirs of the Geological Survey of Great Britain, London*.
- POSTGATE, J.R. 1984. *The Sulphate Reducing Bacteria*. 2nd. Edition, Cambridge University Press, Cambridge.
- POTTER, R.W., CLYNNIE, M.A. & BROWN, D.L. 1978. Freezing point depression of aqueous sodium chloride solutions. *Economic Geology*, **73**, 284-285.

- POWELL, T.G. & MACQUEEN, R.W. 1984. Precipitation of sulphide ores and organic matter: sulphate reactions at Pine Point, Canada. *Science*, **224**, 63-66.
- PUGH, W. 1960. Triassic salt: discoveries in the Cheshire-Shropshire Basin. *Nature*, **187**, 278-279.
- ROEDDER, E. 1984. *Fluid inclusions*. Reviews in Mineralogy, 12. Mineralogical Society of America.
- ROSE, A.W. 1976. The effect of cuprous chloride complexes in the origin of red bed copper and related deposits. *Economic Geology*, **71**, 1036-1048.
- SHEPHERD, T.J. 1981. Temperature-programmable heating-freezing stage for microthermometric analysis of fluid inclusions. *Economic Geology*, **76**, 1244-1247.
- STANTON, R.L. 1972. *Ore Petrology*. McGraw-Hill, New York.
- STEEL, R.J. & THOMPSON, D.B. 1983. Structures in the Bunter Pebble Beds in the Sherwood Sandstone Group, North Staffordshire, England. *Sedimentology*, **30**, 341-367.
- SVERJENSKY, D.A. 1987. The role of migrating oil field brines in the formation of sediment-hosted copper-rich deposits. *Economic Geology*, **82**, 1130-1141.
- TAYLOR, B.J., PRICE, R.H. & TROTTER, F.M. 1963. Geology of the country around Stockport and Knutsford. *Memoirs of the Geological Survey of Great Britain, London*.
- TAYLOR, S.R. 1983. A stable isotope study of the Mercia Mudstones (Keuper Marl) and associated sulphate horizons in the English Midlands. *Sedimentology*, **30**, 11-31.
- THODE, H.G. & MONSTER, J. 1965. Sulphur isotope geochemistry of petroleum, evaporites and ancient seas. *American Association of Petroleum Geologists Memoir*, **4**, 367-377.
- THOMPSON, D.B. 1969. Dome shaped aeolian dunes in the Frodsham Member

- of the so-called 'Keuper' Sandstone Formation (Scythian-/ Anisian: Triassic) at Frodsham, Cheshire, England. *Sedimentary Geology*, **3**, 264-289.
- THOMPSON, D.B. 1970. Sedimentation in the Triassic (Scythian) red pebbly sandstones in the Cheshire Basin and its margins. *Geological Journal*, **7**, 183-216.
- THOMPSON, D.B. 1983. *Permo-Trias of Cheshire and East Irish Sea Basins*. Poroperm Excursion Guide 4, Poroperm-Geochem Ltd, Chester.
- TRUDINGER, P.A., CHAMBERS, L.A. & SMITH, J.W. 1985. Low temperature sulphate reduction: biological versus abiological. *Canadian Journal of Earth Sciences*, **22**, 1910-1918.
- TUCKER, R.M. & TUCKER, M.E. 1981. Evidence of syn-sedimentary tectonic movements in the Triassic halite of Cheshire. *Nature*, **290**, 495-497.
- VAUGHAN, D.J. 1969. Zonal variation in bravoite. *American Mineralogist*, **54**, 1075-1083.
- VINE, J.D. & TOURTELOT, E.B. 1970. Geochemistry of black shale deposits - a summary report. *Economic Geology*, **65**, 253-272.
- WALKER, T.R. 1976. Diagenetic origin of continental red beds. In: FALKE, H. (ed.) *The continental Permian in Central, West and South Europe*. D. Reidel Publishing Co., Dordrecht, Holland.
- WARRINGTON, G. 1965. The metalliferous mining district of Alderley Edge, Cheshire. *Mercian Geologist*, **4**, 69-72.
- WEDD, C.B., SMITH, B., KING, W.E.R. & WRAY, D.A. 1929. The country around Oswestry. *Memoirs of the Geological Survey of Great Britain, London*.
- WEDEPHOL, K.H. 1978. *Handbook of Geochemistry*. Springer-Verlag, Heidelberg.
- WHITTAKER, A. (ed.) 1985. *Atlas of onshore Sedimentary Basins in England and Wales: Post-Carboniferous Tectonics and Stratigraphy*. Blackie.

CHAPTER 3
ASPECTS OF THE DIAGENESIS OF THE SHERWOOD SANDSTONE
AND MERCIA MUDSTONE GROUPS OF THE CHESHIRE BASIN

ABSTRACT

The Triassic Sherwood Sandstone and Mercia Mudstone Group sediments of the Cheshire Basin comprise a series of continental red beds deposited in fluvial, aeolian and marginal marine settings. Maximum burial depths range from shallow (< 1km) in the Sherwood Sandstone Group around the basin margins to deep (> 3km) in the Tarporley Siltstone Formation, Wilkesley. A distinct suite of early diagenetic events including detrital grain dissolution, replacement of detrital silicates by haematite and clays, and the precipitation of authigenic illite, K-feldspar and quartz can be recognised throughout the basin. These processes are similar to those recorded from modern red beds in the southwestern U.S.A. The occurrence of early diagenetic authigenic albite in the Tarporley Siltstone Formation is attributed to the presence of NaCl brines in the marginal marine sandstones. Depth-related diagenetic processes in the deeply buried Tarporley Siltstone Formation of the Wilkesley borehole include the precipitation of anhydrite, quartz and saddle dolomite and minor secondary porosity generation. Basin inversion during the Tertiary resulted in the exposure of the Sherwood Sandstone Group adjacent to the basin margins to modern meteoric waters which have a neutral pH and are capable of dissolving carbonate and sulphate cements. More acidic present-day groundwaters were responsible for kaolinite precipitation in the mineralised sandstones at Alderley Edge. Textural observations support the contention that diagenetic processes in the Cheshire Basin played an important role in the release of base metals from the red beds and may have contributed significantly to the genesis of the mineralisation at the basin margins.

3.1 INTRODUCTION

The Cheshire Basin is located in north-west England (Fig. 3.1) and comprises a fault-bounded basin with the thickest onshore Permo-Triassic section in Britain. The

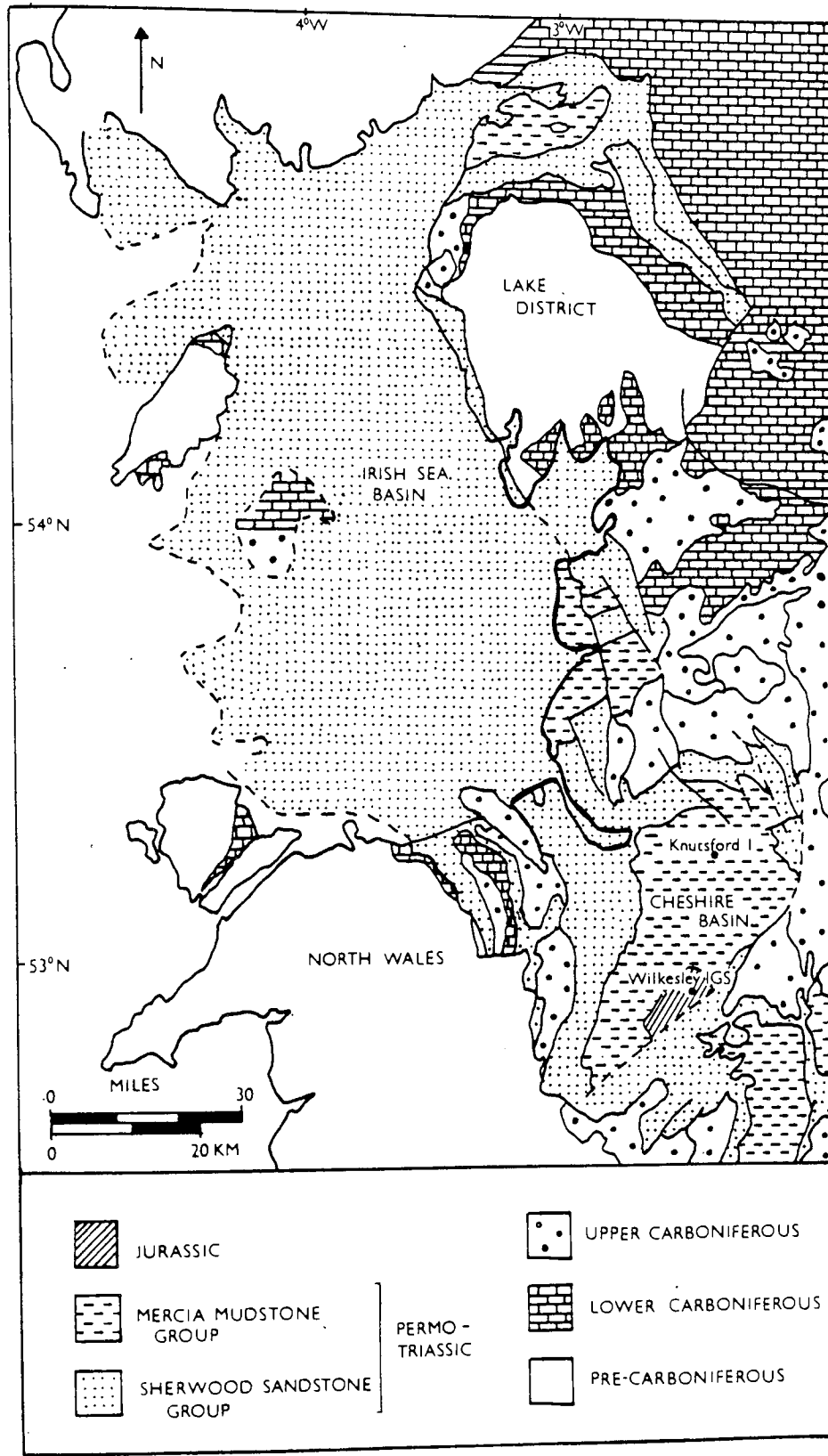


Figure 3.1. Simplified geological map showing the location of the Cheshire Basin relative to the Irish Sea Basin. The sites of the Knutsford and Wilkesley boreholes are also shown.

largely clastic basin fill accumulated rapidly during Permo-Triassic times as a result of movement on syn-sedimentary faults and has a maximum thickness of 4.5 km. The three main lithostratigraphic units of the Triassic in the Cheshire Basin are the Sherwood Sandstone Group, Mercia Mudstone Group and Penarth Group (Warrington et al. 1980). The sediments were deposited in a variety of depositional environments including fluvial, aeolian and shallow marine settings. Basin inversion during the Tertiary caused widespread uplift and erosion of the Mesozoic cover. Extensive Pleistocene drift now covers the Permo-Triassic sediments of Cheshire and only 3% are exposed in the horst blocks around the basin margin.

Petrographic and diagenetic studies of the Sherwood Sandstone Group and Mercia Mudstone Group of Cheshire are scarce in the literature. References to the diagenesis of the Triassic sediments of the Cheshire Basin are made by authors involved in nationwide studies of the British Permo-Triassic (Waugh 1978, Burley 1984). Holmes et al. (1983) noted the authigenic suite of minerals in the Tarporley Siltstone Formation of the Wilkesley borehole, whilst Jeans (1978) described their clay mineralogy from X-ray diffraction analyses. Macchi & Veltkamp (1985) described compound quartz and feldspar overgrowths in the Helsby Sandstone Formation of northern Cheshire and suggested that the early diagenetic trends in the sandstones are consistent with observations made by Walker et al. (1978) in a well-known study of early diagenesis in desert alluvium.

The purpose of this chapter is first to define the depositional and pre-depositional features which have controlled diagenesis in the Sherwood Sandstone and Mercia Mudstone Groups of Cheshire. The aim is to assess the extent to which the depositional environments of the sediments have controlled their early diagenetic history. The Mercia Mudstone Group sediments of the Wilkesley borehole provide the opportunity to identify diagenetic events associated with deep burial, whilst evidence for the diagenetic processes associated with uplift and interaction with present-day groundwaters is provided by the Sherwood Sandstone Group sediments around the basin margins. This investigation of the deep burial diagenetic processes in the Mercia Mudstone Group of Cheshire, is linked to the geochemical and mineralogical studies of Holmes et al. (1983) who proposed that continued dissolution of detrital grains during diagenesis provided metals for the

mineralisation in the Sherwood Sandstone Group adjacent to the basin margins (see Chapter 2).

3.2 METHODOLOGY

The majority of samples studied in this investigation were obtained from the exposures of Sherwood Sandstone Group sandstones in the faulted blocks around the basin margin. The principal sampling sites include Alderley Edge and the Mid-Cheshire Ridge where the Sherwood Sandstone Group is host to sulphide and barite mineralisation. Non-mineralised Sherwood Sandstone Group sediments at Thurstaston, Wirral were also studied (Fig. 3.2). Samples were also collected from the mines at Alderley Edge and from shallow commercial boreholes near Bickerton on the Mid-Cheshire Ridge. Additional samples were obtained from the core of the Wilkesley borehole stored by the Institute of Geological Sciences. The Wilkesley borehole penetrated the entire succession of Mercia Mudstone Group sediments whose lithological characteristics were described by Poole & Whiteman (1966). The sediments described herein belong to the Mercia Mudstone Group and the Tarporley Siltstone Formation in particular, (Fig. 3.3) and currently have burial depths ranging between 1685 and 709m.

In total, 90 samples were impregnated with blue araldite and those containing carbonate were stained using the combined stain of potassium ferricyanide and Alazarin Red-S prior to petrographic examination. 30 thin sections were point counted to quantify the components of the detrital and authigenic assemblages and the porosity. Samples were examined using transmitted light microscopy, cathodoluminescence and scanning electron microscopy with EDAX facilities. Quantitative chemical data were obtained for detrital and authigenic feldspar using a Cameca Camebax microprobe with a 15k.v. accelerating voltage. Standards used and operating conditions are detailed in Appendix. I. The < 2 μ m clay fraction of both the mudstones and sandstones was studied using X-ray diffraction techniques.

3.3 SEDIMENTOLOGY AND STRATIGRAPHY

The stratigraphy of the Cheshire Basin was established following the drilling of three wells; Knutsford No. 1 by British Petroleum-British Gas Group, Prees No. 1 by

FIGURE 3.2

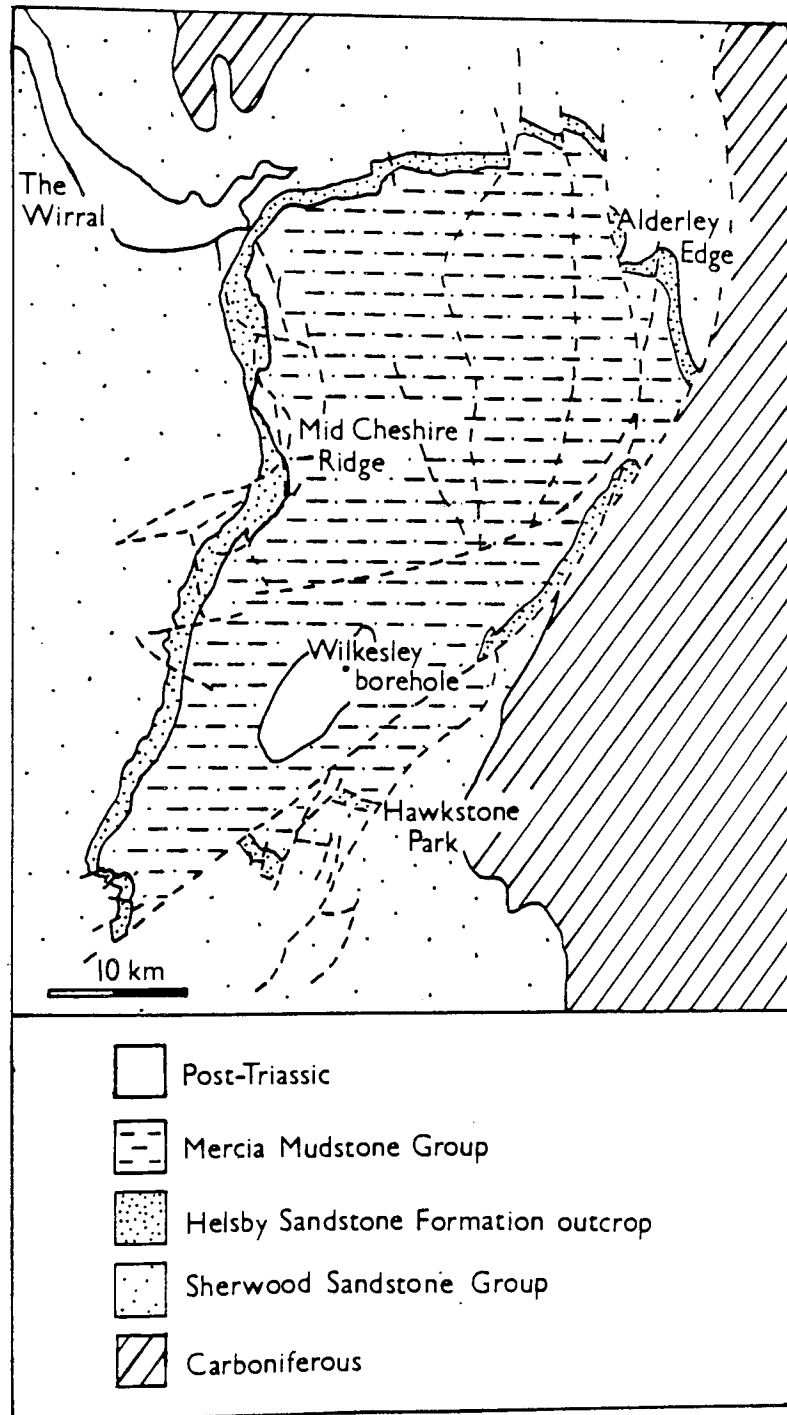


Figure 3.2. Generalised geological map of the Cheshire Basin showing the exposures of the Sherwood Sandstone Group around the basin margins and the position of the Wilkesley borehole in southern Cheshire.

FIGURE 3.3

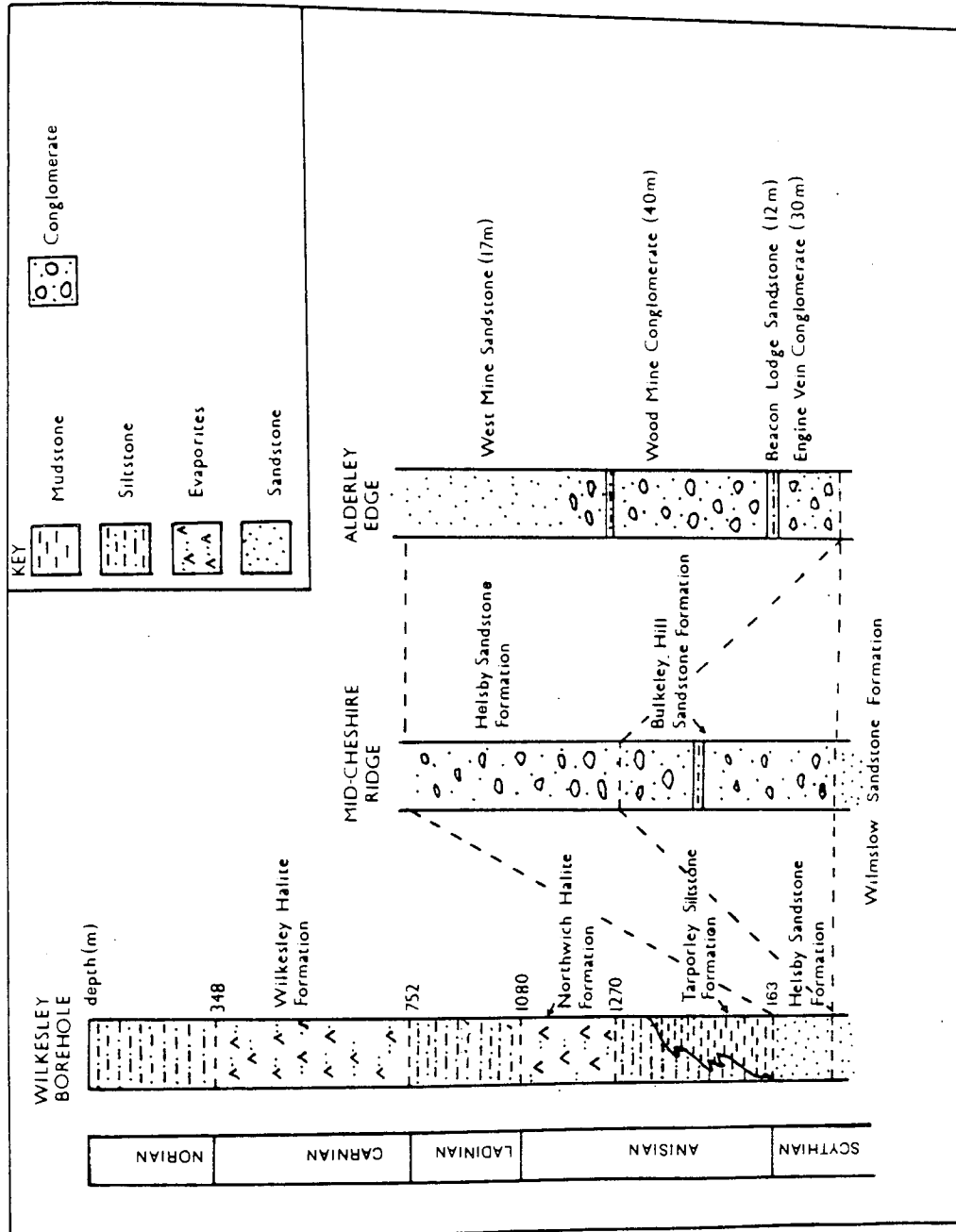


Figure 3.3. Schematic diagram showing the stratigraphical and sedimentological relationships between the Sherwood Sandstone and Mercia Mudstone Groups of the Cheshire Basin. Warrington et al. (1980) assigned the Bulkeley Hill Sandstone Formation as a separate stratigraphic unit that is only present in the exposures near the Mid-Cheshire Ridge.

Trend Exploration Ltd (Colter & Barr 1975) and the Wilkesley borehole by the Geological Survey of Great Britain (Poole & Whiteman 1966). Warrington et al. (1980) reviewed the Triassic stratigraphy of the British Isles and their recommended lithostratigraphical subdivisions of the Sherwood Sandstone, Mercia Mudstone and Penarth Groups are used in the present study.

A detailed description of the sedimentological and tectonic evolution of the Cheshire Basin is given in Chapter 2. In view of this, emphasis is placed on describing the sedimentology and stratigraphy of the Wilmslow and Helsby Sandstone Formations (Sherwood Sandstone Group) and Tarporley Siltstone Formation (Mercia Mudstone Group) from which the samples used in this part of the study were obtained.

The Wilmslow and Helsby Sandstone Formations form the upper part of the Sherwood Sandstone Group in the Cheshire Basin and sedimentological studies by Thompson (1969, 1970) have shown them to be the deposits of braided rivers with minor aeolian input. Thompson (1970) distinguished several lithofacies types within the Wilmslow and Helsby Sandstone Formations ranging from pebbly conglomerates deposited in fluvial channels to shales and mudstones deposited on the bar tops and floodplains. Aeolian sedimentation is less common but aeolian intercalations have been recognised at Frodsham, Alderley Edge and Thurstaston (Thompson 1969, 1970, 1983).

The Tarporley Siltstone Formation lies at the base of the Mercia Mudstone Group and directly overlies the Helsby Sandstone Formation. The samples described in this study from the Wilkesley borehole comprise fine, red coloured cross-bedded sandstones interbedded with anhydrite-bearing mudstones and siltstones. Ireland et al. (1978) interpreted the depositional environment as intertidal following a detailed lithofacies and trace fossil study. According to Ireland et al. (1978), the palaeocurrent directions in the Tarporley Siltstone Formation are not significantly different from those in the underlying Sherwood Sandstone Group, indicating that the sediments continued to be derived from a southerly source area. The remainder of the Mercia Mudstone Group consists of thick halite and mudstone sequences which were interpreted by Arthurton (1980) as the result of periodic marine flooding due to eustatic changes in sea level with intermittent emergent conditions.

3.4 BURIAL HISTORY OF THE CHESHIRE SEDIMENTS

The relationship between the burial history of the Sherwood Sandstone Group and the timing of mineralisation in the Cheshire Basin were discussed in Chapter 2. Knowledge of the burial history of the Sherwood Sandstone Group and Mercia Mudstone Group sediments is critical to this part of the study and consequently is described below in an attempt to relate the diagenetic events to tectonic events and burial depths of the sediments.

Basin evolution was initiated in the Permian as a result of rifting in the North Atlantic (Burke 1976) and intracratonic basins such as the Cheshire and Irish Sea Basins subsided rapidly following vertical movements on synsedimentary faults. The maximum burial depth of the Sherwood Sandstone Group varies throughout the basin and is primarily controlled by the proximity to active faults.

Tectonic inversion affected many of the British Permo-Triassic basins during the Tertiary and resulted in widespread uplift of the Sherwood Sandstone Group to form the basin margin fault-blocks such as at Alderley Edge. The amount of uplift in the Cheshire Basin is thought to be comparable to that in the Irish Sea Basin where Colter (1978) suggested 2 km of uplift from spore colouration and vitrinite reflectance studies. Similar tectonic inversions have been recorded from the Wessex Basin (Stoneley 1982) and Staffordshire Basin (Shell U.K. unpublished data).

Thus, the Tarporley Siltstone Formation sediments of the Wilkesley borehole are thought to have undergone significant burial, possibly in the order of 3.5-4 km. Burial depths for the Sherwood Sandstone Group adjacent to the basin margin remain uncertain, but it is evident that the sediments have been subject to uplift and exposure to modern groundwater systems following burial.

3.5 PETROGRAPHY OF THE SHERWOOD SANDSTONE GROUP

3.5.1 DETRITAL MINERALOGY

The detrital mineral assemblage of the sandstones of the Wilmslow and Helsby Sandstone Formations of the Cheshire Basin is dominated by quartz and the rocks are classified as quartz arenites and sublitharenites after Folk (1974) (see Fig. 3.4). Monocrystalline quartz is the dominant quartz type and occurs as well rounded grains. At

FIGURE 3.4

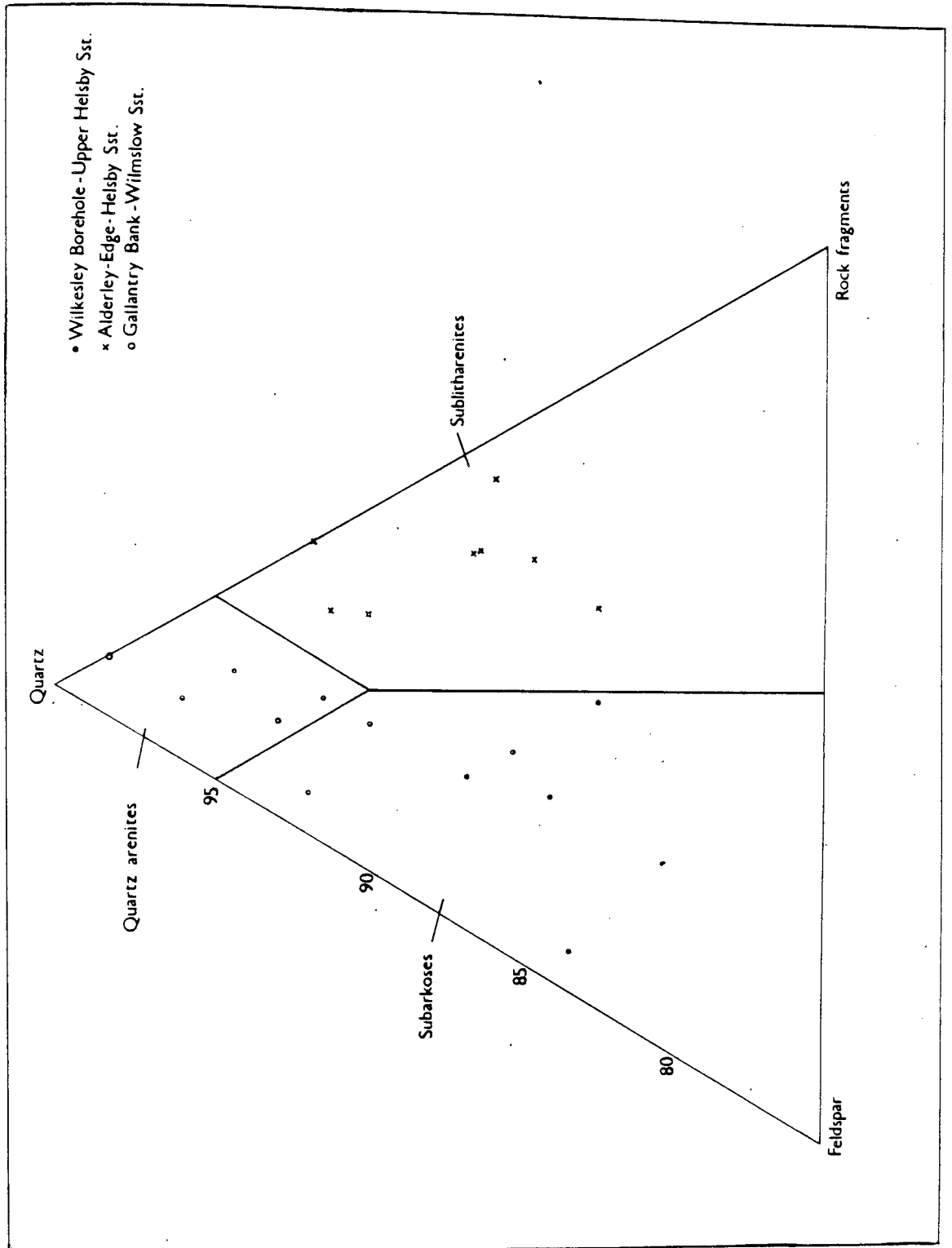


Figure 3.4. Mineralogical classification of the sandstones of the Cheshire Basin (After Folk 1974).

TABLE 3.1

	AE1	AE3	AE4	AE6	AE7	AE9	AE11	AE13	AE5	RA2	RA4	RA5	PH2	BE2	HA2	HA4	G3	GB4	TH4	TH3
Monocrystalline quartz	418	388	276	358	370	408	408	36.8	356	45.4	44.2	42.0	536	346	36.4	45.2	45.2	34.6	55.4	41.0
Polycrystalline quartz	15.4	11.0	14.2	20.0	23.0	17.4	14.4	13.2	20.4	19.2	10.6	11.6	5.2	28.0	8.4	11.0	4.0	22.0	9.0	34.2
Alkali feldspar	1.4	4.8	0.6	TR	2.0	1.8	1.8	2.4	0.2	6.6	0.8	1.6	1.2	TR	3.0	4.8	0.6	1.2	2.2	0.4
Plagioclase	~	0.4	~	TR	~	~	~	~	~	TR	~	~	~	~	~	~	~	1.6	~	~
Rock fragments	4.2	5.0	6.2	5.0	7.4	4.6	7.0	6.6	4.6	4.0	5.8	6.8	12	6.8	5.2	6.2	1.2	1.6	7.6	3.8
Mica	~	0.8	TR	TR	~	0.6	~	0.4	0.2	TR	~	TR	~	~	~	0.2	~	TR	0.4	TR
Opaque/heavy	TR	TR	TR	TR	TR	0.2	TR	TR	TR	TR	TR	TR	TR	~	TR	TR	0.8	TR	TR	TR
Detrital clay	7.0	TR	4.4	3.8	1.4	3.4	0.2	1.0	0.8	TR	TR	TR	TR	TR	~	~	10.6	TR	0.2	TR
Microquartz	~	~	~	~	~	~	~	~	~	~	~	~	362	~	~	~	17.0	3.8	TR	~
Qtz overgrowth	~	2.4	1.0	4.0	3.6	1.2	2.6	1.6	0.4	1.0	~	~	~	~	0.2	~	3.6	4.4	~	8.8
Fsp overgrowth	~	~	~	~	~	TR	TR	TR	~	0.8	~	~	~	~	0.8	TR	~	~	~	~
Calcite	~	~	39.6	~	~	~	~	~	~	~	~	~	~	~	~	~	~	~	~	~
Barite	24.8	1.4	3.0	1.2	0.6	22.2	10.0	32.8	27.2	7.6	23.4	5.2	~	21.2	44.8	3.8	~	~	~	~
Ore minerals	~	27.4	TR	7.2	0.6	~	15.8	~	~	~	~	~	~	~	~	~	~	~	~	~
Replacement clay†	TR	1.6	TR	TR	TR	TR	TR	TR	0.2	1.2	TR	TR	TR	TR	TR	10	16	5.4	~	TR
Authigenic clay‡	5.0	TR	1.8	2.4	4.8	2.0	4.4	1.8	6.8	TR	5.4	3.4	TR	TR	0.4	2.2	2.2	4.8	6.0	0.4
POROSITY	0.4	6.4	1.6	2.0	19.6	5.8	3.0	3.4	3.6	10.0	9.8	2.8	3.4	9.4	0.2	8.0	3.2	3.4	10.0	3.6
intergranular dissolution	TR	~	TR	18.6	~	TR	TR	TR	TR	4.2	TR	26.6	0.2	TR	0.6	18.6	TR	17.2	9.2	7.8
detritus	69.8	60.8	53.0	64.6	70.8	68.6	64.2	60.4	61.8	75.2	61.4	62.0	96.4	69.4	53.0	67.4	89.4	64.8	74.8	79.4
authigenic	29.8	32.8	45.4	14.8	9.6	25.4	32.8	36.2	34.6	10.6	28.8	28.6	~	21.2	46.2	7.0	7.4	14.6	6.0	9.2
porosity	0.4	6.4	1.6	20.6	19.6	5.8	3.0	3.4	3.6	14.2	9.8	9.4	3.6	9.4	0.6	26.6	3.2	20.6	19.2	11.4

TABLE 3.1. Point count data from the Sherwood Sandstone Group sediments of the Cheshire Basin.

Alderley Edge these grains are extensively fractured except where there the sandstones are cemented by calcite.

Feldspars make up between 0.1 and 6.6 % of the Sherwood Sandstone Group sediments of Cheshire (Table 3.1). Orthoclase and microcline are by far the most common feldspars with plagioclase only rarely present. In most cases, orthoclase and perthite have a fresh appearance, but some grains show varying degrees of dissolution and alteration. Microcline is present in small amounts and exhibits the characteristic polysynthetic twinning. Detrital feldspars of the Helsby Sandstone Formation at Thurstaston and the Mid-Cheshire Ridge are often enclosed by authigenic K-feldspar overgrowths.

Rock fragments make up approximately 5% of the whole rock and comprise metamorphic and igneous fragments, some of which are tourmaline and chlorite-bearing. Minor quantities of volcanic rock fragments, coarse-grained igneous fragments and sedimentary clasts are present.

Muscovite and biotite are present in varying amounts in these sediments (up to 0.8%) but are absent in the aeolian sandstones of the Sherwood Sandstone Group. Muscovite and biotite generally occur as undeformed, unaltered flakes, although biotites in the Wilmslow Sandstone Formation of the Mid-Cheshire Ridge are extensively replaced by haematite. The heavy mineral assemblage includes zircon, tourmaline, epidote and garnet and is similar to that in the Sherwood Sandstone Group of the English Midlands (Ali 1982).

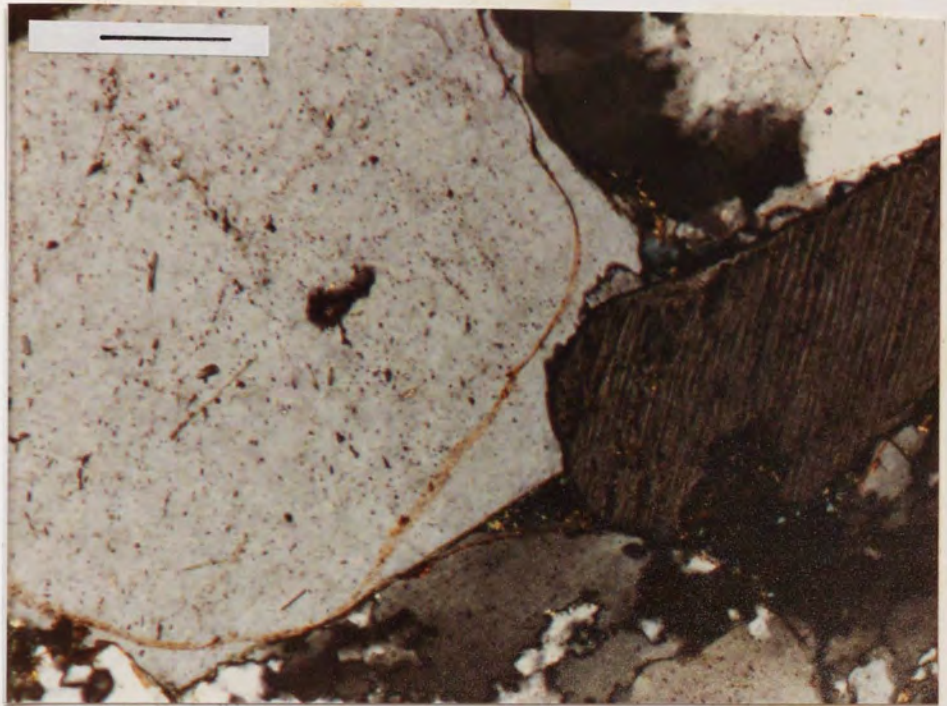
3.5.2 DIAGENETIC HISTORY OF THE SHERWOOD SANDSTONE GROUP

Grain dissolution and replacement textures are widespread in the Sherwood Sandstone Group of Cheshire and are commonly associated with rock fragments, feldspars and heavy minerals. K-feldspar grains are often partially dissolved and, in many cases, enlarged pores contain relicts of haematite-clay pellicles which originally surrounded a detrital grain. Detrital silicates are commonly replaced by chlorite, illite, haematite and calcite. Burley (1984) described intensely leached orthoclase from shallowly buried sandstones on the western Cumbrian Basin margin but Ali (1982) found no evidence of feldspar dissolution in the Sherwood Sandstone Group of central England.

Plate 3.1 Colour photomicrograph showing the relative timing of authigenic K-feldspar and quartz overgrowth formation in the Helsby Sandstone Formation, Thurstaston. Quartz overgrowths enclose epitaxial feldspar overgrowths and clearly developed later. Thin haematite clay pellicles mark the outline of the original quartz grains and predate the formation of euhedral quartz overgrowths. Grain-grain contacts are rare and compactional effects are minimal. Scale bar = 500 μm (Crossed polars).

Plate 3.2 Colour photomicrograph of an epitaxial, authigenic potassium feldspar overgrowth in the Helsby Sandstone Formation, Rawhead, Mid-Cheshire Ridge. Both the detrital orthoclase grain and the overgrowth are partially altered to highly birefringent illitic clays. Scale bar = 100 μm (Crossed polars).

au thigenic
sandstone
ial feldspar
y pellicles
e
acts are
un



sium
awhead,
ne
lays. Scale

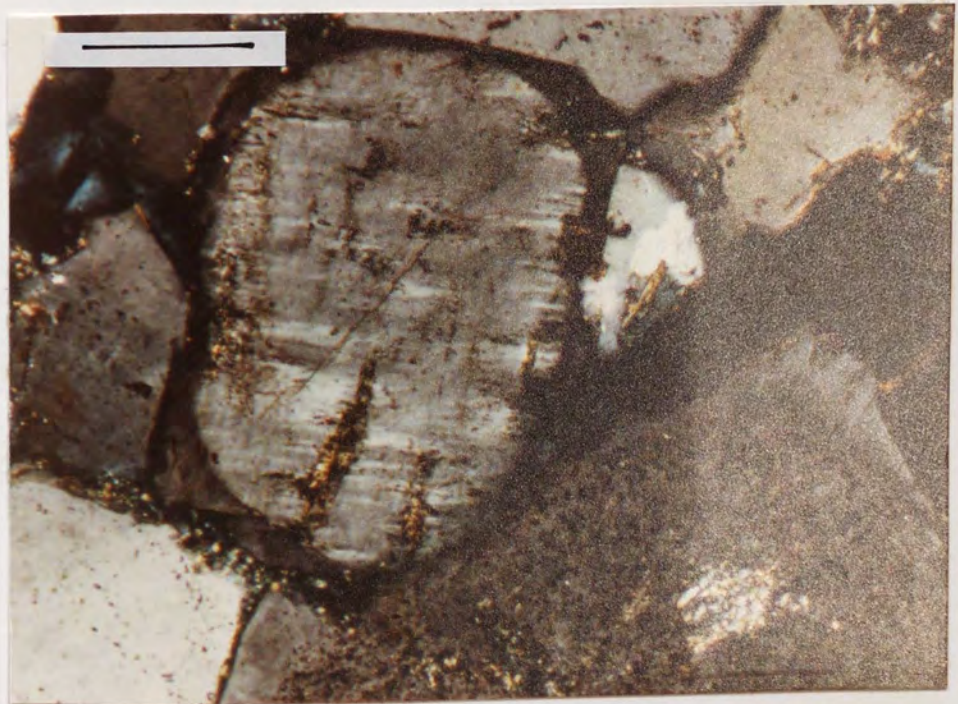
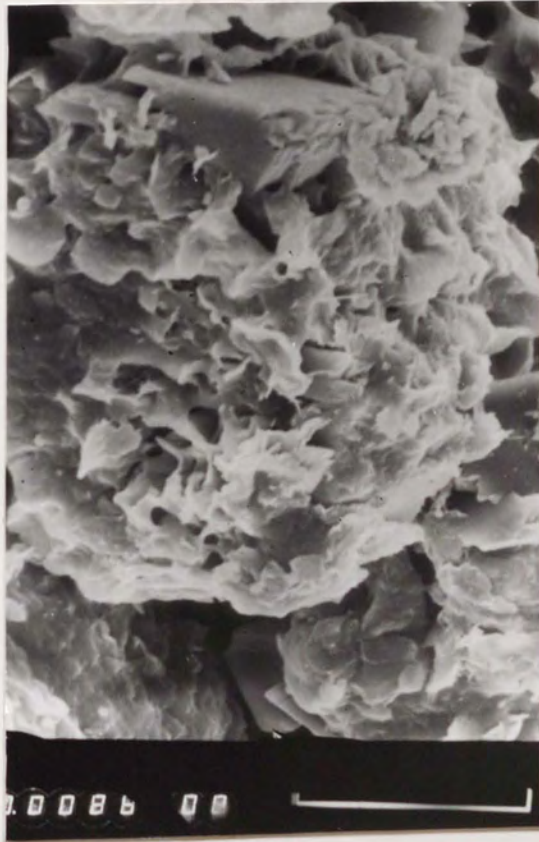
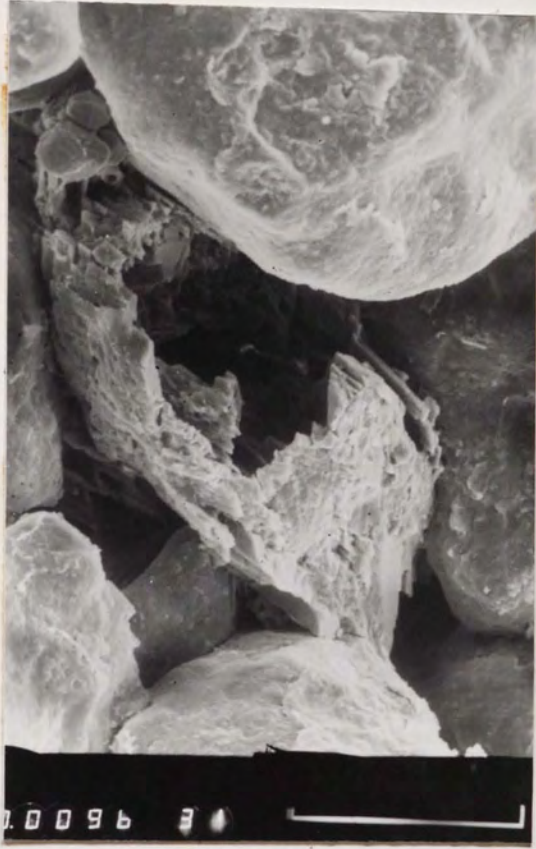


Plate 3.3 Scanning electron micrograph of authigenic cement and porosity in the Helsby Sandstone Formation, Hawkstone Park. Intense dissolution of detrital potassium feldspar with authigenic feldspar overgrowth intact. Scale bar = 86 μm .

Plate 3.4 Scanning electron micrograph of authigenic clays and potassium feldspar overgrowths in the Helsby Sandstone Formation, Grinshill. Poorly developed boxwork texture of illite-smectite mixed layer clay and finely particulate authigenic haematite coating a detrital K-feldspar grain. Scale bar = 96 μm .



The sandstones are cemented by a variety of authigenic minerals including quartz, K-feldspar, illite, kaolinite, haematite and calcite. In addition, barite is a common cementing agent in the Wilmslow and Helsby Sandstone Formations around the basin margins. Barite mineralisation is clearly fault-related (see Chapter 2) and several generations of barite are evident in the Sherwood Sandstone Group sediments around the basin margin (Plate 3.6). The timing of barite deposition relative to the precipitation of the other authigenic phases described in this chapter remains uncertain.

Silica is a common cementing agent and occurs as syntaxial overgrowths on detrital quartz grains. Authigenic quartz is not present in the fine-grained fluvial sediments of the Helsby Sandstone Formation but is an important cement in the open-textured aeolian sediments, where it effectively reduces permeability by blocking pore throats. The well-developed quartz overgrowths are similar to those described by Waugh (1970a) and Waugh (1970b) in the Penrith Sandstones and their development from small crystallographic projections to complete enclosing overgrowths parallels that in the Penrith Sandstone. Quartz overgrowths in the Sherwood Sandstone Group of Cheshire postdate thin authigenic illite-haematite grain coatings and, in some cases, thick haematite-clay pellicles clearly prevented quartz overgrowth development. Macchi & Velkamp (1985) reported that quartz overgrowths in the Helsby Sandstone Formation partially enclose authigenic feldspar overgrowths and observations made during this study confirm that authigenic feldspar precipitation predated quartz overgrowth development (Plate 3.1).

Previous studies on authigenic K-feldspars in the Permo-Triassic include the work of Reynolds (1929), Williams (1973) and Ali & Turner (1982). Authigenic K-feldspar is common in the Sherwood Sandstone Group of Cheshire and typically occurs as epitaxial overgrowths enclosing detrital microcline and orthoclase grains (Plate 3.2). The morphology and development of the overgrowths is closely comparable to that documented by Waugh (1978) in his study of authigenic K-feldspar in British Permo-Triassic sandstones (Plate 3.3). The minor amounts of Fe_2O_3 and CaO detected during electron microprobe analyses of authigenic K-feldspar in Cheshire (Table 3.2) are thought to represent tiny inclusions of haematite and carbonate within an otherwise pure

TABLE 3.3. Electron microprobe analyses of detrital and authigenic feldspars in the Cheshire Basin.

Sample number	SiO ₂	Al ₂ O ₃	Fe ₂ O ₃	CaO	Na ₂ O	K ₂ O	BaO	TOTAL
RAW2*Detrital grain	65.4	18.5	0.1	0.1	0.9	15.4	0.1	100.5
Overgrowth	64.9	17.7	n.d.	0.2	n.d.	16.4	n.d.	99.2
RAW2 Detrital grain	66.0	18.9	0.1	0.1	1.2	15.2	0.2	101.7
Overgrowth	65.8	18.7	n.d.	0.1	n.d.	16.5	n.d.	101.1
RAW2 Detrital grain	65.7	18.1	n.d.	n.d.	0.6	15.5	0.1	100.0
Overgrowth	65.1	18.3	0.2	0.1	n.d.	16.7	n.d.	100.4
RAW2 Detrital grain	68.6	19.9	n.d.	0.4	11.4	0.1	n.d.	100.4
G3 Detrital grain	64.7	18.1	n.d.	0.1	0.2	16.0	0.3	99.4
WB9835								
Detrital K-feldspar	65.9	18.4	n.d.	0.1	1.1	15.1	0.4	101.0
Authigenic albite	69.3	19.8	0.1	n.d.	11.7	n.d.	0.1	101.0

* Sample localities given by the prefix on the sample number: RAW = Rawhead, Mid-Cheshire Ridge; G = Grinshill, southern Cheshire; WB = Wilkesley borehole.

Plate 3.5 Colour photomicrograph of carbonate cements in the Helsby Sandstone Formation, Alderley Edge. Non-ferroan micritic calcite cements enclose detrital quartz and haematite grains. The extensive grain replacement and corrosion and the displacive growth textures are reminiscent of textures associated with calcrete development in fluvial sands. Scale bar = 500 μm (Crossed polars).

Plate 3.6 Colour photomicrograph of barite cements in the Helsby Sandstone Formation, Beeston, Mid-Cheshire Ridge. Well-rounded quartz grains are often isolated by the pervasive, poikilotopic barite cements. The barite cements appear to have inhibited the development of authigenic quartz overgrowths and authigenic clays. Scale bar = 500 μm (Crossed polars).

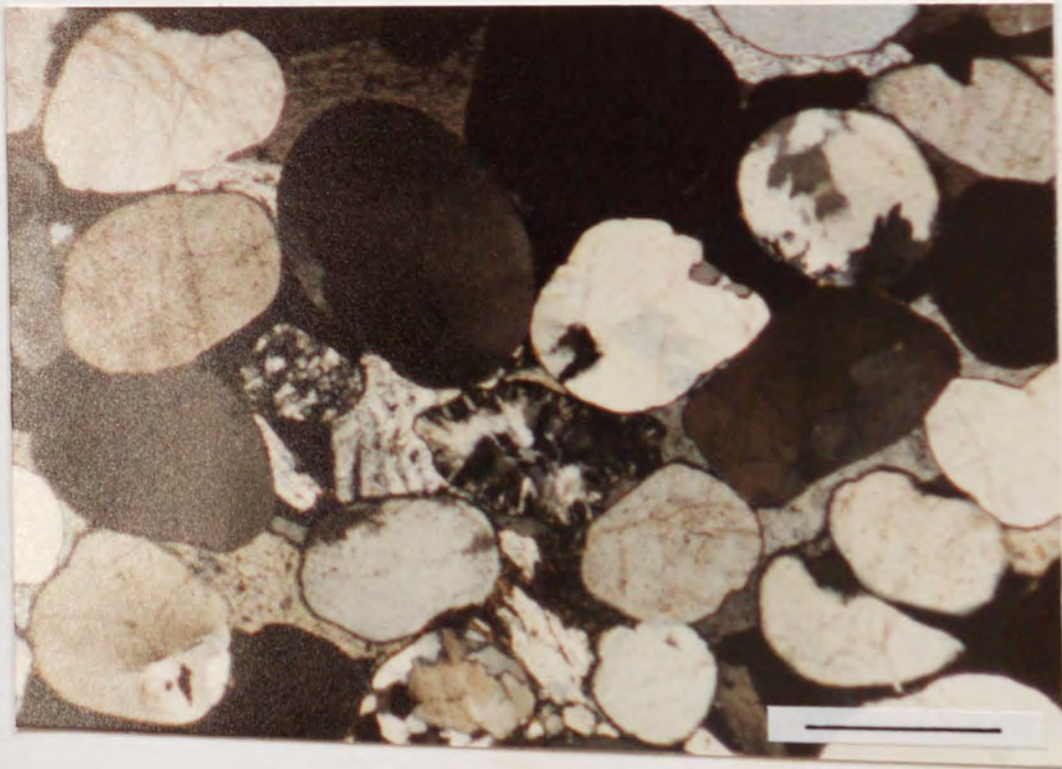
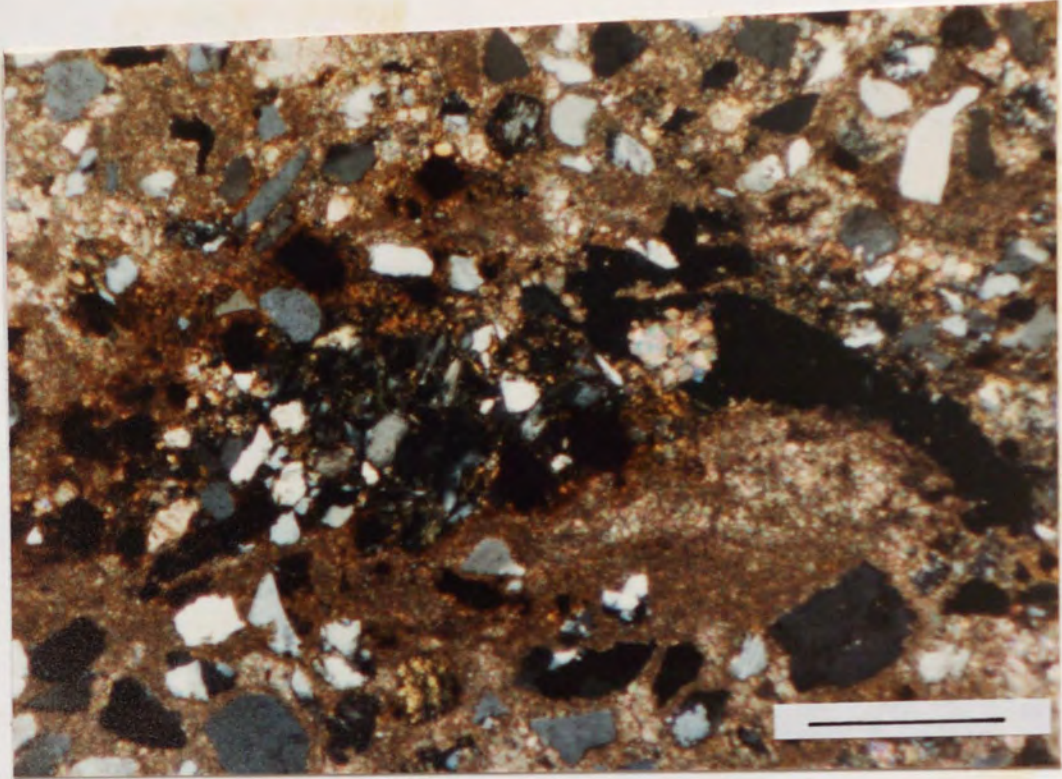
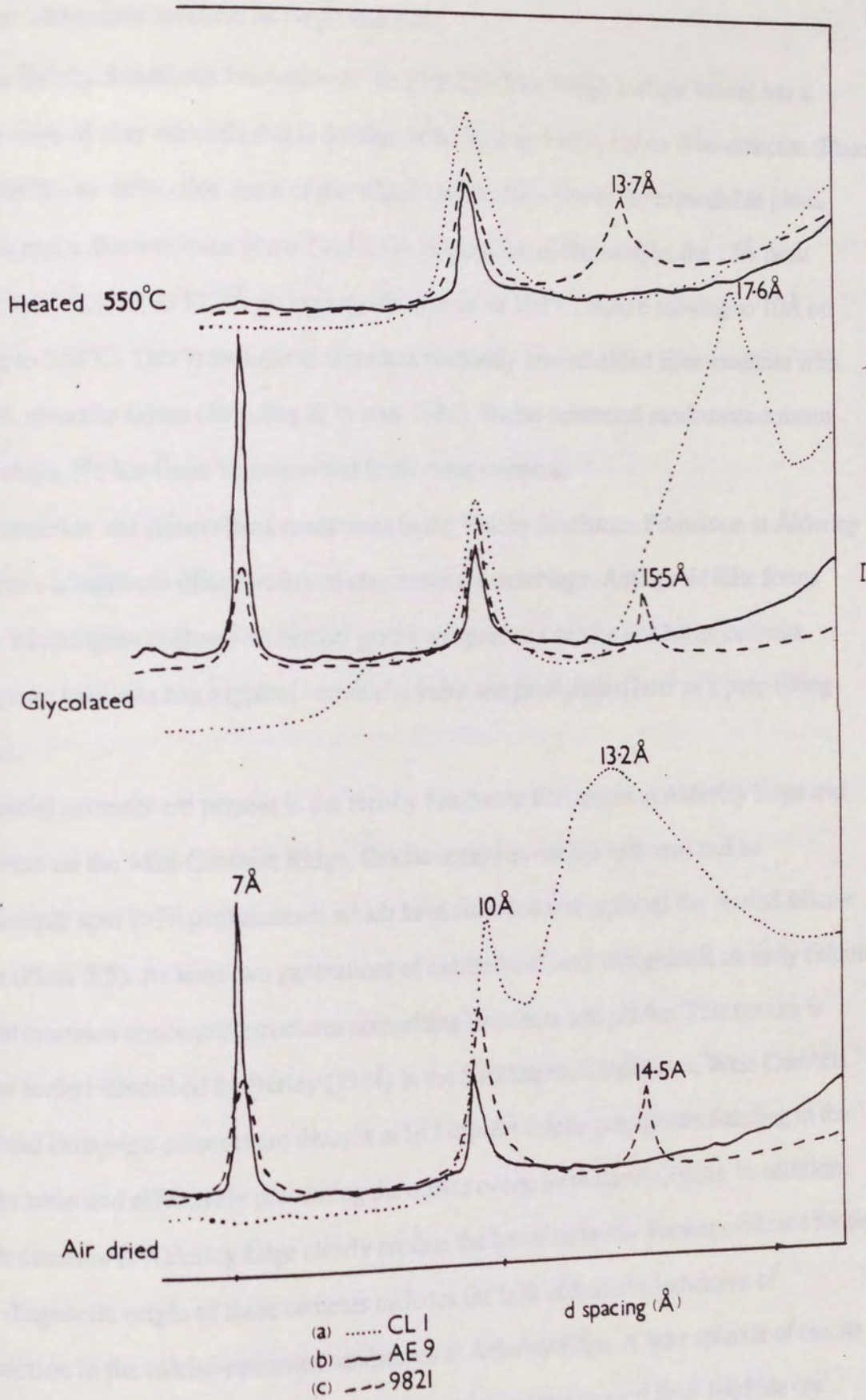


Figure 3.5. X-ray diffraction traces of the $<2\mu\text{m}$ clay fraction of the Cheshire Basin sandstones; (a) a randomly interstratified illite-smectite-dominated assemblage, Helsby Sandstone Formation, Mid-Cheshire Ridge, (b) illite and kaolinite in mineralised sandstones, Alderley Edge and (c) illite-chlorite-kaolinite dominated assemblage, Tarporley Siltstone Formation, Wilkesley borehole.

FIGURE 3.5



overgrowth. Waugh (1978) found the overgrowths to be pure, stoichiometric feldspar whereas Ali & Turner (1982) noted that the overgrowths consisted of potassium low sanidine with minor amounts of Na_2O and BaO .

The Helsby Sandstone Formation of the Mid-Cheshire Ridge and the Wirral has a distinct suite of clay minerals that is dominated by illite and mixed layer illite-smectite (Plate 3.4). The X-ray diffraction trace of the $<2\mu\text{m}$ clay fraction shows an expandable phase (13.2\AA) and a discrete mica phase (10\AA). On glycolation of the sample, the 13\AA peak moves to 17\AA , then to 12.4\AA on heating the sample to 180°C , before moving to 10\AA on heating to 550°C . This is thought to represent randomly interstratified illite-smectite with 40-50% smectite layers (Brindley & Brown 1986). Barite-cemented sandstones contain fewer clays. No kaolinite was recorded from these samples.

In contrast, the mineralised sandstones in the Helsby Sandstone Formation at Alderley Edge have a kaolinite-illite dominated clay mineral assemblage. Authigenic illite forms highly birefringent coatings on detrital grains and predates calcite and barite cements. Authigenic kaolinite has a typical vermicular habit and precipitated later as a pore-filling cement.

Calcite cements are present in the Helsby Sandstone Formation at Alderley Edge and Bickerton on the Mid-Cheshire Ridge. Calcite occurs as micrite ($<5\mu\text{m}$) and as poikilotopic spar ($>70\mu\text{m}$) cements which have corroded and replaced the detrital silicate grains (Plate 3.5). At least two generations of calcite have been recognised; an early calcite cement contains concentric structures comprising haematite and calcite. This texture is similar to that described by Burley (1984) in the Kirklington Sandstones, West Cumbria and these carbonate cements are thought to be incipient calcite precipitates forming in the vadose zone and effectively preventing the quartz overgrowth development. In addition, calcite cements at Alderley Edge clearly predate the barite cements. Further evidence for the early diagenetic origin of these cements includes the lack of features indicative of compaction in the calcite-cemented sandstones at Alderley Edge. A later episode of calcite precipitation occurred at Bickerton where the calcite gangue formed after sulphide ore formation adjacent to the Bickerton-Bulkeley fault (see Chapter 2).

Primary porosity in the Sherwood Sandstone Group is augmented by secondary

porosity. There is strong evidence for the secondary porosity created by the dissolution of framework grains and cements. Enlarged pores commonly contain isolated haematite-clay rims indicating the former presence of detrital silicate or ferromagnesian grains. K-feldspar appears to be prone to grain dissolution (Plate 3.3). Small, irregular embayments in quartz overgrowths and detrital grains and the irregular shape of some grains in the Wilmslow Sandstone Formation of the Mid-Cheshire Ridge are thought to result from dissolution of early carbonate cements during diagenesis. The textures in the Sherwood Sandstone Group of the Cheshire Basin resemble those associated with cement dissolution porosity from the Permo-Triassic sandstones of the Wessex and Irish Sea Basins (Burley & Kantorowicz 1986).

3.6 PETROGRAPHY OF THE MERCIA MUDSTONE GROUP,

WILKESLEY BOREHOLE

3.6.1 DETRITAL MINERALOGY

Quartz is the dominant detrital component in the Wilkesley borehole sediments, constituting between 43 and 63 % of the whole rock (Table 3.3). According to Folk's (1974) classification these sandstones are subarkoses and quartz arenites (Fig 3.4). Ali (1982) reviewed the different types of quartz present in the Triassic of Central England and concluded that the majority of detrital quartz was sourced from medium to low grade metamorphic terrains with minor inputs from igneous and sedimentary sources.

Both alkali and plagioclase feldspar are present in minor amounts (between 1.0 % and 7.4 %) and for the most part have suffered extensive alteration to haematite and clays. Plagioclase feldspar seems to be more abundant than microcline and orthoclase but this may be a function of the easily identifiable multiple twinning. The feldspars are subrounded to subangular and cathodoluminescence reveals that they are more abundant than the point count data suggests. Replacement and dissolution of feldspars is particularly associated with plagioclase. The widespread nature of these phenomena suggest that the original feldspar content of the sediments is likely to have been higher.

Rock fragments derived principally from metamorphic and igneous sources constitute up to 5% of the Wilkesley borehole sediments. Metamorphic clasts predominate and consist mostly of mica schists; fine-grained volcanic fragments, plutonic fragments and siltstone

TABLE 3.3

	9792	9798	9803	9804	9815	9817	9821	9828	9835	9853
QUARTZ (monocrystalline)	36.2	41.6	37.0	43.2	40.8	42.4	40.6	39.6	39.4	37.4
polycrystalline	4.6	4.8	17.4	12.4	8.2	8.2	3.0	1.0	0.6	2.8
K feldspar	1.2	0.6	4.8	3.0	1.8	3.8	1.8	0.6	4.0	5.4
Plagioclase	0.8	0.6	1.0	0.6	3.6	2.8	1.4	0.4	1.2	2.0
Rock fragments	1.8	1.6	3.6	2.2	5.0	3.0	0.6	0.8	2.4	0.6
Mica	TR	TR	TR	0.2	0.4	1.6	0.8	0.6	0.4	0.2
Opaque / heavy	1.2	1.4	1.6	TR	1.0	0.8	3.2	0.4	1.2	TR
Detrital clay†	21.8	7.0	2.0	4.4	5.0	6.6	3.6	4.4	4.4	3.8
Qtz overgrowth	9.0	10.2	7.0	8.2	8.4	18.6	18.2	11.2	14.2	19.4
Fsp overgrowth	-	-	0.2	TR	0.2	TR	0.2	TR	0.8	0.2
Anhydrite	14.0	20.4	0.8	-	-	0.2	0.8	8.8	1.8	20.0
Gypsum	-	0.8	-	-	-	-	-	TR	TR	0.8
Dolomite	1.6	2.8	0.8	6.8	3.2	4.4	2.2	4.0	1.0	0.4
Replacement clay	2.6	TR	1.6	1.4	1.0	1.2	4.2	3.6	3.0	0.6
Authigenic clay†	TR	TR	1.8	6.2	5.4	5.2	16.8	1.2	6.0	5.0
POROSITY intergranular grain dissolution	5.2 TR	8.2 TR	5.0 5.4	11.4 TR	16.0 TR	1.2 TR	2.6 TR	3.4 TR	9.6 TR	1.4 TR
TOTAL detritus	67.6	57.6	67.4	66.0	65.8	69.2	55.0	47.8	63.6	52.2
authigenic phases	27.2	34.2	22.2	22.6	18.2	29.6	42.4	48.8	26.8	46.4
porosity	5.2	8.2	10.4	11.4	6.0	1.2	2.6	3.4	9.6	1.4

TABLE 3.3 Point count data from the Mercia Mudstone Group sediments of the Cheshire Basin

clasts are present in minor quantities.

Detrital micas include muscovite flakes which are abundant in the finer lithologies and are commonly sheared or deformed. Chlorite is occasionally present but biotite mica is notably absent.

The heavy mineral assemblage includes zircon, tourmaline, apatite, epidote and sphene and is closely comparable to that in the underlying Sherwood Sandstone Group.

3.6.2. DIAGENETIC HISTORY OF THE SEDIMENTS

The diagenetic modifications of the Wikesley borehole sediments during burial correspond to the diagenetic features commonly associated with continental red beds (Turner 1980). These include mechanical infiltration of detrital clay, widespread framework grain dissolution affecting metastable silicates such as hornblende and plagioclase, clay replacement of detrital grains and the precipitation of a suite of authigenic minerals which includes quartz, K-feldspar, illite, kaolinite, haematite and carbonate cements. In addition, in the Tarporley Siltstone sediments of the Wilkesley borehole, anhydrite cements and authigenic albite are commonly present.

Mechanically infiltrated clays occur as grain coatings in these sandstones and mudstones and are a common feature of ancient red bed sequences. In common with the Sherwood Sandstone Group of Central England (Ali & Turner 1982, Burley 1984) and Cheshire (see above), these Tarporley Siltstone Formation sediments contain no pyroxene or amphibole. This is thought to reflect the scarcity of these minerals in the source area but is also a function of dissolution of such ferromagnesian grains during diagenesis. Waugh (1978) noted that framework grain dissolution in Triassic sandstones affected minerals such as K-feldspar, which is high in the stability series of Goldrich (1938). SEM techniques and petrographic observations from thin sections in this study have confirmed this, revealing that both K-feldspar and plagioclase have undergone partial dissolution.

Large, well-developed quartz overgrowths are widespread in the Tarporley Siltstone Formation and Lower Keuper Marl of the Wilkesley borehole. Early syntaxial quartz overgrowths predate the patchy quartz cements which do not display optical continuity with adjacent detrital grains. Quartz overgrowths are thought to have formed contemporaneously with feldspar overgrowths, although in one instance authigenic quartz precipitation

occurred after the formation of an albite overgrowth. The scarcity of sutured grain contacts indicates that the majority of authigenic silica precipitated from migrating fluids as opposed to pressure solution processes.

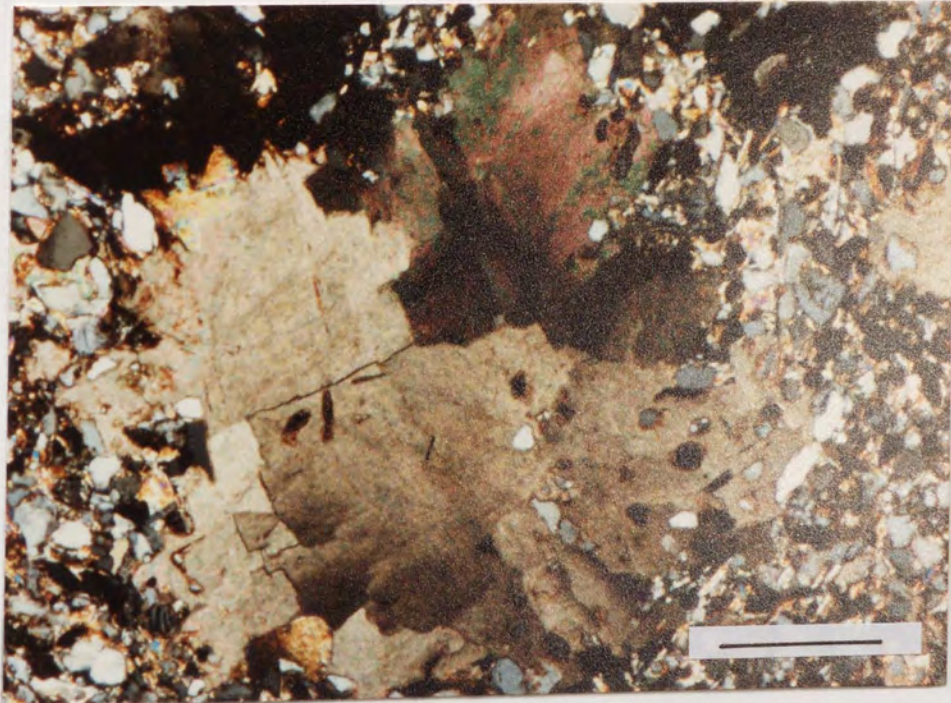
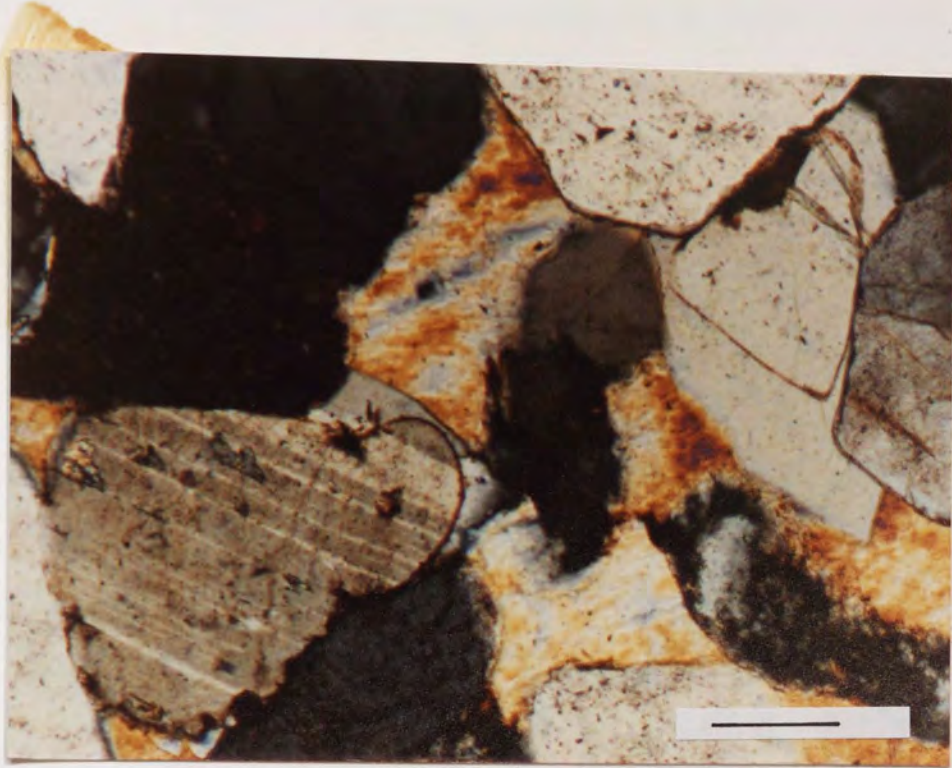
Authigenic K-feldspar is a common constituent of the Sherwood Sandstone Group but is less common in the overlying Mercia Mudstone Group. This is confirmed in the present study where the orthoclase and microcline in the Wilkesley sediments rarely have associated overgrowths. In contrast, the plagioclase grains often have optically continuous, twinned overgrowths (Plate 3.7) which develop preferentially on crystal faces parallel to the twin planes.

The dominant diagenetic minerals of the Tarporley Siltstone Formation are anhydrite and dolomite. Anhydrite is a common constituent of the mudstones and sandstones and constitutes up to 20.4% of the whole rock. Two forms of anhydrite can be recognised; interlocking, lath-shaped crystals occur with gypsum and form nodular masses in the mudstones. CaSO_4 is thought to have been precipitated as gypsum during deposition of the sediments in a coastal sabkha environment. Burial of the sediments to depths in excess of 1.5km caused the gypsum to dehydrate to anhydrite. A later pore-filling, highly birefringent anhydrite cement encloses authigenic quartz and feldspar overgrowths (Plate 3.7). Textural evidence indicates that this later anhydrite precipitated during deep burial as it appears to post-date compaction.

The dolomite content of the sediments ranges from 0.8 to 14.0% (mean 3.1%). Dolomite occurs as euhedral rhombs (0.1 mm) and also as large (~1 mm) spear-shaped crystals which have curved faces and resemble a variety of dolomite known as 'saddle dolomite' (Radke & Matthis 1980) (Plate 3.8). The Wilkesley dolomite is mostly non-ferroan, though the ferroan nature of the outer edge of some rhombs is indicated by the blue colour which develops on staining with potassium ferricyanide. According to Radke & Matthis (1980), saddle dolomite characteristically has a deformed crystal lattice causing sweeping extinction under crossed polars, contains abundant fluid inclusions and is typically enriched in calcium. Radke & Matthis (1980) emphasise the importance of saddle dolomite as a replacement phase, citing solid inclusions of calcite and anhydrite as

Plate 3.7 Colour photomicrograph of saddle dolomite in the Tarporley Siltstone Formation, Wilkesley borehole. The dolomite crystals are spear-shaped and exhibit sweeping extinction. They contain inclusions of quartz and anhydrite, indicating that the dolomite is a replacement phase. Scale bar = 500 μm (Crossed polars).

Plate 3.8 Colour photomicrograph of blocky anhydrite cements in the Tarporley Siltstone Formation, Wilkesley borehole. The highly birefringent, pore-occluding anhydrite cements postdate the formation of quartz overgrowths and epitaxial feldspar overgrowths. Note the common occurrence of pressure solution grain contacts between detrital grains. Scale bar = 100 μm (Crossed polars).



evidence. The spear-shaped forms of dolomite in the Wilkesley borehole exhibit all the features described above, including the presence of widespread anhydrite inclusions indicating that the dolomite is a late diagenetic precipitate. Dolomite is also found to replace detrital silicate grains such as quartz, plagioclase and K-feldspar.

X-ray diffraction traces for the Tarporley Siltstone Formation sediments at Wilkesley are similar to those obtained by Jeans (1978) and show an illite-chlorite dominated assemblage with minor kaolinite (Fig. 3.5). Ordered mixed-layer chlorite-smectite is present in minor amounts in some samples. Chlorite and kaolinite are often grain replacement phases and illite with characteristic box-work texture is the major authigenic phase and is represented by a sharp 10\AA peak on the diffraction trace.

Present-day porosities in the Wilkesley sediments are low (between 1.2 and 11.4%), largely as a result of diagenetic modifications during burial. Compaction and the precipitation of authigenic haematite and quartz have effectively reduced porosity in both the sandstones and argillaceous sediments. Minor secondary porosity arises from the dissolution of anhydrite and gypsum cements. This is particularly evident in the sandstones where strongly etched anhydrite cements are found adjacent to open pore spaces. Dissolution of framework grains is additional form of secondary porosity, but is rarely significant in the Mercia Mudstone Group sediments of Cheshire. Acidic migrating porewaters are capable of generating widespread secondary porosity and the presence of an early framework-supporting cement such as calcite is an essential precursor to secondary porosity. Textural evidence indicates that Mercia Mudstone Group sediments were not subjected to flushing by acidic porewaters and that the sandstones contained no early carbonate cement that may be susceptible to dissolution during burial diagenesis.

3.7 DISCUSSION

The diagenetic history of the Triassic sandstones of the Cheshire Basin are discussed below in the context the diagenetic regimes defined by Schmidt & McDonald (1979). This classification involves a subdivision of diagenetic events, depending on whether they are influenced by the depositional environment and the associated pore water chemistry (eodiagenesis), by conditions prevailing during burial (mesodiagenesis), or by the interaction of near-surface waters following uplift of the sediments (telodiagenesis).

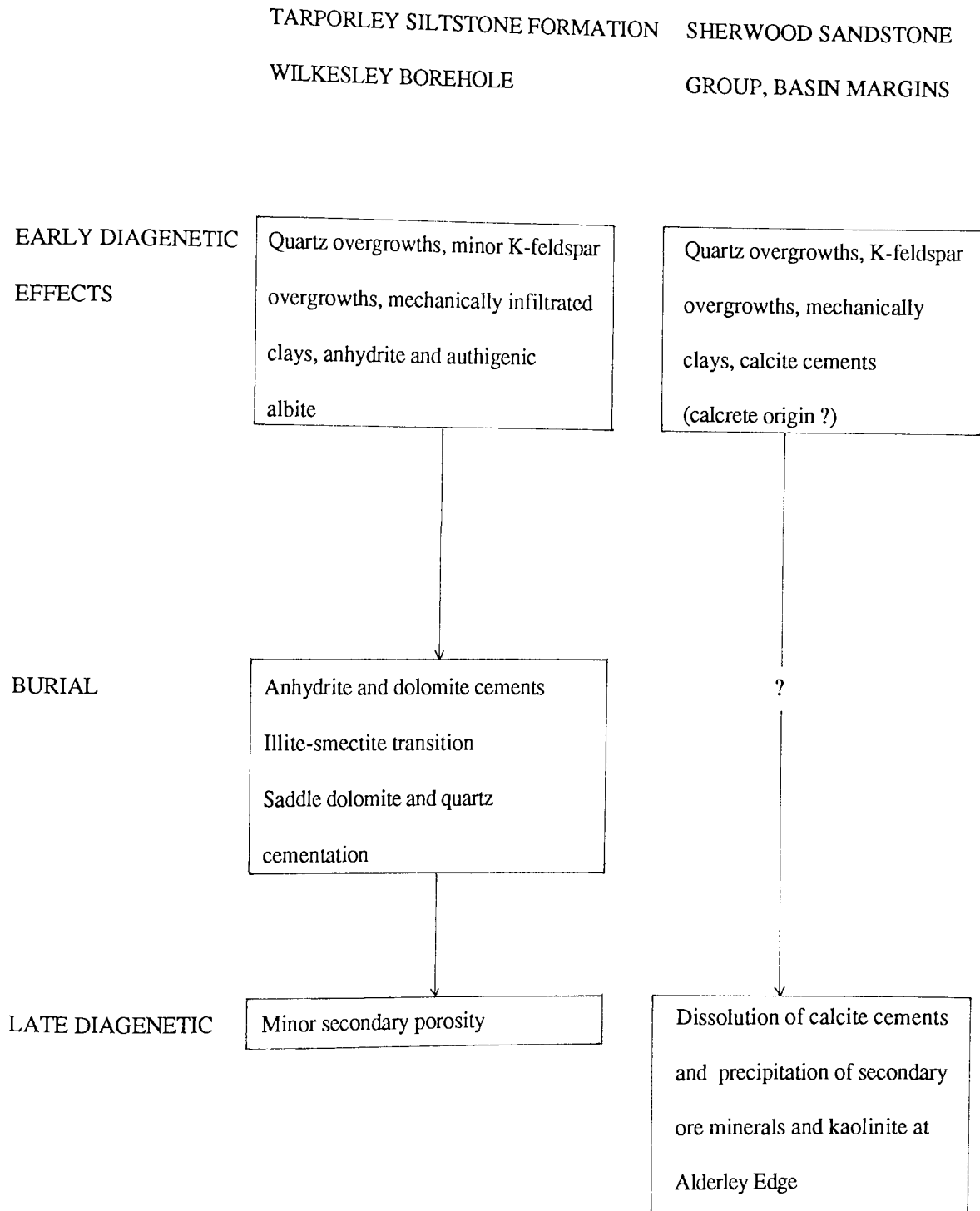
3.7.1 EODIAGENESIS

Textural relationships in the Sherwood Sandstone Group and Mercia Mudstone Group sediments examined in this study indicate that early diagenetic phases have to a certain extent been controlled by the chemical characteristics of porewaters which are, in turn, related to the original depositional environment. It is evident that the presence of anhydrite in the sediments of the Tarporley Siltstone Formation at Wilkesley reflects the intertidal environment in which the sediments accumulated. In addition, the authigenic quartz content of the Sherwood Sandstone Group appears to be partly lithofacies controlled. The aeolian sandstones contain well-developed quartz overgrowths, whereas detrital grains in fluvial sandstones are often surrounded by haematite-clay pellicles which have inhibited quartz overgrowth formation. Textural evidence is consistent with the formation of the quartz overgrowths before any significant burial compaction.

The early diagenetic history of the Triassic sediments of the Cheshire Basin is characterised by grain dissolution and replacement processes and by the precipitation of authigenic minerals including haematite, illite, quartz, albite, K-feldspar and calcite. These events have occurred irrespective of whether the sediments were deposited in fluvial, aeolian or marginal marine environments and are thought to be ancient analogs of early diagenetic features associated with present day red beds in California (Walker et al. 1978).

Illite and K-feldspar are common authigenic constituents of both the Sherwood Sandstone Group and Mercia Mudstone Group and their formation depends on adequate supplies of potassium, aluminium and silicon ions. Potential sources of these ions include K-feldspar, mica, mafic minerals and clays, all of which are present in varying amounts in the Triassic sequence of the Cheshire Basin. Walker et al. (1978) demonstrated that dissolution of relatively unstable grains such as mafic minerals and plagioclase commonly occurs during shallow burial of red beds and results in the release of ions into the interstitial waters. It is proposed that the dissolution of ferromagnesian silicates and K-feldspar can account for the amounts of authigenic illite and K-feldspar in the Triassic sediments of Cheshire. Illite and K-feldspar authigenesis is favoured by high K^+/H^+ ratios or high H_4SiO_4 activity (Ali & Turner 1982). The geochemical environment favouring of authigenic albite formation is similar to that for authigenic K-feldspar (Kastner & Siever

Figure 3.6 Schematic diagram showing the diagenetic history of the Sherwood Sandstone Group and Mercia Mudstone Group sediments of the Cheshire Basin.



1979), although it is likely that albite authigenesis in the Tarporley Siltstone Formation was promoted by the presence of high NaCl brines associated with the marginal marine environment. Thus, the greater abundance of K-feldspar in the Sherwood Sandstone Group may simply reflect the higher primary K-feldspar content of the basin margin sandstones. Detailed textural studies suggest that authigenic albite precipitated during shallow burial of the Tarporley Siltstone Formation.

3.7.2. MESODIAGENESIS

The Tarporley Siltstone Formation of the Wilkesley borehole is currently at a burial depth of approximately 1.5km (maximum burial depths are likely to have been in excess of 3-3.5 km) and diagenetic events occurring during burial are superimposed on the fabric and mineralogy developed during early diagenesis. These later diagenetic modifications occur in both the sandstones of the Tarporley Siltstone Formation and mudstones of the overlying Lower Keuper Marl and are clearly depth-related.

Diagenetic reactions during the mesodiagenetic regime are controlled by the clay mineral transformations such as depth-related conversion of smectite to illite, by the expulsion of interstitial pore waters and by the dehydration of hydrous minerals. The implications of the illite-smectite transformation were documented by Boles & Franks (1979) who showed that the reaction liberates ions such as silicon, calcium, magnesium, sodium and iron into the pore waters. These pore waters may be capable of transporting large quantities of dissolved ionic species from mudrocks into associated sandstones and may ultimately be responsible for the precipitation of quartz overgrowths, ferroan carbonates and chlorite, and for causing albitisation of plagioclase feldspar (Curtis 1983). Other depth-related processes likely to have influenced the deep burial of the Tarporley Siltstone Formation include the expulsion of interstitial pore waters during the smectite-illite transformation and the dehydration of gypsum to anhydrite. Numerous workers since Curtis (1978) have invoked associated mudrocks as sources of ions for deep burial diagenetic processes in sandstones.

The Tarporley Siltstone Formation at Wilkesley underlies anhydrite-bearing mudstones of the Lower Keuper Marl and it is suggested that the diagenetic events occurring during deep burial were influenced by the expulsion of porewaters from the mudstones into the

more porous sandstones below. The deep-burial diagenetic assemblage of the Tarporley Siltstone Formation of the Wilkesley borehole comprises anhydrite, dolomite and quartz cement. The precipitation of anhydrite seems to have occurred relatively late in mesodiagenesis, as it clearly post-dates features associated with compaction.

Supersaturated calcium sulphate brines originating in the Mercia Mudstone Group are thought to have percolated into the sandstones and to have precipitated these anhydrite cements after the formation of quartz and feldspar overgrowths. The poikilotopic anhydrite cements are replaced by non-ferroan dolomite which resembles saddle dolomite as described by Radke & Matthis (1980). According to Radke & Matthis (1980), saddle dolomite is associated with hydrocarbon occurrences, base metal mineralisation, fluorite, calcite and commonly occurs in spalerite-rich carbonate horizons. These authors also stressed the importance of saddle dolomite as a geothermometer, indicating diagenetic events in the temperature range 60-150°C. However, saddle dolomite does not occur exclusively in high temperature diagenetic environments, as it has also been described from low temperature hypersaline marine environments (Friedman & Radke 1979). A microstructural study by Barber et al. (1985) suggests that a limited supply of parent fluid and the presence of impurities such as hydrocarbons or sulphate favour the precipitation of saddle dolomite, and is consistent with its occurrence in the evaporite-rich Tarporley Siltstone Formation of the Cheshire Basin.

Secondary porosity generation is not thought to be of major significance in the Tarporley Siltstone Formation at Wilkesley. This may reflect the early cementation of the sediments by cements such as silica or, alternatively, may be ascribed to the presence of passive, alkaline porewaters in the sediments during burial.

3.7.3 TELODIAGENESIS

The re-introduction of meteoric water into the Sherwood Sandstone Group around the basin margins has led to widespread secondary porosity generation through the removal of calcite and barite cements as well as detrital grains (particularly rock fragments). This is particularly evident at Alderley Edge, northeast Cheshire, where pore-filling kaolinite is common and the sandstones lack red colouration. A hydrogeochemical investigation of the Triassic Budleigh Salterton Pebble Beds of south Devon (Walton 1981) has revealed that

dilute acidic groundwaters (pH 5-6) have caused extensive leaching of haematite and carbonate cements. Furthermore, the *in situ* alteration of detrital K-feldspar to illite-kaolinite-authigenic K-feldspar is thought to result from the interaction with modern pore waters which are currently saturated with respect to kaolinite and illite and contain appreciable quantities of dissolved alumina.

Examination of the textures in the Sherwood Sandstone Group and Mercia Mudstone Group of the Cheshire Basin has revealed that widespread framework grain dissolution and replacement has occurred during diagenesis. This confirms the suggestion by Holmes et al. (1983) that such processes have affected the Triassic sequence of Cheshire and have possibly contributed to the metals in the basin margin mineralisation.

3.8 CONCLUDING REMARKS

The eodiagenesis of the sediments of the Sherwood Sandstone Group and Mercia Mudstone Group of the Cheshire basin is closely comparable to the diagenetic features in modern desert alluvium (Walker et al. 1978). Dissolution of detrital grains, replacement of detrital silicates by haematite and clays and the precipitation of authigenic illite, K-feldspar and quartz occur throughout the Triassic sequence of Cheshire regardless of the original depositional environment (Fig 3.6). The absence of authigenic albite in the Sherwood Sandstone Group is attributed to the lack of Na⁺ ions and is not thought to reflect a difference in the physicochemical conditions.

Deep-burial processes in the anhydrite-bearing mudstones of the Lower Keuper Marl in the Wilkesley borehole are thought to have controlled burial diagenetic events in the Tarporley Siltstone Formation. The consistent deep-burial assemblage of crystalline illite, ferroan carbonates and quartz cement and the secondary porosity from a variety of basins-North Sea (Bjørlykke et al. 1979), Texas Gulf Coast (Milliken et al. 1981) and British Permo-Triassic basins (Burley 1984) differs from that described above for the Tarporley Siltstone Formation of the Cheshire Basin where secondary porosity is of minor importance. Thus, the present study emphasises the importance of the relationship between the facies of the sedimentary environment and the eventual cements, fabric and porosity of the sediments following deep burial.

The Sherwood Sandstone Group adjacent to the basin margin were exposed to dilute,

typically neutral pH meteoric waters capable of dissolving carbonate and sulphate cements, following basin inversion in the Tertiary. More acidic solutions resulted in the precipitation of kaolinite at Alderley Edge. It is clear that interaction of sediments with modern groundwaters causes authigenic phases to become unstable and dissolve and care must be taken to recognise the evidence for the former existence of such cements.

Finally, this investigation has adequately demonstrated the widespread nature of the dissolution of ferromagnesian minerals, quartz and feldspar which is the mechanism suggested by a number of authors including Holmes et al. (1983) to be an important source of metals for red bed-hosted mineralisation.

REFERENCES

- ALI, A.D. 1982. *Triassic stratigraphy and sedimentology in Central England*. Unpublished PhD thesis, University of Aston.
- ALI, A.D. & TURNER, P. 1982. Authigenic K-feldspar in the Bromsgrove Sandstone Formation (Triassic) of Central England. *Journal of Sedimentary Petrology*, **52**, 187-198.
- ARTHURTON, R.S. 1980. Rhythmic sedimentary sequences in the Triassic Keuper Marl (Mercia Mudstone Group) of Cheshire, northwest England. *Geological Journal*, **15**, 43-58.
- BARBER, D.J., REEDER, R.J. & SMITH, D.J. 1985. A TEM microstructural study of dolomite with curved faces (saddle dolomite). *Contributions to Mineralogy and Petrology*, **91**, 82-92.
- BJØRLYKKE, K., ELVERHØI, A. & MALM, O. 1979. Diagenesis in Mesozoic sandstones from Spitzbergen and the North Sea- a comparison. *Geologisches Rundschau*, **68**, 1152-1171.
- BRINDLEY, G.W. & BROWN, G. 1980. (eds) *Crystal structures of clay minerals and their identification*. Mineralogical Society of London.
- BOLES, J.R. & FRANKS, S.G. 1979. Clay diagenesis in Wilcox Sandstones of southwest Texas: implications of smectite diagenesis on sandstone cementation. *Journal of Sedimentary Petrology*, **49**, 55-70.
- BURKE, K. 1976. Development of grabens associated with the initial rapture of the Atlantic Ocean. *Tectonophysics*, **36**, 93-112.
- BURLEY, S.D. 1984. Patterns of diagenesis in the Sherwood Sandstone Group (Triassic) United Kingdom. *Clay Minerals*, **19**, 403-440.
- BURLEY, S.D. & KANTOROWICZ, K. 1986. Thin section and S.E.M. textural criteria for the recognition of cement-dissolution porosity in sandstones. *Sedimentology*, **33**, 587-604.
- COLTER, V.S. 1978. Exploration for gas in the Irish Sea Basin. *Geologisches en Mijnbouw*, **57**, 503-516.

- COLTER, V.S. & BARR, K.W. 1975. Recent developments in the geology of the Irish Sea and Cheshire Basins. In: WOODLAND, A.W. (ed.) *Petroleum and the continental shelf of North-West Europe*, vol.1. Applied Science Publications, London.
- CURTIS, C.D. 1978. Possible links between sandstone diagenesis and depth related geochemical reactions in enclosing mudstones. *Journal of the Geological Society of London*, **135**, 107-118.
- CURTIS, C.D. 1983. Geochemistry of porosity enhancement and reduction in clastic sediments. In: BROOKS, J. (ed.) *Petroleum Geochemistry and Exploration of Europe. Geological Society of London Special Publication*, **12**, 113-126.
- FOLK 1974. *Petrology of sedimentary rocks*, Hemphills, Austin, Texas.
- FRIEDMAN, G.M. & RADKE, B.M. 1979. Evidence for sabkha overprint and carbonates of north-eastern North America and Queensland Australia. *Northeastern Geology*, **1**, 18-42.
- GOLDRICH, S.S. 1938. A study in rock weathering. *Journal of Geology*, **46**, 17-58.
- HOLMES, I.M., CHAMBERS, A.D., IXER, R.A., TURNER, P. & VAUGHAN, D.J. 1983. Diagenetic processes and the mineralization in the Triassic of Central England. *Mineralium Deposita*, **18**, 365-377.
- IRELAND, R.J., POLLARD, J.E., STEEL, R.J. & THOMPSON, D.B. 1978. Intertidal sediments and trace fossils from the Waterstones (Scythian-Anisian?) at Daresbury, Cheshire. *Proceedings of the Yorkshire Geological Society*, **41**, 399-436.
- JEANS, C.V. 1978. The origins of Triassic clay mineral assemblages of Europe with special reference to the Keuper Marl and Rhaetic parts of England. *Philosophical Transactions of the Royal Society*, **A289**, 551-636.
- KASTNER, M. & SIEVER, R. 1979. Low temperature feldspars in sedimentary rocks. *American Journal of Science*, **279**, 435-479.
- MACCHI, L. & VELTKAMP, C.J. 1985. Compound quartz and feldspar

- overgrowths from the Helsby Sandstone Formation (Triassic) of Cheshire, northwest England. *Geological Journal*, **20**, 281-285.
- MILLIKEN, K.L., LAND, L.S. & LOUCKS, R.G. 1981. History of burial diagenesis determined from isotope geochemistry, Frio Formation, Brazoria County, Texas. *Bulletin of the American Association of Petroleum Geologists*, **65**, 1397-1413.
- POOLE, E.G. & WHITEMAN, A.J. 1966. Geology of the country around Northwich and Whitchurch. *Memoirs of the Geological Survey of Great Britain*, London.
- RADKE, B. & MATTHIS, R.L. 1980. On the occurrence and formation of saddle dolomite. *Journal of Sedimentary Petrology*, **50**, 1149-1168.
- REYNOLDS, D.L. 1929. Some new occurrences of potash feldspar. *Geological Magazine*, **66**, 390-399.
- SCHMIDT, V. & McDONALD, D.A. 1979. The role of secondary porosity in sandstones. In: SCHOLLE, P.A. & SCHLUGER, P.R. (eds) Aspects of diagenesis. SEPM Special Publication, 26, 209-225.
- STONELEY, R. 1982. The structural development of the Wessex Basin. *Journal of the Geological Society*, **139**, 545-554.
- THOMPSON, D.B. 1969. Dome-shaped aeolian dunes in the Frodsham Member of the so-called 'Keuper' Sandstone Formation (Scythian-Anisian: Triassic) at Frodsham, Cheshire. *Sedimentary Geology*, **3**, 263-289.
- THOMPSON, D.B. 1970. Sedimentation in the Triassic (Scythian ?) red pebbly sandstones in the Cheshire Basin and its margins. *Geological Journal*, **1**, 183-215.
- THOMPSON, D.B. 1983. *Permo-Trias of Cheshire and East Irish Sea Basins*. Poroperm Excursion Guide, Poroperm-Geochem Ltd, Chester.
- TURNER, P. 1980. *Continental Red Beds*. Elsevier, Amsterdam.
- WALKER, T.R., WAUGH, B. & CRONE, A.J. 1978. Diagenesis in first-cycle desert alluvium of Cenozoic age, southwestern United States and northwestern Mexico. *Bulletin of the Geological Survey of America*,

89, 146-155.

- WALTON, N.R.G. 1981. A detailed hydrogeochemical study of groundwaters from the Triassic sandstone aquifer of south west England. *Report of the Institute of Geological Sciences*. No.81/5.
- WARRINGTON, G., AUDLEY-CHARLES, M.G., ELLIOT, R.E., EVANS, W.B., IVIMEY-COOK, H.C., KENT, P.E., ROBINSON, P.L., SHOTTON, F.W. & TAYLOR, F.M. 1980. *A correlation of the Triassic rocks of the British Isles*. Geological Society of London Special Publication.
- WAUGH, B. 1970a. Formation of quartz overgrowths in the Penrith Sandstone (Lower Permian) of northwest England as revealed by scanning electron microscopy. *Sedimentology*, **14**, 309-320.
- WAUGH, B. 1970b. Petrology, provenance and silica diagenesis of the Penrith Sandstone (Lower Permian) of northwest England. *Journal of Sedimentary Petrology*, **40**, 1226-1240.
- WAUGH, B. 1978. Authigenic K-feldspar in British Permo-Triassic sandstones. *Journal of the Geological Society of London*, **135**, 51-56.
- WILLIAMS, D. 1973. *The sedimentology and petrology of the New Red Sandstone of the Elgin Basin*. Unpublished Ph.D. thesis, University of Hull.

CHAPTER 4
THE DIAGENESIS AND Pb-Ba-F MINERALISATION OF
PERMO-TRIASSIC SANDSTONES OF THE INNER MORAY FIRTH
BASIN.

ABSTRACT

Up to 135m of Permo-Triassic red beds are preserved on the southern margin of the Inner Moray Firth Basin, northeast Scotland, and are exposed on the Moray coast near Lossiemouth. The sequence consists of continental fluvial and aeolian sandstones, overlain by a palaeosol horizon (the Cherty Rock), and range in age from Scythian to Norian. New petrographic evidence has established a sequence of diagenetic and mineralising events including quartz and feldspar overgrowths, illite, haematite, calcite, fluorite and barite. Sulphide mineralisation, in the form of galena and pyrite is largely confined to the Cherty Rock.

Base metals, Ba, F and sulphur are likely to have been derived from the Mesozoic sediments in the Inner Moray Firth Basin. The sulphur isotope data for the barite mineralisation (mean $\delta^{34}\text{S} +29\text{‰}$) are not consistent with simple derivation of sulphur from evaporite horizons, and the range of $\delta^{34}\text{S}$ values for pyrite ($+2.8 \text{‰}$ to 27.0‰) preclude a magmatic source for the sulphides. The sulphur-rich Brora Coal and Kimmeridgian Clay Formations may have supplied the sulphur for the mineralisation at Elgin.

Fluid inclusion studies on quartz gangue revealed that the mineralising fluids were warm ($\sim 100^\circ\text{C}$), saline ($\sim 16\text{wt\% NaCl}$) solutions similar to those thought to have been responsible for some Mississippi Valley-type deposits. Two ore-forming solutions are considered; the first involves a reducing fluid transporting metals and sulphur to the site of ore deposition. On the other hand, oxidising basinal brines may have been responsible for metal transport with sulphide precipitation triggered by the presence of H_2S at the site of ore formation. The favoured genetic model involves expulsion of basinal brines from the Inner Moray Firth Basin. Compaction caused brines to flow

towards the basin margins where sulphides, barite and fluorite were precipitated in porous Permo-Triassic sandstones below the impermeable cover of the Jurassic shales.

4.1. INTRODUCTION

The Moray Firth Basin lies between latitudes 57° 30'N and 59° 10'N and longitudes 1° 00'E and 4° 00'W. The Inner Moray Firth Basin is a half-graben structure in which the major controlling faults are the Great Glen and Helmsdale faults to the north west (McQuillin et al. 1982) (Fig.4.1). Basin development was initiated in the early Permian as a result of large scale E-W extensional tectonism (Glennie 1984). Strike-slip movements along the Great Glen fault continued through to the Cretaceous followed by a period of structural stability prior to the onset of uplift and erosion in the Tertiary. The observed subsidence within the basin (~3 km) corresponds closely to the proposed amount of extension where the lithospheric stretching factor, $\beta = 1.06$ (McQuillin et al. 1982).

Within the basin, continental clastics of Permo-Triassic age rest unconformably upon Devonian red beds and reach thicknesses in excess of 1500m near the Great Glen fault (Frostick et al. 1988). Up to 2200m of Jurassic marginal and marine sediments have been recorded from the basin (Chesher & Lawson 1983). Cessation of fault movement in the Upper Cretaceous was reflected by widespread Chalk deposition (Linsley et al. 1980) whilst tilting towards the north east and tectonic inversion marked the final stages of basin development (McQuillin et al. 1982). A minimum of 500-700m of uplift is indicated by organic maturation data (vitrinite reflectance, sporomorph colour, solvent extract and extractable hydrocarbon: organic carbon ratios and the carbon preference index of nC21-nC33 alkanes; Pearson & Watkins 1983) from the inner basin.

Up to 135m of Permo-Triassic red beds are preserved on the Moray coast near Lossiemouth (Fig. 4.1) and represent deposition on the southern margin of the Inner Moray Firth Basin. These onshore sediments are thought to be laterally equivalent to finer Triassic siliciclastic sediments within the basin; they comprise fluvial and aeolian sandstones which were derived from south westerly sources and are overlain by a complex palaeosol horizon (Peacock et al. 1968; Frostick et al. 1988). The sediments

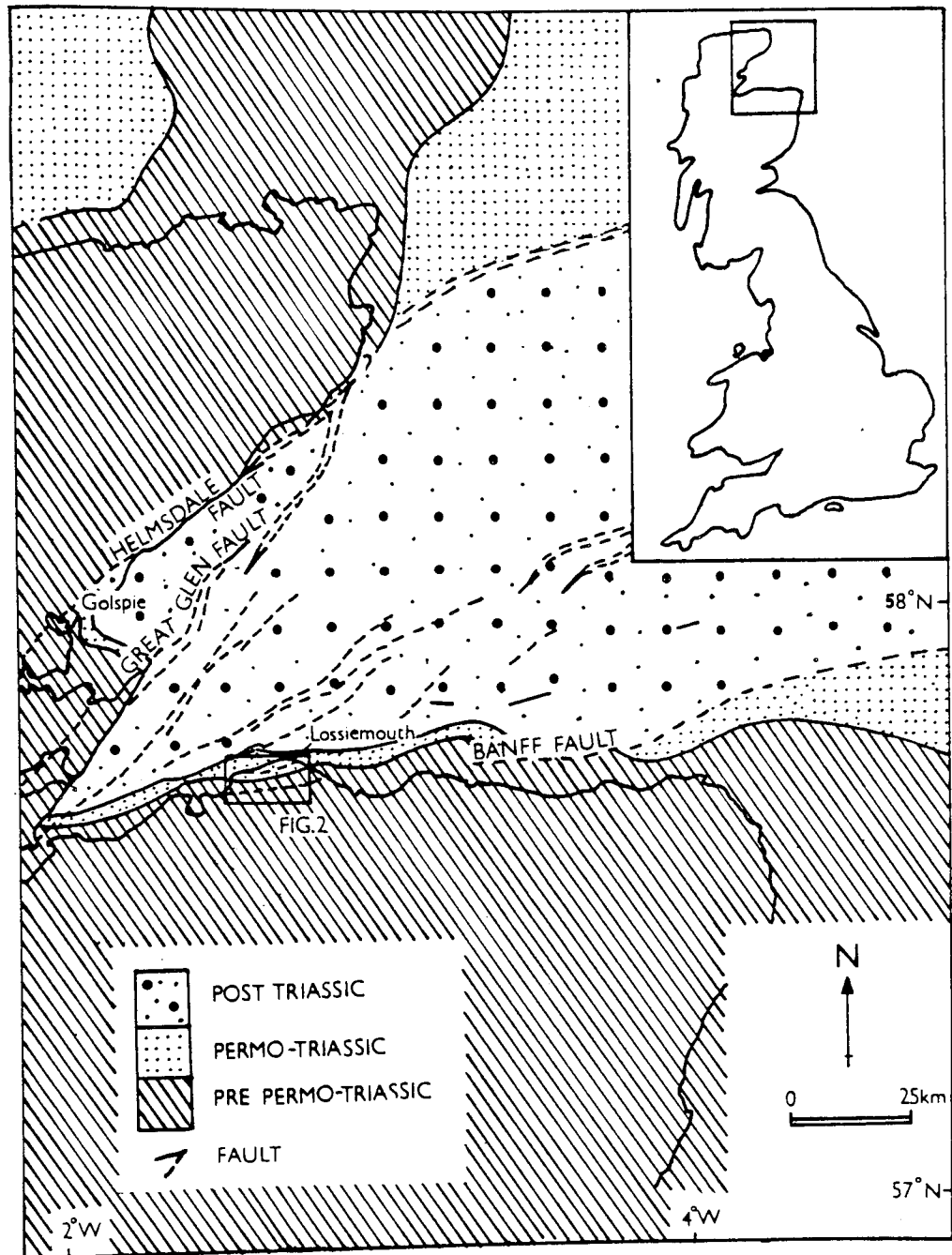


Figure 4.1. Geological map of north east Scotland showing the location of the Inner Moray Firth Basin. The field area on the southern margin of the basin is shown, along with the major faults. Inset shows the location of the Moray Firth Basin in the British Isles.

range in age from Scythian to Norian and are hosts to barite, calcite, haematite, fluorite, silica, pyrite and galena mineralisation (Peacock et al. 1968; Williams 1973).

The controversy and interest concerning the age and stratigraphy of the Elgin sandstones has dominated previous research in the area. Early workers such as Judd (1873) and Newton (1893) assigned the sandstones to the Permo-Triassic with the latter author distinguishing Upper Triassic and Lower Triassic units on the basis of reptilian remains. The Permo-Triassic sandstones were subdivided into the Hopeman, Burghead and Lossiemouth Sandstone Formations in a recent revision of Triassic stratigraphy in the British Isles (Warrington et al. 1980) and this nomenclature is used in this study. Newton (1893) recognised the Hopeman and Lossiemouth Sandstone Formations but the unfossiliferous Burghead Sandstone Formation was not assigned separate status until recently (Watson et al. 1948; Westoll 1951). Later studies by Walker (1961) and Benton & Walker (1985) have resulted in a more precise estimate of the timing of sediment deposition. Early stratigraphic and sedimentological studies include those of Watson & Hickling (1914) and Mackie (1897, 1901a, 1901b). An aeolian origin was postulated by the latter author (Mackie 1901b) whereas a low temperature groundwater origin was invoked for the fluorite. This earlier work is summarised by Peacock et al. (1968), who together with Williams (1973) give a detailed account of the sedimentology and petrology of the quartz arenites and sub-arkoses in the Permo-Triassic succession at Elgin. The interpretation of the deformation structures within the Hopeman Sandstone Formation (Glennie & Buller 1983) and the interpretation of the same unit as a system of complex star dunes (Clemmensen 1988) represent the latest sedimentological studies in the area.

The Permo-Triassic sandstones of Elgin have a complex diagenetic history unlike that generally ascribed to sub-arkosic to quartz arenitic sands. Calcite, barite and fluorite cements are widespread and sulphide mineralisation is concentrated within the Cherty Rock horizon. The overall aim of the present work is to present a detailed model for the diagenesis and mineralisation of the Permo-Triassic sandstones of Lossiemouth.

4.2 BASIN EVOLUTION

The Moray Firth Basin can be subdivided into the Inner and Outer Moray Firth

Basins on the basis of differing fault patterns and Bouger anomaly characteristics (McQuillin et al. 1982; Glennie 1984; Barr 1985). The Inner Moray Firth Basin is characterised by a complex fault pattern with a predominantly NE-SW trend and with major bounding faults including the Great Glen fault to the north and the Banff fault on the southern basin margin. In the Outer Moray Firth Basin, faults are aligned WNW-ESE (Linsley et al. 1980; Frostick et al. 1988). A residual gravity anomaly confined to the Inner Moray Firth Basin is interpreted as being derived from buried Caledonian Granites (Barr 1985). The overall implications of the gravity modelling in the inner basin are that there has been negligible post-Triassic crustal thinning and that the evolution of the inner basin cannot be explained by the uniform lithospheric stretching model of Mackenzie (1978) due to the lack of isostatic compensation (Barr 1985).

McQuillin et al. (1982) envisage four distinct phases of basin evolution, beginning with the development of a half-graben form during the Permo-Triassic tilted towards the Great Glen and Helmsdale faults in the north. Dextral transcurrent movement along the Great Glen fault during the Jurassic and early Cretaceous continued into the late Cretaceous when the basin became more stable. The final stage of basin development occurred in the Tertiary when uplift is thought to have resulted in the erosion of at least 1000m of the sediment deposited within the Inner Moray Firth Basin (McQuillin et al. 1982).

Early Carboniferous igneous activity in the Moray Firth area coincided with the cessation of differential fault movement (Glennie 1984). Basin development in the Inner Moray Firth was initiated in the Permian and throughout the Mesozoic the main control on sedimentation was normal faulting related to the Kimmerian movements (Linsley et al. 1980). Facies distributions and offshore thicknesses of the Permian Rotliegend in the Inner Moray Firth Basin remain incompletely known (Glennie 1984), although up to 600m of conglomerates and shales are preserved in the vicinity of the Great Glen fault. The Hopeman Sandstone Formation is thought to be the onshore equivalent of the Rotliegend and overlying Wiessliend (Glennie & Buller 1983). Approximately 60m of aeolian dune sands have been found to contain reptile footprints (Benton & Walker

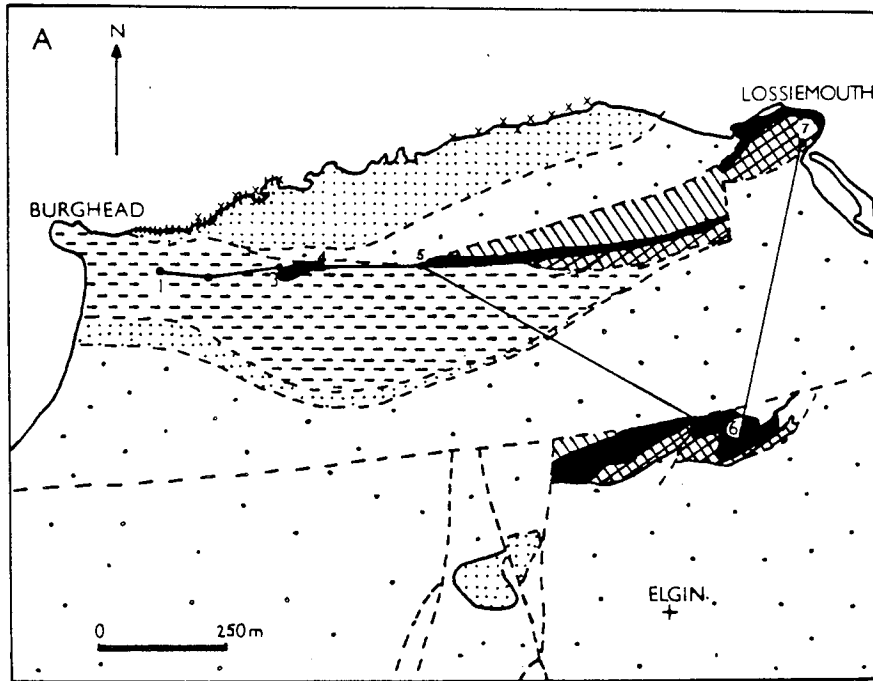
1985) and as a consequence have been tentatively dated as early Triassic or late Permian. Large scale deformation structures within these Hopeman Sandstones were interpreted by Glennie & Buller (1983) as structures formed by air escape through the wet surface of the aeolian dunes during the Zechstein transgression. An alternative hypothesis advocated by Peacock (1966) and supported by Frostick et al. (1988) involves soft sediment deformation due to slumping after heavy rainfall. Widespread barite, calcite and fluorite mineralisation in the Hopeman Sandstone Formation is seen to postdate these deformation structures.

Fluvial and aeolian sandstones were deposited in the Moray Firth Basin during the Triassic and have limited onshore exposure at Golspie, Sutherland (Batten et al. 1986) and at Lossiemouth, Morayshire where they are extensively mineralised. A reconstructed section across the basin at this time shows a wedge-shaped, half-graben structure with the Great Glen fault developing in a dip-slip manner (Frostick et al. 1988) and up to 500m of predominantly fine-grained Triassic sediments adjacent to the fault (McQuillin et al. 1982). The first movements on the Wick and Banff faults are thought to have occurred about this time and were probably concurrent with Triassic rifting in the North Sea (Ziegler 1982). Offshore Triassic sediments can be subdivided into a lower sandy unit and an upper unit comprising inter-bedded sand, silt and clay (Frostick et al. 1988). The onshore succession on the southern basin margin is postulated to be laterally equivalent to the Triassic sequence offshore and consists of the Burghead and Lossiemouth Sandstone Formations and the Cherty Rock (Fig.4.2). The Burghead Sandstone Formation attains a maximum thickness of 73m and comprises fluvial, pebbly sandstones thought to have been deposited in a braided river system. Palaeocurrent directions obtained from foresets show the main direction of flow towards the E and NE. The Lossiemouth Sandstones are mainly aeolian deposits and are, at least partly, contemporaneous with the Burghead Sandstone Formation (Peacock et al. 1968) (see Fig. 4.2). Barite, galena and fluorite are found on joint planes and minor fault surfaces within the Lossiemouth Sandstones. Strong evidence for the assignment of the Lossiemouth Sandstone to the Lower Norian (Upper Triassic) was cited by Benton & Walker (1985) in their study of fossil reptile remains. The Cherty Rock has been

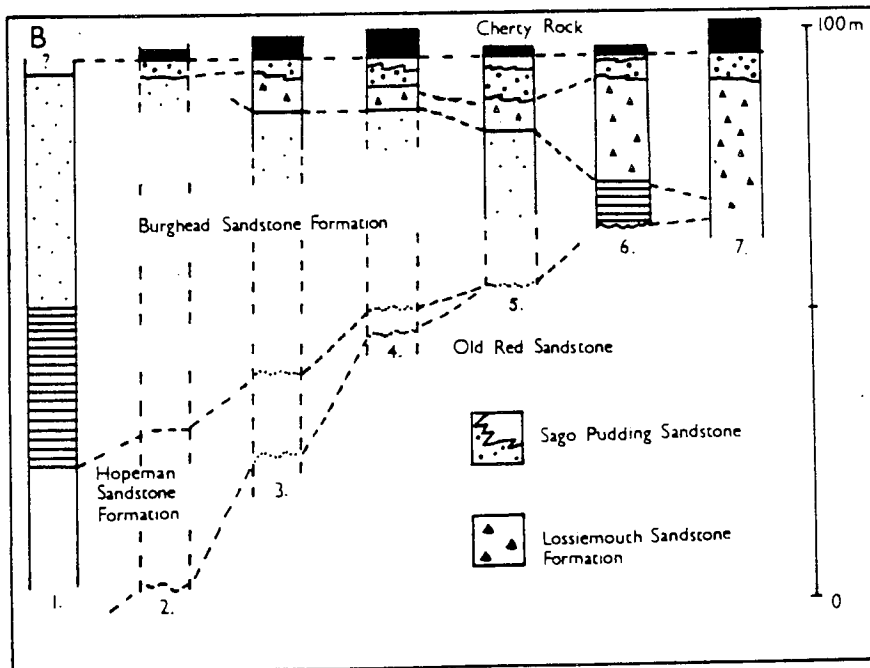
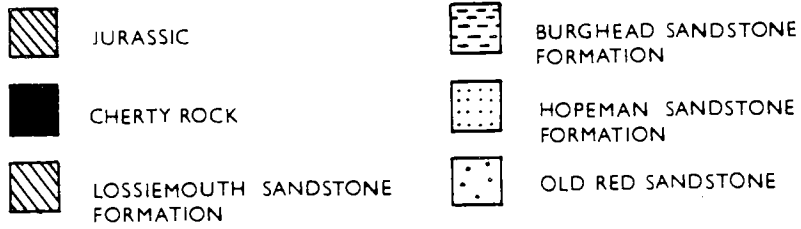
Figure 4.2a. A simplified geological map of the Elgin district. The principal sampling sites for the isotopic study are shown, together with the distribution of fluorite and barite in the Hopeman and Burghead Sandstone Formations. Barite mineralisation is represented by crosses, whereas fluorite is represented by vertical lines.

b. The stratigraphical relationships between the Hopeman, Burghead and Lossiemouth Sandstone Formations, and the Cherty Rock.

FIGURE 4.2



KEY



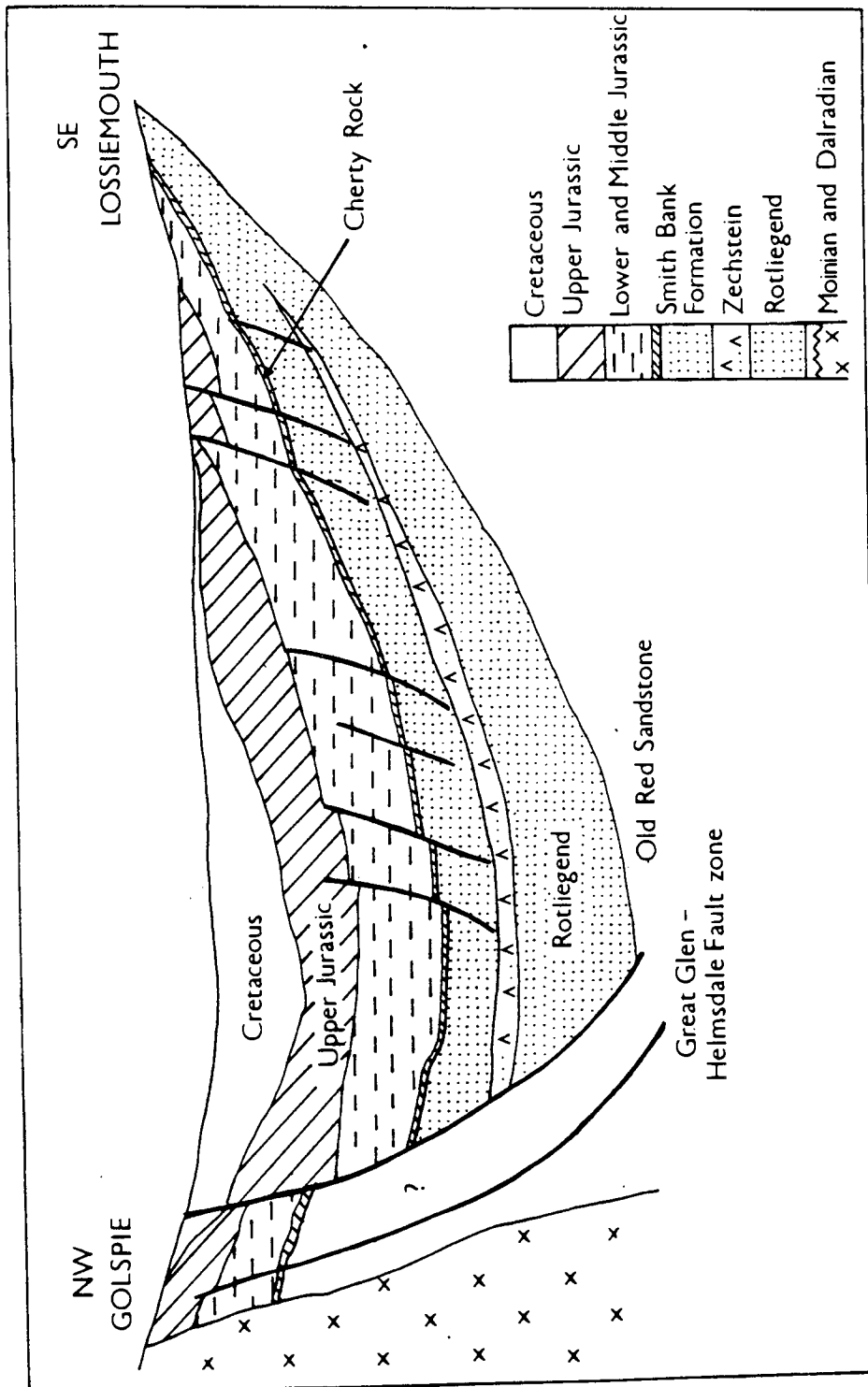
interpreted as a laterally extensive, complex palaeosol horizon (Peacock et al. 1968, Williams 1973, Naylor et al. 1988 in press) which occurs throughout the Moray Firth Basin. Its presence in the basin led Frostick et al. (1988) to suggest that the Rhaetic was a period of tectonic quiescence. Outcrops of the horizon near Lossiemouth show it to host barite-calcite-pyrite-fluorite-galena mineralisation which clearly postdates the early pedogenic evolution of the horizon.

It appears that the depocentre for post-Rhaetic sedimentation shifted to the north-east as the Helmsdale fault (Fig.4.1) became the major tectonic influence in the basin. Jurassic and Lower Cretaceous sediments reach thicknesses in excess of 3000m in the vicinity of the Great Glen fault, with estuarine shales and mudstones of Liassic age overlain by Jurassic marine sediments (McQuillin et al. 1982) (Fig. 4.3). Thicknesses of up to 1000m of Upper Jurassic sediments are preserved in the basin (Chesher & Lawson 1983) and include the Kimmeridge Clay and Heather Formations (Fig. 4.3) which are a suite of organic-rich shales and mudstones. Continued fault activity and related subsidence resulted in the deposition of at least 1000m of Lower Cretaceous sediments (Chesher & Lawson 1983). Basin uplift during the Middle and Late Palaeocene times caused early Tertiary and Upper and Lower Cretaceous sediments of the inner basin to be removed by erosion. Consequently, the Inner Moray Firth Basin must have reached its present day structural configuration by the late Palaeocene.

Thus, basin evolution is thought to have been dominated by dextral strike-slip movements along the Great Glen fault which were initiated in the Permo-Triassic and continued into the Cretaceous (McQuillin et al. 1982). Palinspastic reconstructions by Barr (1985) are consistent with the suggestion by McQuillin et al. (1982) that 6.4 km of post-Triassic dextral strike-slip movements occurred along the Great Glen fault incorporating 2.5 km of post-Jurassic displacement. The mineralisation in the relatively thin sequence of Permo-Triassic red beds on the southern basin margin is thought to be intimately related to the structural and sedimentological development of the Moray Firth Basin as a whole. The aim of the present study is to link the genesis of the barite-fluorite-sulphide mineralisation to the events which marked basin evolution.

Figure 4.3. A schematic section across the Inner Moray Firth Basin showing the relationship between the exposures near Elgin and the sediments in the basin centre. The section also illustrates the present day structural configuration of the Inner Moray Firth Basin. The Great-Glen and Helmsdale faults are thought to have controlled sedimentation during Permo-Triassic times whilst block-faulting dominated the Jurassic. (Based on seismic data from McQuillin et al. 1984).

FIGURE 4.3



4.3 SEDIMENTOLOGY OF THE EXPOSURES ON THE SOUTHERN BASIN MARGIN

The Hopeman Sandstone Formation (Fig. 4.2) comprises a series of aeolian sandstones with large scale cross-stratification (Peacock 1966; Peacock et al. 1968). Individual dunes appear to have reached heights of at least 30m in Clashach Quarry (Fig. 4.2) and have been variously interpreted as a sequence of transverse dunes (Glennie & Buller 1983) or alternatively, as representing a star dune complex (Clemmensen 1988). Individual beds within the dunes have thicknesses ranging from 0.5-2m and palaeocurrent data obtained from deeply-dipping foresets reveal that the palaeowind direction was from the northeast. Rare pebble-bearing and ripple-marked sandstones of fluvial origin were observed in the Hopeman Sandstone Formation but no evidence was found in the onshore succession for the Zechstein marine transgression.

The subdivision of the Hopeman Sandstone Formation by Glennie & Buller (1983) into an upper and lower unit on the basis of varying degrees of large-scale disruption of the dune bedding by soft sediment deformation structures is considered to be largely invalid following detailed field observations during the present study. This subdivision was not supported in a recent study by Clemmensen (1988) who confirmed that the deformation structures are randomly distributed and were not stratigraphically significant. For the purposes of the present study the Hopeman Sandstone Formation is considered as a single unit of aeolian dune sands. A number of mechanisms have been suggested to account for the pervasive deformation within the dune sands; however, the controversy over the origin of these escape structures is beyond the scope of the present study. Suffice to say that cementation and mineralising events appear to postdate these structures.

The sediments of the overlying Burghead Sandstone Formation are fluvial deposits, consisting of shallow cross-stratified coarse sandstone units with low-angle foreset inclinations. The units are stacked in a series of fining-up cycles whose individual thickness varies between 0.5 and 1m (Fig. 4.4). The sediments are generally poorly sorted, they contain mudflake intraclasts as well as abundant pebbles (mean diameter 5cm), the presence of which implies a relatively high energy depositional

environment. Limited palaeocurrent data obtained from foresets and pebble orientations are consistent with flow towards the east and correspond closely to data presented by Williams (1973) and Frostick et al. (1988).

The absence of fine-grained sediments typical of floodplain depositional environments, and the lack of lateral accretion surfaces in the so called 'point bar deposits' described by Williams (1973) have led to the sediments being reinterpreted as channel and bar sands deposited in broad shallow channels associated with a braided river system. Frostick et al. (1988) consider the Burghead Sandstone Formation to represent ephemeral stream deposits on the passive margin of the Moray Firth half-graben structure. Cyclicity within the sediments is thought to be a direct response to fault movements on the northern edge of the basin.

The Lossiemouth Sandstone Formation is approximately 30 m thick and is made up of aeolian dune sands with minor fluvial intercalations. At Lossiemouth these sands succeed a series of water-lain sediments (possibly the eastern equivalent of the Burghead Beds). Due to the unfossiliferous nature of the Burghead Beds the relationship between the two units near Burghead (Fig. 4.2) remains unclear, although it has been suggested that the Lossiemouth Sandstone Formation passes laterally into the Burghead Beds. The sediments within the Lossiemouth Sandstone Formation further east at Lossiemouth and Spynie are predominantly uniformly bedded sands whose attitude suggests that the net sand transport direction was similar to that for the underlying Hopeman sands (north east). With the exception of bedding, internal structures have been obliterated by pervasive cements of silica and occasionally calcite. The Lossiemouth Sandstone Formation is thought to represent an aeolian and lacustrine environment with occasional fluvial input at the top of the sequence. The formation of the laterally extensive Cherty Rock succeeds the deposition of the Lossiemouth Sandstone Formation. This latter horizon has been discussed in detail by Naylor et al. 1988 (in press) and has been interpreted as a silicified calcrete whose deposition marked the end of Triassic sedimentation in the Inner Moray Firth Basin.

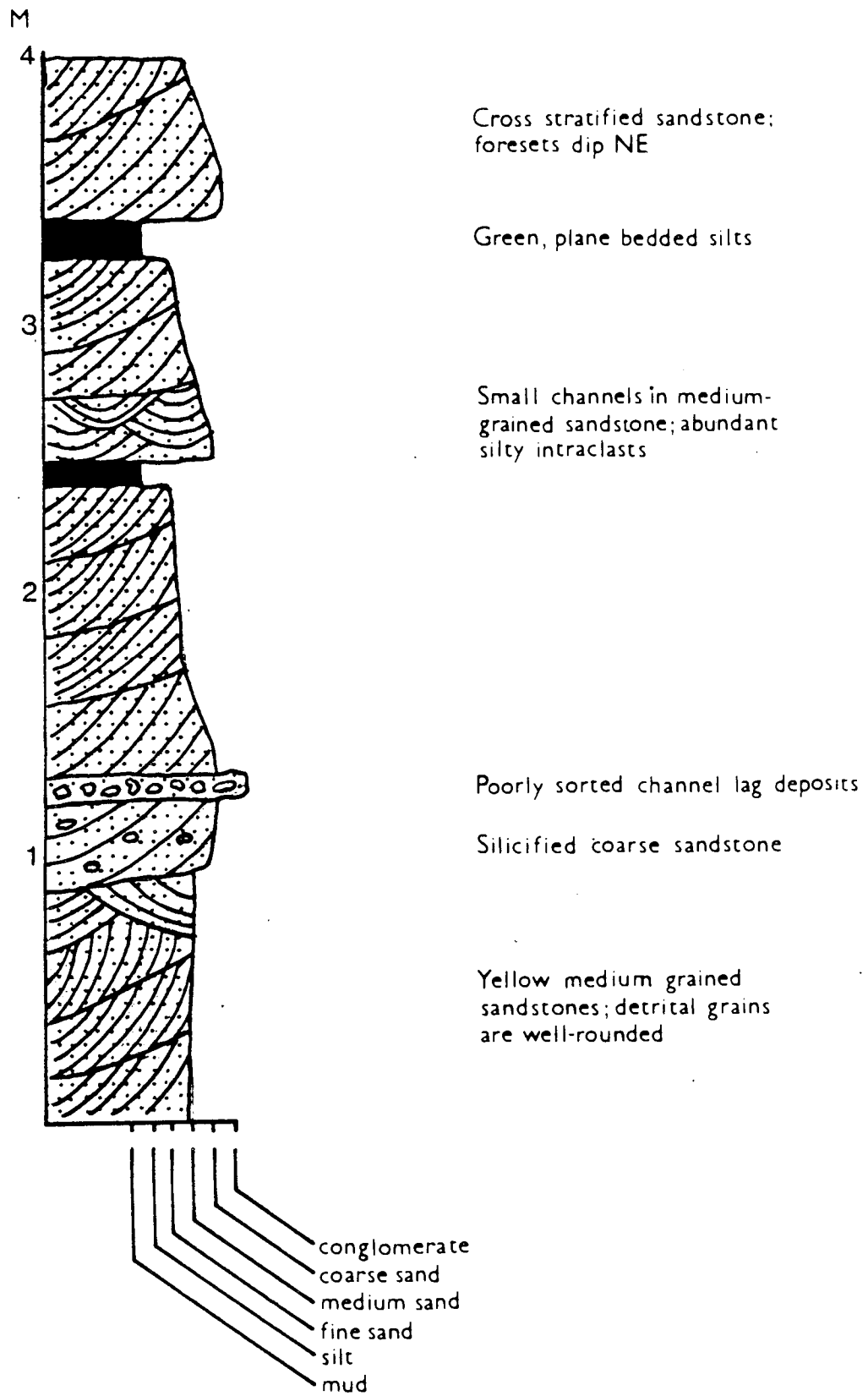


Figure 4.4. Sedimentological log of the Burghead Sandstone Formation, Burghead, GR 69241082.

4.4 PETROGRAPHY

The primary objective of the petrographic study was to delineate a paragenetic sequence for the precipitation of authigenic phases within the Permo-Triassic sediments of Morayshire. Over seventy thin sections were examined petrographically and, of these, more than thirty were point-counted for detrital grain components, authigenic minerals and porosity (Table 4.1). Other techniques employed include cathodoluminescence petrography (CL), scanning electron microscopy (SEM) with energy dispersive analysis to facilitate mineral identification and to provide semi-quantitative chemical analyses. In addition, electron microprobe analysis was carried out on selected samples. The electron probe was operated with an accelerating voltage of 15 k.v. and conventional silicate standards were used throughout with the exception of BaO for which barite was used. (Operating conditions and standards are detailed in Appendix I)

The Hopeman Sandstone Formation, Burghead Beds and Lossiemouth Sandstone Formation have similar detrital mineralogies dominated by quartz and are classified as quartz arenites, sub-arkoses and sub-litharenites (Folk 1974)(Fig. 4.5). Point count data reveal that detrital feldspars are a relatively minor component of the detrital grains comprising approximately 1.9% of the whole rock. The majority of feldspars are tabular microclines with subsidiary orthoclase and remain relatively unaltered. This contrasts with the altered K-feldspars from Permo-Triassic sequences elsewhere in Britain (Waugh 1978). The absence of plagioclase in the Elgin sandstones has been attributed to the high grade metamorphism in the source area (Williams 1973). Muscovite and biotite micas represent a minor constituent in the fluvial sandstones of the Burghead Sandstone Formation but are largely absent in the aeolian sediments of the Hopeman and Lossiemouth Sandstone Formations. Sub-rounded rock fragments consist of meta-quartzites, schists, chert, and altered igneous fragments which are occasionally tourmaline-bearing. Other lithologies recorded by Peacock et al. (1968) and Williams (1973) are aplite, granulite, rhyolite, hornfels and calcrete ('cornstones') and sandstones probably sourced in the Devonian to the south. Zircon is the dominant constituent of the heavy mineral assemblage within the sandstones which also comprises tourmaline, rutile, sphene, epidote, garnet, augite, anatase and enstatite.

FIGURE 4.5

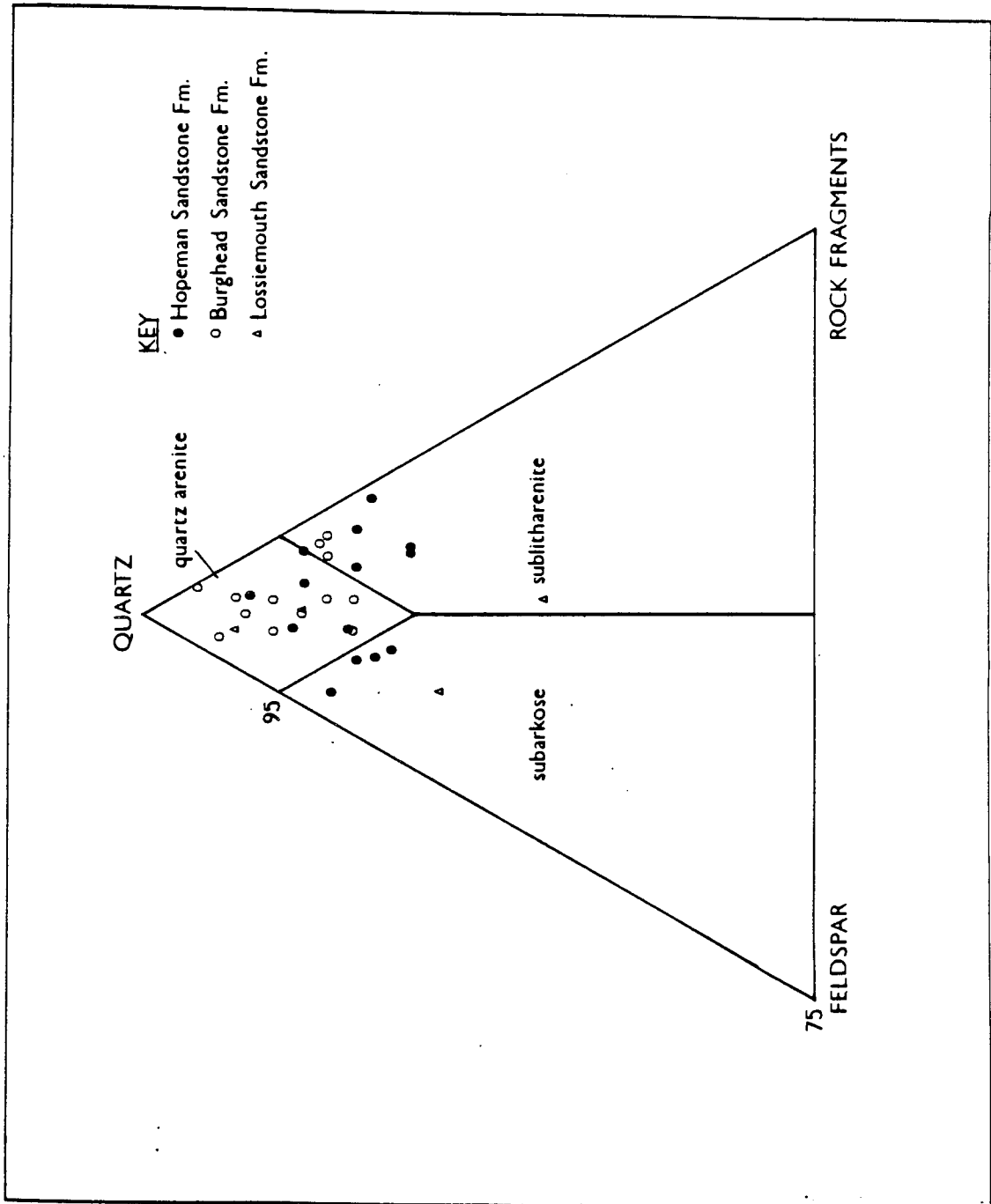


Figure 4.5 Mineralogical classification of the Permo-Triassic sandstones of Elgin (after Folk 1974).

TABLE 4.1

	HSF *										BSF							LSF				
	10	27	61	32	75	77	81	1	2	6	7	5	38	53	55	57	52	92	99	101		
Monocrystalline quartz	48.6	56.2	49.6	44.6	56.6	42.4	52.4	53.2	47.0	71.2	53.0	47.6	48.8	52.0	51.4	56.8	53.6	49.8	63.8	57.0		
Polycrystalline quartz	4.8	3.6	11.4	5.4	3.6	13.0	4.8	13.6	10.4	9.2	10.2	13.2	7.6	6.8	11.4	15.0	2.2	3.4	9.2	3.0		
K feldspar	1.8	0.6	1.2	3.0	2.8	2.0	1.8	1.8	0.8	TR	0.8	0.8	1.2	1.4	1.8	2.0	4.8	4.0	2.0	1.4		
Plagioclase	-	-	-	-	-	-	-	0.8	0.2	-	-	-	-	-	-	-	-	0.2	-	-		
Rock fragments	4.0	3.2	4.0	1.0	2.2	4.4	3.6	3.4	3.2	1.0	1.6	3.6	1.0	1.8	1.0	0.6	2.0	5.0	2.8	0.8		
Mica	-	-	-	-	-	-	-	TR	-	-	-	TR	TR	TR	TR	0.4	-	-	0.2	-		
Opaque/heavy	TR	TR	TR	TR	TR	TR	TR	TR	TR	TR	TR	TR	TR	TR	TR	TR	TR	TR	TR	TR		
Detrital clay†	3.6	10.8	1.0	1.8	2.0	0.6	2.0	5.0	4.8	5.0	1.2	4.4	1.0	1.4	TR	0.2	1.0	TR	2.4	4.0		
Quartz overgrowth	7.0	6.4	5.2	1.4	2.0	2.6	12.6	19.6	8.8	10.4	3.0	11.2	1.2	10.0	9.0	7.6	7.0	31.0	13.6	19.4		
Fsp overgrowth	0.2	0.4	TR	0.2	0.2	0.2	0.2	-	0.2	TR	R	TR	R	0.6	TR	TR	0.2	-	0.2	0.4		
Calcite	-	-	-	29.6	-	-	-	-	-	-	-	17.2	30.0	3.2	-	-	25.6	-	-	-		
Fluorite	-	-	-	-	26.8	32.8	-	-	22.2	0.4	29.0	0.6	-	0.4	-	-	-	-	-	-		
Barite	-	-	21.4	-	-	1.6	1.8	-	-	-	-	TR	-	-	-	-	-	-	-	-		
Replacement illite	0.2	TR	TR	TR	TR	TR	TR	TR	TR	TR	TR	TR	TR	TR	-	-	TR	TR	TR	-		
Pore illite	TR	TR	1.0	TR	0.8	TR	TR	0.2	0.8	2.2	-	0.2	TR	TR	1.8	0.6	2.6	0.6	2.4	4.0		
POROSITY																						
intergranular	29.8	18.8	4.6	13.0	3.0	0.4	20.8	2.4	1.6	0.6	1.2	1.2	9.2	22.0	23.2	17.0	1.0	6.0	3.4	10.0		
dissolution	TR	TR	TR	TR	TR	TR	TR	TR	TR	TR	TR	TR	TR	TR	TR	TR	TR	-	TR	TR		
TOTAL	62.8	74.4	67.8	55.8	67.2	62.4	64.6	77.8	63.4	86.4	66.8	69.6	59.6	63.8	66.0	74.8	63.6	62.4	80.4	66.2		
detritus	8.2	6.8	27.6	31.2	29.8	37.2	14.6	19.8	32.0	13.0	32.0	29.2	31.2	14.2	10.8	8.2	35.4	31.6	16.2	23.8		
authigenic	28.8	18.8	4.6	13.0	3.0	0.4	20.8	2.4	1.6	0.6	1.2	1.2	9.2	22.0	23.2	17.0	1.0	6.0	3.4	10.0		
porosity																						

TABLE 4.1 Point count data for the Elgin sandstones.

Previous petrographic studies (Dunham 1952; Peacock et al. 1968; Williams 1973) are essentially descriptive, although Williams (1973) established a paragenetic sequence for the various cements with respect to the Cherty Rock. Mixed haematite-clay grain coatings, quartz and feldspar overgrowths, calcite, fluorite and barite commonly cement the Permo-Triassic sandstones of Elgin and detailed textural studies have revealed the following sequence of authigenic mineral formation: i) illite ii) quartz iii) feldspar iv) authigenic haematite v) calcite and fluorite and; vi) barite.

4.4.1. QUARTZ AND FELDSPAR

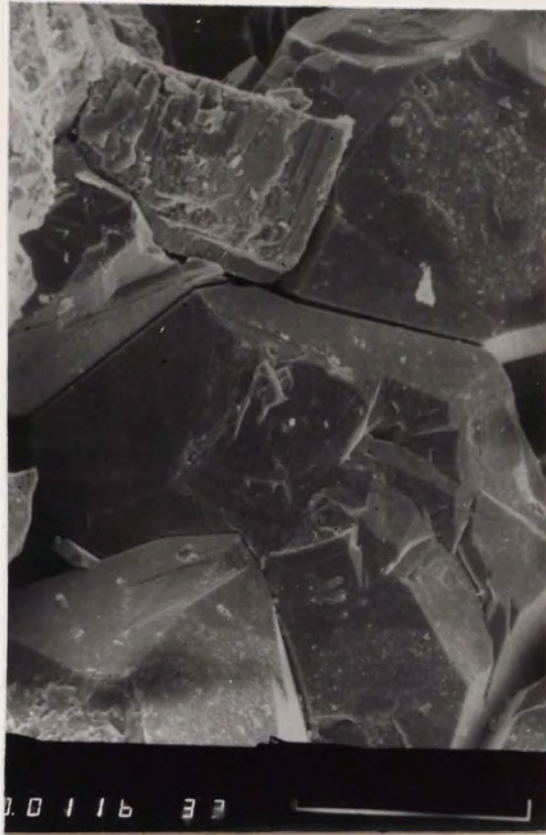
Authigenic quartz and K-feldspar formation postdate the initial precipitation of illite pore-lining cements. Syntaxial quartz overgrowths are common throughout the Hopeman Sandstone Formation and form locally significant pore-occluding cements in both the Burghead and Lossiemouth Sandstone Formations (Plate 4.1). The latter formation is highly silicified in its uppermost part but becomes increasingly calcareous towards the base. It would appear that the development of quartz cements is directly related to the environment of deposition, with fluvial sandstones particularly prone to extensive quartz cementation during early diagenesis. The resulting effective reduction in porosity and permeability may account for the concentration of later fluorite and barite cements in the more porous Hopeman Sandstone Formation.

The precipitation of silica is not confined to the period of authigenic overgrowth formation. Quartz veins occur within the Hopeman Sandstone Formation where they commonly trend E-W and a late phase of quartz deposition is associated with the Cherty Rock where quartz occurs as euhedral, drusy crystals infilling cavities and in the form of veins. The cross-cutting nature of the quartz veins in the silicified calcrete horizon at Lossiemouth illustrates that their emplacement postdates the major silicification events in the Cherty Rock. Most of the fluid inclusion measurements were carried out on fluid inclusions hosted by this later generation of quartz.

Authigenic feldspar occurs as overgrowths developed around detrital microcline and orthoclase grains. The majority of feldspar grains have associated overgrowths comprising rhombic and euhedral crystals (Plate 4.2). These overgrowths are unaltered, they exhibit no twinning or perthitic texture and in the case of microcline are not in

Plate 4.1 Scanning electron micrograph of well-developed authigenic quartz overgrowths in the Burghead Sandstone Formation. Scale bar = 116 μm .

Plate 4.2 Scanning electron micrograph of authigenic K-feldspar in the Hopeman Sandstone Formation. The overgrowths consist of oriented, stacked crystals of adularia habit. Scale bar = 25 μm .



optical continuity with the host grain. Some orthoclase hosts in these sandstones have optically continuous overgrowths but the majority have not. This observation is at variance with Waugh's (1978) description of authigenic feldspars within Permo-Triassic sandstones which are optically continuous with the host grain and are potassium intermediate sanidines. However, authigenic feldspars from Elgin appear similar to those within the Bromsgrove Sandstone Formation, Central England, where optical discontinuity between orthoclase, microcline and authigenic feldspar was documented by Ali & Turner (1982). The development of authigenic feldspar overgrowths in the Elgin sandstones parallels that of feldspars in the Bromsgrove Sandstone Formation (Ali & Turner 1982) and other Permo-Triassic sandstones (Waugh 1978) and is characterised by the initial growth of small (1-10 μ m) rhombohedral crystals on the surface of the detrital grain. The build-up of these crystals results in the formation of larger crystals of similar habit (Plate 4.2) so that eventually the feldspar is entirely enclosed by the overgrowth.

The composition of the detrital grains and their overgrowths was determined by electron microprobe analysis on selected samples from the Hopeman and Lossiemouth Sandstone Formations (Table 4.2). The overgrowths are potassium-low sanidines in contrast to the detrital cores which are generally microcline and orthoclase. Ali & Turner (1982) record trace amounts of barium within authigenic feldspar in contrast to the feldspars of the present study which exhibit uniform chemical compositions corresponding to pure KAlSi_3O_8 (Table 4.2).

It is not usually possible to assess the textural relationships between the authigenic quartz and feldspar in red bed sequences due to the limited occurrence of the latter phase. However within the Hopeman Sandstone Formation authigenic quartz precipitation clearly postdates the feldspar overgrowths which is consistent with the relationship observed between authigenic quartz and feldspar on a compound grain in Triassic sandstones of the Cheshire Basin (Macchi & Veltkamp 1985).

4.4.2 CALCITE

Calcite occurs sporadically throughout the Permo-Triassic sequence near Elgin, typically as a grain-replacive, poikilotopic spar cement. These cements occur in the

TABLE 4.2. Selected electron probe microanalyses of detrital and authigenic K-feldspar in the Hopeman and Lossiemouth Sandstone Formations.

OXIDES (wt%)	<u>DETRITAL K-FELDSPAR</u>					<u>AUTHIGENIC K-FELDSPAR</u>		
	HOP 9	HOP 9	HOP9	LOS 90	HOP30	HOP30	HOP30	HOP30
SiO ₂	64.8	64.9	65.0	66.2	65.1	66.0	65.5	65.7
Al ₂ O ₃	18.4	18.2	18.4	17.6	17.7	17.6	17.2	17.7
Fe ₂ O ₃	n.d.	0.1	n.d.	n.d.	n.d.	n.d.	n.d.	n.d.
CaO	0.1	0.2	0.2	n.d.	n.d.	n.d.	n.d.	n.d.
Na ₂ O	1.6	0.9	1.1	0.5	0.8	n.d.	n.d.	n.d.
K ₂ O	14.2	14.8	14.6	16.1	16.5	16.1	16.3	16.5
BaO	0.7	0.1	1.0	n.d.	n.d.	n.d.	n.d.	n.d.
TOTAL	99.8	99.2	99.7	100.4	100.1	99.8	99.0	99.9

Plate 4.3 Field photograph of calcite nodules in the fluvial sands of the Burghead Sandstone Formation, GR12366922. The upstanding nodules occur on near-horizontal bedding planes and are associated with fluorite mineralisation. (Hammer for scale)

Plate 4.4 Field photograph of barite mineralisation in the Hopeman Sandstone Formation, GR18437103. Barite occurs as clusters of crystals ('rosettes') which are scattered randomly in the aeolian sandstones. These may coalesce along dune foresets to form veinlets which are often displaced by minor faults. (Lens cap for scale).



Hopeman Sandstone Formation at Clashach Quarry (Fig. 4.2) where they are concentrated in the upper part of the beds of aeolian sands, suggesting that they are incipient calcrete-like precipitates. Nodules of 5 to 15cm diameter, consisting of calcite are common within the fluvial units of the Burghead Sandstone Formation (Plate 4.3) whilst within the Lossiemouth Sandstone Formation patchy rhombic and coarsely crystalline calcite occur in aeolian sandstones at Spynie (Fig. 4.2).

Petrographic study has revealed the existence of two generations of carbonate cement, with an early non-ferroan calcite cement possibly of pedogenic origin (Plate 4.5). This interpretation remains open to question due to the absence of textures diagnostic of calcretes such as micritic cements, pisolites and laminar layering. Inclusions of calcite within fluorite cements indicate that the carbonate is a precursor to the fluorite. Non-luminescent non-ferroan and ferroan calcite cements clearly postdate the cubic fluorite crystals scattered throughout the Burghead Sandstone Formation near the contact with the Hopeman Sandstone Formation, and are thus interpreted as representing a later stage of calcite precipitation. The corrosive nature and paragenetic relationship of these cements is illustrated by embayments and surface textures of both the detrital quartz and feldspar grains and their overgrowths. 'Ghosts' of silicate grains totally replaced by the calcite are reflected by surviving thin clay pellicles within the carbonate.

The limited dissolution of these carbonate cements, evident in certain sandstones, has resulted in minor secondary porosity generation and the process may have operated on a larger scale to produce some of the grain framework-supported sands which lack carbonate cements.

4.4.3 FLUORITE

Fluorite is present within the Hopeman and Burghead Sandstone Formations as a cementing agent and according to Peacock et al. (1968) also occurs on joint surfaces within the Lossiemouth Sandstone Formation though this was not confirmed due to the exposures no longer being accessible.

Field evidence from the present study supports the suggestion made by Peacock et al. (1968) that two episodes of fluorite precipitation occurred within the

Hopeman Sandstone Formation. Early fluorite in the form of small (0.5 cm diameter) cubes clearly predates the formation of calcite nodules in sandstones near Greenbrae Quarry (Fig. 4.2), yet fluorite-bearing joints at the same location (along which shearing has taken place) cross-cut and displace the calcite nodules. Thus either fluorite precipitation occurred as two distinct events or the fluorite within the shear zones represents a remobilisation of earlier cements. Fluorite is also present in the Burghead Sandstone Formation where it takes the form of scattered cubes (1-2 cm diameter) and also forms 3-4 cm wide sub-vertical vein whose E-W trend approximates that of local faults.

In thin section, fluorite is a poikilotopic, replacement cement forming up to 29% of the rock and whose precipitation postdates authigenic quartz and feldspar overgrowths (Plate 4.6). The embayments in detrital grains and their overgrowths could be a result of corrosion by solutions responsible for fluorite or alternatively by a precursor cement such as calcite which often replaces detrital silicates.

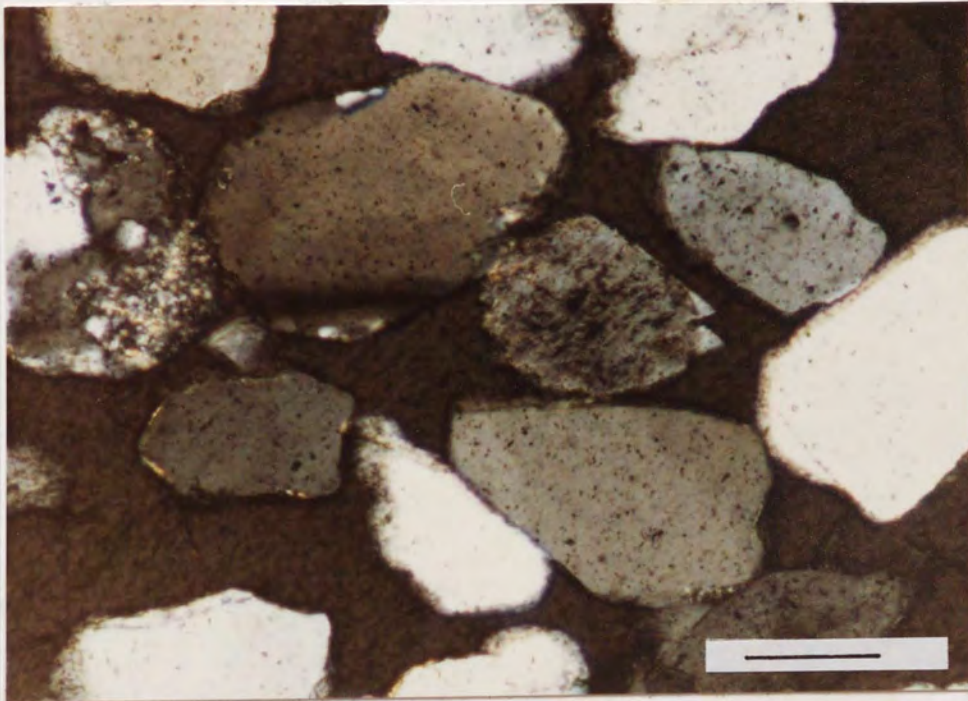
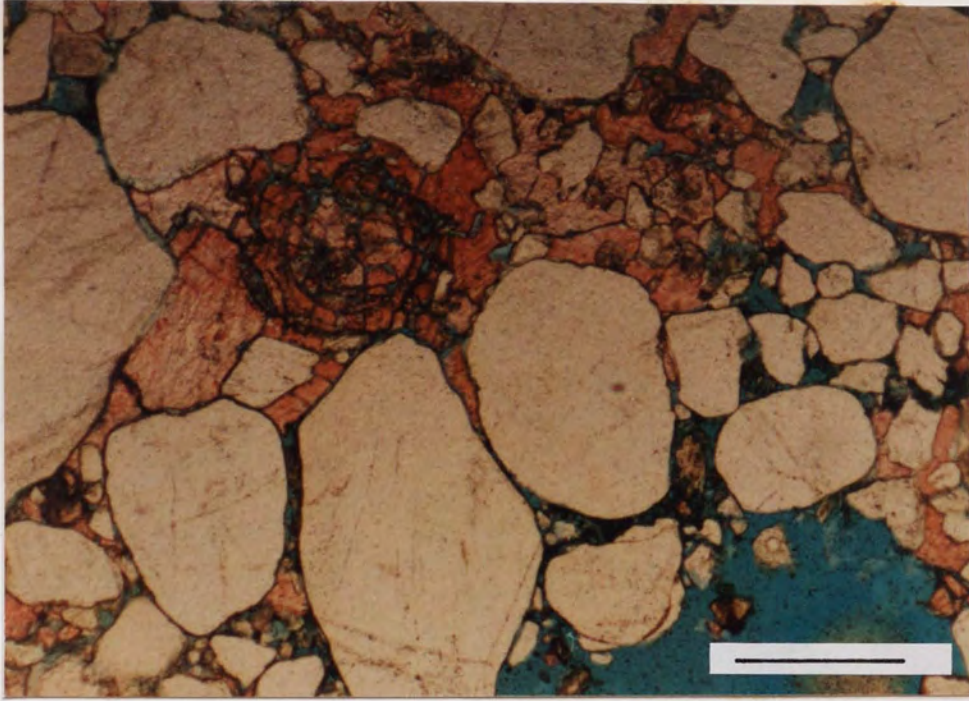
Apparently later fluorite generations in faults and joints at Masonhaugh Quarry for example are associated with sulphide mineralisation and may represent remobilisation of fluorite in the Hopeman Sandstone Formation.

4.4.4 BARITE

Barite cement is concentrated within the Hopeman Sandstone Formation (Fig. 4.2 and Plate 4.4) although barite also occurs as euhedral bladed crystals on joint surfaces within the Lossiemouth Sandstone Formation and as cross-cutting veins within the Cherty Rock. Microscopic examination of barite-cemented sandstones from the Moray coast reveals barite to exist in a variety of forms as either single, small bladed crystals approximately 0.15 mm in length, larger crystals of similar habit which fill three or four consecutive pore spaces, barite 'rosettes' (clusters of radiating crystals 1 cm in diameter) and as a pervasive, pore-occluding cement (Plate 4.7). These cements often have a considerable horizontal extent (on the scale of 10's of metres) and their distribution appears to be intimately related to bedding planes within the dune sands. This reflects the porosity control on the fluids responsible for barite precipitation, with the more permeable, coarser laminae allowing greater access to such fluids. Replacement

Plate 4.5 Colour photomicrograph of nodular non-ferroan calcite cements in the Burghead Sandstone Formation, Burghead. The replacive nature and nodular appearance of the cements are suggestive of incipient calcrete precipitates. Scale bar = 500 μm (PPL).

Plate 4.6 Colour photomicrograph of isotropic fluorite cements in the Hopeman Sandstone Formation, Hopeman. Fluorite forms pore-occluding cements which postdate authigenic K-feldspar overgrowths. Quartz grain margins contain deep embayments, indicating widespread corrosion. Scale bar = 100 μm (Crossed polars)



of detrital silicate grains is a common phenomenon in the Hopeman Sandstone Formation where barite constitutes up to 21.4% of the rock (mean, 10.5%). Thus a 'floating grain' texture is observed, similar to that described from barite-cemented sandstones of the Cheshire Basin (Carlson 1975), with few grain-grain contacts.

Paragenetic relationships involving barite and fluorite proved difficult to establish due to the patchy distribution of the cements and their tendency to occur as spatially separate precipitates. In one instance however, barite encloses and therefore post-dates fluorite cements in sandstones to the east of Hopeman village.

4.4.5 CLAY MINERALOGY

Petrographic and scanning electron microscope studies have been used in conjunction with X-ray diffraction techniques in order to study the relatively simple clay mineralogy of the Elgin Sandstones. Pore-lining or pore-filling authigenic clays, mechanically infiltrated clays and grain replacement clays are present in minor amounts throughout the sequence. The $< 2 \mu\text{m}$ clays are dominated by illite with minor smectitic interlayering (probably a mixture of authigenic and detrital clay) and average only 0.2% of the rock. The different textural varieties of clay cannot be separated for X-ray diffraction analysis. Petrographic observations show that both illite and chlorite replace detrital feldspars and rock fragments, although chlorite was not detected using X-ray diffraction studies.

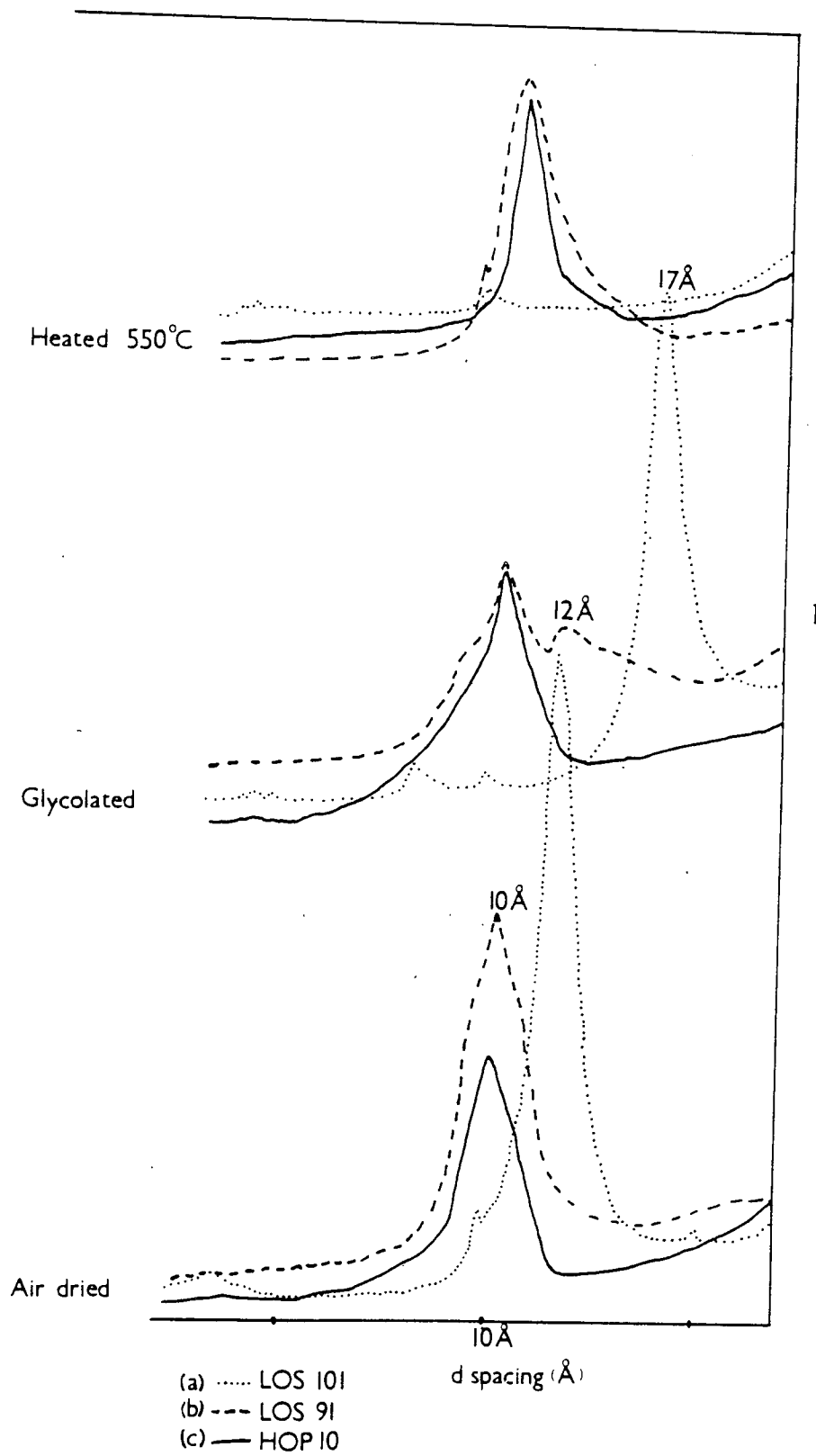
Air dried and glycolated samples from the Hopeman Sandstone Formation produce X-Ray diffraction traces that are dominated by a slightly asymmetrical, 10\AA peak. Heating of the sample to 180°C and 550°C did not alter the position of the 10\AA peak. This behaviour is typical of an illite-dominated assemblage with a minor expandable component in the form of smectite (Fig. 4.6).

The clay mineralogy of the Lossiemouth Sandstone Formation is more variable with sandstones from Lossiemouth (Stotfield) being broadly comparable to that of Devonian sandstones from Rosebrae Quarry. The X-ray diffraction data on the clay mineral assemblage from both these sands is characterised by a distinct 10\AA peak (Fig. 4.6); this peak developed a shoulder at $12\text{-}13\text{\AA}$ on glycolation which was subsequently destroyed on heating to 550°C . Such behaviour is typical of illite-smectite and careful

Figure 4.5. X-ray diffraction traces for the $<2\mu\text{m}$ clay fraction of selected samples;

(a) An illite-smectite dominated clay mineral assemblage of the Lossiemouth Sandstone Formation (b) An illite-dominated clay assemblage with a minor smectite component from the Lossiemouth Sandstone Formation (c) A typical X-ray diffraction trace from the Hopeman Sandstone Formation showing an illite-dominated clay assemblage.

FIGURE 4.6



interpretation of the X-ray trace using parameters defined by Srodon (1984) revealed it to be a mixture of illite and ISII ordered illite-smectite with less than 15% smectite layers. The clay fraction of the Lossiemouth Sandstone Formation samples from Spynie is dominated by an expandable component; X-Ray diffraction traces for air dried samples are dominated by a peak at 12Å, whilst glycolated samples produce a peak at 17Å. This peak collapsed on heating of the sample to 550°C; whereas a minor peak at 10Å remained unaltered throughout. The overall behaviour of the sample indicates an assemblage dominated by Na-rich smectites with subsidiary illite.

4.4.6 POROSITY

Estimates of the porosities of the sandstones are based on point counting thin sections (Table 4.1). In this way several porosity types have been identified, including i) intergranular porosity ii) intragranular porosity and iii) microporosity.

Textural observations show most of the porosity to be intergranular primary porosity which is important especially in the poorly-cemented sands of the Hopeman Sandstone Formation where the porosity reaches a maximum of 29.8%. Enlarged intergranular porosity is evident in certain sandstones from the Burghead Beds and the Hopeman Sandstone Formation and is thought to result from secondary dissolution of detrital grains whose former existence is indicated by the haematite-clay pellicles remaining within the oversized pores. It must be emphasised that this category of enlarged intergranular porosity is not widespread.

Intragranular porosity is the second major porosity type and results from the partial dissolution of detrital silicates such as K-feldspar, such dissolution occurring preferentially along planes of weakness. This secondary porosity generation is evident in all the sandstones, particularly in the poorly-cemented samples. Microporosity within authigenic and pore-filling clays and fracture porosity are rarely important in these sandstones.

A number of the porosity types and textures outlined above correspond to the petrographic criteria defined by Schmidt & McDonald (1979) as characteristic of secondary porosity generation. Secondary porosity formation within these Permo-Triassic sandstones appears to have been episodic resulting in complex textures.

A relatively major event of secondary porosity is envisaged as early carbonate cements were dissolved causing embayments on the edges of quartz and feldspar overgrowths. Another episode of secondary porosity generation is thought to have occurred after clay replacement of detrital feldspars.

4.5 SULPHIDE MINERALISATION

The presence of a 'diagenetic quartz zone' rich in haematite as described by Williams (1973) occurring below the Cherty Rock was not confirmed in the present study. The majority of onshore exposures are devoid of the red colouration typically associated with such ancient continental sands. Walker (1967) attributes the formation of red beds in a semi-arid to arid environment to *in situ* alteration of detrital iron-bearing minerals such as biotite and these red beds constitute the greater part of the Permo-Triassic basin fill throughout Britain (Turner 1980).

Haematite is not entirely absent within the Permo-Triassic rocks examined in the present study but tends to occur locally within the Hopeman Sandstone Formation, Burghead Beds and Lossiemouth Sandstone Formation and appears in places to represent the weathered remnants of original sulphide cements. Stockworks of haematite-filled veins (Plate 4.9) are common in the Hopeman Sandstone Formation near Masonhaugh Quarry (Fig. 4.2) and small concentrations of haematite are widespread throughout the adjacent sands of the Burghead Beds. These roughly spherical patches of haematite are 7-8mm in diameter and are thought to represent the remains of an original sulphide or pyrite cement which has been subjected to intense weathering. This interpretation is consistent with the description of a pyrite cement and pyrite-filled fractures within the Burghead Sandstone Formation at depths greater than 60 m in the Clarkly Hill borehole (Peacock et al. 1968).

Pyrite / marcasite and galena mineralisation is closely associated with the Cherty Rock (Plate 4.8). Starkey (1988) noted the presence of minor amounts of pale yellow spalerite in the Cherty Rock, but no zinc-bearing minerals were observed during this study. The ore in the Cherty Rock was mined briefly in the nineteenth century and six tons of ore were raised from small workings at Lossiemouth (Wilson & Frett 1921). Read in Wilson & Frett (1921) described the ore as closely associated with joint planes

with subordinate galena randomly scattered throughout the cherty matrix.

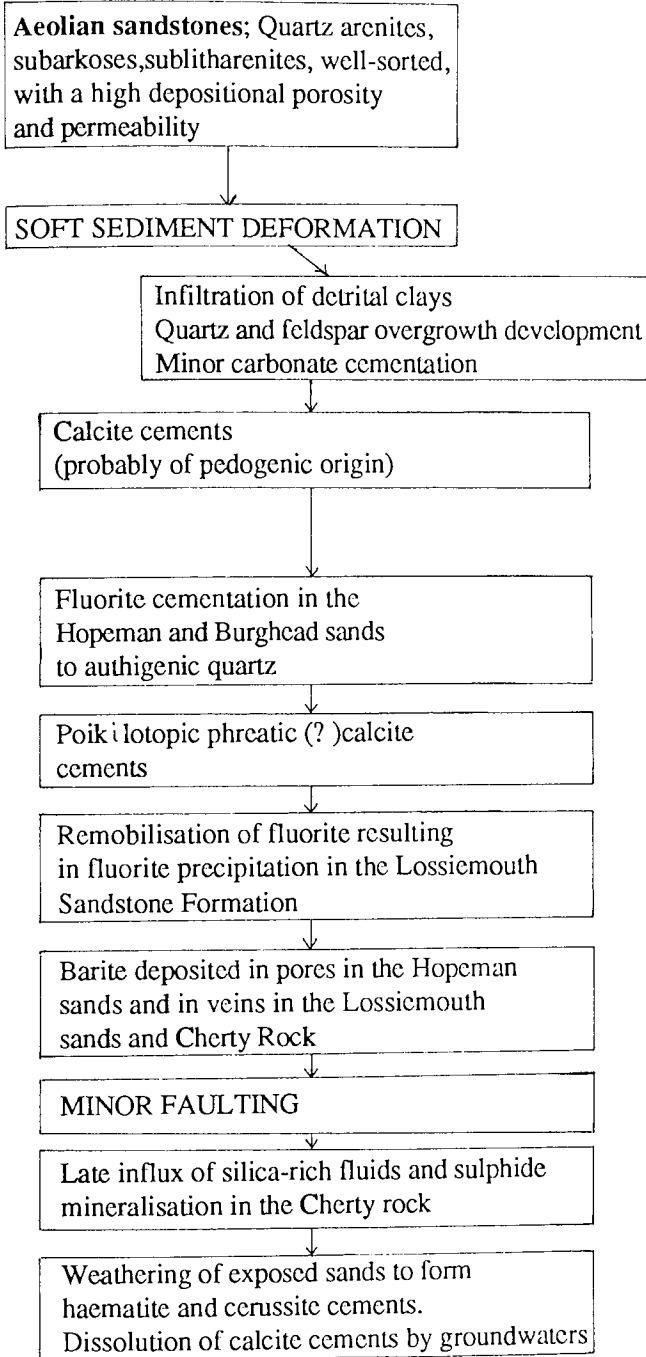
Galena is more widespread than the iron sulphides and is found in the uppermost part of the Lossiemouth Sandstone Formation at Inverugie and Lossiemouth where it occurs as single random crystals cementing the sandstone or on joint surfaces together with barite, calcite, fluorite, and minor pyrite. Fluorite and galena were also recorded from joints in the Lower Jurassic rocks penetrated by the Lossiemouth Borehole (Berridge & Ivimey-Cook 1967). Textural studies indicate that galena mineralisation within the Cherty Rock (Plate 4.10) is the result of two discrete phases of ^{lead} sulphide deposition with earlier crystals of diameter 0.1-0.7 mm occurring within the micritic matrix of the horizon at Inverugie and in the silica-rich zone of the horizon at Lossiemouth. Transgressive quartz veins which have been shown by fluid inclusion studies to have precipitated from fluids at temperatures of 115°C enclose larger crystals of galena and constitute the second phase of lead sulphide deposition (Fig. 4.7).

Two periods of pyrite/marcasite precipitation are recognised where the first mineralising event resulted in the formation of pyrite and marcasite crystals within the micro and macrocrystalline quartz matrix of the Cherty Rock. Iron sulphides are also intimately related to coarsely crystalline quartz cavity fill, and fluid inclusion data confirms that they precipitated from warm (~100°C) mineralising fluids. The matrix-hosted iron sulphides comprise highly fractured crystals which have no distinctive euhedral crystal shape and exhibit no framboidal textures. In one instance this generation of pyrite is enclosed by, and therefore predates, scattered galena crystals.

Selected electron microprobe analyses of the galena and pyrite are shown in Table 4.3. This part of the study revealed the galena and pyrite/marcasite to be pure phases with no evidence of the minor element enrichments described from pyrites in the red beds of the Cheshire Basin and diagenetic sulphides within the Old Red Sandstone of the Orcadian Basin (Muir & Ridgeway 1975).

HOPEMAN AND LOSSIEMOUTH SANDSTONE FORMATIONS

FORMATION



BURGHEAD SANDSTONE

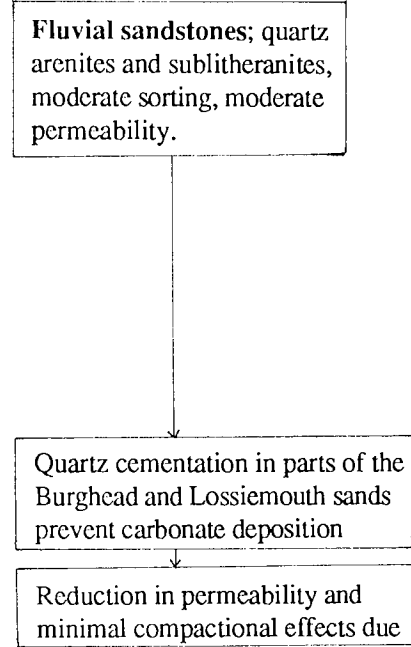


Figure 4.7. The sequence of diagenetic events that have occurred in the Permo-Triassic sandstones of Elgin. Exact paragenetic relationships remain uncertain and some cements may have precipitated concurrently. The diagenetic modifications outlined above are typical of those associated with buried quartzose sandstones in a petroleum basin (e.g. Glennie et al. 1978) with the exception of the widespread barite and fluorite cements.

Plate 4.7 Colour photomicrograph of barite cements in the Hopeman

Sandstone Formation. The detrital orthoclase feldspar in the centre of the field of view has an epitaxial overgrowth which clearly formed before barite precipitation. Haematite pellicles on detrital grains are absent in the sandstones cemented by barite. Scale bar = 500 μm (Crossed polars).

Plate 4.8 Reflected light micrograph of sulphide ores in the Cherty Rock,

Lossiemouth. Pyrite and marcasite crystals are highly fractured and are scattered throughout the matrix of the silicified calcrete. Scale bar = 500 μm .

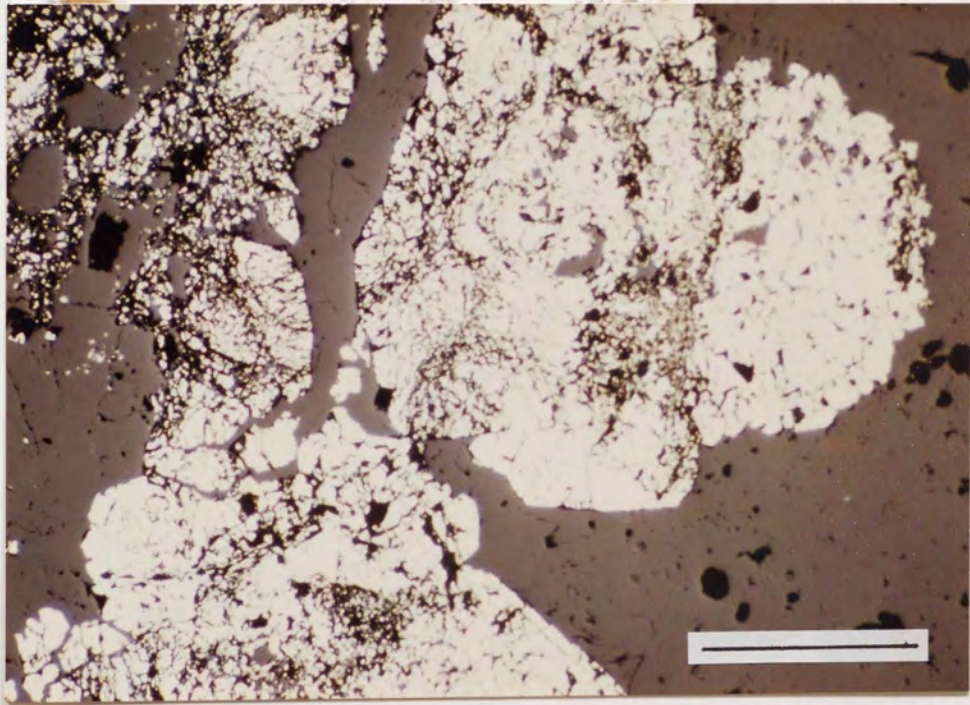
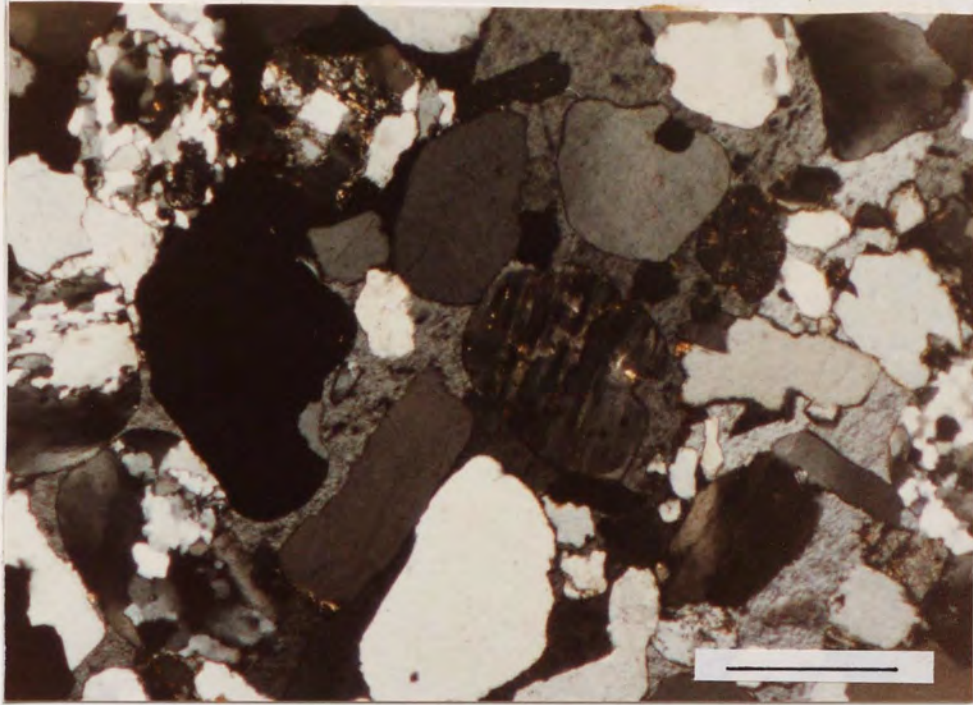


Plate 4.9 Field photograph of sulphide veins in the Hopeman Sandstone Formation, GR12816919. The multiple vein systems consist largely of iron oxides and are generally aligned parallel to the major offshore faults which trend approximately E-W. (Hammer for scale)

Plate 4.10 Field photograph of sulphide ores in the Cherty Rock, Lossiemouth GR22927117. Galena is the dominant sulphide and occurs as disseminated crystals throughout the matrix of the silicified horizon. (Lens cap for scale).





TABLE 4.3. Representative electron probe microanalysis of sulphide phases within the Cherty Rock.*

Mineral species	Zn	Co	Fe	S	Pb	Bi	Ag	Sb	TOTAL
Marcasite C20H	n.d.	n.d.	45.6	53.1	0.3	0.2	n.d.	n.d.	99.3
Marcasite C20H	0.1	0.1	45.2	54.0	0.2	0.2	n.d.	n.d.	99.8
Pyrite C20H	n.d.	0.1	45.8	53.8	0.2	0.1	n.d.	n.d.	100.0
Galena C22H	0.1	n.d.	n.d.	12.7	85.5	0.2	n.d.	0.1	98.6
Galena C22H	0.1	n.d.	n.d.	12.6	85.7	0.2	n.d.	0.1	98.7

* All data expressed in weight percent. Analyses obtained using a Cameca Camebax electron microprobe at 20 k.v. and employing natural and synthetic sulphides as standards (see Appendix I for details).

4.6 GEOCHEMISTRY

Whole rock analysis of samples was undertaken using X-ray fluorescence spectrometry and the results are shown in Table 4.4 and 4.5. Major element contents inevitably reflect the mineralogical characteristics of the sandstones and the silica-rich nature of the Permo-Triassic sediments of Elgin is evidence of their maturity.

There appear to be no systematic differences in the major element geochemistries of sandstones of aeolian and fluvial origin with the exception of the sediments in the Burghead Sandstone Formation which have uniformly low Al_2O_3 contents. This may be a result of early quartz cementation which prevented substantial clay development. MgO and Na_2O contents remain constant throughout the succession, whereas K_2O is more variable, possibly reflecting differing amounts of K-feldspar and illite. The mean Fe_2O_3 content of these sandstones is low (0.47%) compared to that for Triassic red beds in the Wilkesley Borehole, Cheshire (mean Fe_2O_3 content 2.96% ; Holmes et al. 1983). This confirms the relative lack of haematite and is consistent with the bleached nature of the onshore succession at Elgin. The high barium content of sample HOP 81 indicates the presence of a pervasive barite cement. The presence of calcite and fluorite cements in certain samples is reflected by the high CaO contents in some sandstones.

Trace element concentrations correspond closely to those reported by Wedepohl (1978) for sandstones of similar maturity. Nickel is the only element that is significantly enriched and the reasons for this remain unclear.

4.7 FLUID INCLUSION STUDIES

In order to characterise the mineralising fluids and to obtain an estimate for the minimum temperature of the mineralisation microthermometric studies were carried out on fluid inclusions hosted by authigenic phases within the sandstones and coarsely crystalline quartz within the Cherty Rock; these studies met with varying degrees of success.

Inclusions observed within quartz overgrowths in the Burghead Beds were typically small, having diameters in the range 2 to 5 μm . The temperatures obtained for these

TABLE 4.4. Geochemical analyses of samples from the Hopeman, Burghead and Lossiemouth Sandstone Formations.

	Major oxides (wt%)								TOTAL
	SiO ₂	Al ₂ O ₃	Fe ₂ O ₃	MgO	CaO	Na ₂ O	K ₂ O	TiO ₂	
HOP105	88.9	6.4	0.4	0.4	0.1	0.1	3.4	0.3	100.0
HOP79	95.7	2.4	0.1	0.1	N.D.	0.2	1.4	N.D.	99.2
HOP81	96.5	2.1	0.2	0.1	N.D.	0.1	1.3	N.D.	100.3
BUR1H	96.6	1.6	0.6	N.D.	N.D.	0.1	1.0	N.D.	99.0
BUR3H	77.6	1.4	0.2	0.1	19.6	N.D.	1.1	N.D.	100.0
BUR4H	91.7	1.5	0.9	0.1	4.3	0.1	1.1	N.D.	99.7
BUR5	93.2	2.5	1.7	0.1	0.8	0.1	1.4	N.D.	99.3
BUR6H	95.6	2.3	0.3	0.1	0.1	0.1	1.5	N.D.	100.0
BUR7H	71.1	1.3	0.1	0.1	26.4	N.D.	1.1	N.D.	100.1
BUR38	71.5	0.9	0.2	0.1	26.6	N.D.	0.7	0.1	100.1
BUR39	86.6	1.6	0.3	0.5	10.3	N.D.	1.0	0.1	100.4
BUR55	95.6	2.0	0.4	0.1	N.D.	0.3	1.2	0.1	99.7
BUR56	96.8	1.7	0.2	N.D.	N.D.	0.1	1.0	0.1	99.9
LOS51	71.2	4.6	0.5	0.1	20.3	0.0	3.0	0.1	100.1
LOS52	89.7	4.0	0.2	0.2	2.0	0.4	2.7	0.1	100.0
LOS90	89.3	5.6	1.1	0.5	0.1	0.2	3.2	0.1	100.1
LOS91	89.4	5.6	1.0	0.5	N.D.	0.2	3.2	0.1	100.0
LOS92	91.6	5.2	0.2	0.1	N.D.	0.2	2.5	N.D.	99.8
LOS96	92.4	3.8	0.8	0.5	0.1	0.2	1.8	0.5	100.1
LOS99	97.2	1.5	0.2	N.D.	N.D.	0.2	0.8	N.D.	99.9
LOS100	89.4	5.6	0.8	0.1	0.1	0.8	2.1	0.3	99.8
LOS101	90.8	5.4	0.2	0.1	0.1	0.5	2.8	0.1	100.0

Horizons from which the samples were collected are given by the prefix on the sample number: HOP= Hopeman Sandstone Formation; BUR= Burghead Sandstone Formation; LOS= Lossiemouth Sandstone Formation.

TABLE 4.5. Geochemical analyses of samples from the Hopeman, Burghead and Lossiemouth Sandstone Formations.

	Minor elements (ppm)					
	Mn	Cu	Pb	Zn	Ni	Ba
HOP105	171	1	14	57	107	512
HOP79	25	7	16	7	216	231
HOP81	12	7	18	7	241	15886
BUR1H	26	10	32	25	305	235
BUR3H	13	13	30	27	182	221
BUR4H	166	3	139	67	167	201
BUR5	1606	25	14	166	111	253
BUR6H	56	0	23	42	177	216
BUR7H	2	7	19	22	186	239
BUR38	555	0	22	43	31	123
BUR39	474	3	22	77	143	156
BUR55	31	7	39	67	275	190
BUR56	53	3	20	35	215	162
LOS51	173	9	36	70	106	497
LOS52	212	0	17	34	100	396
LOS90	64	1	15	21	202	388
LOS91	59	3	15	15	153	396
LOS92	42	4	25	41	111	899
LOS96	107	0	14	12	56	227
LOS99	61	0	13	4	224	152
LOS100	60	1	20	29	191	374
LOS101	231	0	23	30	198	190

Horizons from which samples were collected are denoted as in Table 4.

inclusions are considered to be erroneously high ($>200^{\circ}\text{C}$). It appears that the inclusions have undergone significant post-trapping alteration in the form of leaking and/or necking down (see Roedder 1984).

Investigation of the fluorite-hosted fluid inclusions from the Hopeman Sandstone Formation revealed the inclusions to be too small for microthermometric study with the exception of a single two-phase inclusion that homogenised at 101.3°C . At room temperature, barite-hosted fluid inclusions are monophasic and were not used in the present study. Microscopic observations confirmed the similarity between these inclusions and those hosted by the barite of the Cheshire Basin, the metastable behaviour of which during freezing was taken to indicate that the barite was deposited from low temperature, weakly saline fluids (Chapter 2).

The bulk of the fluid inclusion study was conducted on the coarsely crystalline quartz that forms veins and infills vugs in the Cherty Rock horizon. The chalcedony-hosted fluid inclusions were too small for microthermometric study. The fluid inclusions within the quartz can be subdivided into those that occur in clusters, solitary inclusions and those inclusions that occur along healed fracture planes. The first two categories are thought to be primary (Roedder 1984). The third type of inclusion is considered to be secondary and these, together with inclusions showing evidence of necking down were not studied as they were considered likely to give erroneous microthermometric results. The primary inclusions show a wide variation in shape and their diameters range from 3-7.5 μm . Two-phase liquid-vapour inclusions were used in the present study although the majority of inclusions are monophasic at room temperature.

All the inclusions homogenised into the liquid state at temperatures varying between 94.8°C and 139°C (mean 114.8°C) (see Fig. 4.8). The final melting temperature of ice ranged from -10.2°C to -14.6°C with a mean of -12.4°C corresponding to a mean salinity of approximately 16 wt% NaCl equivalent (Potter et al. 1978). The uncertainty surrounding the burial history of the basin margin Permo-Triassic sediments renders invalid any attempts at pressure correction. Consequently, the homogenisation temperatures quoted above may only be taken as minimum estimates of the temperature

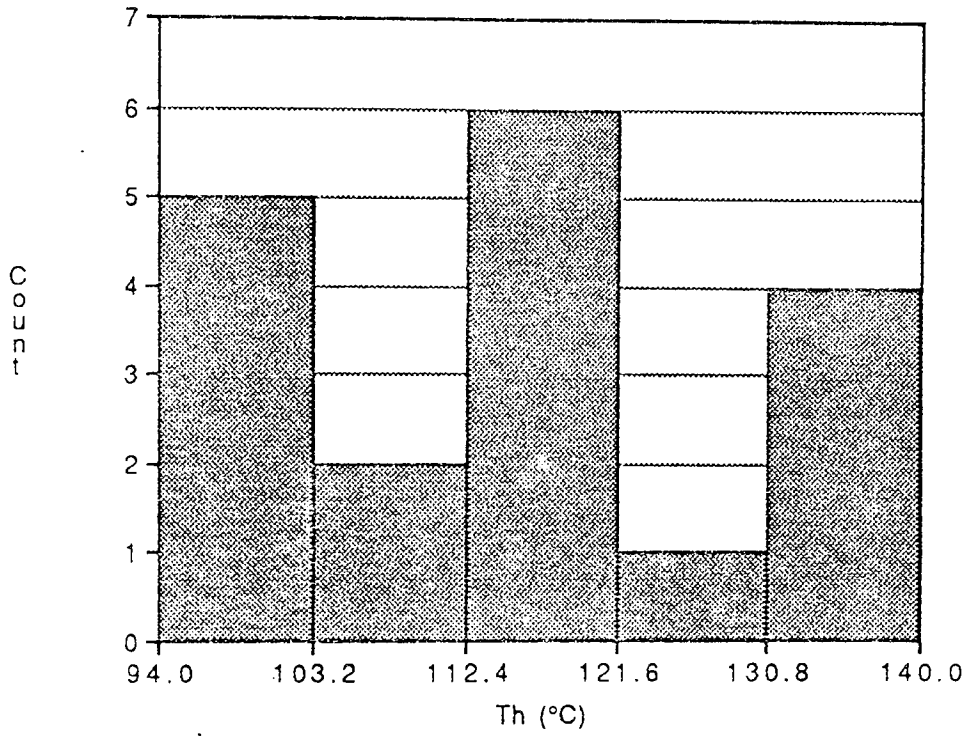


Figure 4.8. Histogram of homogenisation temperatures (T_H) of quartz-hosted fluid inclusions in the Cherty Rock.

of the mineralising event.

4.8 SULPHUR ISOTOPES

A comprehensive sulphur isotope study was carried out on sulphate and sulphide phases within the Permo-Triassic Sandstones of Lossiemouth in order to constrain the source of sulphur in the deposits and to elucidate the mechanism of precipitation of the barite and the sulphides.

Samples analysed include barite cements within the Hopeman Sandstone Formation, barite veins within the Lossiemouth Sandstone Formation and Cherty Rock, as well as galena and pyrite from the Cherty Rock horizon. All the samples studied were collected from onshore exposures between Lossiemouth and Burghead.

Samples preparation and isotopic analysis techniques are documented in Appendix I. The SO₂ produced was analysed using an 'ISOSPEC 64' spectrometer. Reproducibility of the overall procedure is $\pm 0.27\%$, as derived from 20 complete analyses of the internal laboratory standard (including combustion).

The $\delta^{34}\text{S}$ ratios obtained in the study are shown in Table 4.6 and Fig. 4.9 and the results are discussed below.

4.8.1 BARITE

The $\delta^{34}\text{S}$ ratios obtained for the barite cements within the Hopeman Sandstone Formation range from $+24.5\%$ to $+34.0\%$ with a mean of $+27.4\%$ ($n=9$). The $\delta^{34}\text{S}$ values derived from the barite veins within the overlying Lossiemouth Sandstone Formation and the Cherty Rock were indistinguishable with a mean of $+28.2 \pm 0.0\%$ ($n=2$). Thus there is no systematic variation of barite sulphur isotope values with time. In addition, it can be seen from the data in Table 4 that $\delta^{34}\text{S}$ of the barite is not stratigraphically or spatially controlled.

Unlike the $\delta^{34}\text{S}$ values obtained for barite mineralisation in the Cheshire Basin (Chapter 2) which corresponded closely to the $\delta^{34}\text{S}$ ratios of associated evaporites, the $\delta^{34}\text{S}$ values for the barite at Lossiemouth are considerably enriched in ^{34}S relative to the Permian evaporites of the Inner Moray Firth Basin. $\delta^{34}\text{S}$ values for late Permian

evaporites have a $\delta^{34}\text{S}$ of approximately 10.5‰ (Claypool et al. 1980). This indicates that the sulphate in the barite at Lossiemouth was almost certainly not derived from the Permian evaporites via a simple dissolution-reprecipitation mechanism.

4.8.2 GALENA

The $\delta^{34}\text{S}$ values for galena in the Cherty Rock horizon exhibit a narrow range, from -4.8‰ to +0.4‰ (mean -1.9‰). The relative isotopic homogeneity of the galenas suggests that both the early sulphide disseminated in the palaeosol matrix, and the later galena associated with quartz veining had the same sulphur source. Thus, The $\delta^{34}\text{S}$ galena are consistent around a mean of -1.9‰, regardless of locality or position in the paragenetic sequence, indicating deposition from an isotopically homogenous fluid.

4.8.3 PYRITE

The limited $\delta^{34}\text{S}$ data for pyrite appear to indicate the presence of two isotopically distinct groups (see Fig. 4.9) with isotopically light pyrite from the Cherty Rock at Lossiemouth and Spynie yielding $\delta^{34}\text{S}$ ratios between +2.8‰ and +6.9‰ (mean +5.1‰). Samples C94 and C114 have $\delta^{34}\text{S}$ values of +27.0‰ and +25.4‰ respectively. The latter samples are closely associated with quartz veins and are thought to have precipitated from later fluids. The pyrites depleted in $\delta^{34}\text{S}$ are extensively fractured and are disseminated throughout the palaeosol horizon; consequently, they are thought to have precipitated earlier in the history of the horizon and in one instance, clearly predate the galena. In view of the limited data it is not possible to establish whether these two texturally distinct generations have characteristic isotopic signatures, or alternatively, whether the data represent two extremes of a wide range of $\delta^{34}\text{S}$ values.

The sulphur isotope disequilibrium apparent between the galena and pyrite within the Cherty Rock is a common phenomenon in deposits formed at temperatures below 120°C (Ohmoto & Rye 1979). The observed $\Delta_{\text{FeS}_2\text{-PbS}}$ values of the ores are commonly smaller than the equilibrium values in several important groups of mineral deposits such

TABLE 4.7. Sulphur isotope data from the Cherty Rock, Elgin.

Sample no.	Mineral	Remarks	$\delta^{34}\text{S}$ (‰)
C98	Galena	Euhedral crystals in macroquartz, C.R., Lossiemouth	-3.7
C91574	Galena	Massive ore in a quartz vein, C.R., Lossiemouth	-4.8
C18	Galena	Euhedral crystals in macroquartz, C.R., Lossiemouth	-0.3
C24	Galena	Euhedral crystals in macroquartz, C.R., Lossiemouth	-3.5
C26	Galena	0.5cm cubes in siliceous matrix, C.R., Lossiemouth	-3.6
C22	Galena	Euhedral crystals in microquartz, C.R., Lossiemouth	-2.8
C19	Galena	Euhedral crystals in macroquartz, C.R., Lossiemouth	-2.8
C97	Galena	Anhedral crystals in quartz veins, C.R., Lossiemouth	-0.3
C17	Galena	Crystals enclosed in macroquartz, C.R., Lossiemouth	-1.0
C49	Galena	Crystals enclosed in microquartz, C.R., Inverugie	+0.7
C85	Galena	Anhedral crystals in a cavity, C.R., Inverugie	+0.4
C114	Pyrite	Anhedral crystals in microquartz, C.R., Lossiemouth	+24.5
C94	Pyrite	Crystals enclosed in quartz veins, C.R., Lossiemouth	+27.0
C116	Pyrite	Disseminated in microquartz, C.R., Lossiemouth	+2.8
C20P	Pyrite	Fractured crystals in microquartz, C.R., Lossiemouth	+6.9
C103	Pyrite	Anhedral phase in microquartz, C.R., Lossiemouth	+5.5
HOP61	Barite	Cement in Hopeman Sst., W. Hopeman G.R. 11426993	+26.3
HOP66	Barite	Cement in Hopeman Sst., W. Hopeman G.R. 14196975	+28.0
HOP73	Barite	Cement in Hopeman Sst., E. Hopeman, G.R. 14586998	+26.5
HOP74	Barite	Cement in Hopeman Sst., E. Hopeman, G.R. 14586998	+27.8
HOP76	Barite	Cement in Hopeman Sst., E. Hopeman, G.R. 14896993	+31.3
HOP77	Barite	Cement in Hopeman Sst., E. Hopeman, G.R. 14896993	+34.0
HOP78	Barite	Cement in Hopeman Sst., Covesea, G.R. 19211727	+24.5
HOP80	Barite	Cement in Hopeman Sst., Covesea, G.R. 18437101	+25.6
HOP81	Barite	Cement in Hopeman Sst., Covesea, G.R. 18437101	+24.7
LOS113	Barite	Crystals in a joint, Lossiemouth Sst., G.R. 23837088	+28.2
C115	Barite	Cross-cutting vein, C.R., Lossiemouth, G.R. 23237137	+28.2

Horizon key: C.R. = Cherty Rock

FIGURE 4.9

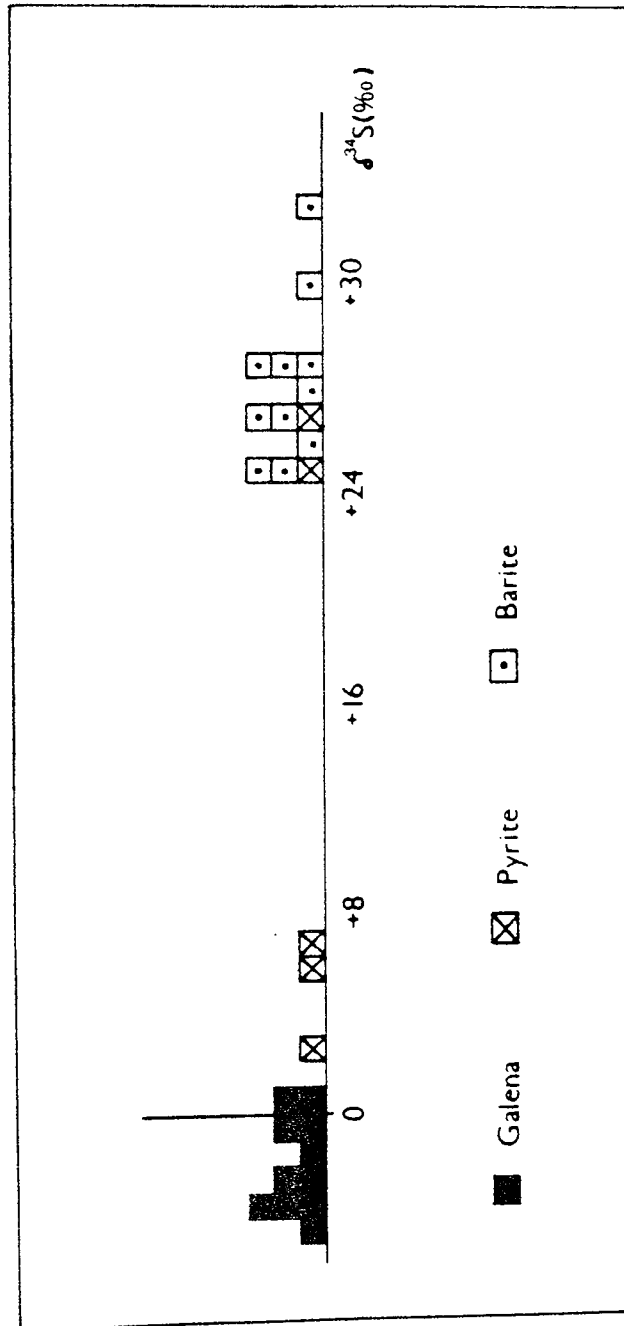


Figure 4.9. Histogram of sulphur isotope data for galena, pyrite and barite mineralisation near Elgin.

TABLE 4.6. The oxygen isotopic composition of late quartz in the Cherty Rock, Lossiemouth.

Sample no. and description	$\delta^{18}\text{O}^*$
C86 Euhedral quartz cavity fill	20.3
C23 Euhedral quartz cavity fill	17.7
C94 Quartz cavity fill enclosing pyrite	17.8
C103 Complex quartz veins	23.0

* Oxygen isotope results are expressed as per mil derivation of the $\delta^{18}\text{O}/\delta^{16}\text{O}$ ratio of Standard Mean Ocean Water (SMOW).

as red-bed associated Cu deposits, sandstone lead deposits and some Mississippi Valley-type deposits (Ohmoto 1986). Sulphur isotopic disequilibrium also occurs frequently where sulphide mineral pairs involve pyrite such as at Lossiemouth. Pyrite does not always co-precipitate with the simple sulphides, as illustrated by the textures in the Cherty Rock and this is thought to contribute significantly to the apparent isotopic disequilibrium (Ohmoto 1986).

The discrepancy between the observed and calculated equilibrium fractionation factors between coexisting barite and sulphide minerals in the Permo-Triassic sandstones of Lossiemouth reflects the isotopic disequilibrium between the phases. The sulphur isotope exchange kinetics suggest that isotopic equilibrium between aqueous sulphate and sulphide is only to be expected at temperatures greater than 100°C (Ohmoto & Lasaga 1982).

4.9 DISCUSSION

Various hypotheses have been proposed for the sources of the fluids responsible for barite, fluorite and sulphide deposition in the Inner Moray Firth Basin with early authors such as Mackie (1923) suggesting derivation of the fluorite from the fluorite-rich granite intrusions of Helmsdale and Peterhead. Dunham (1952) advocated a 'hydrothermal' origin for the fluorite in the Hopeman Sandstone Formation, but no evidence was put forward in support of this theory. Williams (1973) proposed a remobilisation of early fluorite and galena phases in association with haematite-quartz-galena-calcite mineralisation of Mid-to Upper Jurassic age where mineralising fluids were introduced along basin margin faults. Previous authors including Williams (1973) were unable to establish the source and nature of these fluids due to the lack of geochemical data and in the absence of evidence for a method of fluid introduction at Elgin. According to Peacock et al. (1968), the impermeable Jurassic shales were responsible for trapping the mineralising fluids resulting in the precipitation of sulphides in the underlying Cherty Rock.

4.9.1 TECTONIC CONTROL AND TIMING OF THE MINERALISATION

Tectonic control of the spatial distribution of the mineralisation is suggested by the

alignment of quartz and fluorite-bearing veins in the Hopeman and Burghead Sandstone Formations with the local E-W trending post-Liassic faults. The concentration of ores adjacent to joints in the Cherty Rock suggest that the mineralisation is to some extent fault-controlled, and may be connected to movements along basin margin fault systems during Jurassic to Lower Cretaceous times and during basin inversion during the Tertiary.

A lower age limit is placed on the mineralisation by the fluorite and galena recorded from Lower Jurassic rocks in the Geological Survey borehole at Lossiemouth (Berridge & Ivimey-Cook 1967). Moorbath (1962) gives a date of 140 ± 60 M.y. for the mineralisation in the Cherty Rock from a lead isotope study. This date corresponds to late Jurassic times but it remains uncertain which of the two galena generations this result refers to.

Williams (1973) suggested that barite and fluorite precipitation was penecontemporaneous and occurred prior to, and during, the deposition of the Burghead Sandstone Formation. This is inconsistent with the post-overgrowth fluorite and barite cements in the Hopeman and Burghead Sandstone Formations observed during the course of the present study. Thus, textural evidence indicates that Ba-F-bearing fluids were introduced into the sediments after early diagenesis.

4.9.2 SOURCES OF Pb, F, Ba, Si, Fe AND S

Williams (1973) noted the similarity between the mineral assemblage at Elgin and that of the mineralisation associated with the Newer Granites to the south and west of the Inner Moray Firth (Gallagher et al. 1971) and favoured a deep hydrothermal source for the fluorite and barite mineralisation at Elgin. A recent lead isotope study conducted by Parnell & Swainbank (1985) has revealed that galena from the Moray Firth has a significantly lower $^{207}/^{206}$ ratio than the galena hosted by the Devonian sediments in the Orcadian Basin to the north east. The lead isotope data from the Inner Moray Firth Basin suggests that the lead at Lossiemouth was not derived directly or from weathering of a Caledonian granitic source (Parnell & Swainbank 1985). Furthermore, the geological setting of the mineralisation and the sulphur isotope data are inconsistent with a hypothesis invoking the direct derivation of sulphur from hydrothermal fluids of

magmatic origin. The deposits are not associated with magmatic activity; the New Granites nearby were emplaced during the early Ordovician, prior to the deposition of the Devonian siliciclastic sediments in the Orcadian Basin (Chesher & Lawson 1983). In addition, the wide range of $\delta^{34}\text{S}$ values for the pyrite at Lossiemouth is incompatible with a magmatic sulphur source which is characterised by a narrow range of sulphur isotope values ($0\text{‰} \pm 4\text{‰}$; Ohmoto & Rye 1979).

The validity of a hypothesis invoking a detrital sulphide source is questioned as there is no textural evidence in the present sandstones for there ever having been detrital sulphide grains, there also is no obvious sulphide source to the south-west of the basin from where the sediments were derived. Furthermore, the semi-arid environment thought to be in existence in the Inner Moray Firth Basin during Permo-Triassic times is not considered conducive to transportation and survival of such material.

Possible 'sedimentary' sources of sulphur for the mineralisation at Elgin include evaporite sulphur from the Zechstein of the Inner Moray Firth Basin, Jurassic seawater sulphate, pyrite and other sulphides fixed in the Jurassic marine shales in the basin or finally the organically-bound sulphur from the Jurassic Brora Coal Formation or the Kimmeridgian Clay Formation. Potential 'sedimentary' sources of metals, fluorine and barium include the Permo-Triassic redbeds and Jurassic shales in the Inner Moray Firth Basin. To the north of the mineralised area lies a sedimentary basin containing approximately 1500m of Permo-Triassic red beds and evaporites in addition to at least a 2200m thickness of Jurassic siliciclastics and organic-rich shales. Basinal fluids originating in this sedimentary sequence are likely to have migrated along porous horizons and up-dip towards from the basin centre towards the edges of the basin with compaction as the major driving force.

Holmes et al. (1983) suggested that the dissolution of detrital grains and subsequent release of major and minor elements into solution could more than account for the concentrations of metals (particularly Cu) comprising the Cheshire Basin ore deposits. Dissolution of detrital phases such as K-feldspar and ferromagnesian grains has been shown to be an integral part of the diagenesis of red bed sequences (eg. Walker 1967, Turner 1980). BaO commonly occurs in minor amounts in K-feldspar as

illustrated by the electron microprobe analyses of detrital microcline and orthoclase in the present study (Table 4.2). A worldwide study of trace element contents in K-feldspar has revealed that lead contents of feldspar may reach 11,000 ppm (mean 62.3 ppm; Wedepohl 1978). Textural studies of the feldspars within the mineralised Hopeman, Burghead and Lossiemouth Sandstone Formations have revealed that they have suffered minor alteration and dissolution and consequently are not thought to have contributed significantly to the Ba and Pb mineralisation within the onshore succession.

Trace amounts of fluorite occur in illite, muscovite, biotite and apatite, and iron is present in the ferromagnesian minerals; hence, dissolution of these detrital grains during burial of the basin-fill sediments would result in the release of F and Fe into solution. In spite of this, basinal fluids are not generally rich in fluorine and it is likely that the mineralising fluids circulated down into basement rocks. The potential clearly exists to derive Ba, F, Ca, Si, Pb and Fe from detrital phases during diagenesis of thick clastic sequences and the depth-related clay dehydration reaction whereby smectite is transformed to illite is proposed to be the major source of diagenetic pore fluids in the Inner Moray Firth Basin.

The mineralised sediments at Elgin are associated with Zechstein evaporites in the Inner Moray Firth Basin and are overlain by Jurassic sediments deposited in marginal marine and marine settings (Berridge & Ivimey-Cook 1967). Data from North America and Europe (Claypool et al. 1980) indicate that $\delta^{34}\text{S}$ of evaporites ranged from 15.5‰ to 10.5‰ during the Permian, and that the $\delta^{34}\text{S}$ of evaporites from mid-Triassic to Late Jurassic times remained constant with $\delta^{34}\text{S} = 16.1\text{‰} \pm 1.5\text{‰}$. Hence the $\delta^{34}\text{S}$ values for barite are consistently enriched in the heavier isotope relative to both the Permian evaporites and Jurassic seawater sulphate. This suggests that barite sulphur was not derived directly from either the anhydrite/gypsum facies of the Zechstein or from Jurassic seawater percolating into the underlying Triassic sediments. Bacterially mediated sulphate reduction processes in the evaporite-bearing horizons of the Zechstein or in the Jurassic sediments may have resulted in an enrichment of $\delta^{34}\text{S}$ in the residual fluid and this may account for the heavy $\delta^{34}\text{S}$ values obtained for barite at Elgin.

Organically-bound sulphur and diagenetic sulphide in the form of pyrite, are common constituents of the Jurassic shales in the Inner Moray Firth Basin and are potential sources of sulphur for the mineralisation. Kimmeridgian samples from the Moray Firth have a mean sulphur content of 200-300 ppm, whilst some whole rock samples contain up to 27% diagenetic sulphide. The Brora Shale has a mean sulphur content of 511 ppm and the Bituminous Shales contain up to 2126 ppm (Duncan 1986). Leaching of this sulphide and reprecipitation of the sulphide in the Permo-Triassic sandstones may have occurred, and if this were the case, we would expect to see isotopically light sulphur isotope values. The $\delta^{34}\text{S}$ values obtained for sulphides at Elgin are not negative and are inconsistent with simple derivation of sulphate or sulphide sulphur from the Jurassic shales in the Moray Firth Basin.

Mackie (1901) proposed that fluorite and barite cements in the Hopeman Sandstone Formation were deposited in a lacustrine environment and, indeed, the occurrence of fluorite in Cenozoic lacustrine facies deposited in saline, alkaline environments was recently described by Sheppard & Mumpton (1984). In this latter study, fluorite was thought to precipitate as a result of mixing of high pH, F and Si-bearing lake waters with relatively dilute Ca-bearing waters that entered the lakes from streams or springs. Sheppard & Mumpton (1984) did not specify the source of the fluorine but noted that modern lakes enriched in fluorine are commonly found in volcanic terrains and are sodium carbonate-bicarbonate in composition. The fluorite mineralisation at Elgin is hosted by aeolian and fluvial sandstones which have no association with volcanic rocks, and it is considered unlikely that fluorite is a primary precipitate from saline lake waters or groundwaters.

In view of the evidence presented above, the favoured source of sulphur is the Zechstein evaporites, whilst base metals, silica, fluorine and barium are thought to have originated in the red bed and shale horizons of the Inner Moray Firth Basin.

4.9.3 NATURE OF THE MINERALISING SOLUTIONS

The physicochemical characteristics of some of the ore-forming fluids associated with the mineralisation have been constrained as a result of integration of the geological, fluid inclusion and stable isotope data from the present study. Fluid inclusion data from

the quartz veins and cavity-fill in the Cherty Rock have shown that the mineralising fluids responsible for their precipitation were warm ($\sim 115^{\circ}\text{C}$) and saline (~ 16 wt % NaCl equivalent). The quartz-water fractionation equation for environments at low temperature ($< 200^{\circ}\text{C}$) of Knauth & Epstein (1975) was used to calculate the $\delta^{18}\text{O}$ of the ore-forming fluids:

$$1000\ln \alpha_{\text{qtz-water}} = 3.09 (10^6 T^{-2}) - 3.29$$

The $\delta^{18}\text{O}$ of the quartz (mean 19.7 ‰ SMOW) reflects the relative temperature of quartz precipitation ($\sim 115^{\circ}\text{C}$) and the isotopic composition of the waters from which it formed. Using the above equation the $\delta^{18}\text{O}$ value of the mineralising fluid is estimated to range from -5.8 ‰ to -0.5 ‰ (mean -2.5 ‰ SMOW). These values are compatible with a meteoric origin for the fluid, and basinal fluids emanating from the sediments in the Inner Moray Firth Basin are likely to have had a similar isotopic signature. The data presented above effectively eliminate from consideration any genetic model involving the precipitation of the second generation of lead from groundwaters. However, the possibility that barite and fluorite were derived from groundwaters cannot totally be disregarded.

Any attempt to characterise the potential ore-forming solutions in the Inner Moray Firth Basin must take into account their ability to silicify the host rock and to dissolve carbonates (albeit on a small scale). A fundamental question concerning the nature of the fluids is whether the lead and sulphur were transported in the same solution to the site of ore deposition. Several aspects of the nature of the mineralising fluids at Elgin remain problematical a genetic model is suggested involving transport of lead and sulphur in the same solution. Two possible genetic models involving transport of lead and sulphur in the same solution are also considered below.

Models involving ore deposition following mixing of two solutions are popular among workers on carbonate-hosted Pb-rich deposits (Mississippi Valley type deposits). Anderson (1975) favoured a model for precipitation of Mississippi Valley-type ores involving base metal-bearing basinal brines precipitating sulphides on encountering

either gaseous H_2S in the carbonate host rock or H_2S dissolved in groundwater. The sedimentological setting of the mineralisation at Elgin is not thought conducive to the accumulation of significant amounts of H_2S and consequently this mixing model is considered unlikely.

Oxidising fluids, capable of transporting Cu, Pb, Zn and SO_4 are thought to play a major role in the genesis of red bed-hosted Cu-rich deposits (eg. Rose 1976, Holmes et al. 1983, Sverjensky 1987), hence they have been invoked as the dominant ore-forming fluids in the Cheshire Basin deposits. Despite the presence of red beds and evaporites in the Inner Moray Firth Basin, it is clear from the distribution of the $\delta^{34}S$ values and the Pb-F-Ba rich nature of the deposits near Elgin, that the relatively simple genetic model proposed for the Cheshire Basin deposits cannot be applied to the mineralisation in the Moray Firth. These oxidising fluids are thought likely to transport copper in significant amounts as chloride complexes, with only minor amounts of lead and zinc, under conditions of relatively high Eh values. The absence of Cu mineralisation in the Moray Firth is thought to indicate that such brines did not contribute significantly to the genesis of the Pb-Ba-F mineralisation.

Sverjensky (1984) demonstrated that low pH (pH <4) brines containing no more than a few ppm Pb and Zn could form potential ore solutions. These ore-forming fluids are thought to be directly analogous to modern oilfield brines which are known to contain dissolved H_2S , Pb and Zn. However, the mode of metal transport within these solutions is still poorly understood, with authors such as Giordano and Barnes (1981) presenting theoretical data revealing that chloride and bisulphide complexes are inadequate to account for the lead transport and suggesting that organic ligands may be important complexing agents. Sverjensky (1984) also proposed that the migration of such brines through a sandstone aquifer would increase the amounts of base metals through dissolution and alteration of detrital grains such as K-feldspar. Sverjensky (1984) suggests that the initial stage of ore deposition from these solutions would be sphalerite-rich, and that when the reaction capacity of the aquifer is exhausted, solutions undersaturated with respect to sphalerite deposit galena during a second episode of ore

deposition. Furthermore, Sverjensky (1984) notes the association of Pb-rich deposits with sandstone aquifers similar to those in the Inner Moray Firth, this neat model is in accord with the geological setting and the low Zn/Pb ratio of the mineralisation at Elgin.

4.9.4 PRECIPITATION MECHANISMS FOR THE SULPHIDES,

BARITE AND FLUORITE.

Deduction of the precipitation mechanisms is limited by the poorly defined spatial and paragenetic relationships between the sulphide ores and the barite and fluorite deposits. Thus, sulphide deposition and precipitation of barite and fluorite are discussed separately.

Mechanisms involving the formation of sulphides from a metal-reduced sulphur bearing brine can include a decrease in temperature, dilution by groundwaters or reaction of the fluid with a carbonate horizon (Anderson 1983). A decrease in the chloride concentration of the fluid will bring about sulphide formation and this latter process can be triggered either by mixing with dilute groundwaters or reaction with carbonate-rich lithologies. An increase in the pH of the ore-forming solution on encountering carbonates will have a similar effect. The extent to which any of the above processes were involved in sulphide deposition within the Elgin succession remains unknown, with one or more of these mechanisms equally likely to have been significant in the light of the present data.

On the other hand, processes whereby sulphate in an oxidising fluid could be reduced in a sedimentary or diagenetic environment include bacterial sulphate reduction, thermochemical reduction by hydrocarbons, or inorganic sulphate reduction by iron minerals fixed in the host sediments. The $\delta^{34}\text{S}$ values of the galena and pyrite in the Cherty Rock are consistently lower than those in the barite and thus the distribution of the $\delta^{34}\text{S}$ values conform to a model involving sulphate-reduction of a fluid with initial sulphur isotope value similar to that of the barite (Ohmoto & Rye 1979). Thus, sulphate reduction may have been responsible for sulphide precipitation in the Cherty Rock, however, in view of the fact that the mineralising fluids are likely to have transported both metals and reduced sulphur, sulphate reduction is not thought to be a major mechanism for sulphide precipitation.

Barite depositional mechanisms have been documented by Leach (1980) and include oxidation of a barium and reduced sulphur-bearing solution, dilution of a barium-bearing brine with sulphate-rich meteoric waters or mixing of a barium-rich solution with a sulphate-bearing fluid. The latter mechanism was favoured by Leach (1980) following a detailed fluid inclusion study on paragenetically late barite in the southeast Missouri barite district which confirmed suggestions made by previous authors such as Sawkins (1968). A process of barite precipitation invoking oxidation of reduced sulphur would ultimately lead to a lowering of the pH resulting in significant dissolution of carbonate cements in the host sandstone. No evidence was found for a precursor carbonate cement in the barite-bearing sediments but it is clear that a period of widespread silica dissolution predated or was penecontemporaneous with barite formation in the aeolian sandstones. It has not been possible to elucidate the most significant mechanism of barite precipitation in terms of the present data.

Fluorite deposition can be brought about by a fall in temperature, by increase in solution pH and by mixing of solutions rich in Ca^+ with F^- saturated solutions (Richardson & Holland 1979). These authors favoured the simple cooling mechanism for fluorite deposition in the Cave-in Rock district, Illinois. The delicate colour banding noted by Richardson & Holland (1979) in the fluorite from Illinois is not present in the fluorite cements in the Hopeman Sandstone Formation. It is therefore not possible to preclude any of the fluorite depositional mechanisms outlined above but the presence of calcite inclusions in the fluorite in the Hopeman Sandstone Formation suggests that fluorite deposition may have resulted from the interaction between an F-bearing, almost pure NaCl solution with calcite cements in the Permo-Triassic sandstones of Elgin.

4.10 CONCLUDING REMARKS

It has not been possible to relate the timing of the mineralisation to the tectonic events in the Inner Moray Firth Basin. However, the limited evidence for fault control of the mineralising fluids in the exposures near Elgin, suggest that the mineralisation may be related to the intense fault activity in the basin during Jurassic to Lower Cretaceous times and during the Tertiary.

A sedimentary source for the base metals, Ba, F and sulphur is favoured, as

alternatives such as hydrothermal fluids of magmatic origin, groundwaters and seawater have been discounted in the light of the fluid inclusion and sulphur isotope data. The pattern of sulphur isotope values suggests that neither Permian evaporites or Jurassic seawater were the dominant source of sulphur for the mineralisation. Alternative sulphur sources in the Inner Moray Firth Basin are the sulphur-bearing horizons of the Jurassic Brora Coal and Kimmeridgian Clay Formations. The ore-forming fluids are envisaged as warm ($\sim 100^{\circ}\text{C}$), saline (~ 16 wt % NaCl) solutions similar to the basinal brines proposed by several authors (eg. Sverjensky 1984) as responsible for the transport of metals and sulphur during genesis of Mississippi Valley-type ore deposits.

Two genetic models are favoured for the mineralisation at Elgin; the first involves a reducing ore fluid transporting base metals, Ba, F and sulphur to the site of ore deposition. Sulphide precipitation is likely to be triggered by a fall in temperature, dilution with groundwaters or reaction with carbonates. Alternatively, the mineralising fluids may have been oxidising, with sulphide precipitation caused by H_2S at the site of ore deposition. The former model is preferred, as problems exist with the sulphate reduction mechanism inherent in the model involving oxidising fluids. In addition, it is suggested that the absence of copper in the mineralisation at Elgin may be a function of the reducing nature of the mineralising fluids.

In view of the evidence presented in this chapter, it is possible that genetic processes operating at Elgin were comparable to those invoked for certain Mississippi Valley-type ore deposits (Sangster 1983).

REFERENCES

- ALI, A.D. & TURNER, P. 1982. Authigenic K-feldspar in the Bromsgrove Sandstone Formation (Triassic) of Central England. *Journal of Sedimentary Petrology*, **52**, 187-197.
- ANDERSON, G.M. 1975. Precipitation of Mississippi Valley-type ore deposits. *Economic Geology*, **70**, 937-942.
- ANDERSON, G.M. 1983. Some geochemical aspects of sulfide precipitation in carbonate rocks. In: KISVARSANYI, G., GRANT, S.K., PRATT, W.P. & KOENIG, J.W. (eds) *International Conference on Mississippi Valley type lead-zinc deposits: Proceedings Volume*, 61-76. Univ. Mo. Rolla, U.S.A.
- BARR, D. 1985. The palinspastic restoration of normal faults in the Inner Moray Firth : implications for extensional basin development. *Earth and Planetary Science Letters*, **75**, 191-203.
- BATTEN, D.J., TREWWIN, N.H. & TUDHOPE, A.W. 1986. The Triassic-Jurassic junction at Golspie, Inner Moray Firth Basin. *Scottish Journal of Geology*, **22**, 1-44.
- BENTON, M.J. & WALKER, A.D. 1985. Palaeoecology, taphonomy and dating of Permo-Triassic reptiles from Elgin, north-east Scotland. *Palaeontology*, **28**, 207-234.
- BERRIDGE, N.G. & IVIMEY-COOK, H.C. 1967. The geology of a Geological Survey borehole at Lossiemouth, Morayshire. *Bulletin of the Geological Survey of Great Britain*, **27**, 155-169.
- CARLON, C.J. 1975. *The Geology and Geochemistry of some British barite deposits*, Phd. Thesis, University of Manchester.
- CHESHER, J.A. & LAWSON, D. 1983. *The geology of the Moray Firth*. Report 83/5. Institute of Geological Sciences.
- CLAYPOOL, G.E., HOLSTER, W.T., KAPLAN, I.R., SAKAI, H. & ZAK, I. 1980. The age curves of sulphur and their mutual interpretation. *Chemical Geology*, **28**, 199-260.

- CLEMMENSEN, L.B. 1987. Complex star dunes and associated aeolian bedforms, Hopeman Sandstone (Permo-Triassic), Moray Firth Basin, Scotland. In: FROSTICK, L. E. & REID, I. (eds) *Desert Sediments: Ancient and Modern*. Geological Society of London Special Publication, 356, 213-231.
- DUNCAN, A. 1986. *Organic geochemistry applied to source potential and the tectonic history of the Inner Moray Firth Basin*. PhD Thesis, University of Aberdeen.
- DUNHAM, K.C. 1952. *Fluorspar*. Special Report on the Mineral Resources of Great Britain, vol. IV. Memoirs of the Geological Survey of Great Britain.
- FOLK, R.L. 1974. *Petrology of Sedimentary Rocks*. Hemphills, Austin, Texas.
- FROSTICK, L.E., REID, I., JARVIS, J. & EARDLEY, H. 1988. Triassic sediments of the Inner Moray Firth, Scotland: early rift deposits. *Journal of the Geological Society*, **143**, 235-248.
- GALLAGHER, M.J., MICHIE, U.M^CL., SMITH, R.I. & HAYNES, L. 1971. New evidence of uranium mineralisation in Scotland. *Transactions of the Institute of Mining and Metallurgy*, **80B**, 150-173.
- GIORDANO, T.H., & BARNES, H.L. 1981. Lead transport in Mississippi-type ore solutions. *Economic Geology*, **76**, 409-425.
- GLENNIE, K.W. (ed.) 1984. *Introduction to the Petroleum Geology of the North Sea*. Blackwell Scientific Publications, Oxford.
- GLENNIE, K.W., MUDD, G.C. & NATEGAAL, P.J.C. 1978. Depositional environment and diagenesis of Permian Rotligendes Sandstone in Leman Bank and Sole Pit areas of the U.K. southern North Sea. *Journal of the Geological Society of London*, **135**, 25-34.
- GLENNIE, K.W. & BULLER, A.T. 1983. The Permian Wiessliegend of North-West Europe. The partial deformation of aeolian dune sands caused by the Zechstein transgression. *Sedimentary Geology*, **35**, 43-81.
- HOLMES, I., CHAMBERS, A.D. IXER, R.A., TURNER, P. & VAUGHAN, D.J.

1983. Diagenetic processes and the mineralization of the Triassic of Central England. *Mineralium Deposita*, **18**, 365-377.
- JUDD, J.W. 1873. The secondary rocks of Scotland. *Quarterly Journal of the Geological Society*, **29**, 97-197.
- LEACH, D.L. 1980. Nature of mineralizing fluids in the barite deposits of central and southeast Missouri. *Economic Geology*, **75**, 1168-1180.
- LINSLEY, P.N., POTTER, H.C., M^CNAB, G. & RACHER, D. 1980. The Beatrice field, Inner Moray Firth, U.K., North Sea. In: HALBOUTY, M.T. (ed) *Giant oil and gas fields of the decade 1968-1978*. Memoir of the American Association of Petroleum Geologists, **30**, 117-129.
- M^CQUILLIN, R., DONATO, J. & TULSTRUP, J. 1982. Development of basins in the Inner Moray Firth and the North Sea by crustal extension and dextral displacement of the Great Glen Fault. *Earth and Planetary Science Letters*, **60**, 127-139.
- M^CQUILLIN, R., BACON, M. & BARCLAY, W. 1984. *An Introduction to Seismic Interpretation*. Graham & Trotman, London.
- MACCHI, L. & VELTKAMP, C.J. 1985. Compound quartz and feldspar overgrowths from the Helsby Sandstone Formation (Triassic) of Cheshire, northwest England. *Geological Journal*, **20**, 281-285.
- M^CKENZIE, D.P. 1978. Some remarks on the development of sedimentary basins. *Earth and Planetary Science Letters*, **40**, 25-32.
- MACKIE, W. 1897. The sands and sandstones of Eastern Moray. *Transactions of the Edinburgh Geological Society*, **7**, 148-172.
- MACKIE, W. 1901a. The occurrence of barium sulphate and calcium fluoride as cementing agents in the Elgin Trias. *Report for the British Association for the Advancement of Science, Glasgow*, 649-650.
- MACKIE, W. 1901b. The pebble band of the Elgin Trias and its windworn pebbles. *Report for the British Association for the Advancement of Science, Glasgow*, 650-651.

- MOORBATH, S. 1962. Lead isotope abundance studies on mineral occurrences in the British Isles. *Philosophical Transactions of the Royal Society of London*, **A245**, 295-360.
- MUIR, R.O. & RIDGEWAY, J.M. 1975. Sulphide mineralisation of the continental Devonian sediments of Orkney (Scotland). *Mineralium Deposita*, **10**, 205-215.
- NAYLOR, H., FALLICK, A.E., TURNER, P. & VAUGHAN, D.J. (in prep) The genesis of the Cherty Rock, Elgin. (submitted to *Geological Journal*).
- NEWTON, E.T. 1893. On some reptiles from the Elgin Sandstones. *Philosophical Transactions of the Royal Society*, **184B**, 431-503.
- OHMOTO, H. 1986. Stable Isotope Geochemistry of Ore Deposits. In: VALLEY, J.W., TAYLOR, H.P., & O'NEIL, J.R. (eds). *Stable Isotopes and High Temperature Geological Processes*. Reviews in Mineralogy, 16. Mineralogical Society of America.
- OHMOTO, H. & LASAGA, A.C. 1982. Kinetics of reactions between aqueous sulphates and sulphides in hydrothermal solutions. *Geochimica et Cosmochimica Acta*, **46**, 1727-1745.
- OHMOTO, H. & RYE, R.O. 1979. Isotopes of Sulphur and Carbon. In: BARNES, H.L. (ed) *Geochemistry of Hydrothermal Ore Deposits*, 2nd. edition. Wiley and Sons, New York.
- PARNELL, J. & SWAINBANK, I. 1985. Galena mineralisation in the Orcadian Basin, Scotland; geological and isotopic evidence for sources of lead. *Mineralium Deposita*, **20**, 20-56.
- PEACOCK, J.D. 1966. Contorted beds in the Permo-Triassic aeolian sandstones of Morayshire. *Bulletin of the Geological Survey of Great Britain*, **24**, 157-162.
- PEACOCK, J.D., BERRIDGE, N.G., HARRIS, A.L. & MAY, A.F. 1968. *The geology of the Elgin district*. Memoir of the Geological Survey, Edinburgh.
- PEARSON, & WATKINS. 1983. Organo facies and early maturation effects in Upper Jurassic sediments from the Inner Moray Firth Basin. In: BROOKS, J. (ed) *Petroleum Geochemistry and Exploration of Europe*.

Geological Society of London Special Publication, 12, 147-160.

POTTER, R.W., CLYNNIE, M.A. & BROWN, D.L. 1978. Freezing point depression of aqueous sodium chloride solutions. *Economic Geology*, **73**, 284-285.

RICHARDSON, C.K. & HOLLAND, H.D. 1979. Fluorite deposition from hydrothermal solutions. *Geochimica et Cosmochimica Acta*, **43**, 1327-1336.

ROEDDER, E. 1984. *Fluid Inclusions*. Reviews in Mineralogy 12, Mineralogical Society of America.

ROSE, A.W. 1976. The effect of cuprous chloride complexes in the origin of red bed copper and related deposits. *Economic Geology*, **71**, 1036-1048.

SANGSTER, D.F. 1983. Mississippi Valley-type deposits: a geological melange. In: KISVARSANYI, G., GRANT, S.K., PRATTT, W.P. & KOENIG, J.W. (eds) *International conference on Mississippi Valley type lead-zinc deposits: Proceedings Volume*, 7-19, University, Mo. Rolla, U.S.A.

SAWKINS, F.J. 1968. The significance of Na/K and Cl/SO₄ ratios in fluid inclusions with respect to the genesis of Mississippi Valley-type ore deposits. *Economic Geology*, **63**, 935-942.

SCHMIDT, V. & McDONALD, D.A. 1979. The role of secondary porosity in sandstones. In: SCHOLLE, P.A. & SCHLUGER, P.R. (eds) *Aspects of diagenesis*. SEPM Special Publication, 26, 209-225.

SHEPPARD, R.A. & MUMPTON, F.A. 1984. Sedimentary fluorite in a lacustrine zeolitic tuff of the Gila Conglomerate, Grant County, New Mexico. *Journal of Sedimentary Petrology*, **54**, 853-860.

SRODON, J. 1984. X-ray powder diffraction identification of illitic materials. *Clays and Clay Minerals*, **32**, 337-349.

STARKEY, R.E. 1988. Phosgenite from Losseimouth, Grampian Region: confirmation of the first Scottish occurrence. *Scottish Journal of Geology*, **24**, 15-19.

- SVERJENSKY, D.A. 1981. The origin of a Mississippi Valley-type ore deposit in the Viburnum Trend, southeast Missouri. *Economic Geology*, **76**, 1848-1872.
- SVERJENSKY, D.A. 1984. Oil field brines as ore-forming solutions. *Economic Geology*, **79**, 23-37.
- SVERJENSKY, D.A. 1987. The role of migrating oil field brines in the formation of sediment-hosted Cu-rich deposits. *Economic Geology*, **82**, 1130-1141.
- TURNER, P. 1980. *Continental Red Beds*. Developments in Sedimentology, 29, Elsevier, Amsterdam.
- WALKER, A.D. 1961. Triassic reptiles from the Elgin area : *Stagonolepis*, *Dasygnathus* and their allies. *Philosophical Transactions of the Royal Society*, **B244**, 103-204.
- WALKER, T.R. 1967. Formation of red beds in modern and ancient deserts. *Bulletin of the Geological Society of America*, **78**, 353-368.
- WARRINGTON, G., AUDLEY-CHARLES, M.G., ELLIOT, R.E., EVANS, W.B., IVIMEY-COOK, H.C., KENT, P.E., ROBINSON, P., SHOTTON, F.W. & TAYLOR, F.M. 1980. *A correlation of Triassic rocks in the British Isles*. Geological Society of London Special Publication.
- WATSON, D.M.S. & HICKLING, G. 1914. On the Triassic and Permian rocks of Moray. *Geological Magazine*, **1**, 399-402.
- WATSON, D.M.S., WESTOLL, T.S., WHITE, E.I. & TOOMBS, H.A. 1948. Guide to excursion 16 vertebrate palaeontology. 18th International Geological Congress.
- WAUGH, B.W. 1978. Authigenic K-feldspar in British Permo-Triassic sandstones. *Journal of the Geological Society of London*, **135**, 51-56.
- WEDEPOHL, K.H. 1978. *Handbook of Geochemistry*. Springer-Verlag, Heidelberg.
- WESTOLL, T.S. 1951. The vertebrate-bearing strata of Scotland. 18th

International Geological Congress, 9, 5-21.

WILSON, G.V. & FLETT, J.S. 1921. *The lead, zinc, copper and nickel ores of Scotland.*

Memoirs of the Geological Survey of Great Britain Special Report on the Mineral Resources of Great Britain, vol XVII, 110-111.

WILLIAMS, D. 1973. *The sedimentology and petrology of the New Red Sandstone of the Elgin Basin, North-east Scotland.* Ph.D. thesis, University of Hull.

ZIEGLER, P.A. 1982. *Geological Atlas of Western and Central Europe.* Elsevier, Amsterdam.

CHAPTER 5

THE GENESIS OF THE CHERTY ROCK, ELGIN

ABSTRACT

The Cherty Rock is a laterally persistent horizon that extends across the Inner Moray Firth Basin, northeastern Scotland. The southern exposures of the Cherty Rock near Elgin reveal an indurated carbonate and silica-rich horizon (0.75-10m thick) developed in the uppermost part of the largely aeolian Lossiemouth Sandstone Formation. Laminated, pisolitic and brecciated textures within the Cherty Rock confirm that the horizon represents an analogue to Recent calcretes of semi-arid areas. Textures characteristic of silcretes are widespread in the Cherty Rock but these originate from silica replacement of calcite. The carbon and oxygen stable isotopic composition of the Cherty Rock (mean $\delta^{13}\text{C} = 7.3 \text{‰}$, mean $\delta^{18}\text{O} = 8.9 \text{‰}$, both relative to PDB) is comparable to that of other Permo-Triassic calcretes and modern soil carbonate, suggesting that similar processes were responsible for their formation. Carbon and oxygen isotope techniques can be used to constrain the source materials, the temperature and processes involved in ancient calcrete development and to assess the post-depositional changes. The $\delta^{13}\text{C}$ and $\delta^{18}\text{O}$ values for calcite in the Cherty Rock may indicate that evaporative processes contributed to its development.

The Cherty Rock is a useful stratigraphical and palaeoclimatic indicator, and its presence in the Inner Moray Firth basin suggests a period of tectonic stability in the basin during late Triassic times.

5.1 INTRODUCTION

The Cherty Rock is an enigmatic, carbonate-rich, laterally extensive horizon which occurs throughout the Inner Moray Firth Basin, northeastern Scotland (Linsley et al. 1980) (see Fig. 5.1) and is generally less than 15m thick. It is developed in the upper part of a sequence of continental aeolian and fluvial sands (Peacock et al. 1968) whose maximum thickness at Lossiemouth reaches 135m. The horizon is developed in the thin fluvial deposits in the uppermost part of the predominantly aeolian Lossiemouth

Sandstone Formation. The Cherty Rock is also instantly recognisable on seismic sections (Linsley et al. 1980) and is thus an invaluable stratigraphic marker horizon.

The complexity of the carbonate and silica-rich microfabrics within the Cherty Rock horizon have resulted in controversy over its origin. Early authors such as Watson & Hickling (1914) compared it to the superficial chalcidony of modern semi-arid areas. More recent discussions have favoured an origin analogous to modern calcretes (Peacock et al. 1968; Williams 1973; Frostick et al. 1988) which are commonly subject to silicification (eg. Watts 1980) similar to that associated with the Cherty Rock. Numerous references to calcrete exist in the descriptions of ancient sedimentary sequences (eg. Allen 1974; Steel 1974; Hubert 1978) as do various general reviews (Netterberg 1967; Goudie 1973; Reeves 1976). The term 'calcrete' is used to describe a carbonate-rich, dominantly indurated profile or a horizon resulting from pedogenic carbonate accumulation. Calcretes have considerable geological significance for a variety of reasons, including their use as palaeoclimatic and palaeoenvironmental indicators (Goudie 1973). The presence of a laterally extensive, reasonably thick calcrete in ancient sedimentary sequences is often indicative of a period of stable tectonic conditions and of minimal erosion. In addition, calcretes are often distinctive marker horizons which may be used for stratigraphic correlation purposes, and some calcretes are economically important, as demonstrated by Carlisle (1983) in his description of uranium ores hosted by the groundwater calcretes of Western Australia.

An alternative origin for the Cherty Rock is as a limestone deposited in a lagoonal or lacustrine environment; the presence of freshwater ostracods being cited as supporting evidence for this theory (Robertson Research Report 1978).

In the present study, the southern exposures of the Cherty Rock near Lossiemouth (Fig. 5.2) have been examined in detail. The investigation has revealed a complex diagenetic history, which includes carbonate cementation prior to barite, fluorite, haematite, galena and marcasite mineralisation. This paper is primarily concerned with the early development of the Cherty Rock horizon which will be shown largely to predate the mineralisation. The horizon is poorly exposed and, as a result of the lack of large-scale features, the main aim has been to examine critically the analogy between the

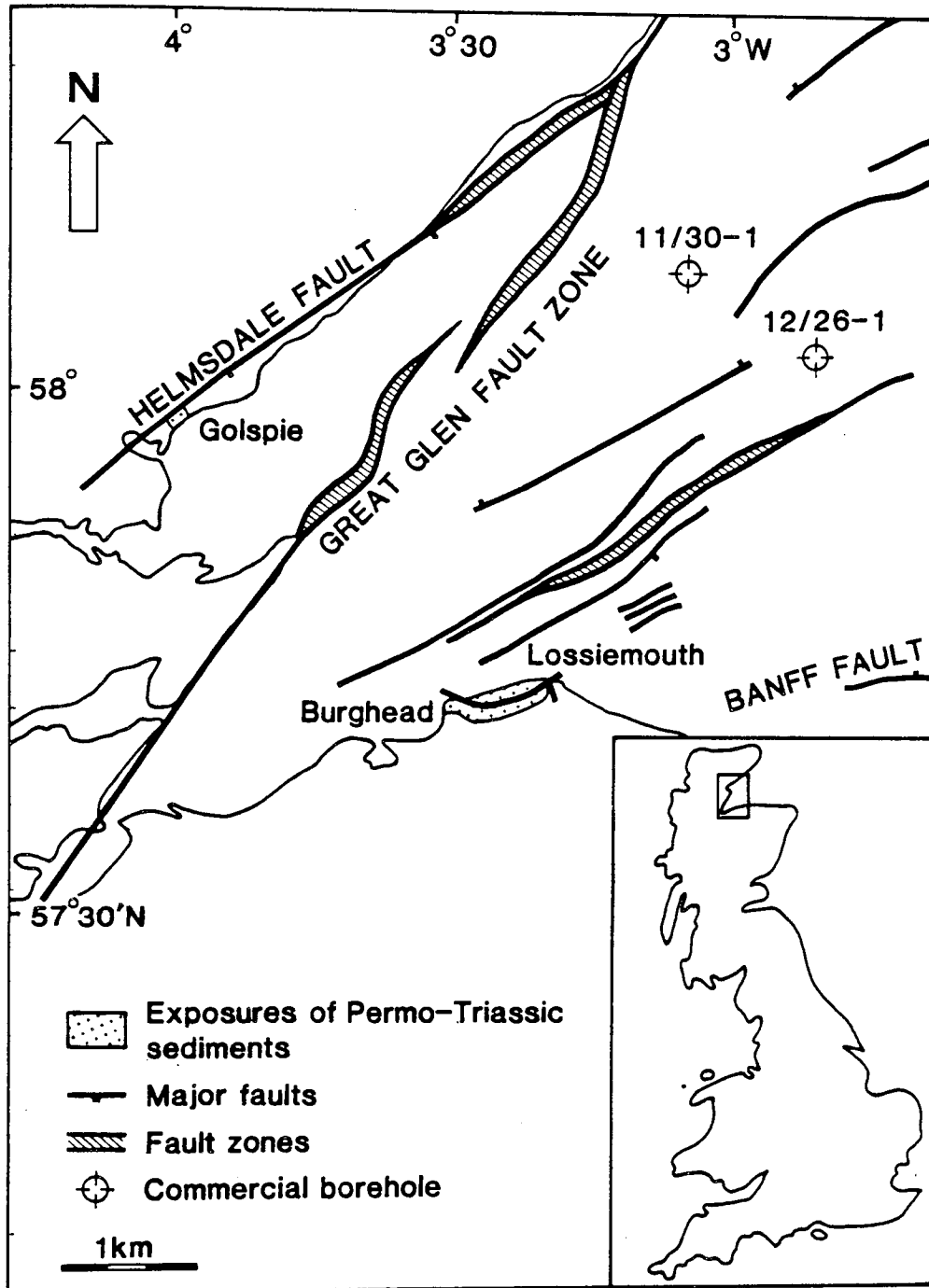


Figure 5.1. A map showing the geological setting and the exposures of the Cherty Rock on the southern edge of the Inner Moray Firth Basin, north east Scotland. The location of commercial offshore wells in which the horizon is present is also shown.

Cherty Rock and Recent calcretes (eg. Watts 1980) in the light of textural, geochemical and stable isotope data. The pedogenic and diagenetic history of the Cherty Rock is described herein, and for comparative purposes, petrographic and isotopic data have also been obtained from calcretes in the New Red Sandstone of the Hebridean Basin, Western Scotland (Steel 1974). In discussing the results of this work, emphasis is placed on the palaeogeographic, palaeoclimatic, stratigraphic and tectonic importance of the laterally persistent Cherty Rock horizon within a structurally complex basin.

5.2 GEOLOGICAL SETTING

The Cherty Rock is a chemically precipitated horizon which developed in the upper part of the Lossiemouth Sandstone Formation in the Rhaetic (Fig. 5.1). It is a pale grey, massive, strongly indurated horizon which is exposed at a small number of localities on or near the southern Moray coast e.g. at Inverugie Quarry and at Stotfield, Lossiemouth (Fig. 5.2) where it is extensively silicified and mineralised (Peacock et al. 1968).

The horizon was first described by Judd (1873) who noted its similarity to a marly limestone with chert which is poorly exposed near Golspie, Sutherland (Fig. 5.1). Later authors (eg. Lee 1925; Peacock et al. 1968) agreed with this observation and it is generally accepted that the exposures near Golspie are stratigraphically equivalent to the Cherty Rock of Lossiemouth. Benton & Walker (1985) dated the Lossiemouth Sandstone Formation as Lower Norian on the basis of a detailed study of reptile fauna. At Golspie, the Lower Jurassic Dunrobin Pier Conglomerate contains pebbles derived from the underlying Cherty Rock and this is interpreted by Batten et al. (1986) as evidence for an erosive contact between the two. These authors also presented palynological data which suggested that the Dunrobin Pier Conglomerate is Hettangian in age. On the southern basin margin, Early Jurassic non-marine sediments overlie Triassic continental facies in the Lossiemouth Borehole, although the contact is not seen (Berridge & Ivimey-Cook 1967). In view of the evidence outlined above, the Cherty Rock is tentatively assigned to the Upper Triassic (Rhaetic). The lateral extent of the Cherty Rock horizon remains incompletely known but it is a strong seismic reflector throughout the Inner Moray Firth Basin, and has been recognised in the Beatrice Field where it forms the base of the reservoir section (Linsley et al. 1980). The Cherty Rock is

also present in a dry hole drilled by Hamilton Brothers in 1976 (well 12/26-1) and its absence in well 12/23-1 (a dry hole drilled by Total) (see Fig. 5.1) has been attributed to erosion (Linsley et al. 1980).

5.3 FIELD OCCURRENCE

The Cherty Rock occurs within the Lossiemouth Sandstone Formation, which comprises intensely silicified sandstones that contain patchy carbonate cements. Field studies have shown that sporadic nodular calcite cements are also present in the underlying Burghead and Hopeman Sandstone Formations and at least some of these cements may represent pedogenic carbonate accumulations. The Cherty Rock itself varies in thickness from 0.75m to a maximum of 10m at Inverugie Quarry (Fig. 5.2) where it has a shallow dip to the north. In offshore well 12/26-1, it is represented by a thin, flat-lying calcareous horizon containing siliceous veins and chert. Williams (1973) suggested that vertical variations within the Cherty Rock represented different stages of calcrete profile development. However, the complex silica and calcite textures observed in the present study render invalid any attempt to subdivide this complex horizon. Overall, the southern exposures of the Cherty Rock comprise highly silicified Lossiemouth Sandstone which grades up into an increasingly carbonate-rich, indurated horizon with occasional 'pockets' of unaltered sandstone. This main horizon, of probable pedogenic origin, is generally massive with 1-1.5m thick beds separated by stylolitic contacts. The thickness of the Cherty Rock suggests that this is a composite palaeosol representing recurring episodes of calcrete development.

5.4 ANALYTICAL METHODS

Textural and mineralogical studies involved the examination of more than 50 thin and polished sections using transmitted and reflected light microscopy as well as cathodoluminescence petrography. Thin sections were stained with potassium ferricyanide and Alazarin Red-S (following Dickson 1965). Calcrete mineralogy was also determined by X-ray diffraction and the minor elements analysed by X-ray fluorescence spectrometry.

Isotopic analyses were performed on calcite hand-picked from stained polished rock slices. CO₂ was extracted from the powdered calcite on reaction with phosphoric acid

This page has been left intentionally blank

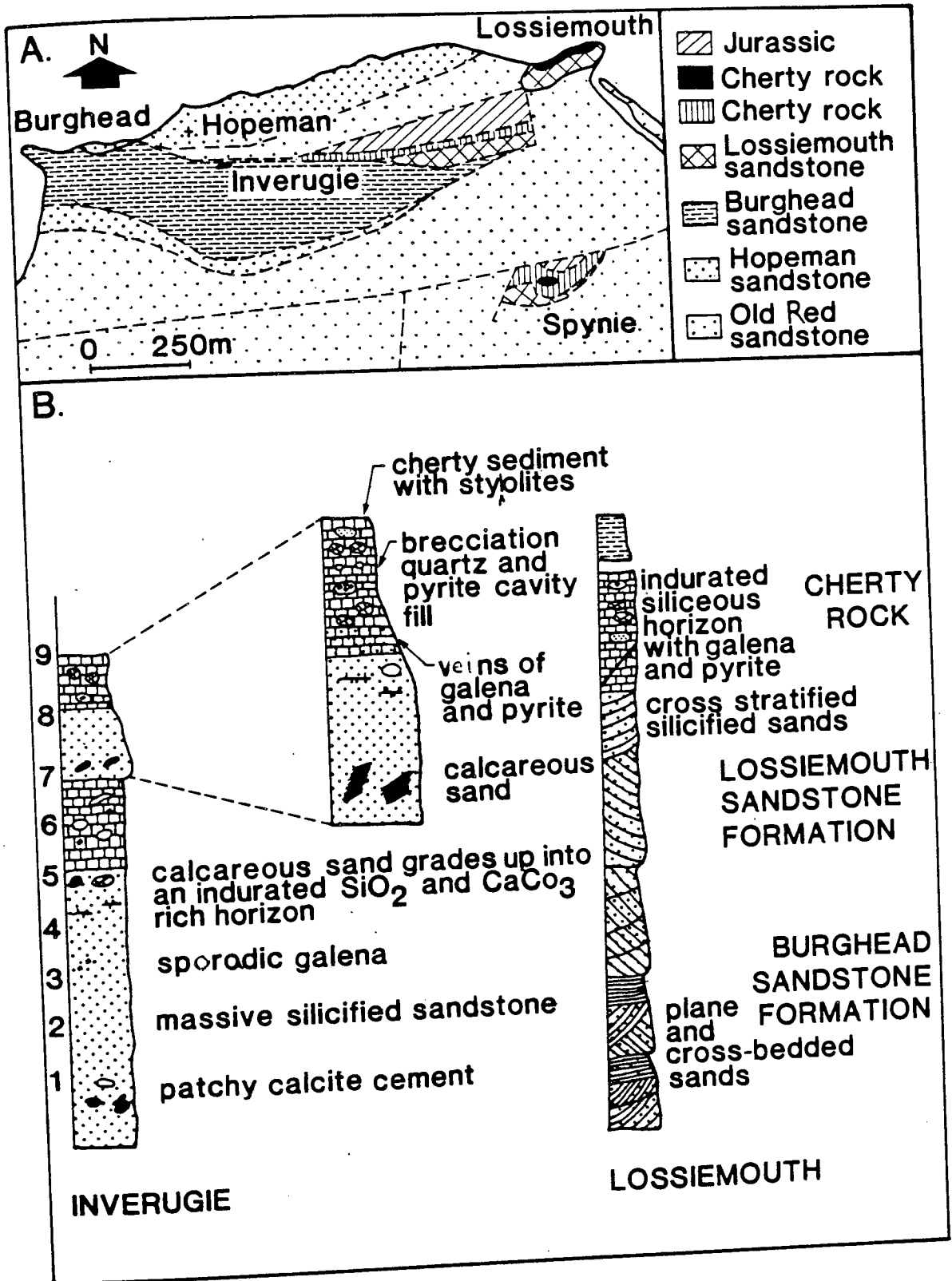
Figure 5.2.A. A detailed geological map of the Permo-Triassic sequence at the southern margin of the Inner Moray Firth Basin, near Lossiemouth (adapted from Peacock et al. 1968). The Cherty Sandstone was studied in the exposures at Lossiemouth, Spynie and Inverurie.

B. Schematic logs of the upper Lossiemouth Sandstone Formation and Cherty Rock at Inverurie and Lossiemouth to show the lithological characteristics of the sediments. At least two distinct, indurated horizons are present in a shallow borehole at Inverurie, while silicification and mineralisation prevail in the single horizon at Lossiemouth.

Figure 5.2.A. A detailed geological map of the Permo-Triassic sediments on the southern margin of the Inner Moray Firth Basin, near Lossiemouth (adapted from Peacock et al. 1968). The Cherty Rock was studied in the exposures at Lossiemouth, Spynie and Inverugie.

B. Schematic logs of the upper Lossiemouth Sandstone Formation and Cherty Rock at Inverugie and Lossiemouth to show the lateral characteristics of the sediments. At least two distinct, indurated horizons are present in a shallow borehole at Inverugie, whilst silicification and mineralisation prevail in the single horizon at Lossiemouth.

FIGURE 5.2



using the procedures outlined by McCrea (1950). The carbon and oxygen isotopic ratios were measured using a 'VG SIRA 10' mass spectrometer. Carbon and oxygen isotope values are reported in the standard notation relative to the PDB standard; reproducibility of results was $\pm 0.1\text{‰}$ for both carbon and oxygen. Chalcedony was prepared for isotopic analysis by first crushing and then handpicking under a binocular microscope. The powdered samples were treated with ClF_3 at 650°C (after Borthwick & Harmon 1982) and analysis of the CO_2 performed on a 'VG SIRA 10' mass spectrometer. NBS 28 quartz gives $\delta^{18}\text{O} = 9.6\text{‰}$ (SMOW) and NBS 19 carbonate gives $\delta^{13}\text{C} = 1.96\text{‰}$ (PDB), $\delta^{18}\text{O} = -2.19\text{‰}$ (PDB) by these techniques.

5.5 PETROGRAPHIC STUDIES

5.5.1 DESCRIPTION

The textures developed in the Cherty Rock are outlined below and references made to similar fabrics described in the Quaternary calcretes of the Kalahari (Watts 1980) and to other well-documented Triassic calcretes (Steel 1974). The Lossiemouth Sandstone Formation, which hosts the Cherty Rock horizon, consists of mature, medium-grained, well sorted sands similar to those of the Kalahari. Quartz is the predominant detrital mineral with subsidiary orthoclase feldspar, microcline, rock fragments and negligible amounts of muscovite. The clay assemblage is dominated by detrital illite which occurs as thin grain coatings. The original sandstone fabric comprises subrounded detrital silicate grains, poorly cemented by quartz overgrowths. It is rarely preserved in the main horizon as a result of the pervasive carbonate cements, but where it does occur, quartz and feldspar overgrowths are seen to predate calcite micritic cements.

Low Mg calcite is widespread throughout the Cherty Rock where it occurs as micrite, microspar and spar cements. The microfabric of the horizon comprises crystals of size $2\text{--}12\ \mu\text{m}$ which are generally equant or subhedral in form. Rhombic calcite crystals are scattered within the micrite and have a mean length of $130\ \mu\text{m}$ (Fig. 5.3). Cathodoluminescence petrography reveals the concentric zoning within these rhombs. The presence of rhombic calcite in palaeosols has been noted by several authors

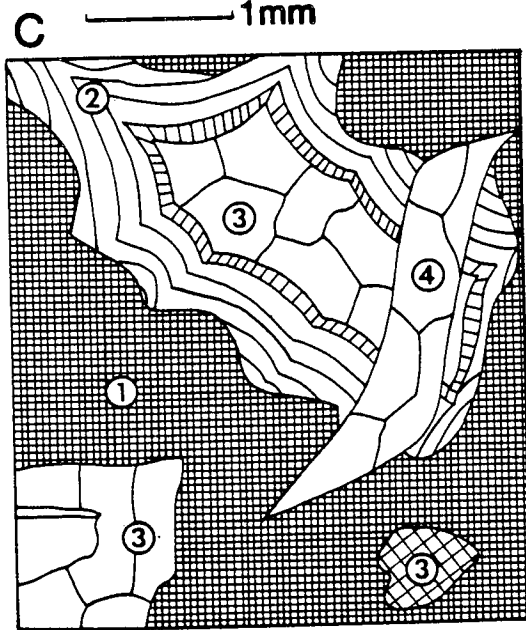
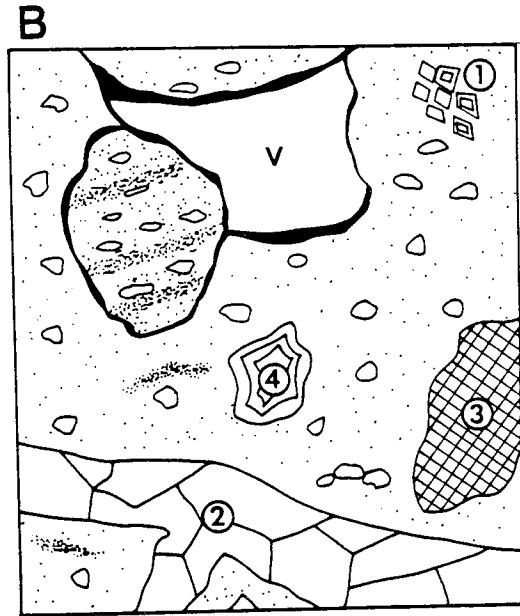
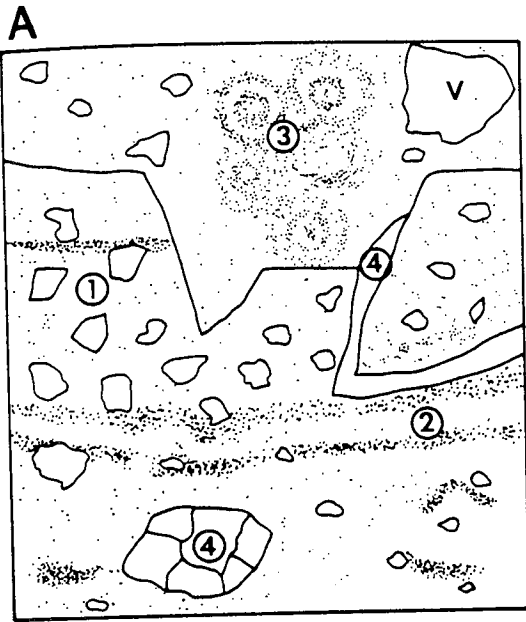
This page has been left intentionally blank

Figure.5.3. A schematic diagram to show the textural evolution of the Cherty Rock.

(A). The original sandstone fabric with illitic grain coatings and quartz and feldspar overgrowths enclosing detrital quartz grains (1) predates the precipitation of pervasive micritic cements. Corroded sandstone grains (1) are isolated in a micritic matrix and thickening of micritic laminae on the underside of detrital silicate grains (2) illustrates that downward percolation of carbonate-rich groundwaters occurred during the development of the Cherty Rock. Voids (V) are common, as are pisolites (3) and veinlets of sparry calcite (4).

(B). Scattered dolomite and calcite rhombs are observed (1). Recrystallisation and dissolution-reprecipitation processes result in the deposition of cross-cutting sparite veins (2) and non-ferroan calcite spar in cavities. Silicification of the horizon is heralded by the precipitation of microquartz (3) and sporadic development of length-slow and length-fast chalcedony.

(C). Advanced silicification of the Cherty Rock is reflected by the widespread precipitation of microquartz (1) containing calcite inclusions. Alternating bands of length-slow and length-fast chalcedony (2) predate the deposition of macroquartz (3) in cavities and vugs. Later, transgressive veins of coarsely crystalline quartz are commonly sulphide-bearing. Sigmoidal tension gashes are filled with non-ferroan calcite (4) and are interpreted as the last phase of cementation in the horizon prior to the onset of mineralisation.



including Folk (1974) and Chafetz & Butler (1980) who attributed it to precipitation from slow-moving solutions in a freshwater environment. The 'floating' fabric of quartz and feldspar grains within micrite, which is common in the Cherty Rock, is thought to be the result of a combined process of displacive micritic growth and grain dissolution. Fabrics observed in the Cherty Rock include laminar layering comprising sub-parallel laminae of micrite (Plate 5.1). The different colours and luminescence characteristics of the individual laminae are probably determined by the relative concentrations of Mn and Fe within them (Machel 1986). Concentric structures comprising several laminae of micrite and having diameters ranging between 90 and 100 μm are abundant in the Cherty Rock (Plate 5.2). These features are common in calcretes and three main types were recognised by Hay & Wiggins (1980). The concentric structures in the Cherty Rock are similar to the authigenic calcite 'pellets' described by Hay & Wiggins (1980). Pellets in the Cherty Rock are commonly dissected by veins of sparry calcite. Detailed cathodoluminescence studies of the spar have revealed that individual growth zones may only be traced between adjacent pores and cannot be used for correlation purposes. Cathodoluminescence defines several generations of spar cements (Plate 5.3) but the complexity of the textures makes it impossible to distinguish between meteoric spar cements and burial cements. Several generations of calcite veins occur in a cross-cutting pattern with the later spar tending to be ferroan calcite.

Minor amounts of dolomite occur as small (115-150 μm in size) euhedral rhombs scattered within the micritic fabric. Highly birefringent illite grain coatings are common. X-ray diffraction confirms the presence of minor amounts of subsidiary, non-swelling illite. In contrast, in the underlying Lossiemouth Sandstone Formation illite-smectite clays predominate. Palygorskite, sepiolite and montmorillonite have been widely reported from Permo-Triassic and Recent calcrete profiles (eg. Watts 1976, 1980) but are thought to result from weathering processes during calcrete development.

Silica cements in the Cherty Rock can be subdivided and consist of i) zones of chalcedony in the form of concentric structures or bands of alternating length-slow and length-fast chalcedony; ii) an interlocking fabric of equant crystals of 20-35 μm in size (microquartz); iii) elongate, semi-opaque crystalline silica, and iv) coarsely crystalline

quartz infilling vugs and veins (Plate 5.4). This idealised sequence of phase deposition (Fig. 5.3) is rarely complete in any one sample but corresponds closely to the sequence of crystallisation described by Thiry & Millot (1987) in Tertiary silcretes. The silcretes show complex textures reflecting the deposition of poorly crystalline silica phases, such as opal followed by dissolution and reprecipitation to form ordered and more coarsely crystalline phases lacking in impurities. X-ray diffracton analyses are consistent with the petrographic observation that authigenic silica within the Cherty Rock occurs as well crystallised quartz that produces sharp peaks on the diffraction trace. Opal-CT is not present but the textural evolution from chalcedonic quartz and microquartz through to macrocrystalline, limpid quartz parallels that seen in the Tertiary silcretes. Thiry & Millot (1987) suggested that a sequence of continued deposition, dissolution and recrystallisation within the palaeosols resulted in the growth of microcrystalline quartz, quartz overgrowths, and finally, the evolution of large quartz crystals in the voids; a similar process is envisaged for the Cherty Rock.

Occasionally, later ferroan calcite spar forms the final cement in the Cherty Rock where it infills sigmoidal tension gaps. Limited brecciation is observed; it generally postdates calcite and chalcedony precipitation with the exception of a late ferroan calcite spar which fills the fractures. Thus, overall, a complex history of cementation, dissolution, reprecipitation and brecciation has been revealed .

5.5.2 INTERPRETATION

The mineralogical and textural characteristics of the Cherty Rock are similar to those of both ancient Permo-Triassic calcretes (Steel 1974) and Recent calcretes (Watts 1980, Esteban & Klappa 1983). Textures diagnostic of calcretes including pervasive micrite, laminar layering, concentric structures and cross-cutting sparry calcite are common. No textural evidence was found to indicate the presence or former existence of the aragonite or high Mg calcite precursor, described by Watts (1980) in Kalahari calcretes. The low Mg calcite of the Cherty Rock is more commonly associated with calcrete development and is thought to precipitate from low Mg/Ca ratio waters in the vadose zone as a result of evaporation, CO₂ loss, or both (Watts 1980).

The presence of dolomite has been interpreted by Frostick et al. (1988) as the first

This page has been left intentionally blank

Plate 5.1 Colour photomicrograph of the original sandstone fabric of the Cherty Rock, Inverugie. Textural evidence indicates that the horizon consisted of a quartz-rich sandstone cemented by illitic clays prior to the precipitation of the micritic calcite cements. Scale bar = 500 μm (PPL).

Plate 5.2 Colour photomicrograph of laminar layering in the Cherty Rock, Inverugie. The structures are composed of micrite and are commonly disrupted by microbrecciation fabrics. Scale bar = 500 μm (Crossed polars)

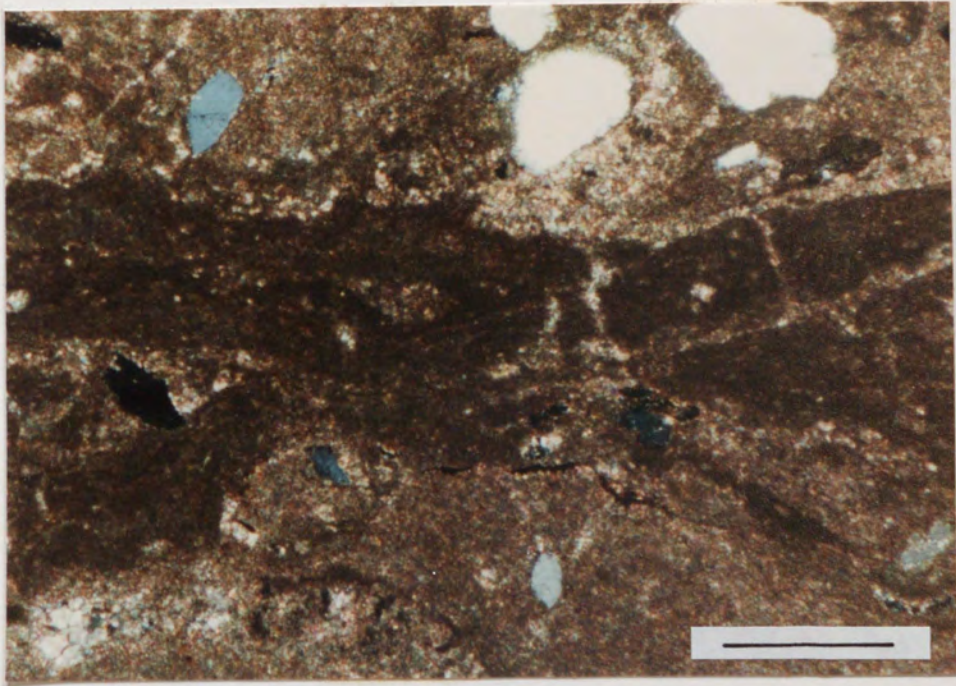
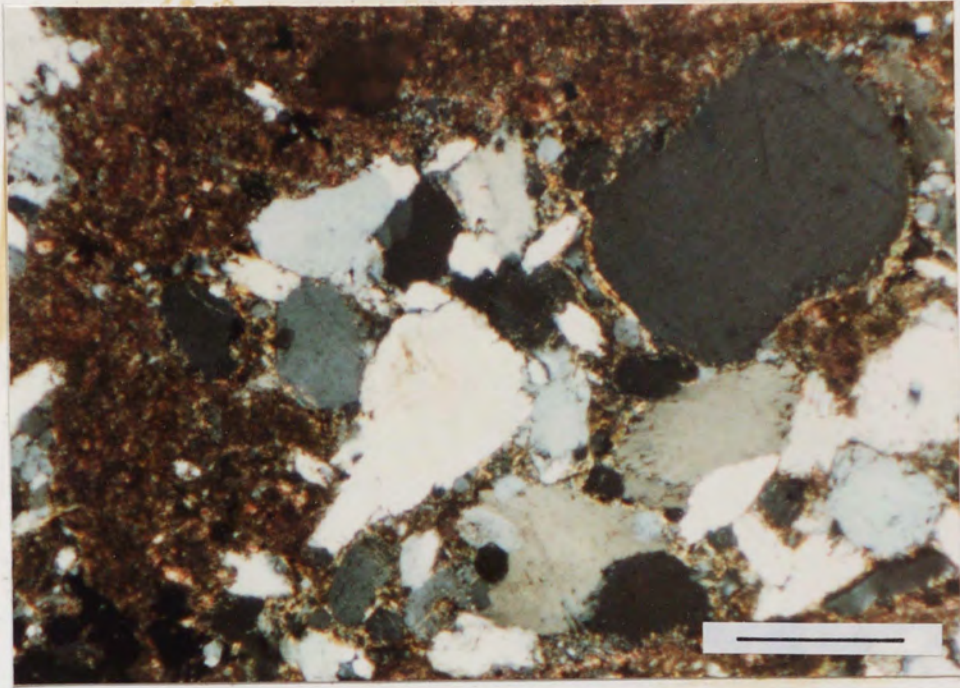


Plate 5.3 Colour photomicrograph of concentric structures (pellets) composed of micritic calcite in the Cherty Rock, Inverugie. Detrital quartz and potassium feldspar are completely enclosed within the micritic matrix. Scale bar = 500 μm (Crossed polars).

Plate 5.4 Colour photomicrograph of the cathodoluminescence characteristics of the cements in the Cherty Rock, Inverugie. Micritic cements typically exhibit dull orange luminescence (M). Two distinct generations of spar cement can be distinguished by their luminescence; an early brightly luminescent cement (S1) and a non-luminescent cement with brightly luminescent 'hairlines' (S2). Scale bar = 500 μm .

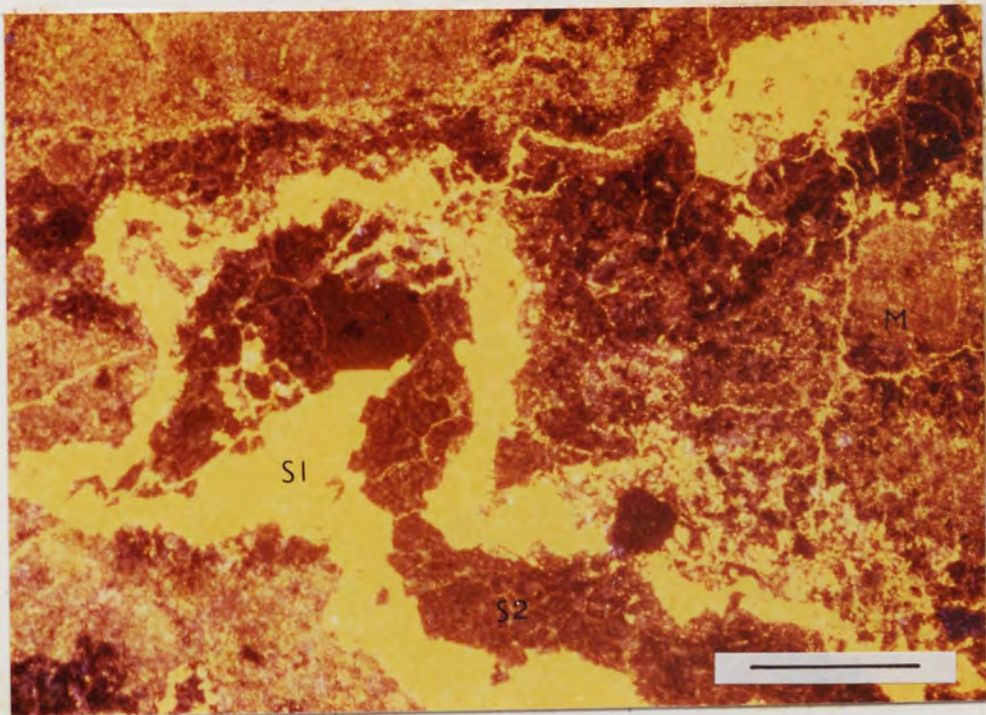
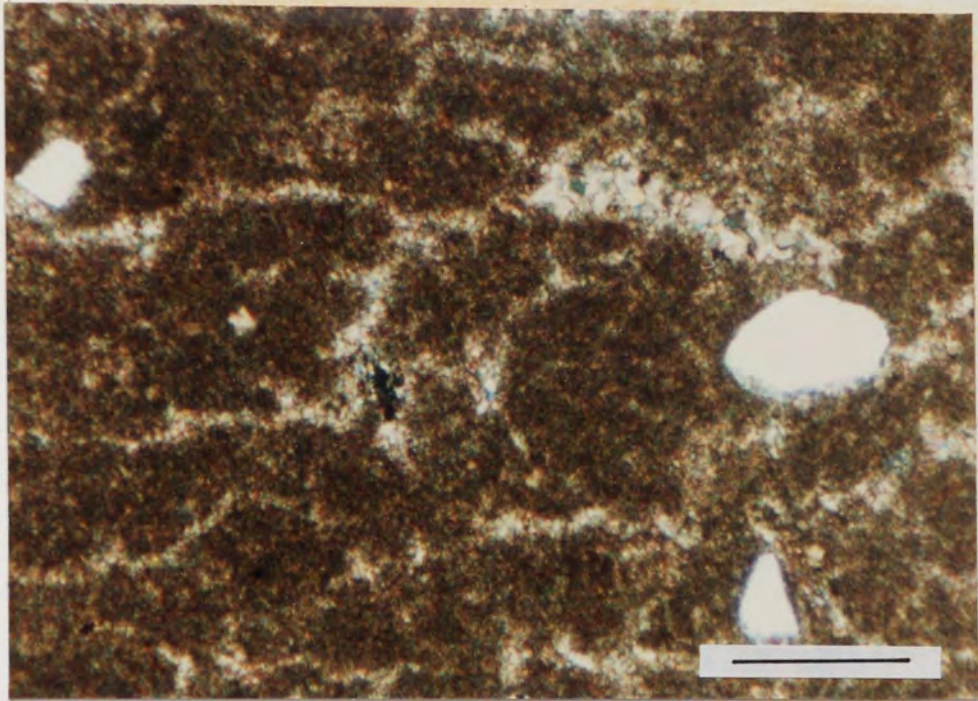
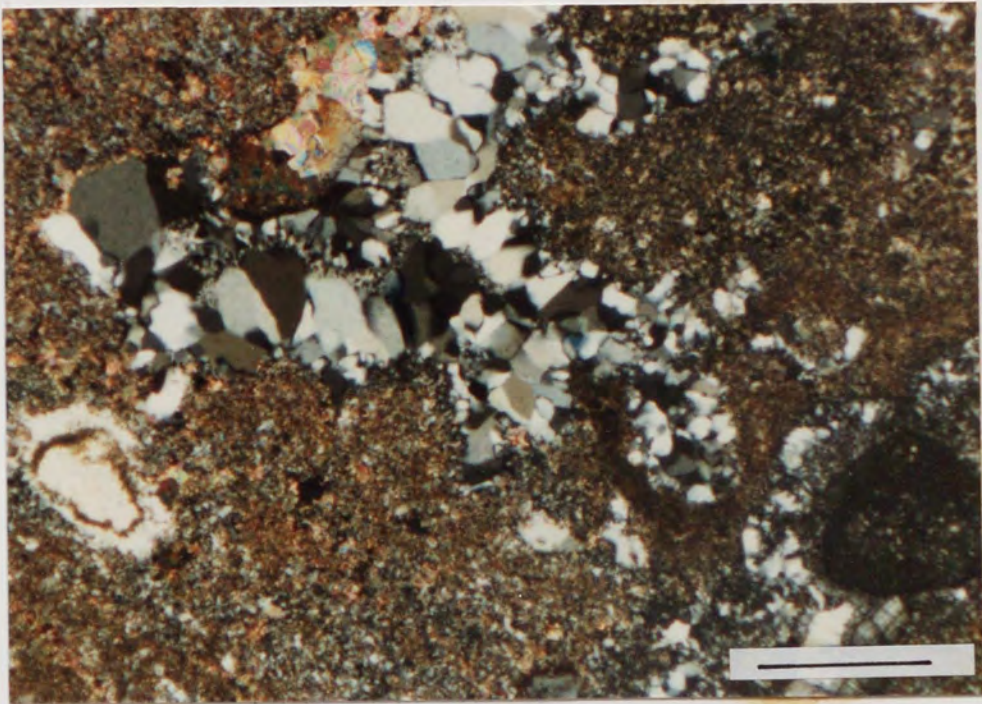
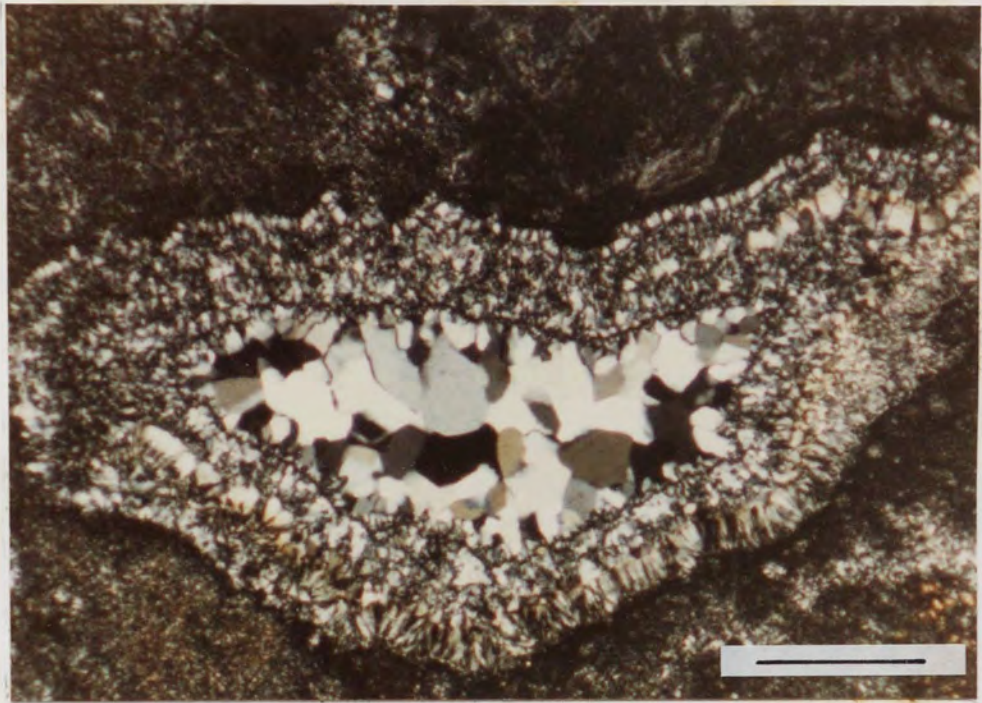


Plate 5.5 Colour photomicrograph of complex silica void fill in the Cherty Rock, Lossiemouth. The main fabric of the rock consists of microcrystalline quartz, whilst alternating bands of length-slow and length-fast chalcedony and coarsely crystalline quartz infill vugs and veins. Scale bar = 500 μm (Crossed polars).

Plate 5.6 Colour photomicrograph of complex carbonate and silica fabrics in the Cherty Rock, Inverugie. Calcite inclusions are widespread in the microquartz, but are not as abundant in the chalcedony and coarsely crystalline quartz. Scale bar = 500 μm (Crossed polars).



evidence for brackish water in the Inner Moray Firth Basin, but the finely crystalline dolomite is more likely to have precipitated from freshwater solutions with high Mg/Ca ratios as a result of evaporation (Watts 1980). In the latter case, Mg-enrichment of pore fluids may be caused by the concurrent precipitation of low Mg calcite within the Cherty Rock. It is suggested that Mg-rich groundwaters may have been sourced from Caledonian gabbros to the south of Elgin.

Finally, the intimate relationship between calcrete profile development and silicification has been noted by several authors (eg. Steel 1974; Watts 1980; Goudie 1983) and appears to be an integral part of the evolution of the Cherty Rock during the Rhaetic. Authigenic silica is common in highly-developed mature calcretes, but unlike the other palaeosols described in the literature where silicification is concentrated in the base of the profile, silicification of the Cherty Rock appears to be totally random. The silicification appears to have been a multi-stage process whereby silica replacement of carbonate and repeated dissolution and reprecipitation of silica occurred.

There is a striking similarity between the textures observed in the Cherty Rock and those described from silcretes (Summerfield 1983a, 1983b; Thiry & Millot 1987) but the abundance of calcite inclusions (as observed from cathodoluminescence studies) within silica generations i), ii), and iii) above (Fig. 5.3) is considered as unequivocal evidence that widespread replacement of carbonate by silica has occurred. Glaebules are concentric structures common in silcretes (Summerfield 1983a, 1983b) which have maximum diameters of several cm. Similar structures in the Cherty Rock are interpreted as inherited features from calcretes where silica replacement of pellets and pisolites has occurred.

5.6 GEOCHEMISTRY

Major element analyses of bulk samples of the Cherty Rock was carried out using atomic absorption spectrophotometry and the results shown in Table.5.1. Samples whose textures and mineralogy are similar to those of modern calcretes have a mean CaCO_3 content of 55.55% and a mean SiO_2 content of 20.44%. The samples in the present study are more silica-rich than the three hundred calcretes analysed by Goudie (1973)

TABLE 5.1. Whole rock chemical analyses (major oxides, wt%) of the Cherty Rock and calcretes from Gribun, Isle of Mull.

	CaCO ₃	SiO ₂	Al ₂ O ₃	TiO ₂	MgO	K ₂ O	Na ₂ O	MnO	Fe ₂ O ₃	TOTAL
C41H	n.d.	96.5	0.7	0.1	-	0.4	0.1	-	0.6	98.4
C50H	10.2	83.6	0.3	-	-	0.4	-	0.1	0.4	95.2
GRI4*	55.4	16.6	1.5	0.1	6.3	0.6	0.2	0.2	0.6	81.5
GRI8*	48.3	24.7	2.7	0.2	2.9	1.7	0.1	0.2	1.3	81.5
C42H*	68.8	18.9	1.4	0.1	0.6	0.8	0.1	0.2	0.4	93.0
GRI2*	49.8	21.5	2.1	0.1	5.2	0.8	0.2	0.2	4.2	84.1
Worldwide										
Data†	79.3	12.3	2.1	-	3.1	-	-	-	2.01	98.8

* indicates a texture and mineralogy similar to modern calcretes. Sample localities are given by the prefix on the sample number: C= Cherty Rock, Lossiemouth; GRI= Gribun, Isle of Mull.

† from Goudie (1973).

TABLE 5.2. Geochemical analyses of samples (in ppm) from the Cherty Rock, Lossiemouth and Gribun, Mull.

	Zn	Cu	Ni	Sr	Ba	U	Pb	Ti	V	Cr
C41H	8	4	101	16	165	2	91	409	7	36
C50H	42	12	23	38	86	2	79	258	3	17
GRI4*	56	34	10	1052	254	2	7	394	12	8
C42H*	50	32	8	260	127	3	22	295	6	9
GRI2*	12	22	19	940	322	2	5	526	17	13

* as in Table 1

whose mean SiO₂ content is 12.3%. Furthermore, the mean MgO content of the Triassic calcretes is greater than that quoted by Goudie (1973; mean MgO content = 3.05%) and reflects the abundance of dolomite, particularly in the Mull samples. Further comparison has revealed that the Al₂O₃, Fe₂O₃ and MnO contents of the Triassic samples are similar to the values obtained by Goudie (1973). In agreement with the limited data of Frostick et al. (1988), calcium, magnesium, potassium and phosphorous are not depleted in the Cherty Rock relative to the underlying sandstones. The titanium enrichment and aluminium depletion characteristic of some silcretes (Summerfield 1983a, 1983b) is not observed in the present study. Titanium and aluminium levels correspond to concentrations in underlying sandstones even in the highly silicified zones of the Cherty Rock (Table 5.1). Petrographic observations confirm this, because alkali feldspars are present in all the samples studied.

Minor element analysis was undertaken using X-ray fluorescence spectrometry and the results given in Table 5.2. The matrix of the Cherty Rock at Lossiemouth is not enriched in base metals, despite the presence of pyrite and galena mineralisation. In addition, only trace concentrations of base metals were detected regardless of whether the enclosing matrix is carbonate or silica-rich (see Table 5.2). A slight lead enrichment is observed in the Cherty Rock relative to the underlying sandstones and to the Mull calcretes. More data are required to establish whether these preliminary results are significant.

5.7 CARBON AND OXYGEN ISOTOPES

5.7.1. INTRODUCTION

The $\delta^{18}\text{O}$ value for calcite is directly related to that of the water from which it precipitated with a temperature effect (0.24‰/°C; Craig 1965). Thus, if the isotopic composition of a soil carbonate is preserved without diagenetic alteration, it should reflect the past meteoric water composition (Cerling 1984). Oxygen isotopes in meteoric waters are related to climate, particularly to mean annual temperature, but are also related to altitude and latitude (Gat 1980). Enrichment of ¹⁸O relative to ¹⁶O occurs during initial evaporation from free-standing bodies of water (Enhalt & Knott 1965).

The $\delta^{13}\text{C}$ content of soil CO_2 varies between approximately -25 and -7 ‰ and is controlled by the depth, local vegetation types and the diffusion rate to the surface (Dorr & Munnich 1980). Cerling (1984) showed that the $\delta^{13}\text{C}$ content of modern soil carbonates is related to the proportion of C_4 biomass present where C_4 plants are mostly arid-zone grasses with $\delta^{13}\text{C}$ values ranging from -13 ‰ to $+3$ ‰ (Vogel et al. 1978). Goodfriend & Magaritz (1988) emphasised that carbon isotopic composition is ultimately determined by rainfall which is responsible for the level of plant activity. The spread of $\delta^{13}\text{C}$ values for calcite in palaeosol horizons may be used to assess the relative importance of CO_2 loss and evaporation as mechanisms of profile development (Salomons et al. 1978; Talma & Netterberg 1983).

The extent to which palaeosols can be used to determine palaeoclimates and the mode of calcite precipitation is severely restricted if the calcrete formed during several climatic episodes. The textures within the Cherty Rock and the field occurrence of the horizon suggest it formed during a single climatic episode. The diagenetic alteration of the isotopic composition of the carbonate also poses a potential problem which is difficult to evaluate. Data from Quaternary pedogenic carbonates of the Olduvai Gorge (Cerling & Hay 1986) and the presence of seemingly primary micrite in ancient calcretes indicate that diagenetic effects may be minimal. In view of this, isotopic measurements were made on calcite from the Cherty Rock and Triassic calcretes from Mull in order to investigate the carbon and oxygen sources and the processes involved in calcrete formation. The results are given in Table. 5.3.

5.7.2 RESULTS

The $\delta^{13}\text{C}$ values for early micrite cements in the Cherty Rock and Mull samples range from -8.5 ‰ to -5.3 ‰ with a mean of -6.9 ‰ whilst $\delta^{18}\text{O}$ values vary between -8.6 ‰ and -3.8 ‰.

Later sparry calcite in veins and cavities has $\delta^{13}\text{C}$ values between -10.1 ‰ and -6.0 ‰ (mean = -7.4 ‰) whilst $\delta^{18}\text{O}$ values range from -16.4 ‰ to -8.5 ‰. A sample

TABLE 5.3. The isotopic composition of calcite from the Cherty Rock, Lossiemouth, Isle of Mull calcretes and cements in the New Red Sandstones of Moray.

		$\delta^{13}\text{C}$	$\delta^{18}\text{O}$
		(‰PDB)	(‰PDB)
Micrite	C84 Cherty Rock, Inverugie	-6.4	-6.6
	C44 Cherty Rock, Inverugie	-6.2	-6.4
	C83 Cherty Rock, Inverugie	-7.3	-6.4
	C42 Cherty Rock, Inverugie	-6.8	-6.0
	C43 Cherty Rock, Inverugie	-7.1	-5.5
	C85 Cherty Rock, Inverugie	-5.8	-4.8
	C82 Cherty Rock, Inverugie	-5.3	-3.8
	C45 Cherty Rock, Inverugie	-8.5	-8.2
	C88 Cherty Rock, Inverugie	-7.6	-7.0
	GRI4 Gribun, Mull	-6.7	-5.1
Spar	C88 Cherty Rock, Inverugie	-8.1	-11.2
	C98 Cherty Rock, Inverugie	-6.7	-15.4
	C98 Cherty Rock, Inverugie	-8.4	-16.4
	C89 Cherty Rock, Inverugie	-10.1	-14.1
	C85 Cherty Rock, Inverugie	-8.9	-11.3
	C84 Cherty Rock, Inverugie	-8.3	-10.4
	C82 Sparite vug fill, Inverugie	-7.1	-9.7
	C44 Cherty Rock, Inverugie	-6.7	-9.1
	C82 Cross-cutting veins, Inverugie	-6.7	-8.5
	C103 Late calcite, post-silica, Spynie	-6.1	-9.1
	GRI2 Spar enclosing chalcedony, Gribun	-7.1	-5.9
	GRI4 Vein calcite, Gribun	-6.0	-8.5
	GRI2 Vug fill, Gribun	-6.2	-8.7
	BUR39 Burghead Beds, Morayshire	-5.5	-6.0
	HOP32 Hopeman Sandstone, Morayshire	-9.7	-6.2

of vein calcite precipitated after silicification, and forming one of the last phases of calcite deposition, has a $\delta^{13}\text{C}$ value of -6.1‰ and a $\delta^{18}\text{O}$ value of -9.1‰ . The $\delta^{18}\text{O}$ values for both the spar and late calcite are significantly lower (at the 95% confidence level) than values obtained for 'co-existing' micrite.

Poikilotopic calcite cements from the Burghead Beds and the Hopeman Sandstone Formation which underly the Lossiemouth Sandstone Formation (see Fig.5.2) have similar $\delta^{13}\text{C}$ values to those of the calcites in the Cherty Rock. Nodular calcite cement in the aeolian Hopeman Sandstone Formation has a $\delta^{13}\text{C}$ value of -9.7‰ with $\delta^{18}\text{O} = -6.2\text{‰}$ and pervasive non-ferroan calcite in the fluvial Burghead Beds has a $\delta^{13}\text{C}$ value of -5.5‰ whilst $\delta^{18}\text{O} = -6.0\text{‰}$.

Preliminary $\delta^{18}\text{O}$ values for chalcedony in the Cherty Rock range from 22.9‰ to 25.9‰ (relative to SMOW). The chalcedony is isotopically distinct from the later macrocrystalline quartz ($\delta^{18}\text{O} = 19\text{‰}$ SMOW) which was shown from fluid inclusion studies to have precipitated at higher temperatures and is associated with sulphide mineralisation (see Chapter 4).

5.8 DISCUSSION

The striking similarity between the field appearance of the indurated calcretes of the Hebridean Province, Western Scotland and the Cherty Rock leads the present author to suggest that the latter is indeed a silicified calcrete which formed as a result of pedogenic carbonate accumulation in the Moray Firth during the Triassic. Steel (1974) devised a morphogenic classification of calcretes based on the maturity of various profiles, with stage 1 relating to the initial random deposition of calcite in the sediments, whilst the final stage 4, is represented by an indurated horizon composed entirely of carbonate. It is this final stage of mature calcrete formation resulting in a hard, impermeable, often silicified horizon that the Cherty Rock closely resembles. This comparison is used as a basis for the following discussion involving petrographic, isotopic and geochemical data from the Cherty Rock and similar measurements and observations from both modern and ancient calcretes.

The fundamental controls on calcrete development are climate, parent material, sediment accretion rate, the proximity and availability of a carbonate source, local vegetation abundance and types, and time. Aeolian dust often contains appreciable quantities of carbonate; such dust in Iraq has been shown to contain up to 69.5% carbonate (Kulal & Saadallah 1973). This has led several authors such as Goudie (1973) to suggest that aeolian dust may represent a significant source of carbonate for calcrete development. Thus, in view of the semi-arid continental setting of the Cherty Rock, aeolian dust is considered to be a possible contributor of carbonate to the horizon. Local contributions from rainwater (Gardner 1972) may have been important. The thickening of micritic laminae below detrital silicates within the Cherty Rock is consistent with Goudie's (1973) model for calcrete formation where carbonate is precipitated from downward-moving solutions. In agreement with Watts (1980), the pervasive low Mg calcite is thought to have precipitated from low Mg/Ca ratio solutions, either as a result of mild evaporation and/or CO₂ loss. The growth of displacive calcite is not thought to be wholly responsible for the minor brecciation fabrics observed within the Cherty Rock, where passive void fillings of sparry calcite are found in place of the fibrous displacive cements described by Watts (1978).

Watts (1980) tentatively attributed the dolomite rhombs often present in palaeosols (eg. Steel 1974) to mixing of vadose and phreatic waters near the water table, but finely crystalline dolomite may also form from solutions with a high Mg/Ca ratio where precipitation may be triggered by mild evaporative conditions. Simultaneous precipitation of low Mg calcite within the profile is envisaged as a viable mechanism for Mg-enrichment of the pore fluids. Dolomite is prevalent in areas with elevated groundwater salinities (Mann & Horowitz 1979) and the suggestion by Frostick et al. (1988) that dolomite in the Cherty Rock represents an influx of brackish water cannot be discounted.

In agreement with Williams (1973), it is proposed that the major source of silica for the silicification of the Cherty Rock and the underlying sandstones is the detrital silicates which released silica on replacement by calcite. At high pH (>9) calcite precipitation is favoured whilst silica remains in solution, and at low pH the reverse is true. Thus,

silica-rich solutions become unstable in low pH or high CO₂ environments, resulting in rapid SiO₂ precipitation. The length-slow chalcedony is thought to be due to high salinities and high pH, whilst later coarse quartz was precipitated due to the slow crystallisation of SiO₂ as a void-fill.

The isotopic data are consistent with the interpretation of the Cherty Rock as an ancient calcrete. The similarity between carbon and oxygen isotope data from the Mull calcretes and the Cherty Rock, Lossiemouth (see Table 5.3 and Fig. 5.6) is consistent with both horizons being formed by similar processes. The isotopic ratios for calcite cements in the underlying sandstones at Lossiemouth suggest that these cements were precipitated from fluids similar to those responsible for deposition of calcite in the Cherty Rock.

The Cherty Rock and Mull calcretes have $\delta^{13}\text{C}$ contents within the reported range for Recent calcretes on a world-wide scale ($\delta^{13}\text{C}$ values range from -12 to +4‰; Talma & Netterberg 1983) (see also Fig. 5.4) and freshwater carbonates (-18 to 0‰, mean -7‰; Degens 1967). A review of stable isotope abundances in calcretes (Talma & Netterberg 1983) suggests that the stable isotopic composition of these soil horizons is a good indicator of the source materials, the temperature, the nature and extent of calcrete development and of post-depositional changes.

The carbon isotopic composition of the Cherty Rock is consistent with values expected for carbonates precipitating from modern soil solutions which derive their carbon from soil-CO₂ dominated by C₄ vegetation (Salomons & Mook 1986) (see Fig. 5.5). Calcite deposited from soil solutions deriving the majority of their carbon from atmospheric CO₂ would exhibit higher $\delta^{13}\text{C}$ values (-1 to 0‰) than those observed for the Cherty Rock and Mull calcretes (Fig. 5.5). According to Cerling (1984), the variation of $\delta^{13}\text{C}$ within a single profile, can be explained in terms of varying precipitation conditions and may to a lesser degree, reflect a change in C₄ plant

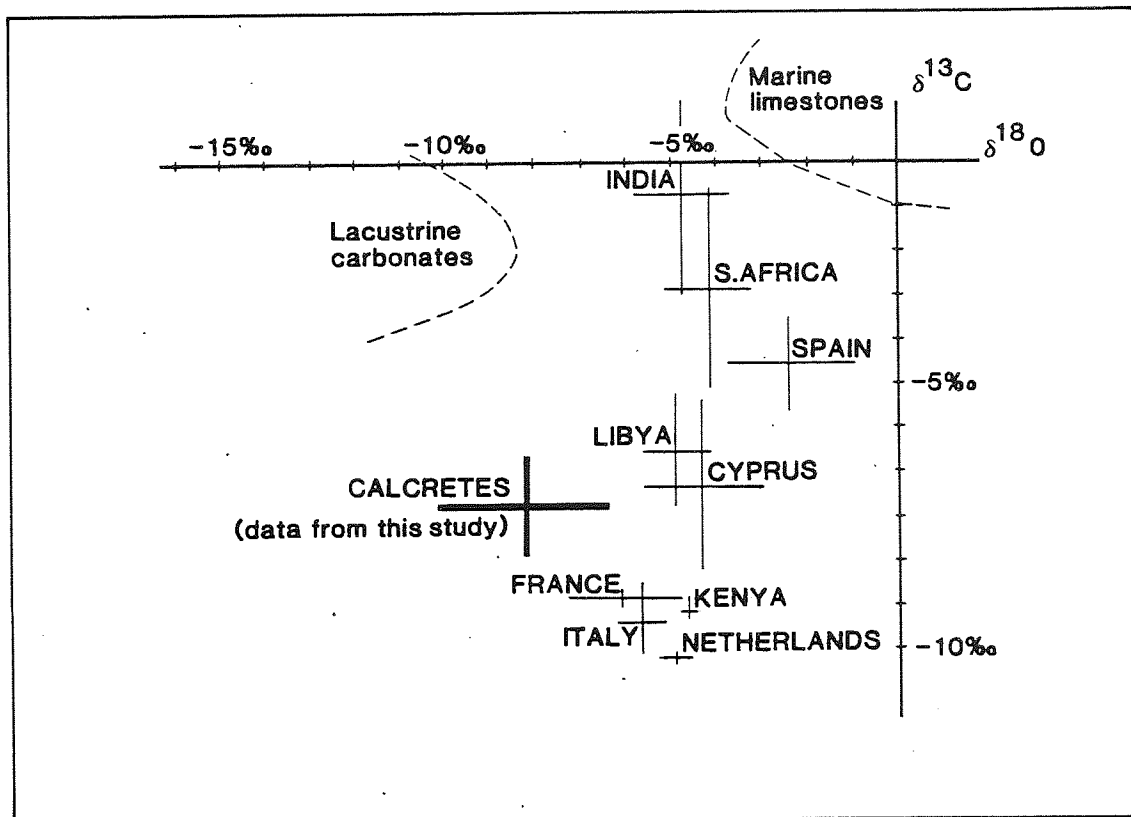


Figure 5.4. Carbon and oxygen stable isotopic compositions of calcretes on a world-wide scale (data from Salomons et al. 1978) plotted with the isotopic data obtained from the present study.

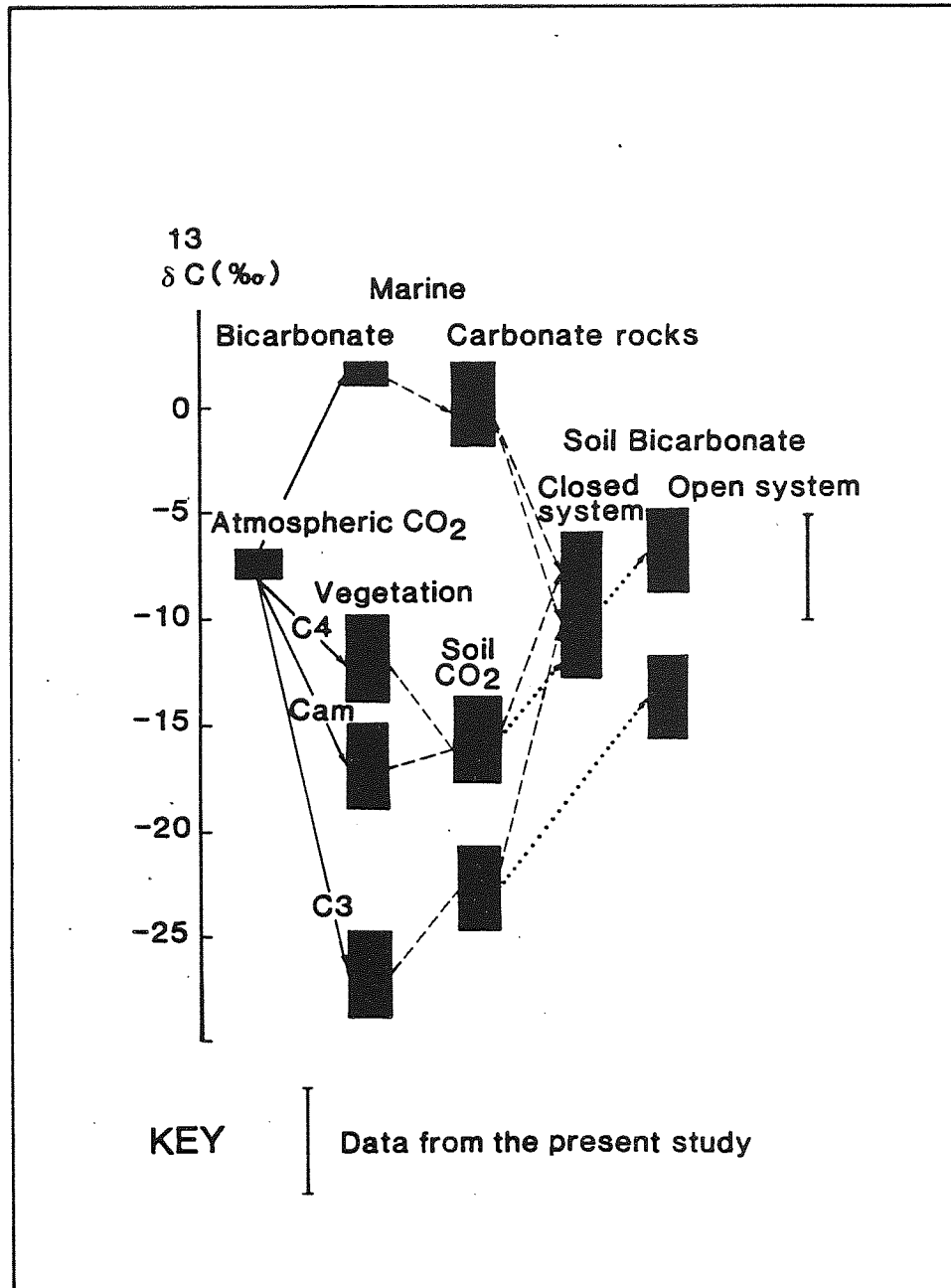


Figure 5.5. Schematic diagram showing the carbon isotopic composition of vegetation, soil- CO_2 and the soil solutions in the weathering zone (After Salomons & Mook 1986).

activity. The $\delta^{13}\text{C}$ values observed in these ancient calcretes could also have been generated by mixing of two components with 'extreme' carbon isotopic compositions such as C3 plants and marine carbonate (see Fig.5.5). However, it is unlikely that carbon derived from marine sources was involved in the formation of these horizons which developed in a continental environment. The variation in $\delta^{13}\text{C}$ of calcite in the Cherty Rock and Mull calcretes may be caused by a change in temperature, conditions of calcite deposition or rainfall (associated with plant activity).

The range of $\delta^{18}\text{O}$ values for calcite in the Cherty Rock and Mull calcretes is wider than that noted by Talma & Netterberg (1983) in their compilation of data ($\delta^{18}\text{O}$ ranged from -9‰ to -3‰); the carbonate $\delta^{18}\text{O}$ of calcite in the present study range from -16.45‰ to -3.0‰ with a mean of -7.8‰ (Fig 5.4). As has been previously stated, the $\delta^{18}\text{O}$ of pedogenic carbonate is determined by the soil water whose isotopic composition is related to climate and particularly to mean annual temperature (Cerling 1984). Hence, the $\delta^{18}\text{O}$ of micrite in the Cherty Rock may reflect past meteoric water composition providing that $\delta^{18}\text{O}$ has remained unmodified by burial diagenesis. The $\delta^{18}\text{O}$ of the Triassic waters responsible for micrite precipitation in the Cherty Rock can be estimated from $\delta^{18}\text{O}_{\text{micrite}}$ (mean = -6.1‰ PDB) combined with an estimate of the surface temperatures during Triassic times in the Inner Moray Firth Basin of 30°C.

$$1000\ln \alpha = -\delta^{18}\text{O}_{\text{water}} + \delta^{18}\text{O}_{\text{calcite}} = 2.78 \times 10^6 / T^2 - 3.39$$

(O'Neil et al. 1969)

where $\delta^{18}\text{O}_{\text{micrite}} = 24.15\text{‰ (SMOW)} = -6.1\text{‰ (PDB)}$

$T = 303\text{K}$ and α is the oxygen isotope fractionation factor between calcite and water.

The meteoric water responsible for micrite precipitation has a mean calculated $\delta^{18}\text{O}$ value of -2.74‰ (SMOW). This corresponds to the oxygen isotopic composition of modern meteoric water in southern Africa ($\delta^{18}\text{O} = -0.1$ to -3.0 ‰ (SMOW); Cerling

1984), and is a reasonable value for Triassic meteoric water in the Inner Moray Firth Basin which was at latitude of approximately 15°N during Triassic times. The relatively high $\delta^{18}\text{O}$ values estimated for the Triassic meteoric water is likely to reflect evaporation effects in a semi-arid to arid climate.

In the Cherty Rock no systematic variations either in $\delta^{13}\text{C}$ or $\delta^{18}\text{O}$ are observed with depth. This is consistent with the data from Recent calcrete profiles in India, Cyprus and Libya (Salomons et al. 1978) and is thought to indicate that isotopically similar processes were responsible for calcite precipitation irrespective of depth in the profile. In areas with little vegetation, a high rate of exchange between CO_2 present in the soil and atmospheric CO_2 may ultimately control the $\delta^{13}\text{C}$ of soil carbonate and lead to increased $\delta^{13}\text{C}$ values of calcite precipitating in the uppermost part of the profile. The uniform $\delta^{13}\text{C}$ values obtained in the present study are consistent with the data from Recent soil carbonates (Salomons et al. 1978) and suggest that no significant exchange occurred between atmospheric CO_2 and soil CO_2 . Overall, more detailed measurements are required to constrain the mechanisms of precipitation and to assess the relative importance of degassing and evaporation in the development of the Cherty Rock.

A positive correlation is observed between $\delta^{13}\text{C}$ and $\delta^{18}\text{O}$ of the sparry calcite in the Cherty Rock and Mull calcretes at the 95% confidence level (Fig. 5.6). A similar relationship exists between $\delta^{13}\text{C}$ and $\delta^{18}\text{O}$ of micritic cements but is not as pronounced. Evaporation has been cited by several authors (eg. Salomons et al. 1978) as being largely responsible for calcite precipitation in calcretes; evaporation results in an increase in both the carbon and oxygen isotopic composition of the precipitated calcite. Thus, the relationship between $\delta^{13}\text{C}$ and $\delta^{18}\text{O}$ in micrite is tentatively attributed to evaporative processes. The positive correlation between the carbon and oxygen composition of the spar cements is more difficult to explain as these cements are likely to have precipitated below the zone of intense degassing and evaporation near the soil surface.

There is no significant difference at the 95% confidence level between $\delta^{13}\text{C}$ values for micrite and spar, however, the $\delta^{18}\text{O}$ values for the spar are consistently lower (at the 95% confidence level) than values obtained for 'coexisting' micrite. The consistency of $\delta^{13}\text{C}$ irrespective of the carbonate cement type or generation is attributed to an isotopically homogenous carbon source which was present during the development of the Cherty Rock. If the two cement types were precipitated at similar temperatures, then $\delta^{18}\text{O}$ of the water from which they were deposited must have been different. This variation may be attributed to differing climatic conditions, different water sources or to isotopic modification as a result of evaporation. The former two suggestions are more consistent with the data, as evaporation also causes changes in carbon isotopic composition and this is not observed in the Cherty Rock where $\delta^{13}\text{C}$ values for micrite and spar are indistinguishable. Independent evidence on the palaeotemperatures of spar precipitation are required, but are not as yet, available for the Cherty Rock, and it is possible that some spar cements formed at higher temperatures during burial. Thus the discrepancy between the $\delta^{18}\text{O}$ values for micrite and spar is likely to have been caused by a combination of the following; changes in climatic conditions, changes in water source or spar precipitating at higher temperatures during burial diagenesis. It is also possible that some of the sparry calcite is recrystallised; recrystallised calcite will have an isotopic composition reflecting that of the surrounding interstitial waters. In view of this, there seems to be no satisfactory explanation for the correlation between $\delta^{13}\text{C}$ and $\delta^{18}\text{O}$ in the spar cements. More data are clearly required to resolve the reason for this relationship.

Calcretes have proved useful as palaeoclimatic indicators (Allen 1974; Hubert 1978) and modern pedogenic carbonate accumulations occur in warm to hot, semi-arid or arid climates where the seasonal rainfall has a marked distribution (Goudie 1973). A similar climate is thus inferred during Upper Triassic times in the Inner Moray Firth Basin.

Radiocarbon dating of arid zone calcretes by Williams & Polach (1971) suggests that mature profiles require approximately 10,000 years to develop. These values cannot be applied indiscriminately to any calcrete as was shown by Hay & Reeder (1978) who

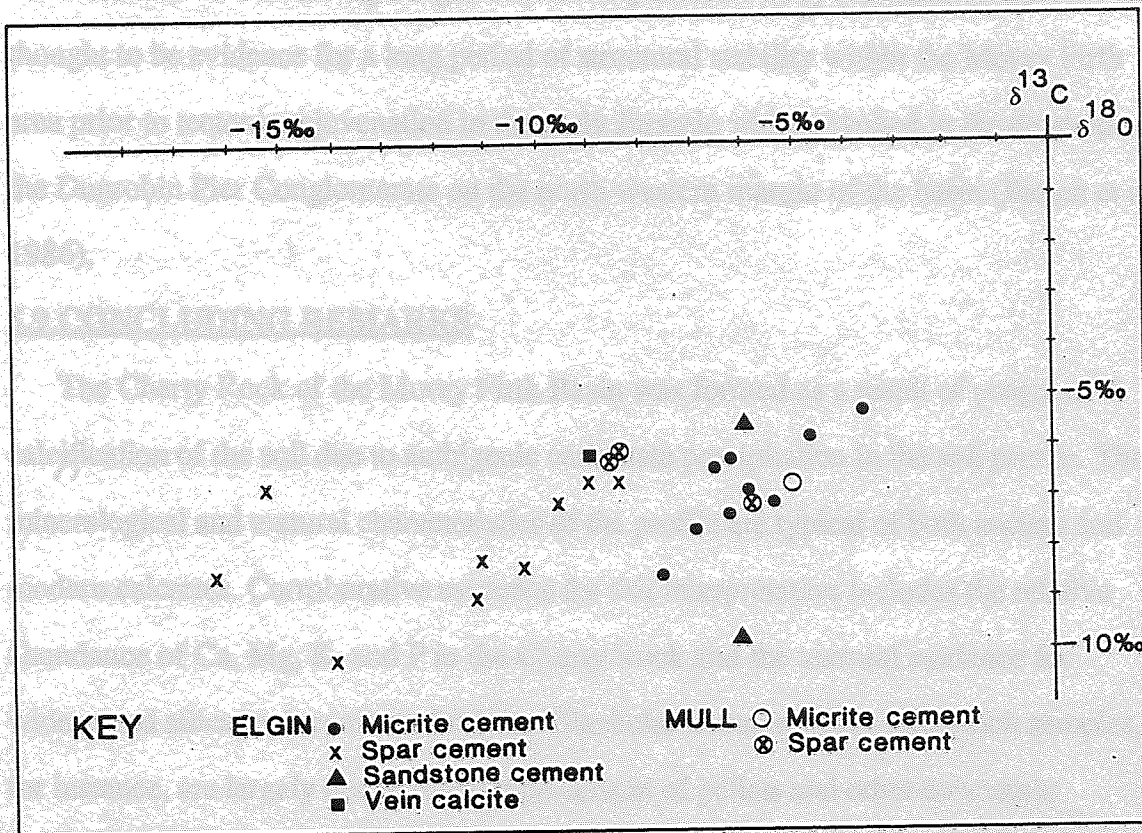


Figure 5.6. Carbon and oxygen compositions of calcite cements in the Cherty Rock and Triassic calcretes from Mull.

estimated that calcretes in East Africa formed in the order of a few thousand years. However, this is at least partly due to a local, readily available source of carbonate which may not have applied to the development of the Cherty Rock whose composite profile is thought to represent a significant time period in the order of tens of thousands of years.

The sheer extent and high degree of maturity of the Cherty Rock calcrete profile are thought to be evidence for a long period of structural stability within the Moray Firth area prior to tectonic rejuvenation in the early Jurassic which resulted in the deposition of the Dunrobin Pier Conglomerate on the north-western margin of the basin (Batten et al. 1986).

5.9 CONCLUDING REMARKS

The Cherty Rock of the Moray Firth Basin was formed as a result of progressive calcification of the soil due to authigenic carbonate precipitation in the soil profile. The mineralogical and textural characteristics of the profile are typical of both ancient and modern calcretes. Corroborative evidence for this interpretation includes the relative abundance of Ca, Mg, K, and P in the Cherty Rock and the textural evidence for widespread silica replacement of calcite. Glaebular textures within silica-rich samples, for instance, are largely due to direct replacement of pellets and other concentric carbonate structures by silica.

The close agreement between carbonate carbon and oxygen stable isotope values from the present study and those obtained for recent soil carbonates is thought to indicate that similar solutions and precipitation mechanisms were responsible for soil carbonate formation during Triassic times. The complexity of these processes within a single horizon is demonstrated by the $\delta^{13}\text{C}$ and $\delta^{18}\text{O}$ values obtained for calcite of different generations and at varying depths within the profile. Providing that no diagenetic overprinting has occurred, careful application of stable isotope techniques to ancient calcretes can lead to a greater understanding of the relative roles of CO_2 loss and evaporation in profile formation.

The stratigraphic importance of the Cherty Rock is well illustrated by recent seismic work in the Moray Firth area and its presence marks a significant period of tectonic stability during the Upper Triassic. The existence of a laterally extensive composite

calcrete profile within the basin constrains the palaeo-climatic conditions and implies that a semi-arid climate prevailed during the formation of the Cherty Rock.

REFERENCES

- ALLEN, J.R.L. 1974. Sedimentology of the Old Red Sandstone (Siluro-Devonian) in the Cleve Hills area, Shropshire, England. *Sedimentary Geology*, **12**, 73-167.
- BATTEN, D.J., TREWIN, N.H. & TUDHOPE, A.W. 1986. The Triassic-Jurassic junction at Golspie, Inner Moray Firth Basin. *Scottish Journal of Geology*, **22**, 85-98.
- BENTON, M.J. & WALKER, A.D. 1985. Palaeoecology, taphonomy and dating of Permo-Triassic reptiles from Elgin, North-east Scotland. *Palaeontology*, **28**, 207-234.
- BERRIDGE, N.J. & IVIMEY-COOK, H.C. 1967. The geology of a Geological Survey borehole at Lossiemouth, Morayshire. Bulletin of the Geological Survey of Great Britain **27**, 155-169.
- BORTHWICK, J. & HARMAN, R.S. 1982. A note regarding ClF_3 as an alternative to BrF_5 for oxygen isotope analysis. *Geochimica et Cosmochimica Acta*, **46**, 1665-1668.
- CARLISLE, D. 1983. Concentration of uranium and vanadium in calcretes and gypcretes. In: WILSON, R.C.L. (ed) *Residual Deposits: Surface Related Weathering Processes and Materials*. Geological Society Special Publication, **11**, 185-195.
- CERLING, T.E. 1984. The stable isotopic composition of modern soil carbonate and its relationship to climate. *Earth and Planetary Science Letters*, **71**, 229-240.
- CERLING, T.E. & HAY, R.L. 1986. An isotopic study of paleosol carbonates from Olduvai Gorge. *Quaternary Research*, **25**, 63-78.
- CHAFETZ, H.S. & BUTLER, J.C. 1980. Petrology of recent caliche pisolites, spherulites and speleothem deposits from central Texas.

- Sedimentology*, **27**, 497-518.
- CRAIG, H. 1965. The measurement of oxygen palaeotemperatures. *Spoletto conference on Stable Isotopes in Oceanographic Studies and Palaeotemperatures*, Pisa.
- DEGENS, E.T 1967. Stable isotope distribution in carbonates. In: CHILINGAR, G.V., BISSELL, H.J. & FAIRBRIDGE, R.W. (eds) *Carbonate Rocks Part B*, 194-208, Elsevier, Amsterdam.
- DICKSON, J.A.D. 1965. A modified staining technique for carbonates in thin section. *Nature*, **205**, 587.
- DORR, H. & MUNNICH, K.O. 1980. Carbon-14 and Carbon-13 in soil CO₂. *Radiocarbon*, **22**, 909-918.
- ENHALT, D.H. & KNOTT, K. 1965. Kinetische Isotopentrennung bei der Verdampfung von Wasser. *Tellus*, **17**, 388-397.
- ESTEBAN, M. & KLAPPA, C.F. 1983. Sub-aerial exposure. In: SCHOLLE, P.A., BEBOUT, D.G. & MOORE, C.H. (eds) *Carbonate Depositional Environments. Memoir of the American Association of Petroleum Geologists*, 33.
- FOLK, R.L. 1974. *Petrology of Sedimentary Rocks*. Hemphills Publishing Co., Austin, Texas.
- FROSTICK, L., REID, I., JARVIS, J. & EARDLEY, H. 1988. Triassic sediments of the Inner Moray Firth, Scotland : early rift deposits. *Journal of the Geological Society of London*, **143**, 235-248.
- GARDNER, L.R. 1972. Origin of the Mormon Mesa Caliche, Clark County, Nevada. *Bulletin of the Geological Society of America*, **83**, 143-156.
- GAT, J.R. 1980. The isotopes of hydrogen and oxygen in precipitation. In: FRITZ, A.P. & FONTES, J.Ch. (eds) *Handbook of Environmental Geochemistry, 1. The Terrestrial environment*. Elsevier. Amsterdam.
- GOODFRIEND, G.A. & MAGARITZ, M. 1988. Paleosols and late Pleistocene

- rainfall fluctuations in the Negev Desert. *Nature*, **332**, 144-146.
- GOUDIE, A.S. 1973. *Duricrusts in Tropical and Sub-tropical Landscapes*. Clarendon Press, Oxford.
- GOUDIE, A.S. 1983. Calcrete. In: GOUDIE, A.S & PYE, K. (eds) *Chemical Sediments and Geomorphology : precipitates and residua in the near-surface environment*. Academic Press, London.
- HAY, R.L. & REEDER, R.J. 1978. Calcretes of Olduvai Gorge and the Ndolanya Beds of northern Tanzania. *Sedimentology*, **25**, 649-673.
- HAY, R.L. & WIGGINS, B. 1980. Pellets, ooids, sepiolite and silica in three calcretes of the southwestern United States. *Sedimentology*, **27**, 559-576.
- HUBERT, J.F. 1978. Paleosol caliche in the New Haven arkose, Newark Group, Connecticut. *Palaeogeography, Paleoecology and Palaeoclimatology*, **24**, 151-168.
- JUDD, J.W. 1873. The secondary rocks of Scotland. *Quarterly Journal of the Geological Society*, **29**, 97-195.
- KULAL, Z. & SADAALLAH, A. 1973. Aeolian admixtures in the sediments of the northern Persian Gulf. In: PURSER, B. H. (ed). *The Persian Gulf*, Springer-Verlag, Berlin.
- LEE, G.W. 1925. The geology of the country around Golspie, Sutherland. *Memoirs of the Geological Survey of Great Britain*. H.M.S.O.
- LINSLEY, P.N., POTTER, H.H., McNAB, G. & RACHER, D. 1980. The Beatrice Field, Inner Moray Firth, U.K. North Sea. In: HALBOUTY, M.T. (ed.) *Giant oil and gas fields of the decade 1968-1978. Memoir of the American Association of Petroleum Geologists*, **30**, 117-129.
- MACHEL, H.G. 1985. Cathodoluminescence in calcite and dolomite and its chemical significance. *Geoscience Canada*, **12**, 137-147.
- MANN, A.W. & HOROWITZ, R.C 1979. Groundwater calcrete deposits in Australia: some observations from Western Australia. *Journal of the Geological Society of Australia*, **26**, 293-303.

- MCCREA, J.M. 1950. On the isotopic composition of carbonates and a paleotemperature scale. *Journal of Chemical Physics*, **18**, 849-857.
- NETTERBERG, F. 1967. Some road-making properties of South African calcretes. *Proceedings of the fourth regional conference on Soil Mechanics and Foundation Engineering*, 77-81.
- O'NEIL, J.R., CLAYTON, R.N. & MAYEDA, T.K. 1969. Oxygen isotope fractionation in divalent metal carbonates. *Journal of Chemical Physics*, **51**, 5547-5558.
- PEACOCK, J.D., BERRIDGE, N.G., HARRIS, A.L. & MAY, F. 1968. *The geology of the Elgin district*. Memoir of the Geological Survey, Edinburgh.
- REEVES, C.C. 1976. *Caliche : Origin, Classification, Morphology and Uses*. Estacado Books, Lubbock.
- ROBERTSON RESEARCH REPORT 1978. *The Moray Firth area of Scotland- The stratigraphy, reservoir rocks and source rock potential of the Devonian to Lower Cretaceous sediments*. A non-exclusive industry report, Robertson Research Ltd.
- SALOMONS, W., GOUDIE, A.S & MOOK, W.G. 1978. Isotopic composition of calcrete deposits from Europe, Africa and India. *Earth Surface Processes*, **3**, 43-57.
- SALOMONS, W. & MOOK, W.G. 1986 Isotope geochemistry of carbonates in the weathering zone. In; FRITZ, P. & FONTES, J.Ch. (eds.) *Handbook of Environmental Chemistry vol.2. The Terrestrial Environment, B*. Elsevier, Amsterdam.
- STEEL, R.J. 1974. Cornstone (fossil caliche)-its origin, stratigraphic and sedimentological importance in the New Red Sandstone, western Scotland. *Journal of Geology*, **82**, 351-369.
- SUMMERFIELD, M.A. 1983a. Geochemistry of weathering profile silcretes, southern Cape Province, South Africa. In. WILSON, R.C.L. (ed) *Residual Deposits: Surface Related Weathering Processes and*

- Materials*. Geological Society of London Special Publication, 11, 167-178.
- SUMMERFIELD, M.A. 1983b. Silcrete. In: GOUDIE, A.S & PYE, K (eds) *Chemical Sediments and Geomorphology; precipitates and residua in the near-surface environment*. Academic Press, London.
- TALMA, A.S. & NETTERBERG, F 1983. Stable isotope abundances in calcretes. In: WILSON, R.C.L. (ed) *Residual deposits: Surface Related Weathering Processes and Materials*. Geological Society of London Special Publication, 11, 221-233.
- THIRY, M. & MILLOT, G. 1987. Mineralogical forms of silica and their sequence of formation in silcretes. *Journal of Sedimentary Petrology*, 57, 343-352
- VOGEL, J.C., FULLS, A. & ELLIS, R.P. 1978. The geographical distribution of Kranz grasses in South Africa. *South African Journal of Science*, 74, 209-215.
- WATSON, D.M.S. & HICKLING, G. 1914. On the Triassic and Permian rocks of Moray. *Geological Magazine*, 1, 399-402.
- WATTS, N.L. 1976. Palaeopedogenic palygorskite from the basal Permo-Triassic of northwest Scotland. *American Mineralogist*, 61, 299-302.
- WATTS, N.L. 1978. Displacive calcite: evidence from recent and ancient calcretes. *Geology*, 6, 699-703.
- WATTS, N.L. 1980. Quaternary pedogenic calcretes from the Kalahari (southern Africa): mineralogy, genesis and diagenesis. *Sedimentology*, 27, 661-686.
- WILLIAMS, D. 1973. *The sedimentology and petrology of the New Red Sandstone of the Elgin Basin, north east Scotland*. Phd thesis, University of Hull.
- WILLIAMS, G.E. & POLACH, H.A. 1971. Radio-carbon dating of arid-zone calcareous paleosols. *Bulletin of the Geological Society of*

[Faint, illegible text]

ABSTRACT

[Faint, illegible text]

[Faint, illegible text]

[Faint, illegible text]

[Faint, illegible text]

[Faint, illegible text]

[Faint, illegible text]

[Faint, illegible text]

[Faint, illegible text]

[Faint, illegible text]

[Faint, illegible text]

[Faint, illegible text]

[Faint, illegible text]

[Faint, illegible text]

[Faint, illegible text]

[Faint, illegible text]

[Faint, illegible text]

[Faint, illegible text]

[Faint, illegible text]

[Faint, illegible text]

[Faint, illegible text]

[Faint, illegible text]

[Faint, illegible text]

CHAPTER 6

ASPECTS OF THE GENESIS OF BASE METAL MINERALISATION IN THE TRIASSIC OF NORTH WEST EUROPE WITH SPECIAL REFERENCE TO MAUBACH AND MECHERNICH Pb DEPOSITS

ABSTRACT

The Triassic sandstones of the Eifel and Oberpfalz regions of the Federal Republic of Germany are host to Pb-Zn-(Cu) mineralisation. In the Eifel region, economic concentrations of Pb, Zn and Cu sulphides are found in the fluvial sandstones and conglomerates of the Middle Buntsandstein. Elevated lead concentrations have been reported from the Middle Buntsandstein to Upper Keuper (c.a 500m) in the Oberpfalz area where rare primary sulphides are closely associated with organic matter which accumulated in a marginal marine depositional environment.

Textural evidence points to the ores having been emplaced during and after early diagenesis of the host sediments. The relationship between mineralisation and faulting has been obscured by widespread supergene enrichment.

The genetic model favoured for the Oberpfalz involves groundwaters/diagenetic fluids transporting lead from the Bohemian Massif mixing with sulphate-bearing pore fluids or seawater, with sulphide precipitation resulting from sulphate reduction in horizons containing abundant organic debris. The genetic models proposed for the Eifel mineralisation include 1) remobilisation of hydrothermal vein sulphides in the Devonian basement by brines or 2) groundwaters or basinal brines transporting sulphur from the evaporites in the overlying Muschelkalk to the site of ore deposition. The provenance of lead remains poorly constrained and sulphate reduction is suggested to be an important sulphide precipitation mechanism on the basis of the light sulphur isotope values ($\delta^{34}\text{S}$ -20‰).

6.1 INTRODUCTION

Deposits of lead occur in the Triassic sandstones of the Eifel Mountains and the Oberpfalz, Federal Republic of Germany (Fig. 6.1). The characteristics of the

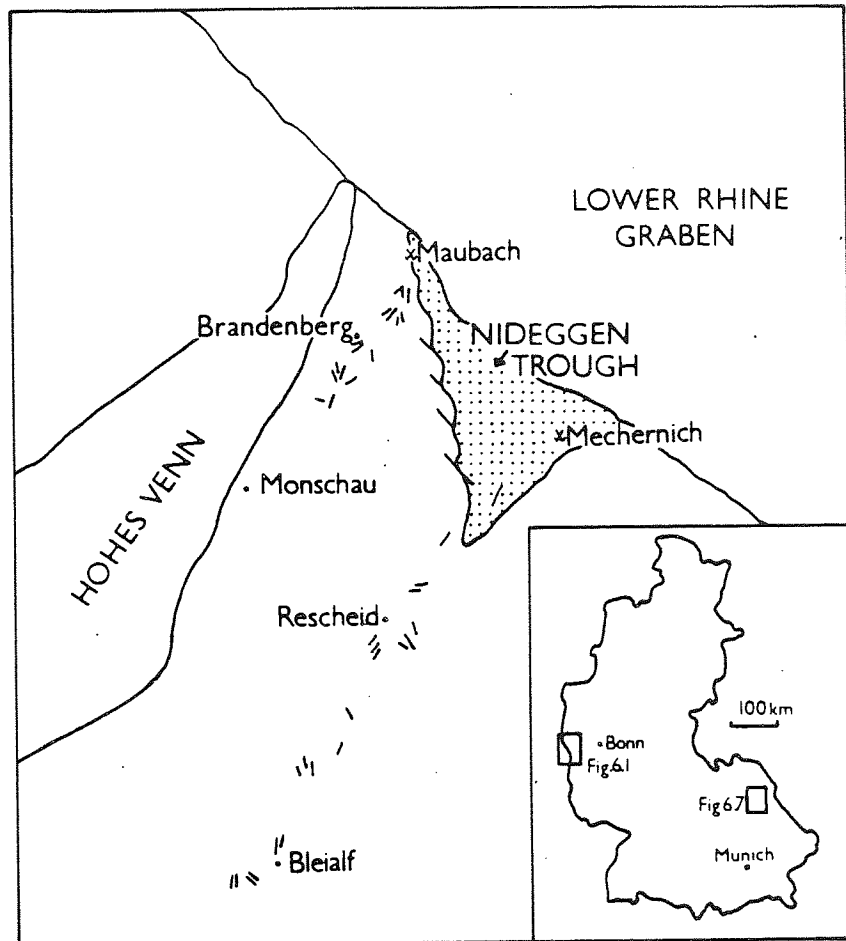
mineralisation in each region are described in this chapter in order to emphasise the similarities and differences between the individual ore deposits and to compare the mineralisation history of each area.

The Maubach and Mechernich ore deposits are located in the North Eifel area of West Germany (Fig. 6.1), which formed the north west margin of the Mid-European Triassic basin. The lower Triassic Buntsandstein was deposited in a roughly N-S trending trough bounded by basement massifs. The ore bodies are situated in a small (25 km²) sedimentary basin at the northern end of this shallow trough which lies along the Variscan tectonic trend (Fig. 6.2a). This basin is known as the Nideggen Trough and comprises a triangle-shaped, fault-bounded depression in which Triassic sediments were deposited on a Devonian basement (Knapp 1980). The Triassic sediments consist of continental red beds of fluvial origin (the Middle Buntsandstein) which are overlain by shales and sandstones, carbonates and evaporites of fluvial, marginal marine and marine origin (the Upper Buntsandstein and Muschelkalk). The Triassic succession in the Northern Eifel has a maximum thickness of only 200-300m.

At Maubach, on the northern margin of the Nideggen Trough (Fig. 6.2a), 40-50m of Middle Buntsandstein sediments lie unconformably on a basement of Devonian sediments. The sulphide mineralisation is dominated by Pb with minor Zn, Cu, Ni, Co, As and Ag and is hosted by Triassic fluvial conglomerate and sandstone units. Mechernich is a larger ore body (225 mt of ore) and is situated on the south east margin of the Nideggen Trough. The ore mineralogy is closely comparable to that at Maubach and the sulphides in both deposits occur as cements in the sandstones and conglomerates which had high primary porosities.

Elevated lead contents have been reported from the Middle Buntsandstein through to Upper Keuper sediments in the Oberpfalz; a thickness of 550m (Walther 1984). Material from two lead occurrences at Parkstein (Schmid 1981) and Freihung (Klemm & v. Schwarzenberg 1977) were examined during the present study.

This chapter presents detailed descriptions of the sedimentology and diagenesis of the Middle Buntsandstein as well as the ore mineralogy and paragenesis at Maubach and Mechernich. Sulphur isotope studies have been undertaken to supplement a recent study by Bayer et al. (1970). The purpose of the present study is to use the isotopic data



KEY

 Triassic


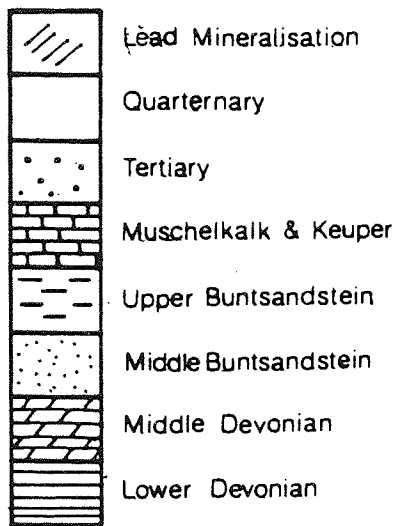
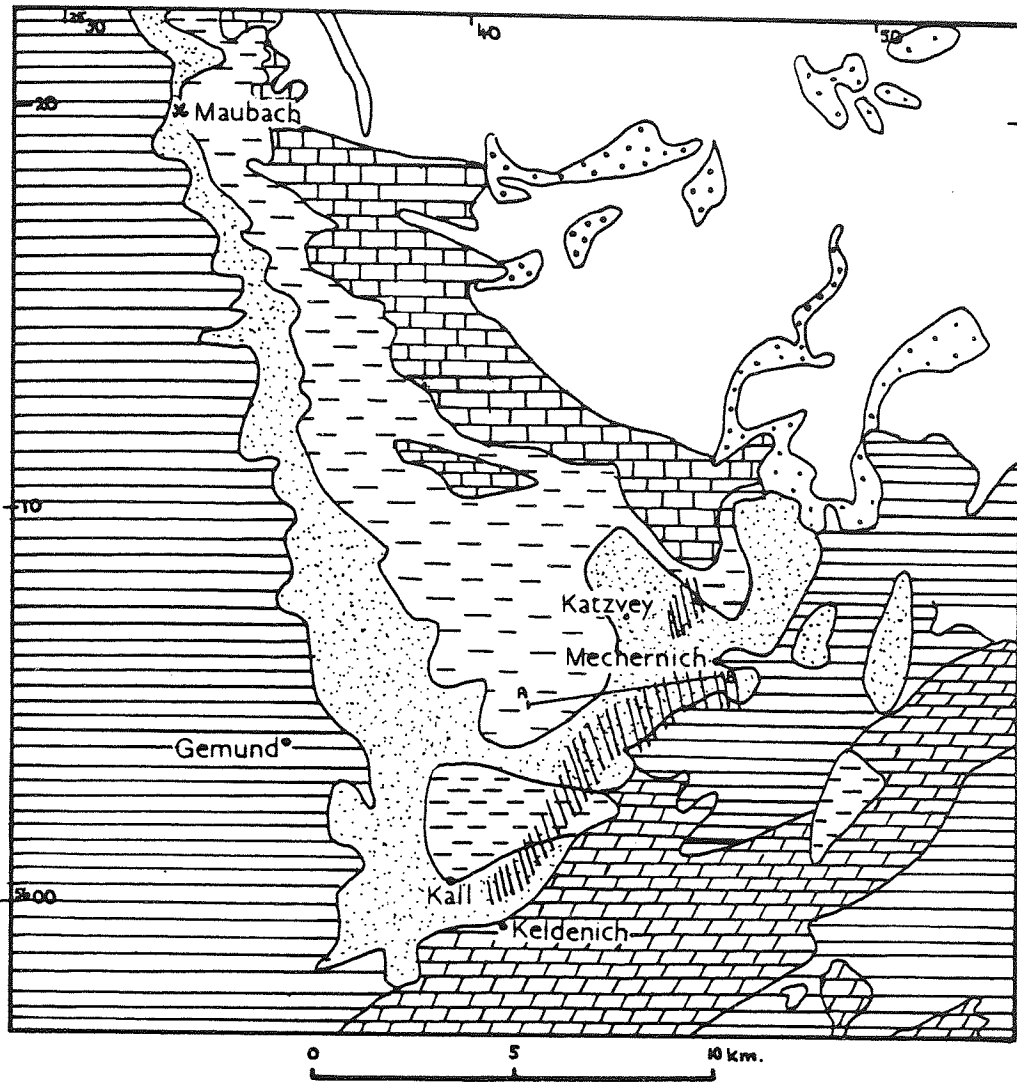
 Sulphide veins in Devonian sediments

Figure. 6.1. Location map showing the situation of Maubach and Mechernich in relation to the lead-zinc and copper vein systems in Devonian rocks in the North Eifel Mountains (adapted from Bayer et al 1970). Inset shows an outline of the the Federal Republic of Germany and the location of the Eifel and Oberpfalz deposits.

Figure. 6.2. Geological situation of the Mechernich and Maubach deposits in the North Eifel. Diagonal shading shows the extent of the Pb-Zn mineralisation at Mechernich on the south eastern margin of the Nideggen Trough.

FIGURE 6.2



available in the literature (Large et al. 1983, Bayer et al. 1970), in conjunction with the sedimentological, mineralogical and sulphur isotope data obtained in the present study, to constrain the mineralisation history of the Buntsandstein of the North Eifel. The overall aim is to critically examine the genetic model applied to the Oberpfalz mineralisation by several authors (eg. von. Gehlen & Nielsen 1985), and to discuss the application of this model to the deposits in the North Eifel.

6.2 MAUBACH AND MECHERNICH

6.2.1 GEOLOGICAL SETTING

The Lower Buntsandstein is absent at Maubach so that the ore-bearing Middle Buntsandstein rests unconformably upon steeply-dipping greywackes and slates of Lower Devonian age. The Upper Buntsandstein comprises a series of fine sandstones and siltstones with abundant palaeosols and overlies the mineralised horizons at Maubach. It has a maximum thickness of approximately 70m and is itself succeeded by the carbonate facies of the Lower Muschelkalk.

The oldest Triassic rocks are basal breccias which underlie the bleached conglomerates with interbedded sandstones that constitute the main ore horizon. This is succeeded by another bleached conglomerate, extensively cemented by sulphides, that in turn is overlain by unmineralised red-coloured conglomerates representing the last phase of deposition in the Middle Buntsandstein. The two ore-bearing horizons are devoid of the red colouration which characterises the Upper Buntsandstein sediments. Sulphide cements are particularly common in the sandstone units and are concentrated near joints and small faults (Walther 1986). Massive galena and chalcopyrite cements also occur within the conglomerates.

At Mechernich, the mineralised Middle Buntsandstein sediments lie unconformably upon strongly deformed Middle Devonian greywackes and carbonates (Fig. 6.2). To the south west of Mechernich and Maubach, these Devonian lithologies are host to the Bleialf-Rescheid and Brandenburg vein systems (Bonhardt 1912, Voigt 1952, Schachner 1960). The mineralised area at Mechernich is approximately 9km² (Fig. 6.3) and the ores occur predominantly in the four massive sandstone units which are interbedded with massive structureless conglomerates. A detailed discussion of the sedimentology of the ore-bearing horizons follows in a later section. At Kallmuther Berg

Figure. 6.3a. A tectonic map of the Mechernich district showing the extent of faulting near the basin margin. Diagonal shading represents Lower Devonian lithologies, whilst stipple indicates Triassic sediments. Unornamented areas are Middle Devonian rocks (adapted from Ribbert 1985).

6.3b. A geological section across the Mechernich ore deposit showing the stratigraphic position of the ores in the Middle Buntsandstein (after Voigt 1952).

(see Fig. 6.3), galena cements typically occur as single crystals (~2mm diameter) encompassing several detrital quartz grains and these are known as 'knotten'. The distribution of these cements is generally random, although in one sample galena was concentrated along bedding planes and the 'knotten' were aligned parallel to the foresets of a cross-stratified sandstone. The sulphides at Mechernich also occur in veins and are found cementing fractured clasts within the conglomerates.

The Middle Buntsandstein at Mechernich has been subjected to several periods of faulting. Some of the faulting was contemporaneous with sediment deposition, whilst later faulting occurred after the mineralisation as evidenced by the slickensides on the ore surfaces and by the truncation of galena 'knotten' by minor faults. It is likely that these later faults were active during the Tertiary, when Alpine orogenic events resulted in the inversion of Permo-Triassic basins throughout North West Europe.

6.2.2 SEDIMENTOLOGY

Lower Triassic gravel and coarse sand-dominated alluvial fan and braided river systems in the North Eifel were examined in the field, through detailed sedimentary logging at Kallmutherberg Pit, Mechernich. The sediments comprise sheet-like conglomerates which are typically structureless with poorly developed imbrication and pebble orientation. Medium to coarse-grained sands make up approximately 50% of the Buntsandstein succession and are characterised by shallowly-dipping cross-stratification and are host to the base metal mineralisation. They are interbedded with siltstones and thin indurated horizons stained with Mn and Fe (Fig. 6.4).

Four major lithofacies groups can be distinguished; i) normally-graded framework-supported conglomerates; ii) inversely or normally graded matrix-supported conglomerates; iii) massive cross-stratified sandstones and iv) red siltstones and thin, indurated horizons.

Normally-graded framework-supported conglomerates

The normally graded clast-supported conglomerates are generally poorly sorted and are seldom imbricated. The clast composition is dominated by vein quartz and metamorphic rocks which are well-rounded and range in size from 4 to 30cm. In contrast, minor locally-derived sandstone and siltstone intraclasts are angular. The

conglomerate matrix is composed of medium to coarse-grained sand. The main characteristics of the conglomerates include the normal grading, the absence of cross-stratification, channel or bar-form geometries and the rare presence of imbrication. The conglomerate units are well defined, often with non-erosive bases. They are laterally extensive and range from 0.5 to 5.0m thick.

A similar facies was documented in the Devonian sediments of the Orcadian Basin by Allen (1981) who noted that thick framework conglomerates such as these had been previously interpreted as deposits of debris flows or other mass flows (eg. Heward 1978, Larson & Steel 1978). In common with Allen (1981), recent authors of sedimentological studies on clast-supported, crudely stratified, coarse alluvial lithofacies (Ballance 1984, Flint et al. 1986) have favoured a sheet flood or stream flow depositional environment. The thick, sheet-like conglomerates of the Middle Buntsandstein in the Eifel are suggested to have been deposited as a result of combined powerful sheet floods on low-angle fan surfaces, and by deposition from high energy fluvial processes operating in a wide river system with minor channelling and no substantial bank or bar formation. Allen (1981) interpreted similar conglomerates as representing deposition under waning stream flow, and suggested that the plane bedded sand wedges in the conglomerates were deposited under a high flow regime, during and after the last phases of gravel deposition.

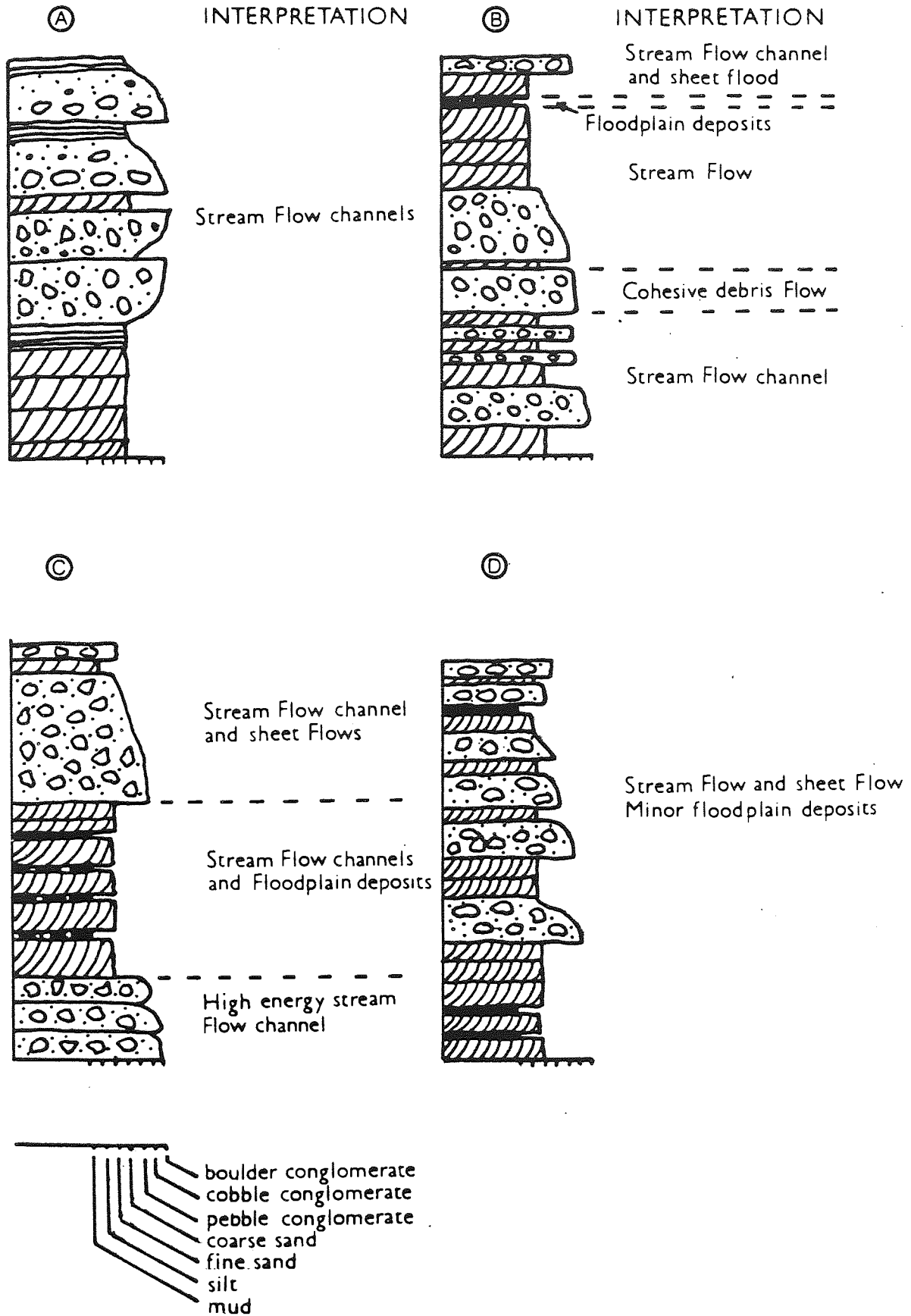
Inversely and normal graded matrix-supported conglomerates

These conglomerates are volumetrically minor in the Middle Buntsandstein and are present only in the exposures at Kallmuther Berg near Mechernich (Plate 6.1). Two types of matrix-supported conglomerates exist; the first type is typically thin (< 1m) and occurs as discrete units within cross-stratified sandstones. The second type of matrix-supported conglomerate is of varying thickness (0.5-1.0m), contains well-rounded clasts and has a matrix of medium to coarse grained sand. The bases of these units are usually planar and non-erosive, and, in some cases, within a single conglomerate the matrix support grades up into slightly coarser clast-supported sediment.

The matrix-supported conglomerates can be variously interpreted as debris flow deposits, reworked debris flow deposits, or alternatively, as the deposits of powerful

Figure 6.4 Interpretive logs through the Middle Buntsandstein succession at Kallmuther Berg, Mechernich. A and B illustrate the dominance of stream flow channel and sheetflood deposits in the lower part of the sequence; C and D show the gradual increase in fine sediments and cross-bedded sands towards the top of the Middle Buntsandstein.

FIGURE 6.4



streams. The thin non-continuous conglomerates are interpreted as debris flows on the basis of the matrix-supported nature of the sediment, their slightly inverse grading and the lack of imbrication. However, it must be stated that these conglomerates are of minor significance compared with the thicker, laterally extensive units of matrix-supported conglomerate which often grade up into clast-supported conglomerates and are thought to be waterlain deposits.

Cross-stratified sandstone units

The sandstone : conglomerate ratio in the Middle Buntsandstein sequence is approximately 50:50. Thick sandstone units range between 0.5 and 5.0m in thickness and are characterised by low-angle cross stratification, although horizontal stratification occurs in the uppermost part of the fining upwards cycle (Fig.6.4). Trough cross-stratification is absent, but the cross-stratification azimuths indicate transport directions from the south. These thick sandstone units comprise medium to coarse-grained sandstones where the latter contain angular, locally derived intraclasts of sandstone and mudstone (Plate 6.2), in addition to well-rounded quartz pebbles. In some cases, the occurrence of mud and siltstone intraclasts in the sandstones directly overlying the conglomerates suggests that mud and silt drapes coated the top surfaces of the conglomerates prior to sandstone deposition. This indicates that some of the sandstones and conglomerates represent separate depositional events. This is supported by the highly irregular base of the sandstones succeeding coarse clast-supported conglomerates with protruding pebbles along their upper surface.

In contrast to the thin sandstone wedges that occur within the conglomerates and are interpreted as representing deposition during waning flow, the massive sandstone units reflect deposition in wide channels with low angle margins, or alternatively, may represent sheet-like deposition. The low angled planar cross-sets result from avalanching of material down slip-faces during the infilling of basal scours, whilst the planar laminations represent deposition during the upper flow regime.

Sandstones at Katzvey (Fig. 6.2) are characterised by planar and trough cross-bedding and horizontal stratification, and commonly contain pebbles up to 3cm in diameter. Mader (1982) identified aeolian sandstones in the Northern Eifel on the basis of microlamination and large-scale cross-bedding, but it is suggested here that the pebbly

Plate 6.1 Field photograph of massive, structureless, matrix-supported conglomerate overlain by a sandstone unit at Kallmuther Berg Pit, Mechernich. Note the bleached nature of the sediments and the lenses of dolomite in the sandstone unit. (Hammer for scale).

Plate 6.2 Field photograph of the erosive contact between a poorly sorted, clast-supported conglomerate and a cross-stratified sandstone unit, Kallmuther Berg Pit, Mechernich. Note the abundance of yellow coloured silty intraclasts at the base of the sandstone unit and the random occurrence of galena 'knotten' in the upper part of the sandstone. (Pencil for scale).



sands and overlying cross-stratified sandstones reflect deposition in fluvial channels. The pebbles within the sandstones are approximately 2-5 cm in diameter and could not have been transported by the wind (Bagnold 1954).

Red siltstones and siderite-rich horizons

Thin (20cm) units of red and green coloured, finely laminated siltstones are preserved within the massive sandstone units. Immature carbonate accumulations in the form of small dolomitic nodules occur within the horizontally laminated siltstones. More mature palaeosol horizons are represented by thin (2-10cm), laterally continuous indurated horizons composed of dolomite and stained with Mn and Fe. These palaeosols often occur at the top of fining upwards sequences, but are unusual in that in some cases they directly overlie sandstones, whilst they themselves are overlain by siltstones. The presence of siltstone intraclasts in the sandstone units suggests fine sediments were more abundant in the system during deposition but have since been eroded.

This is the first description of palaeosols from the Middle Buntsandstein of the Northern Eifel. Palaeosols similar to those described above were seen at the base of the Upper Buntsandstein at Kall (Fig. 6.2) and according to Mader (1981) are also common in the Upper Buntsandstein of the western Eifel. The palaeosols indicate sub-aerial exposure but their immaturity demonstrates the long term instability of the bar top or floodplain surfaces on which they were deposited. Lateral channel migration and subsequent flooding resulted in the deposition of the finely bedded silts prior to, during, and after palaeosol development.

Summary

Depositional processes operating during Lower Triassic times included powerful sheet flood and stream flood events, minor debris flows and floodplain sedimentation as a result of deposition from waning flood waters. Observations made in the course of this work are broadly consistent with the sedimentological interpretations of Mader (1985) whose data indicate a northerly sediment transport direction and deposition in a braided river environment. However, further detailed interpretation of the previously unstudied conglomerate units at Kallmuther Berg Pit, Mechernich (Fig. 6.3) have shown that alluvial fan processes such as debris flows, may have been important on a local scale. A more detailed examination of the exposures in the Mechernich area may help to assess

the extent to which local alluvial fans sourced from the western margin of the Nideggen Trough contributed to the Middle Buntsandstein succession of the northern Eifel.

6.2.3 PETROGRAPHIC AND DIAGENETIC STUDIES

Over 30 thin and polished sections were examined using transmitted light microscopy, cathodoluminescence petrography and scanning electron microscopy in order to determine the diagenetic history of the sandstones and conglomerates hosting the mineralisation at Maubach and Mechernich.

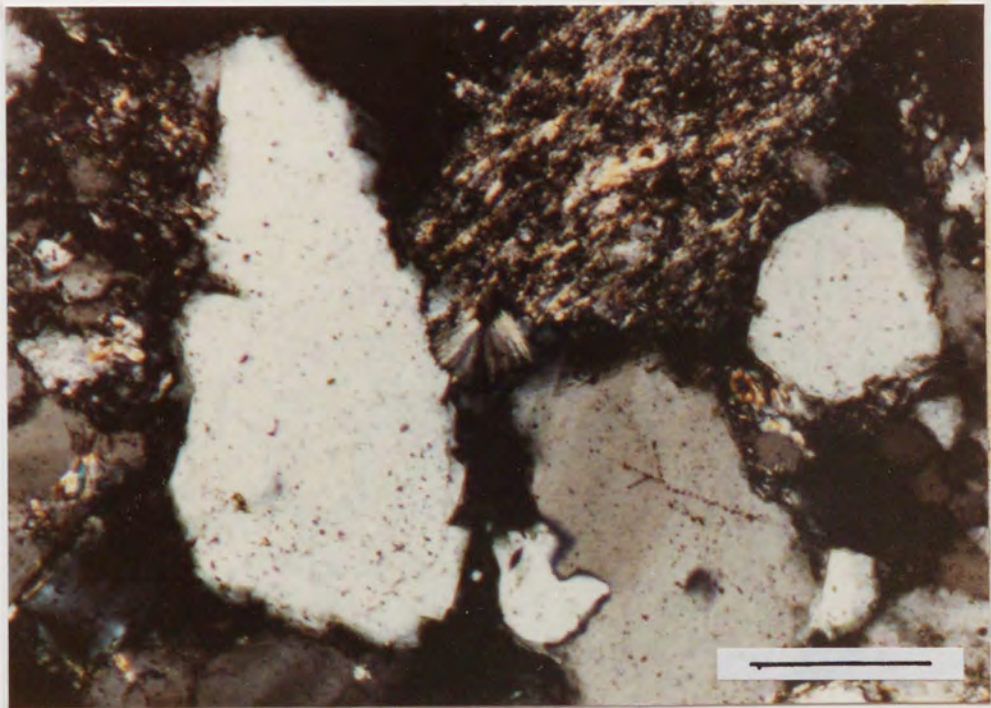
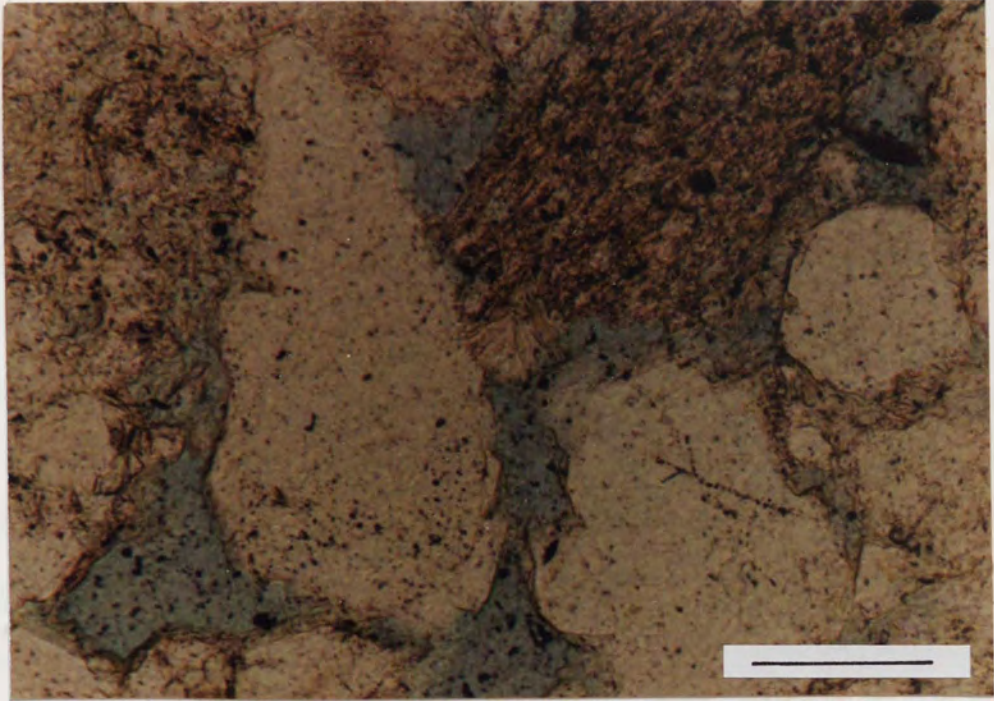
The sandstones are medium-grained, well sorted and mineralogically mature, with detrital quartz grains making up approximately 98% of the detrital assemblage. The sediments are accordingly classified as quartz arenites (Folk 1974). Detrital feldspar contents are low (between 0.7 and 2.3%) and rock fragments make up approximately 3% of the detrital grains. Rock fragments consist mainly of quartzites containing subsidiary muscovite, although fine-grained igneous rocks are also present. These clasts are typically altered to illite and kaolinite group minerals and are highly deformed (Plates 6.1 and 6.2). Muscovite mica is rarely present in the sandstones but is abundant in the finer siltstones and is a detrital component of the palaeosol horizons. The sandstones lack a heavy mineral assemblage.

Authigenic phases within the sandstones and conglomerates include quartz overgrowths, dickite, illite, dolomite and haematite. The sulphide ores, particularly galena and its alteration product cerussite, are important cementing phases. Euhedral syntaxial quartz overgrowths are commonly developed on both monocrystalline and polycrystalline quartz grains and were the first authigenic phase to precipitate. The overgrowths only constitute 1.5% of the whole rock and it is anticipated that their precipitation caused a reduction in permeability; sandstone porosity is not likely to have been greatly affected by their development.

The relative timing of the blocky dickite cements and the rhombic dolomite is problematical. Both phases clearly postdate quartz overgrowth formation and, in some cases, the dickite is enclosed by dolomite crystals. This implies that dickite precipitation preceded the formation of the dolomite. The dickite was identified by a combination of scanning electron microscopy and X-ray diffraction techniques. It forms a coarse, pore-occluding cement (Plate 6.5) and has peaks at 2.56Å and 7.16Å on an X-ray

Plate 6.3 Colour photomicrograph of unmineralised sediments in the Middle Buntsandstein, Kall. Authigenic cements include pore-filling kaolinite (K) and quartz overgrowths. Primary porosity is augmented by secondary porosity which has created the enlarged pores (P). Scale bar = 100 μm (PPL).

Plate 6.4 Colour photomicrograph of unmineralised sediments in the Middle Buntsandstein, Kall. The same view as Plate 6.3. Scale bar = 100 μm (Crossed polars).



diffraction trace. In most of the sandstones, dolomite cements are absent but in the ore-bearing sandstones at both Maubach and Mechernich, a pervasive dolomite cement precedes the main sulphide cements. The dolomite cements consist of interlocking rhombs which have clearly replaced detrital silicate grains and authigenic quartz overgrowths. Fluid inclusions hosted by the dolomite are characteristically small ($< 10\mu\text{m}$); they commonly contain a single liquid phase. Roedder (1984) suggests that such single-phase inclusions are often formed by trapping at low temperatures ($\sim 70^\circ\text{C}$), and have existed in a metastable condition without the formation of a vapour bubble for millions of years.

The mineralised sediments are devoid of the red colouration caused by haematite pellicles on detrital grains. Haematite occurs as isolated patchy cements in the ore-bearing sediments, and it seems likely that these represent weathered and oxidised primary sulphide cements.

The primary porosities of the barren sandstones at Kall (Fig. 6.2) and the ore-bearing sandstones at the present time ranges from 4.8 to 32.0% (mean 19.4%). This porosity is enhanced by the presence of secondary porosity as evidenced by enlarged pores, minor intragranular porosity in altered rock fragments, and minor fracture porosity where detrital grains have been subjected to brittle deformation during burial and/ or mineralisation.

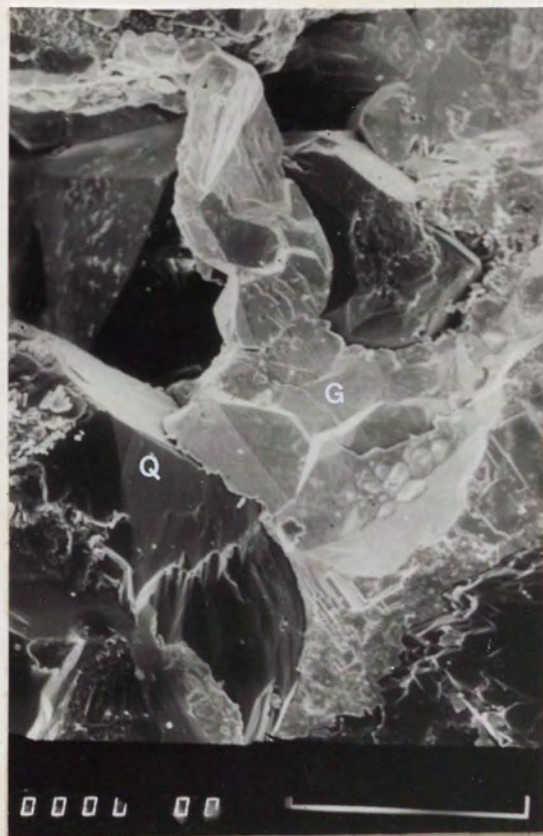
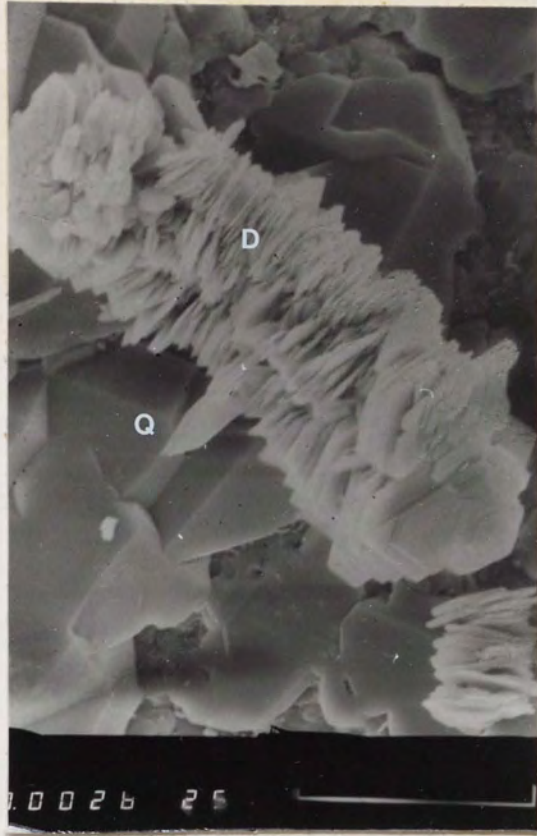
Summary

The burial history of these sediments is uncertain but the ductile deformation of detrital fragments of schistose and quartzite rock and the pressure solution grain contacts suggest that the ore-bearing middle Buntsandstein has been buried to depths considerably greater than the present 200-300m.

Quartz overgrowth formation results from silica dissolution and reprecipitation during early diagenesis of mineralogically mature sandstones. However, with the exception of the quartz overgrowths and also the illite cements, the authigenic mineral assemblage outlined above is not commonly associated with the diagenesis of continental red beds, and has obviously been influenced by the mineralising fluids which have flowed through the sediments.

Plate 6.5 Scanning electron micrograph of a large crystal aggregate of dickite, Middle Buntsandstein, Mechernich. Euhedral highly crystalline dickite (D) postdates euhedral quartz overgrowths (Q). Scale bar = 26 μm .

Plate 6.6 Scanning electron micrograph of galena cements in the Middle Buntsandstein sandstones at Mechernich. Pore-filling galena clearly postdates the formation of euhedral quartz overgrowths. Scale bar = 166 μm .



According to Brindley (1984), 'higher temperatures and hydrothermal pressures' are sometimes thought to favour dickite formation. Rosch & Zimmerle (1988) and Keller (1988) report the occurrence of dickite as a gangue phase in Mississippi Valley-type ore deposits and suggest that dickite precipitation is favoured by elevated temperatures (as high as 140°C). These authors also propose that dickite is an indicator of a regional thermal event. However, authigenic kaolinite and dickite are common constituents of unmineralised sandstones and are widely believed to be either the product of freshwater flushing through the sands (eg. Bjørlykke et al. 1979) or to form in the presence of highly saline pore fluids during burial diagenesis (eg. Hurst & Irwin 1982). It is likely therefore, that dickite in the ore-bearing sandstones of the Eifel Buntsandstein is not related to the mineralisation. Dolomite precipitation cannot be triggered by simple cooling, however, cation exchange, redox reactions, or both, can cause the precipitation of dolomite provided that there is a readily available source of Ca^{2+} and Mg^{+} ions (Holland & Malinin 1979). Sulphate reduction processes for example, involve the extraction of H^{+} from the ore fluid and can lead to the deposition of dolomite, as a result of an increase in the CO_3^{2-} concentration at a given total carbon species concentration.

Thus, the presence of dolomite and dickite may be related to the mineralising fluids moving through the sediments. The absence of haematite and the bleached appearance of the sediments may result from the acidic nature of the mineralising fluids or, alternatively, may be a consequence of weak acid generation accompanying sulphate reduction (see Chapter 7).

6.2.4 ORE MINERALOGY

Previous studies of the ore mineralogy and textures of the mineralisation at Maubach and Mechernich are restricted to the work by Puffe (1953) and Schachner (1960, 1961). Several other unpublished studies carried out between 1926 and 1958 were noted by Walther (1984). Puffe (1953) described the ores and their overall trace metal content from assays before invoking a hydrothermal origin for the mineralisation. Schachner (1960) established a paragenetic sequence for the mineralisation with dolomite, siderite, bravoite, quartz and chlorite predating the main sulphide cements. The major sulphide depositional event involved pyrite, sphalerite, chalcopyrite and galena with subsidiary

barite mineralisation. Finally, weathering processes are thought to have been responsible for the development of secondary minerals such as cerussite and covellite.

In view of the scarcity of published mineralogical, petrological and geochemical data, the main purpose of this part of the study was to establish the mineralogy and paragenesis of the sulphide assemblages. Ores hosted by Devonian carbonates at Keldenich (Fig. 6.2) were also examined for comparative purposes following the suggestion by Schachner (1960) that the Devonian and Triassic ores were precipitated during the same mineralising event.

Five sequential ore mineral assemblages can be distinguished at Maubach and Mechernich (Fig. 6.5). One such assemblage exists within detrital grains, whilst quartz overgrowths host the second phase of deposition. Sulphide precipitation is associated with a widespread dolomite gangue which precedes the main sulphide mineralisation event where galena, sphalerite, chalcopyrite and pyrite were deposited as cements in the existing pore spaces. These sulphides have been altered to carbonates and sulphates as a result of weathering processes.

Rare sulphides and haematite occur within the conglomeratic clasts at Mechernich and within detrital silicate grains in the sandstones; small (20-40 μ m) bravoite and pyrite crystals are enclosed within the silicates. It appears that they are merely replacement phases rather than a true detrital sulphide assemblage, because detrital grains in the non-mineralised sandstones contain no sulphides.

The Middle Buntsandstein sediments were weakly cemented by quartz overgrowths prior to the main sulphide cements and dolomite gangue (Plate 6.6). These overgrowths enclose small (20-50 μ m) pyrite and bravoite crystals similar to those observed in the quartz overgrowths in the mineralised sandstones of the Cheshire Basin (see Chapter 2). Authigenic quartz overgrowths such as these are formed during early sandstone diagenesis and it can therefore be assumed that the enclosed sulphides were also deposited as a result of early diagenetic processes.

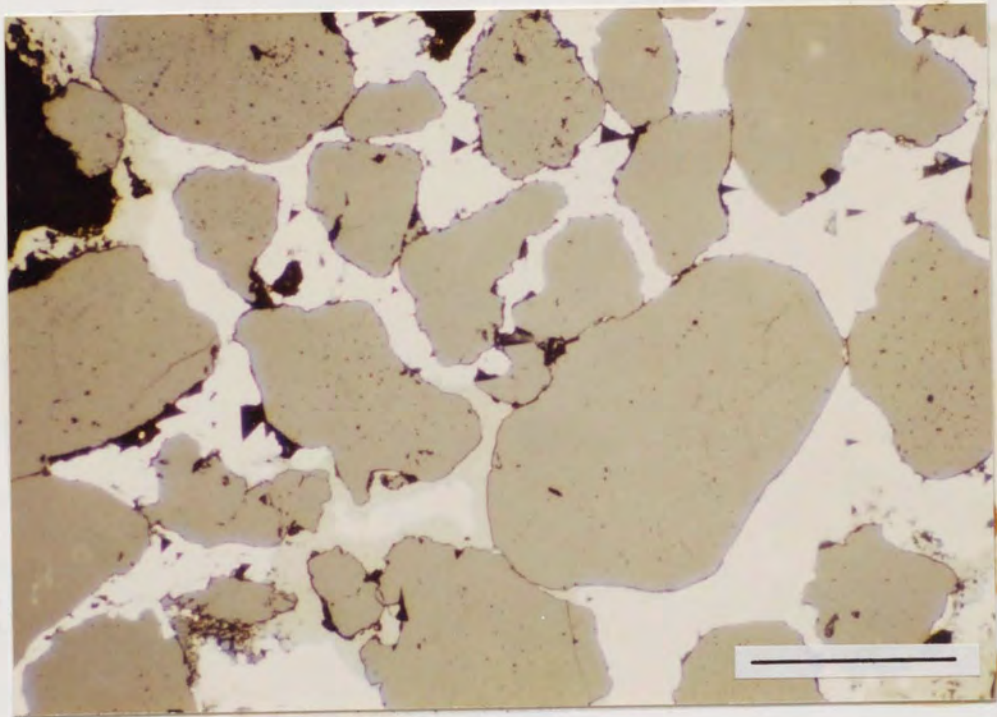
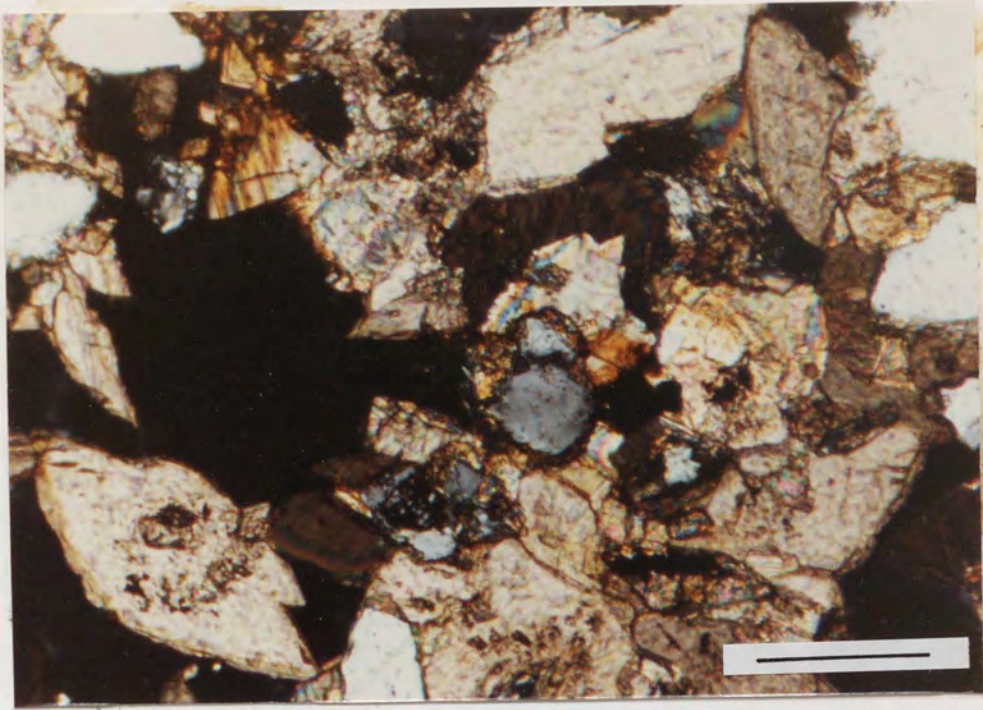
The third sulphide assemblage comprises small (~70 μ m) euhedral and anhedral crystals of pyrite and chalcopyrite associated with a pervasive dolomite cement. The majority of the sulphides predate the large (50-500 μ m) dolomite rhombs (Plate 6.7),

Figure 6.5. Paragenetic diagram for the sulphide mineralisation at Maubach and Mechernich.

	Detrital assemblage	Quartz Overgrowths	Dolomite Gangue	Main sulphide Cement	Secondary Minerals
Qtz and Fsp overgrowths		_____			
Dolomite			_____		
Bravoite	_____	_____		_____	
Pyrite	_____	_____	_____	_____	
Chalcopyrite		_____	_____	_____	
Sphalerite				_____	
Galena				_____	
Haematite	_____	_____			
Azurite					_____
Malachite					_____
Dickite					_____

Plate 6.7 Colour photomicrograph of dolomite gangue in the Middle Buntsandstein sediments, Mechernich. Scale bar = 500 μm (Crossed polars).

Plate 6.8 Reflected light micrograph of sulphide ores in the Middle Buntsandstein at Mechernich. Galena is the dominant sulphide and occurs as a cement infilling the pore spaces between the detrital quartz grains. Scale bar = 300 μm .



although some more massive pyrite and chalcopyrite were precipitated in joints and cavities in the gangue. Pyrite and bravoite crystals are also intimately intergrown with a quartz gangue at Mechernich, but the timing of this cement remains unconstrained due to its rare occurrence.

The main sulphide precipitation event is represented by the widespread sulphide cements in the sediments of the Middle Buntsandstein. This episode postdates the early diagenetic history of the host sediments as euhedral quartz and feldspar overgrowths are cemented by the sulphides. Galena is the dominant cement throughout the Maubach and Mechernich deposits (Plate 6.8) and is commonly intergrown with sphalerite, chalcopyrite, pyrite and bravoite. Walther (1986) noted the occurrence of tetrahedrite, bournonite, gersdorffite and an unidentified Bi-Pb sulphosalt but none of these phases were detected during this investigation. The sulphide paragenesis established during the present study is consistent throughout the mineralised areas at Maubach and Mechernich and agrees closely with the observations of Puffe (1953). Bravoite and pyrite were the first sulphides to precipitate, followed by chalcopyrite and sphalerite. In most cases galena was the last phase to precipitate, although at Maubach chalcopyrite was deposited on the surface of massive (1cm) cubes of galena crystals cementing a conglomerate. Euhedral chalcopyrite crystals also occur in veins and fractures in the host conglomerate and may represent a later, distinct mineralisation event. These primary sulphides are extensively altered to a suite of secondary minerals including cerussite, malachite, azurite and pyromorphite.

At Maubach, bravoite and minor chalcopyrite are hosted by carbonate veins which extend from the Triassic sediments down into the underlying Devonian basement. Ores examined during this study are from Keldenich (Fig. 6.2) and consist solely of massive (3-5mm) monomineralic galena crystals in cavities.

Bravoite Bravoite occurs as small (20-40 μ m) crystals enclosed by galena and sphalerite. The crystals often exhibit concentric zoning similar to that described in bravoites from the Cheshire Basin ore deposits. Results of microprobe analyses on bravoites from Maubach (Vaughan 1969) revealed that nickel and cobalt exhibit a sympathetic relationship, antipathetic towards iron. This is consistent with the limited number of analyses performed during this study on massive bravoite ore from

Mechernich which contains violet-coloured zones enriched in Ni and Co, and pale yellow zones containing up to 33.1 wt% Fe but lesser amounts of Ni (Table 6.1).

Bravoite crystals from Mechernich often have rims of pyritic composition.

Pyrite Electron probe analyses of pyrite from Mechernich show it to contain significant Ni (up to 4.5 wt%) and As (up to 3.2 wt%) but minor amounts of Co (up to 0.8 wt%) and Cu (up to 0.4 wt%). However, paragenetically similar pyrites from Maubach generally contain less than 1 wt% Ni, As, Co and Cu.

Chalcopyrite Anhedral chalcopyrite is intergrown with galena and is enclosed by both sphalerite and galena. Analyses of the chalcopyrite show it to be virtually pure.

Sphalerite The sphalerite is honey-coloured, is intergrown with galena and chalcopyrite but is not associated with any other sulphides at Maubach. The sphalerite is iron-poor (Table 6.1) containing only up to 0.1 wt% Fe but significant amounts of Cd (up to 0.8 wt%) and Ag (up to 0.2 wt%). Both sphalerite and galena have clearly replaced detrital grains.

Galena Galena is by far the most widespread sulphide cement and encloses all the other sulphide phases. Analyses of the galena (Table 6.1) show it to contain negligible Ag and no evidence was found for the sulphosalts described by Schachner (1960). The low Ag tenor of the sulphides is consistent with assay results (Puffe 1953) which showed the sulphide ores to contain only 1.6-2.6 g/t of silver.

6.2.5 SULPHUR ISOTOPES

Samples were prepared for sulphur isotopic analysis using the methods described in Appendix I. The SO₂ was extracted from the samples using the procedure described by Robinson and Kusakabe (1977).

The results are given in Table 6.2 and are compared to data obtained by Bayer et al. (1970) in Fig. 6.6.

The $\delta^{34}\text{S}$ values for galena hosted by the Devonian carbonates at Keldenich range from -16.8‰ to -15.1‰, whilst galena in the overlying Triassic sediments at Mechernich have a narrow $\delta^{34}\text{S}$ range from -22.2‰ to -19.4‰ (mean, -20.4‰). Two

TABLE 6.1

MINERAL SPECIES	ZN	CU	NI	CO	FE	AS	S	PB	BI	AG	CD	SB	TOTAL
GALENA 4554	-	-	-	-	-	-	13.2	87.4	0.1	-	-	0.1	100.8
GALENA 4554	-	-	-	-	-	-	12.8	86.5	0.3	-	-	-	99.6
GALENA WG8	-	-	-	-	-	-	12.9	86.8	0.1	-	-	-	99.8
SPHALERITE 4554	65.8	-	-	-	0.1	-	34.1	-	-	-	0.6	-	100.7
SPHALERITE 4554	64.6	-	-	-	-	-	33.9	-	-	0.2	0.8	-	99.5
SPHALERITE 4554	65.4	-	-	-	-	-	34.1	-	-	-	0.2	-	99.7
PYRITE 4554	-	-	0.1	0.1	45.6	-	54.1	-	-	-	-	-	99.9
PYRITE 4554	-	0.1	-	0.1	45.6	-	54.2	-	-	-	-	-	100.0
PYRITE 4554	-	-	-	0.1	44.7	-	53.7	-	-	-	-	-	98.5
PYRITE 4554	-	-	-	0.1	45.1	-	53.5	-	-	-	-	-	98.7
PYRITE 11425	-	0.2	0.1	0.1	46.3	0.3	54.3	0.2	0.2	-	-	-	101.0
PYRITE 11425	-	0.4	4.5	0.1	40.9	0.3	54.3	0.5	0.1	-	-	-	100.7
PYRITE 11425	-	-	-	0.1	44.9	3.2	51.6	0.2	0.2	-	-	-	100.1
PYRITE 11425	-	0.1	0.1	0.1	45.6	1.0	53.0	0.2	0.1	-	-	-	100.2
PYRITE 11425	-	0.7	2.6	0.2	41.6	2.3	51.7	0.3	0.1	-	-	-	100.1
PYRITE 11425	-	0.1	0.5	0.8	44.3	0.3	55.7	0.4	0.1	-	-	-	101.6
PYRITE 11425	-	0.7	2.6	0.2	41.6	2.3	51.7	-	-	-	-	-	99.7
PYRITE WG22	-	-	0.1	0.1	46.2	1.5	52.3	-	-	-	-	-	101.1
CHALCOPYRITE WG22	-	34.9	-	-	30.2	-	34.2	-	-	-	-	-	99.3
CHALCOPYRITE WG22	-	34.9	-	-	29.7	-	34.8	-	-	-	-	-	99.4
CHALCOPYRITE 11425	-	33.4	-	-	28.8	-	36.6	-	-	-	-	-	98.8
GALENA WG17	-	-	-	-	-	-	12.7	86.2	0.1	-	-	-	99.1
BRAYOITE 886	-	0.9	12.4	0.2	33.1	-	55.0	-	-	-	-	-	101.6
SPHALERITE 4554	61.7	-	-	-	-	-	34.9	-	-	0.1	1.1	0.1	97.9
SPHALERITE 4554	62.6	-	-	-	-	-	31.7	-	-	-	4.1	0.1	98.5

Table 6.1 Electron microprobe data for sulphides from the Eifel and Oberpfalz regions.

galena samples from Maubach have similar $\delta^{34}\text{S}$ values of -21.3‰ and -15.8‰ .

Massive bravoite ores from Mechernich have a $\delta^{34}\text{S}$ ratio of -12.2‰ .

The results obtained in the present study are roughly comparable to those obtained by Bayer et al. (1970). In the latter study, $\delta^{34}\text{S}_{\text{galena}}$ values at Maubach range between -21.3‰ and -18.1‰ , and $\delta^{34}\text{S}_{\text{galena}}$ at Mechernich range from -27.3‰ to -13.7‰ (Fig. 6.6). Minor discrepancies between the two sets of $\delta^{34}\text{S}$ results for Triassic sulphides include the galena cement at Maubach which when analysed during this investigation gave a $\delta^{34}\text{S}$ value outside the range quoted by Bayer et al. (1970). In addition, the $\delta^{34}\text{S}$ value for the massive bravoite cement (-12.2‰), is less negative than the values obtained by Bayer et al. (1970) for similar ores (Fig. 6.6). Barite was not observed during the present investigation but analyses by Bayer et al. (1970) yielded $\delta^{34}\text{S}$ values of approximately $+18\text{‰}$.

The sulphide veins hosted by Devonian lithologies to the southwest of Mechernich and Maubach have $\delta^{34}\text{S}$ values around 0‰ according to Bayer et al. (1970). This contrasts sharply with $\delta^{34}\text{S}$ values of approximately -16‰ for galena in cavities in Devonian carbonates at Keldenich. Samples analysed by Bayer et al. (1970) were from the fairly distant vein systems of Bleialf, Rescheid and Monschau (Fig. 6.1) whilst Keldenich is adjacent to the Mechernich ore body.

6.2.6 DISCUSSION

Early workers including Schneiderhöhn (1944) and Witte (1957) considered Maubach and Mechernich to be truly syngenetic ore deposits in which detrital sulphides were deposited contemporaneously with the host sediments. Witte (1957) cited the lack of 'roots' to the mineralisation and some of the textures involving galena and cerussite as supporting evidence for a syngenetic accumulation of ore. It is unlikely on the basis of what we now know, that the Maubach and Mechernich ores are of syngenetic origin, as at Maubach, mineralised veins clearly extend into the Devonian. Also, there is no evidence for mineralised clasts in the host sediments. It is also unlikely that economic

TABLE.6.2. Sulphur isotope data for sulphides from Maubach, Mechernich and Keldenich.

Sample no.	Phase	Remarks	$\delta^{34}\text{S}^*$ (‰)
WG3	Galena	Cavity fill in Devonian carbonates, Keldenich	-15.1
WG14	Galena	Cavity fill in Devonian carbonates, Keldenich	-15.4
WG26	Galena	Cavity fill in Devonian carbonates, Keldenich	-16.8
WG8	Galena	Cement in conglomerate, Mechernich	-22.2
WG13	Galena	Galena 'knotten' in sandstone, Mechernich	-20.9
WG15	Galena	Poikilotopic cement in sandstone, Mechernich	-19.9
WG17	Galena	Veins cross-cutting sandstone, Mechernich	-19.6
1345	Galena	Cement in sandstone, Mechernich	-19.4
4554	Galena	Cement in sandstone, Maubach	-21.3
11425	Galena	Cement in sandstone, Maubach	-15.8
886	Bravoite	Massive ore, Mechernich	-12.2

*With reference to the Canon Diablo Meteorite standard.

Figure. 6.6. Sulphur isotope data from Maubach-Mechernich and the

Bleialf-Rescheid-Brandenberg vein Systems, North Eifel.

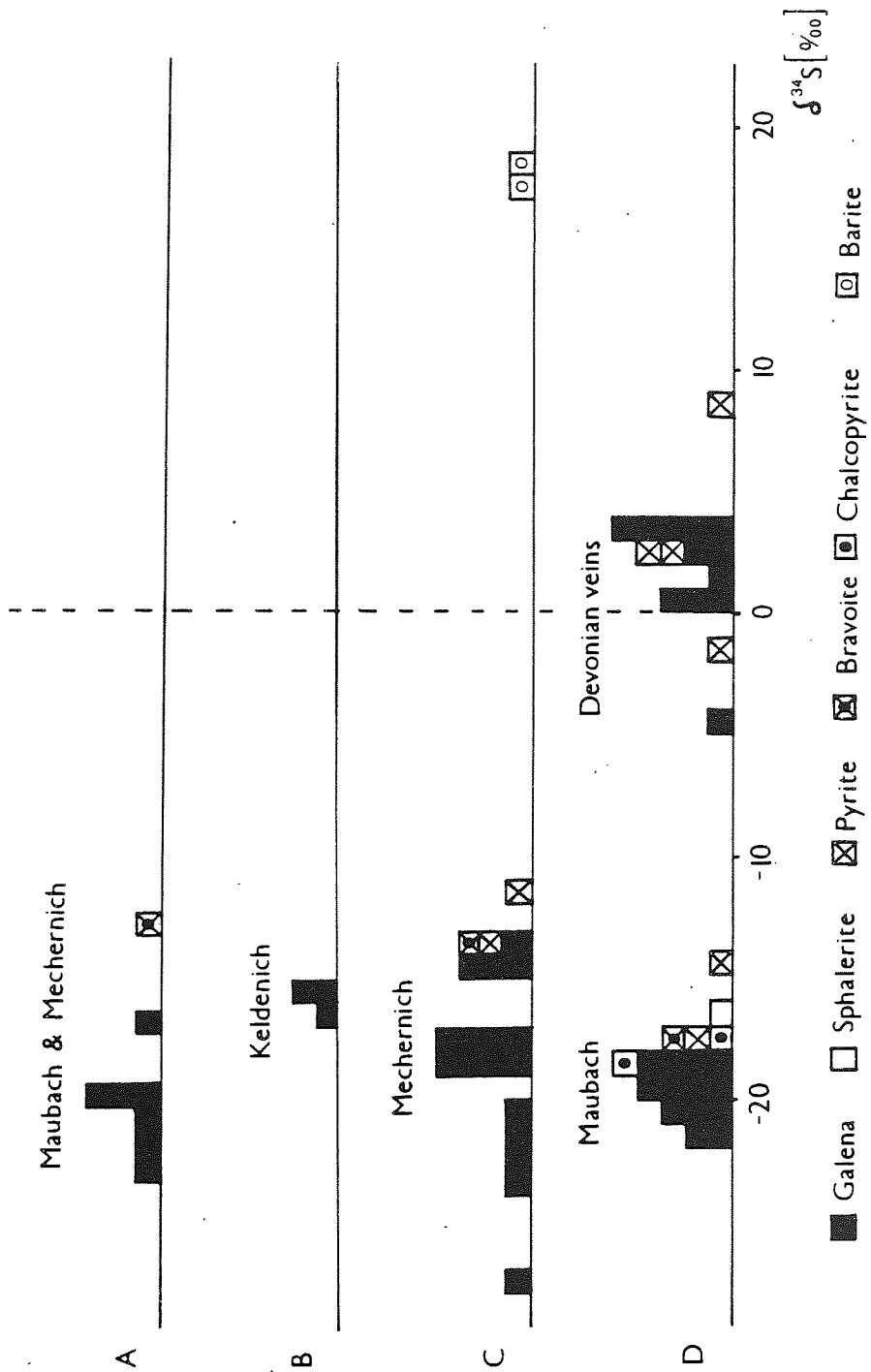
A. Data from the present study for sulphide cements in the Triassic sediments at Maubach and Mechernich.

B. Data from the present study for galena cavity fill in Devonian carbonates at Keldenich.

C. Data from Bayer et al. (1970) for Mechernich ore deposit including analyses on barite.

D. Data from Bayer et al. (1970) for Maubach and the Bleialf-Rescheid-Brandenberg vein systems to the south west of Maubach and Mechernich.

FIGURE 6.6



quantities of ore could have accumulated by such a syngenetic mechanism during the deposition of the thin sequence (200-300m) of Triassic sediments in the North Eifel.

Like the majority of investigators since Bonhardt (1912), Schneiderhöhn (1955) invoked a hydrothermal origin for the mineralisation. Behrend (1950) noted the tectonic and mineralogical relationships between Maubach and Mechernich and the vein-type carbonate-hosted mineralisation in the basement and proposed a single hydrothermal event to account for their occurrence. However, it is evident from the brief review of the literature provided by Walther (1984) that little is known concerning the possible nature and origins of any hydrothermal mineralising fluids. Walther (1984) lists the workers who have invoked an epigenetic or hydrothermal origin for the mineralisation; the most important contributions have been from Puffe (1953), Picard (1954) and Schachner (1960, 1961). Walther (1984) also reviews the attempts to establish the age of the ore deposits and favours a Late Cretaceous to Tertiary age in view of the available stratigraphic and structural data. Bjørlykke & Sangster (1981) classified Maubach and Mechernich as 'sandstone lead deposits' which are characteristically hosted by quartzitic sandstones and favoured a genetic model involving groundwater transport of the metals to an environment rich in H_2S where sulphides are likely to precipitate.

An alternative theory is presented here; it is suggested that during Carboniferous or Permian times, hydrothermal fluids were introduced into Devonian sediments resulting in Pb-Zn vein systems. Triassic sediment deposition followed, and remobilisation of the sulphides in the Devonian occurred as a result of brine circulation or a second hydrothermal event.

6.2.6.1 TIMING OF THE MINERALISATION

The precise timing of the mineralisation remains unclear, but textural studies have revealed that paragenetically early sulphides precipitated during early diagenesis of the host sandstones. The main sulphide cements enclose euhedral quartz and feldspar overgrowths and are thought to have been deposited during burial diagenesis of the Buntsandstein sediments.

Fractured pebbles are commonly cemented by galena and chalcopyrite, indicating that tectonic reworking occurred during mineralisation. Some faulting clearly postdates

the mineralisation at both Maubach and Mechernich. The extent to which the mineralisation was controlled by fault patterns is difficult to establish because of the poor exposure.

6.2.6.2 SOURCES OF METALS AND SULPHUR

Possible sources of lead that have been proposed include an ultimately magmatic source, local granitic basement with elevated lead contents and a sedimentary source where lead is released from K-feldspar during burial diagenesis.

A recent lead isotope study was carried out by Large et al. (1983) on the galena from the Bleialf-Rescheid and Brandenburg vein systems, Keldenich and Maubach and Mechernich. The absolute age of the mineralisation in all these areas remains unknown. Pb isotope results from the north Eifel, irrespective of the age of the host sediment, plot along a linear trend the gradient of which is too steep to define an isochron. According to Large et al. (1983), this trend results from the mixing of lead from two or more different sources with different μ ($^{238}\text{U}/^{204}\text{Pb}$) values and represents Pb derived from the Variscan orogen (shales, siltstones and minor volcanics) mixed with lead from the Mesozoic cover. The uniformity of the data along this trend indicates that the mineralising solutions responsible for both the Devonian and Triassic hosted deposits had a common lead source and that lead is not directly of magmatic origin (Large et al. 1983).

Bjørlykke & Sangster (1981) suggested that granitic basement within the drainage areas of Maubach and Mechernich could have supplied the lead in the deposits. Unfortunately, such a source of lead is not present in the vicinity of the North Eifel.

A sedimentary source of lead has been proposed for the mineralisation in the deep Permo-Triassic basins of Cheshire and the Inner Moray Firth, Great Britain (see chapters 2 and 4). However, Maubach and Mechernich are associated with a relatively small sedimentary basin containing only 200-300m of sandstones and conglomerates. Diagenetic reactions within the sediments of the Nideggen Trough could provide only a fraction of the 225 Mt of Pb ore at Mechernich.

Sulphur isotopes have contributed to the understanding of the Maubach and Mechernich ore deposits. A sulphur isotope study was undertaken by Bayer et al. (1970)

in order to compare the $\delta^{34}\text{S}$ values of sulphides in the Bleialf-Rescheid and Brandenburg vein systems in the Devonian with sulphur isotope data from the sulphides in the Triassic at Maubach and Mechernich. The obvious disparity in the $\delta^{34}\text{S}$ values for Pb-Zn mineralisation in the Devonian (mean 0‰) and Pb mineralisation in the Triassic (mean $\sim -20\%$) suggests that the deposits are not related (at least in any simple way) and are the product of distinct mineralising events. However, $\delta^{34}\text{S}$ values for galena at Keldenich are approximately -16% and this indicates that the mineralisation at Keldenich may have a similar sulphur source to that at Maubach and Mechernich.

The isotopically light values for the sulphides at Maubach and Mechernich are typical of sulphides precipitating as a result of sulphate reduction processes; if this were the case, then the evaporites in the overlying Muschelkalk are a likely source of sulphate. The close correspondence between $\delta^{34}\text{S}$ values for barite ($\sim +18\%$; Bayer et al. 1970) and Triassic seawater sulphate (Claypool et al. 1980) suggests that the barite sulphur was largely derived from evaporites in the Muschelkalk or from Triassic seawater percolating down into the Bundsandstein.

The exact nature and physicochemical characteristics of the mineralising fluids in the North Eifel remain conjectural due to the lack of fluid inclusion data. The relatively simple ore mineral assemblage cannot be used to constrain the conditions of sulphide precipitation at Maubach and Mechernich.

6.2.6.3 PRECIPITATION MECHANISMS AND GENETIC MODELS

Various sulphide precipitation mechanisms have been invoked for the Maubach and Mechernich deposits and, recently, attention has focused on the sulphur isotope results. The negative values for the sulphides at Maubach and Mechernich were attributed by Bayer et al. (1970) to bacteriogenic sulphate reduction processes. Bayer et al. (1970) suggested that bacterial sulphate reduction of sulphate occurred in the Muschelkalk and that H_2S was transported by groundwaters into the underlying Buntsandstein. Bjørlykke & Sangster (1981) proposed that sulphate reduction of oxidising groundwaters occurred at the site of ore deposition due to the accumulation of significant amounts of organic debris. Indeed, the range of $\delta^{34}\text{S}$ values are similar to those obtained for the Freihung

deposit where the ores are clearly associated with fossil wood fragments (see below). However, the high energy depositional environments of the Middle Buntsandstein sediments in the North Eifel are not conducive to the accumulation and preservation of large amounts of organic matter which are an essential nutrient for sulphate-reducing bacteria. Thus, sulphate reduction is not thought likely to have occurred at the site of ore deposition at Maubach and Mechernich, but may have been an important process in the overlying Muschelkalk.

Nielsen (1985) suggests an analogy with sandstone uranium deposits in the U.S.A. (Warren 1972) which have similar $\delta^{34}\text{S}$ characteristics to Maubach and Mechernich. This author proposed that oxidation of diagenetic pyrite fixed in the sediments could cause the formation of thiosulphate which would then disproportionate into isotopically light sulphide and heavy sulphate under different Eh and pH conditions. This mechanism would result in a pattern of $\delta^{34}\text{S}$ values similar to that seen at Maubach and Mechernich. It is doubtful whether this process could have contributed significantly to the genesis of the North Eifel deposits as a diagenetic sulphide source was not readily available during post Triassic times.

The only firm conclusion that can be drawn from the sulphur isotope data is that Maubach and Mechernich have the same sulphur source, although the slightly narrower range of $\delta^{34}\text{S}$ values at Maubach may reflect a later remobilisation of the sulphides.

Simple cooling or mixing with dilute groundwaters could cause sulphide precipitation from hydrothermal fluids. Two genetic hypotheses are favoured in view of the discussion above and involve; i) remobilisation of hydrothermal sulphides in the Devonian basement and ii) groundwaters or low temperature diagenetic fluids deriving sulphur from the evaporite horizons in the Muschelkalk and Pb from the Devonian sediments and volcanics. The sulphur isotope data from this study and from Bayer et al. (1970) are more consistent with the model involving groundwaters or diagenetic fluids as such isotopically light sulphides are characteristic of sulphate reduction processes. Also, the discrepancy between the $\delta^{34}\text{S}$ of sulphides in the Devonian and Triassic sediments suggest that no simple genetic relationship exists between them.

6.3 OBERPFALZ DEPOSITS

6.3.1 GEOLOGICAL SETTING

Galena and other base metal sulphides occur in the Triassic sandstones of the Oberpfalz area, northeastern Bavaria (Fig. 6.7a). The ores occur on the margins of a sedimentary basin containing Permo-Triassic sediments derived from the Bohemian Massif to the east.

The Rotliegendes underlies the poorly mineralised Buntsandstein sediments which consist of fluvial sandstones and conglomerates (Fig. 6.7b). The Muschelkalk succeeds Buntsandstein deposition and comprises poorly cemented sandstones interbedded with carbonates and evaporites. The sediments are thought to reflect deposition in a transitional brackish estuarine and fluvial environment. Lower Keuper sediments are similar, consisting of muddy dolomite horizons interbedded with mudstones and plant-bearing sands. In contrast, the Upper Keuper succession is made up of medium sandstones of both fluvial and marine origin. To the west, the Muschelkalk becomes increasingly dominated by marine carbonates and the Upper Keuper sediments contain gypsum. The well documented 'Bleiglanzbank' is hosted by the dolomitic marl beds of the Muschelkalk (Brockramp 1973). The ore-bearing sediments of the Oberpfalz range from continental fluvial clastics to the east through to more distal marine (partly evaporitic) sediments to the west (Fig. 6.7b).

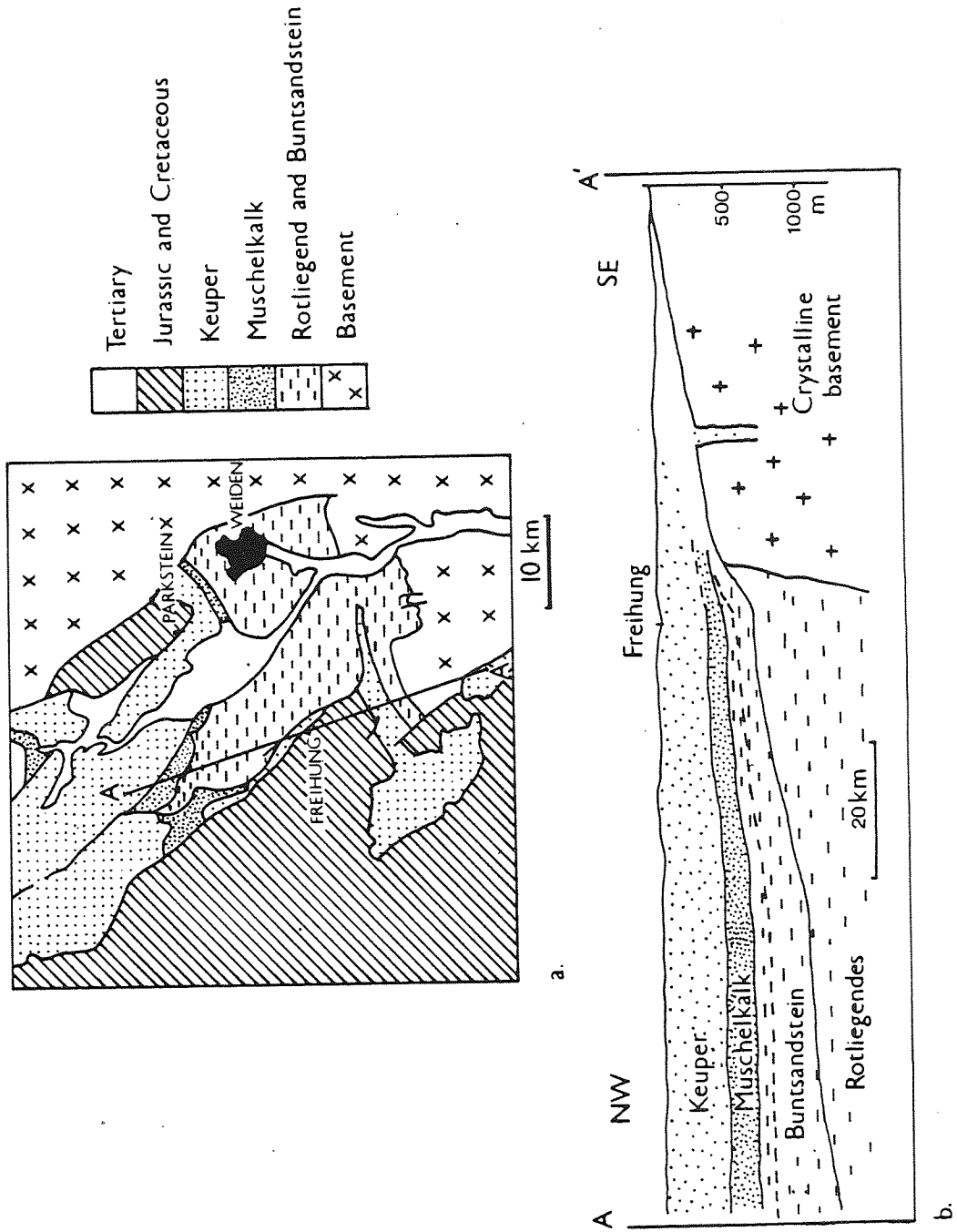
At Freihung (Fig. 6.7), Upper Muschelkalk sandstones are cemented by cerussite and galena and the total ore reserves are estimated at 200,000 tons of Pb (Tillman 1958). Ores are often concentrated below thin shale horizons and consist mainly of cerussite (Tillman 1958, Gudden 1975, Klemm & v. Schwarzenberg 1977). Other primary ore minerals at Freihung include minor sphalerite and pyrite. To the north near Parkstein (Fig. 6.7), a series of boreholes have revealed extensive lead mineralisation in the Lower Muschelkalk and lower Keuper sediments (Schmid 1981). Lead-bearing sediments extend 5km and the lead is concentrated in thin shale layers containing fossil plants (Bjørlykke & Sangster 1981). Galena in the Oberpfalz occurs as a cementing phase in sandstones and also as a replacement phase in fossilised wood fragments (Klemm & v. Schwarzenberg 1977).

The purpose of this part of the study is to briefly describe the ore occurrence, the

Figure. 6.7a. Geological map of the Oberpfalz, northeastern Bavaria showing the Permo-Triassic sedimentary basin to the west of the Bohemian Massif.

6.7b. A cross-section across the Permo-Triassic basin showing the stratigraphic position of the Pb-bearing Lower Keuper and Muschelkalk sediments (after Schroder 1975).

FIGURE 6.7



sulphide mineralogy, the diagenesis of the host sandstones and finally, in view of the results obtained to assess the genetic interpretation of the deposits by previous authors. An additional aim of the study is to compare the mineralisation with the ore deposits in the North Eifel.

6.3.2 PETROGRAPHIC AND DIAGENETIC STUDIES

The Lower Muschelkalk succession in the Parkstein boreholes comprises cross-stratified pale grey sandstones interbedded with thin (2-10cm) dark grey carbonate horizons. The sandstones have high detrital feldspar contents ranging from 7.6 to 18.0% of the whole rock and are accordingly classified as subarkoses and arkoses (Folk 1974). In most cases the sands are fine to medium grained, containing angular and subrounded clasts. The main detrital components are monocrystalline and polycrystalline quartz which together make up approximately 40% of the whole rock. Orthoclase is by far the most common feldspar; perthite and microcline are present only in minor amounts. The remaining detrital constituents are muscovite, quartzitic rock fragments, hornblende and zircon.

Quartz and feldspar overgrowths were the first authigenic phases to precipitate. Euhedral epitaxial feldspar overgrowths are commonly associated with detrital orthoclase grains. Limited electron microprobe analyses on detrital feldspars showed the orthoclase to contain minor amounts of Na and revealed the feldspar overgrowths to be pure stoichiometric K-feldspar. Overgrowth formation precedes the precipitation of micritic dolomite and later dolomite spar. The two generations of dolomite have distinctive cathodoluminescence characteristics, with earlier micrite consisting of small crystals (<10 μ m) of non-ferroan dolomite that luminesce bright orange. Later ferroan dolomite crystals (0.1-0.2mm diameter) have a predominantly dull luminescence, which is cross-cut by narrow zones of brightly luminescent cement. The iron in the ferroan dolomite is responsible for quenching the luminescence (Machel 1985). The clay mineral assemblage in the Lower Muschelkalk sandstones includes blocky, pore-filling kaolinite and illite.

Pyrite is a minor constituent of these sediments but no galena was observed. Pyrite occurs as individual crystals \sim 80 μ m in size, or as clusters of crystals within detrital

grains and in pore spaces. Pyrite distribution is concentrated along the foresets of the sandstones but, on a microscopic scale, occurs randomly. Dolomite-rich lithologies also contain minor amounts of pyrite.

Porosity in the sandstones ranges from 12-19.6% where dolomite cements are absent. Secondary porosity is widespread and is particularly associated with the partial or total dissolution of framework feldspar grains (Plate 6.9).

Textural evidence for widespread feldspar dissolution indicates that the original feldspar content of the sandstones is likely to have been considerably higher. The implications of framework grain dissolution on this scale is discussed further below.

The diagenetic mineral assemblage of the Lower Muschelkalk sandstones closely resembles the early authigenic illite-chlorite- K-feldspar-quartz-pyrite-carbonate cements which characterise marine and marginal marine sandstones (Burley et al. 1985). The presence of kaolinite is an exception to this comparison, and is thought to reflect leaching of the sediments by acidic fluids at some stage of diagenesis. The pyrite in such sediments is typically early diagenetic, resulting from the action of sulphate-reducing bacteria during shallow burial (Berner 1980).

6.3.3 SULPHIDE MINERALOGY

Sulphides occur both as cements, as outlined above, and as replacement phases in fossil wood fragments (Ziehr & Jacobec 1967, Klemm & v. Schwarzenberg 1977). Minor amounts of sphalerite and pyrite were deposited before the precipitation of galena in wood fragments whose cell structure is preserved despite sulphide replacement (Plate 6.10). The higher degree of deformation associated with the cells replaced with galena rather than pyrite is further evidence that pyrite predates galena. This is consistent with observations by v. Gehlen & Nielsen (1985).

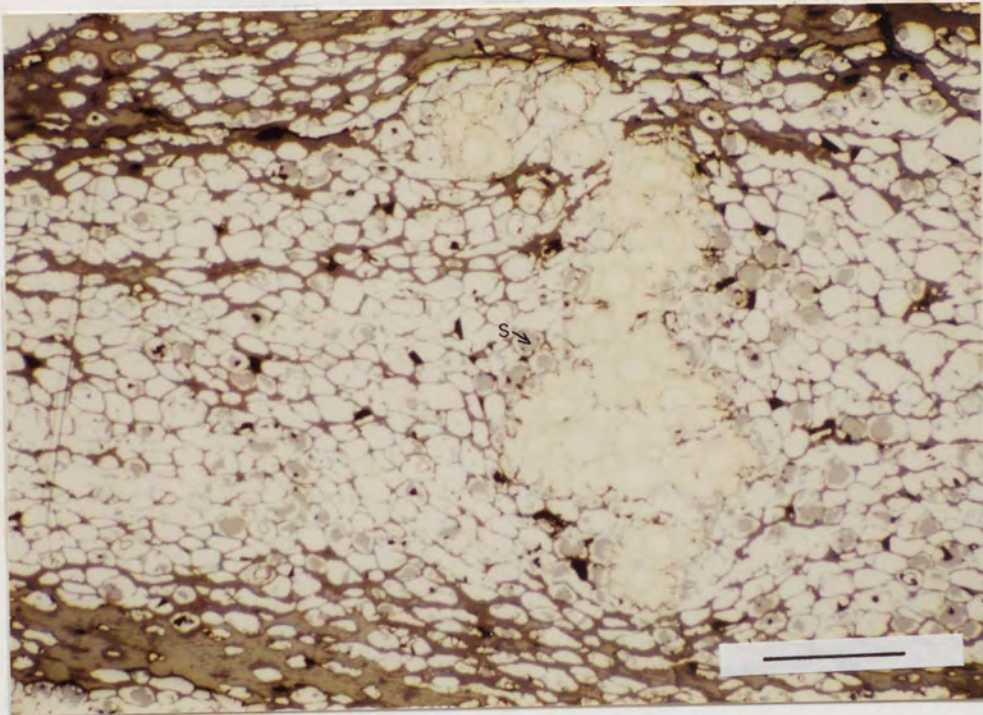
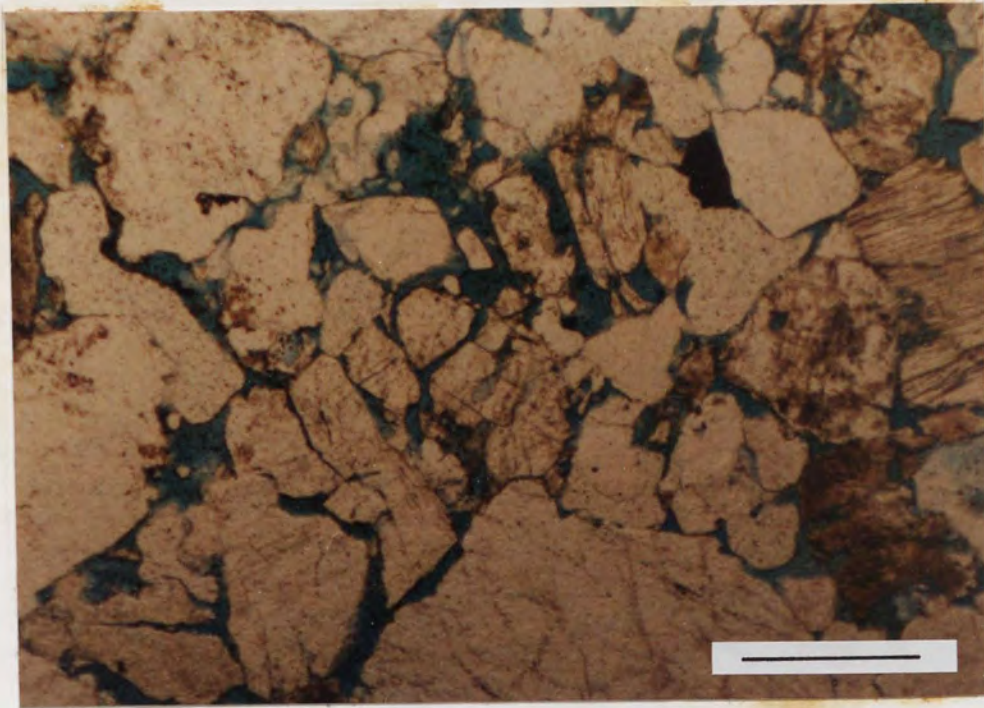
Electron microprobe analyses of the ores show the sphalerite to contain minor amounts of Cd (up to 4.1 wt%) and Ag (up to 0.1 wt%) but no Fe. Pyrite contains minor amounts of Cu (up to 0.4 wt %), Co (up to 0.1 wt %) and As (up to 1.1 wt%). Analyses of galena show it to be pure stoichiometric PbS.

Witte (1957) proposed that some of the cerussite in the deposits is of primary origin but the results of the present work are more in accordance with Klemm & v. Schwarzenberg (1977) and suggest that the galena is the primary ore and that the

Plate 6.9 Colour photomicrograph of Upper Muschelkalk / Lower Keuper sandstones in the Parkstein borehole, PA6. Evidence for secondary porosity includes the oversized pores and pore throats and the dissolution of detrital potassium feldspar grains (F). Scale bar = 500 μm (PPL).

Plate 6.10 Reflected light micrograph of sulphide ores at Freihung, Oberpfalz.

Galena, sphalerite (S) and pyrite replace the cellular structure in wood fragments. The lack of deformation observed in those cells replaced by pyrite suggests that galena and sphalerite precipitated later in the paragenesis, after the deformation of the surrounding cells. Scale bar = 300 μm .



widespread cerussite is a weathering product. This is particularly obvious at Freihung where later faulting is thought to be responsible for remobilisation of lead and for the formation of cerussite, following interaction with oxidising groundwaters (v. Schwarzenberg 1975).

6.3.4 DISCUSSION

Schmid (1981) and Walther (1984) have reviewed the hypotheses invoked by previous authors concerning the genesis of the Oberpfalz deposits. Recent authors have agreed on a syngenetic/diagenetic origin for the ores involving sulphide precipitation contemporaneous with, or occurring shortly after, sediment deposition. Evidence cited by previous authors in support of this theory includes the replacement of fossil wood fragments by pyrite prior to their deformation during burial. In addition, the ores are not fault-related except at Freihung and are of very low grade. The general consensus of opinion on the origin of the lead is that it was derived from the weathering detritus of the Variscan orogen (Gudden 1975, Klemm & v. Schwarzenberg 1977, Schmid 1981).

Sulphur isotope results from a comprehensive study by v. Gehlen & Nielsen (1985) have contributed significantly to the understanding of the deposits and are discussed briefly below. The $\delta^{34}\text{S}$ values for sulphides in the Oberpfalz region are strongly negative and show a fairly wide range within an individual deposit. The uniformly negative results are thought to indicate a bacteriogenic source for the sulphide sulphur (v. Gehlen & Nielsen 1985). The $\delta^{34}\text{S}$ values for galena at Freihung range from -29‰ to -18‰ whilst $\delta^{34}\text{S}$ ratios for sulphides at Wollau and Eichelberg lie in the range -30‰ to -40‰ . v. Gehlen & Nielsen (1985) interpreted these discrepancies as reflecting variations in rates of bacterial sulphate reduction and sulphate supply. At both Wollau and Freihung, the galena hosted by the fossil wood fragments is isotopically lighter (enriched in ^{32}S) than the galena cementing the sandstones. Textural studies have failed to establish a paragenetic relationship between the two types of galena. However, isotopic results may reflect the fact that galena associated with the fossil wood precipitated first, then as sulphate reduction continued in a relatively closed system and isotopically light sulphur was extracted, later galena inevitably has less negative $\delta^{34}\text{S}$

values.

The $\delta^{34}\text{S}$ of pyrite in fossilised wood fragments at Freihung are lower than those values obtained for associated galena. Under equilibrium conditions, thermodynamic fractionation results in the enrichment of $\delta^{34}\text{S}$ in the more strongly bonded sulphide species, so that $\delta^{34}\text{S}$ increases in the sequence galena-chalcopyrite-sphalerite-pyrite (Nielsen 1985). In view of this, it is clear that pyrite and galena at Freihung are not in isotopic equilibrium and according to v. Gehlen & Nielsen (1985), the $\delta^{34}\text{S}$ values suggest that pyrite precipitated first in a relatively open system followed by galena deposition under more closed system conditions where the sulphate supply was limited. This was confirmed by the textural observations of Klemm & v. Schwarzenberg (1977) and during the present study.

On the basis of the sulphur isotope results, v. Gehlen & Nielsen (1985) concluded that the sulphides hosted by Triassic sandstones in northeast Bavaria were precipitated from H_2S produced by bacteriogenic reduction of sulphate. The $\delta^{34}\text{S}$ values of associated barite fall in the range $+15\text{‰}$ to $+20\text{‰}$, corresponding closely to the $\delta^{34}\text{S}$ of Triassic seawater (Claypool et al. 1980). The pattern of $\delta^{34}\text{S}$ values for sulphides in the Oberpfalz is consistent with the distribution pattern defined by Ohmoto & Rye (1979) as indicative of bacterial reduction in euxinic environments (eg. the Kupferschiefer) where rates of sulphate reduction and sulphate supply are low.

Having established that sulphate reduction was the means by which most, if not all, the Oberpfalz sulphide precipitated, the possible sources of sulphate need to be considered. Oxidation of sulphides in the hinterland, leached evaporite/seawater sulphur and brackish porewaters in the host sediments are possible sources of sulphate. The latter possibility is considered unlikely to be a major contributor as a larger sulphate reservoir is required to account for the extensive sulphides. It is not possible to differentiate between the other two alternatives purely on a sulphur isotope basis, although v. Gehlen & Nielsen (1985) favoured a model involving groundwaters which transported the lead and oxidised sulphide from the Bohemian Massif to the site of ore deposition.

6.4 SWITZERLAND

Mineralised samples from the Permo-Triassic sequences of northern Switzerland were examined at Bern University. A recent programme of boreholes by NAGRA (Nationale Genossenschaft für Lagerung radioaktiver Abfälle) has revealed the presence of an extensive sedimentary basin containing up to 3000m of Carboniferous and Mesozoic sediments. Carboniferous Coal Measures are overlain by thick Permian red beds which are succeeded by thin (2-30m) Buntsandstein sediments. A marine transgression followed resulting in the deposition of evaporites, mudstones and carbonates in the Muschelkalk and Keuper.

Table 6.3. lists the types of mineralisation and the sedimentary facies with which they are associated in northern Switzerland. The mineralisation will be discussed in the wider context of Triassic sediment-hosted base metal deposits in the concluding chapter.

6.5 CONCLUDING REMARKS

Maubach, Mechernich and the Oberpfalz deposits are all Triassic sandstone-hosted Pb deposits, but it is clear from the descriptions and discussions above that a single genetic model cannot be applied to the mineralisation in all of these areas.

The timing of the mineralisation at Maubach and Mechernich and the character of the ore-forming fluids responsible for their formation remains uncertain. Textural studies reveal that paragenetically early sulphides precipitated during early diagenesis shortly after burial, whilst the main sulphide cements were deposited during burial diagenesis. Fluid inclusion data are required to constrain the nature of the mineralising fluids.

The likely sources of sulphur for the North Eifel deposits are the Triassic evaporites in the Muschelkalk and the sulphides in the Devonian basement. The sulphur isotope results favour an evaporite origin for the sulphur. The origin of the lead is somewhat problematical, a basement source is preferred as the thickness of the Triassic sediments in the Nideggen Trough is insufficient to account for the amount of ore at Maubach and Mechernich.

Two genetic models are favoured following the integration of geological, diagenetic and isotopic data. The first involves remobilisation of hydrothermal vein sulphides in the Devonian basement by brine circulation or by a second hydrothermal event. Alternatively, groundwaters or diagenetic fluids may have been responsible for

TABLE 6.3. Base metal deposits in the Permo-Trias of northern Switzerland and southern Germany.

Age	Lithology	Mineralisation	Mineralogy
MUSCHELKALK	Marine sediments.	Pb-Zn-Cu-As	Bornite, sphalerite, chalcopyrite, arsenic, galena, covellite, pyrite and marcasite, tennantite, (Weinelt 1955), (Hofmann 1980).
BUNTSANDSTEIN	Cross-stratified sandstones deposited in a marginal marine environment.	Pb-Cu-Fe	Galena, chalcopyrite and copper sulphides.* (Hofmann 1980)
PERMIAN	Continental red muds, evaporites and silcretes.	Ni-Co-Cu U-V	Reduction haloes associated with galena, chalcopyrite, sphalerite and niccolite.* (Hofmann 1986)

*Borehole material from Weiach, Riniken and Bottstein, northern Switzerland

transporting sulphur to the site of ore deposition, the sulphur isotope data are more consistent with the latter hypothesis.

On the other hand, convincing geological and isotopic evidence supports the theory that the Oberpfalz sulphides were precipitated during and immediately following sediment deposition. The close association with terrestrial debris, the lack of post-Triassic magmatic activity, the general absence of fault-related ores and the negative $\delta^{34}\text{S}$ values indicate that the ores were precipitated in a low temperature sedimentary environment during the early diagenesis of the host sediments. Pb was derived from the Bohemian Massif which also acted as a source area for the host sediments. Likely sulphur sources include oxidised sulphur from the basement and leached evaporite/seawater sulphate. Isotopically light sulphur isotope values are consistent with a theory involving sulphate reduction as the dominant mechanism of sulphide precipitation and the abundant organic material in the Oberpfalz acted as a valuable nutrient for sulphate-reducing bacteria.

REFERENCES

- ALLEN, P.A. 1981. Sediments and processes on a small stream-flow dominated Devonian alluvial fan, Shetland Islands. *Sedimentary Geology*, **29**, 31-66.
- BAGNOLD, R.A. 1954. *The physics of blown sand and desert dunes*, 2nd edition, Chapman and Hall, London.
- BALLANCE, P.F. 1984. Sheetflow dominated gravel fans of the non-marine Cenozoic Simmler Formation, central California. *Sedimentary Geology*, **38**, 337-359.
- BAYER, H., NIELSEN, H. & SCHACHNER, D. 1970. Schwefelisotopenverhältnisse in sulfiden aus Lagerstätten der Nordeifel im Raum Aachen-Stolberg und Maubach-Mechernich. *Neues Jahrbuch für Mineralogie Abhandlungen*, **113**, 251-273.
- BEHREND, F. 1948. Die blei- und zinkerz führenden imprägnationslagerstätten im Buntsandstein am Nordrand der Eifel und ihre Entstehung. Rep. 18. International Geological Congress, 7, 325-339.
- BERNER, R.A. 1980. *Early diagenesis a theoretical approach*. Princetown University Press.
- BJØLYKKE, A. & SANGSTER, D.F. 1981. An overview of sandstone lead deposits and their relation to red-bed copper and carbonate-hosted lead-zinc deposits. *Economic Geology 75th Anniversary Volume*, 179-213.
- BJØRLYKKE, K., ELVERHOI, A. & MALM, O. 1979. Diagenesis in Mesozoic sandstones from Spitzbergen and the North Sea - a comparison. *Geologisches Rundschau*, **68**, 1152-1171.
- BONHARDT, W. 1912. Über die gangverhältnisse des Siegerlandes und Seiner umgebung. *Archive für Lagerstättenforsch*, **8**, 515.
- BRINDLEY, G.W. 1984. X-ray analysis of clays. In: BRINDLEY, G.W. & BROWN, G. (eds). *Crystal structures of clay minerals and their identification*. Mineralogical

- Society, London.
- BROCKAMP, O. 1973. Zur metallogense der Bleiglanzbank im mittleren Keuper Südwestdeutschlands. *Neues Jahrbuch für Mineralogie Monatsch.*, , 461-473.
- BURLEY, S.D., KANTOROWICZ, J.D. & WAUGH, B. 1985. Clastic diagenesis. In: BRENCHLEY, P.J. & WILLIAMS, B.P.J. (eds) *Sedimentology: Recent Developments and Applied Aspects..* Geological Society of London Special Publication, **18**, 189-228.
- CLAYPOOL, G.E., HOLSTER, W.T., KAPLAN, I.R., SAKAI, H. & ZAK, I. 1980. The age curves of sulphur and oxygen isotopes and their mutual interpretation. *Chemical Geology*, **28**, 199-260.
- FLINT, S., CLEMMEY, H. & TURNER, P. 1986. The Lower Cretaceous Way Group of Northern Chile: an alluvial fan-fan delta complex. *Sedimentary Geology*, **46**, 1-22.
- FOLK, R.L. 1974. *Petrology of Sedimentary Rocks*. Hemphills Publishing Company, Austin, Texas.
- GEHLEN, K.von. & NIELSEN, H. 1985. Sulphur isotopes and the formation of stratabound lead-bearing Triassic sandstones in northeastern Bavaria. *Geologische Jahresberichte*, **70**, 213-223.
- GUDDEN, H. 1975. Zur bleierz-führung in Trias-sedimenten der nördlichen Oberpfalz. *Geologica Bavarica*, **74**, 33-55.
- HEWARD, A.P. 1978. Alluvial fan and lacustrine sediments from the Stephanian A and B (La Magdalena, Cinera-Matallana and Sabero) coalfields, northern Spain. *Sedimentology*, **25**, 451-488.
- HOFMANN, B. 1980. Blei, zink, kupfer und arsenvererzungen im Wellengebirge (unterer Muschelkalk, Trias) am südlichen und östlichen, Schwarzwaldrand. *Mitt. Naturforsch Ges. Schaffhausen*, **31**, 157-196.
- HOFMANN, B. 1986. Small-scale multi-element accumulations in Permian red beds of northern Switzerland. *Neues Jahrbuch für Mineralogie Monatsch.*, **8**, 367-375.

- HOLLAND, H.D. & MALININ, S.D. 1979. The solubility and occurrence of non-ore minerals. In: BARNES, H.L. (ed.) *Geochemistry of Hydrothermal Ore Deposits*, 2nd edition. Wiley & sons, New York.
- HURST, A. & IRWIN, H. 1982. Geological modelling of clay diagenesis in sandstones. *Clay Minerals*, **17**, 5-22.
- KELLER, W.D. 1988. Authigenic kaolinite and dickite associated with metal sulphides - probable indicators of a regional thermal event. *Clays and Clay Minerals*, **36**, 153-158.
- KLEMM, D.D. & SCHWARZENBERG, T.von. 1977. Die Bleierzvorkommen am Rande des Oberpfälzer Waldes. *Erzmetall*, **30**, 531-536.
- KNAPP, G. 1980. *Erläuterungen zur Geologischen Karte der nördlichen Eifel*, (1:100000) Geologisches Landesamt Nordrhein-Westfalen, Krefeld.
- LARGE, D., SCHAEFFER, R. & HOHNDORF, A. 1983. Lead isotope data from selected galena occurrences in the North Eifel and North Sauerland, Germany. *Mineralium Deposita*, **18**, 235-243.
- LARSEN, V. & STEEL, R.J. 1978. The sedimentary history of a debris flow dominated Devonian alluvial fan - a study of textural inversion. *Sedimentology*, **25**, 37-59.
- MACHEL, H.G. 1985. Cathodoluminescence in calcite and dolomite and its chemical interpretation. *Geoscience Canada*, **12**, 137-147.
- MADER, D. 1981. Genesis of the Buntsandstein (Lower Triassic) in the Western Eifel (Germany). *Sedimentary Geology*, **29**, 1-30.
- MADER, D. 1985. Fluvial conglomerates in continental red beds of the Buntsandstein (Lower Triassic) in the Eifel (F.R.G.) and their palaeoenvironmental, palaeogeographical and palaeotectonic significance. *Sedimentary Geology*, **44**, 1-64.
- NIELSEN, H. 1985. Sulphur isotope ratios in stratabound mineralizations. *Geologische Jahrbichte*, **70**, 225-262.
- OHMOTO, H. & RYE, R.O. 1979. Isotopes of sulphur and carbon. In BARNES, H.L. (ed.) *Geochemistry of Hydrothermal Ore Deposits*, 2nd edition, Wiley & Sons, New York.

- PICARD, K. von. 1954. Beiträge zur erforschung der bleierzlagerstätte bei Mechernich (Eifel). *Geologische Jahresberichte*, **69**, 653-680.
- PUFFE, E. 1953. Die blei-zink-erzlagerstätte der Gewerkschafte Mechernicher werke in Mechernich in der Eifel. *Erzmetall*, **6**, 302-310.
- RIBBERT, K.H. 1985 *Erläuterungen zur Geologischen Karte der 5405 Mechernich* (1: 25000). Geologisches Landesamt Nordrhein Westfalen, Krefeld.
- ROBINSON, B.W., & KUSAKABE, M. 1975. Quantative preparation of sulphur dioxide from $^{34}\text{S}/^{32}\text{S}$ anlayses from sulphides by combustion with cuprous oxide. *Analytical Chemistry*, **47**, 1179-1181.
- ROBINSON, B.W. & KUSAKABE, M. 1975. Quantative preparation of sulphur dioxide for $^{34}\text{S}/^{32}\text{S}$ analyses from sulphides by combustion with cuprous oxide. *Analytical Chemistry*, **47**, 1179-1181.
- ROEDDER, E. 1984. *Fluid Inclusions*. Reviews in Mineralogy, 12, Mineralogical Society of America.
- ROSCH, H. & ZIMMERLE, W. 1988. Diagenetic and petrogenetic significance of dickite occurrences in sedimentary rocks. (Abs.) *Clay Diagenesis in Hydrocarbon Reservoirs and Shales*, Mineralogical Society Conference, Cambridge.
- SCHACHNER, D. 1960. Bravoiitführende blei-zinkvererzungen im Devon und Buntsandstein der Nordeifel. *Neues Jahrbuch für Mineralogie Abhandlungen*, **94**, 469-478.
- SCHACHNER, D. 1961. Blei-zinkerz-lagerstätten im Buntsandstein der Triasmulde Maubach-Mechernich. *Aufschluss Supp.*, **10**, 43-49.
- SCHMID, H. 1981. Zur bleiführung in der Mittleren Trias der Oberpfalzergebnisse neuerer bohrungen. *Erzmetall*, **34**, 652-658.
- SCHNEIDERHÖHN, H. 1944. Erzlagerstätten. Kurzvorlesungen, Fischer, Jena. Aufschluss Fischer, 375.
- SCHRODER, B, von. 1975. Die geologische entwicklung des Vorlandes der

- Oberpfalz. *Der Aufschluss Sonderband*, 26, 277-288.
- SCHWARZENBERG, T. von. 1975. *Lagerstättenkundliche Untersuchungen an sedimentaren Bleivererungen der Oberpfalz*. Unpublished D.Sc dissertation, University of Munich.
- TILLMAN, H. 1958. *Erläuterungen zur Geologisches Karte von Bayern* (1: 25000), Munich sheet no. 6337, Kaltenbrunn.
- VAUGHAN, D.J. 1969. Zonal variation in bravoite. *American Mineralogist*, **54**, 1075-1083.
- VOIGT, A. 1952. Die bleizinkerzvorkommen im Buntsandstein und Unterdevon der Nordeifel. *Geologisches Jahresberichte*, **66**, 1-13.
- WALTHER, H.W. 1984. Criteria on syngensis and epigenesis of lead-zinc ores in Triassic sandstones in Germany. In: WAUKSCHKUHN, A. KLUTH, C. & ZIMMERMAN, R.A. (eds) *Syngensis and Epigenesis in the Formation of Mineral Deposits*. Springer Verlag, Berlin.
- WALTHER, H.W. 1986. Federal Republic of Germany. In: DUNNING, F.W. & EVANS, A.M. (eds) *Mineral Deposits of Europe, volume 3 Central Europe*. The Institute of Mining and Metallurgy and the Mineralogical Society, London.
- WARREN, C.G. 1972. Sulphur isotopes as a clue to the genetic geochemistry of roll-type uranium deposits. *Economic Geology*, **67**, 759-767.
- WEINELT, W. 1955. Bleiträge zur paläogeographie und lithologie der Bleiglanz-Bank des mittleren Keupers im Raum Zwischen Klettgau und Coburg. Unpublished Dissertation, Würzburg.
- WITTE, G. de. 1957. Über die entstehung der Mechernicher bleierz. *Neues Jahrbuch für Mineralogie Monatsch*, **1957**, 121-128.
- ZIEHR, H. & JAKUBEC, F. 1967. Erzminerale von Freihung und Wollau (Oberpfalz) und die spurenelemente in bleiglanz und cerussit. *Aufschluss Sonderheft*, **16**, 292-300.

CHAPTER 7

CONCLUSIONS

7.1. INTRODUCTION

Genetic theories that ascribe the origin of sediment-hosted Pb-Cu-Zn deposits largely to deposition from basinal, connate water brines have become widely accepted over the past twenty five years. Beales & Jackson (1966) were among the first authors to propose that basinal fluids generated by diagenetic processes played a significant part in the formation of carbonate-hosted Pb-Zn deposits (Mississippi Valley-type deposits). The role of similar basinal fluids in the genesis of sediment-hosted copper deposits is more controversial (Rose 1976, Sverjensky 1987) because of the scarcity of fluid inclusion and stable isotope data.

The close association between Cu-Pb-Zn-U-V mineralisation and red beds is a common phenomenon in the Permo-Triassic sediments of Great Britain, Western Europe, Morocco and the southwestern U.S.A. The aim of this chapter is to compare the features of the ore deposits hosted by the Permo-Triassic red beds of Western Europe. A summary of the main characteristics of the mineralisation examined during this work is complemented by a discussion of the features of similar, well-documented deposits in Western Europe.

7.2 A REVIEW OF SIMILAR EUROPEAN DEPOSITS

Samama (1976) reviewed the distribution of Pb-Cu-Zn deposits in the Triassic sandstones of France and noted their common occurrence on the borders of ancient massifs. Examples of such deposits on the edge of the Massif Central include Pb-Zn mineralisation at Largentière (Fogliérini et al. 1980), Pb-Zn-Ba mineralisation in the Lower Triassic sandstones at Carnoulès (Alkaaby et al. 1985) and fluorite deposits hosted by Triassic, Hettangian and Sinemurian clastic sediments in the Morvan area of the Paris Basin (Soulé et al. 1980) (see Fig. 7.1).

The Largentière orebody is located on the southeastern border of the Hercynian Massif Central and is the largest of these deposits with reserves totalling 10 million tons of ore (3.8% Pb, 0.75% Zn, 80g/ton Ag; Fogliérini et al. 1980). The ores at Largentière are hosted by arkosic sandstones of the Buntsandstein which lie directly on Hercynian

basement rocks. The Triassic succession at Largentière varies in thickness from 200 to 250 m and comprises the Buntsandstein (Upper Anisian), overlain by clay-rich dolomites (Ladinian and Carnian), followed by a series of interbedded sandstones and dolomites (Carnian) (Figs. 7.2 and 7.3). The Triassic succession reaches a maximum thickness of over 1 km to the east, in the centre of the Southeast Basin of France. The sedimentary structures in the sandstone units of the Buntsandstein include ripple marks, cross-stratification, channelling, dessication cracks, reptile footprints, anhydrite nodules, and are consistent with deposition by fluvial processes on a coastal plain adjacent to a shallow marine basin (Samama 1976). Palaeocurrent data from foresets indicates that the sediments were derived from the Massif Central and were transported towards the southeast. The palaeogeographic setting of the host sediments at Carnoulès and Morvan is essentially similar, with the ores being hosted by fluvial and marginal marine sediments which accumulated on the border of shallow evaporitic basins in a semi-arid climate.

The ores at Largentière occur as impregnations in the sandstones and comprise galena, sphalerite, pyrite, chalcopyrite, freibergite, bournonite, jamesonite with quartz, fluorite and ankerite gangue (Bernard & Samama 1970). It has proved impossible to establish a paragenetic sequence for the sulphide cements and gangue phases, although authigenic quartz overgrowths appear to have formed contemporaneously with galena (see Fogliérini et al. 1980, p. 54). The precipitation of microcrystalline quartz is followed by the deposition of galena, sphalerite and pyrite, and finally, by widespread deposition of fluorite and barite cements in feldspathic sandstones at Antully, Morvan (Soulié et al. 1980). The principal sulphides at Carnoulès are galena, marcasite and pyrite. Barite is replaced and corroded by the sulphides and both barite and galena crystals occur as inclusions within authigenic quartz overgrowths (Alkaaby et al. 1985).

The orebodies at Largentière are aligned roughly parallel to the palaeocurrent directions (NW-SE), whilst the local faults trend N-S and have throws of ~100m in the Malets fault system (Fogliérini et al. 1980). The faults extending to the basement are mostly Tertiary in age and are generally normal with a minor strike-slip component. The fractures are often mineralised but there is no evidence for any movement along the faults after the mineralising event(s). The deposits in the Morvan area are located near faults

Figure 7.1 Map showing the location of the Triassic and Liassic sediment-hosted ore deposits in France. The majority of Pb-Zn and Ba-F deposits are situated on the margins of deep sedimentary basins adjacent to basement massifs such as the Massif Central.

FIGURE 7.1

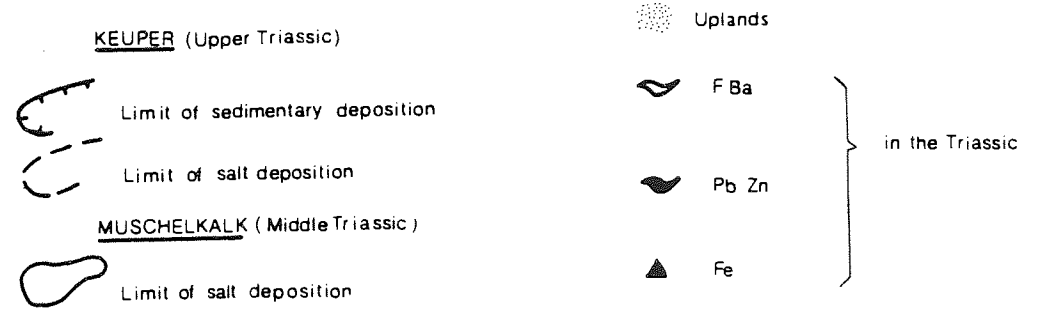
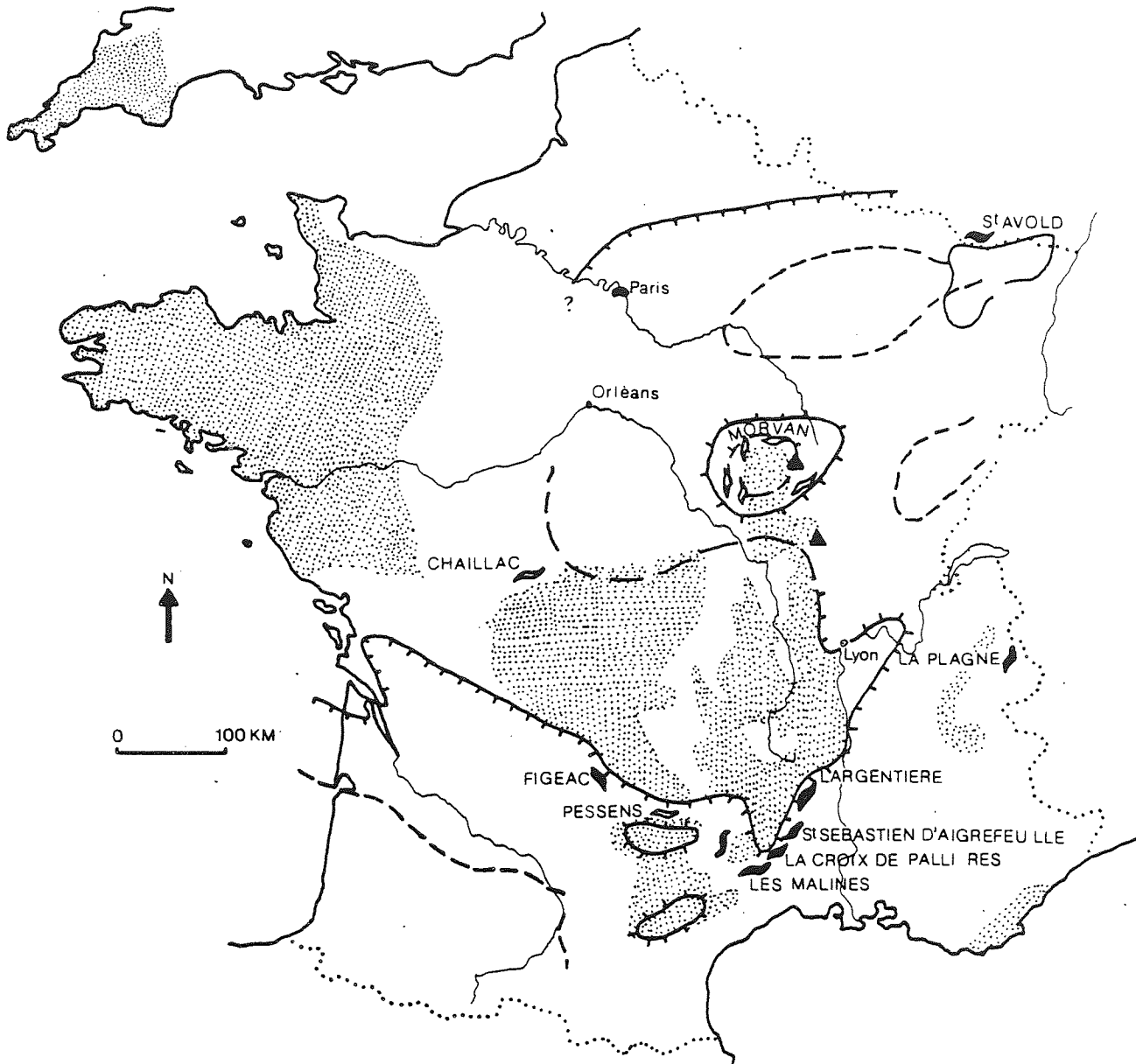


Figure 7.2 Isopach map of the Triassic succession in the southeastern basin of France showing the extent of the evaporite horizons and the location of the Largentiere orebody. (Adapted from Foglierini et al. 1980).

FIGURE 7.2

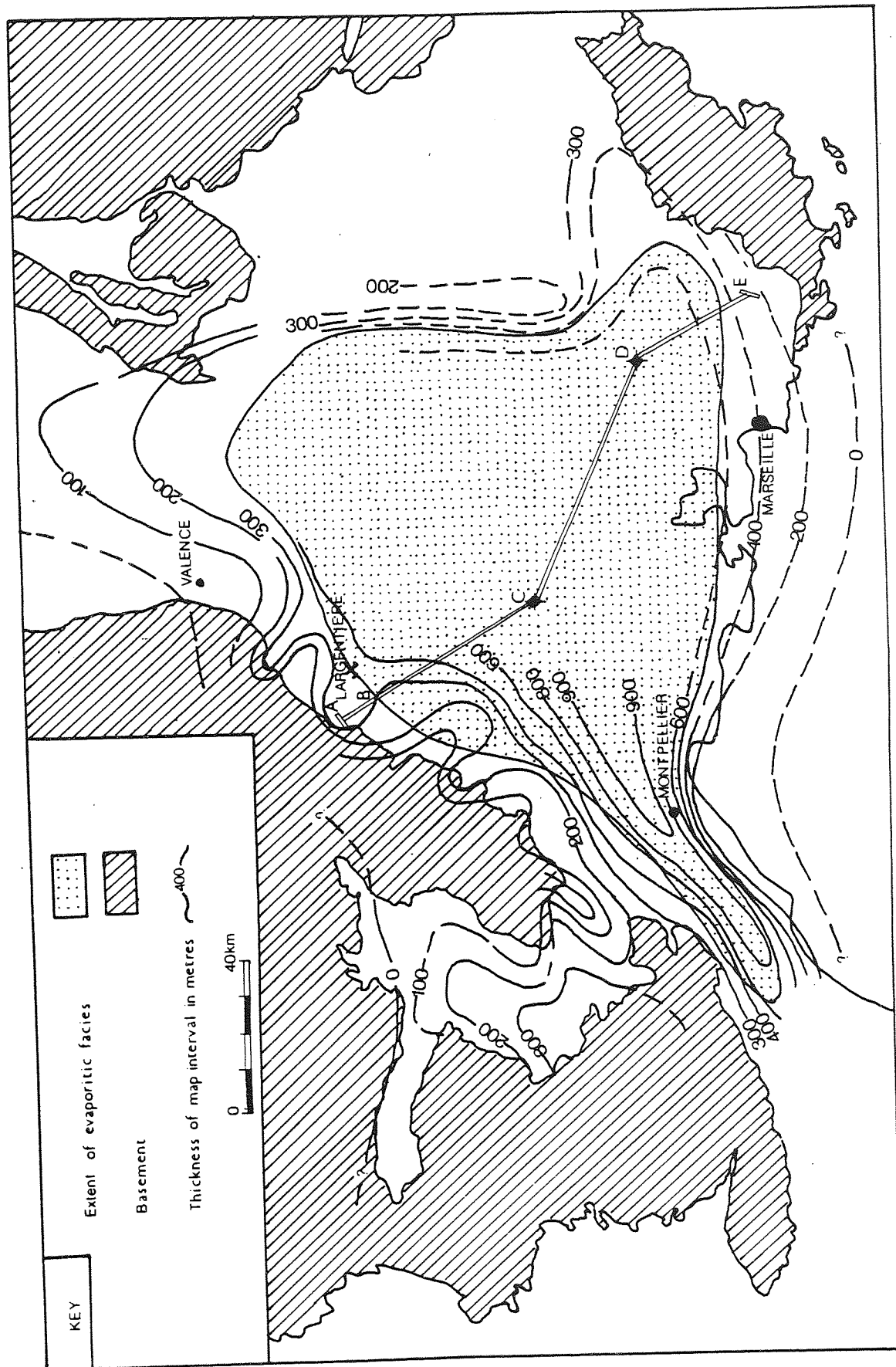
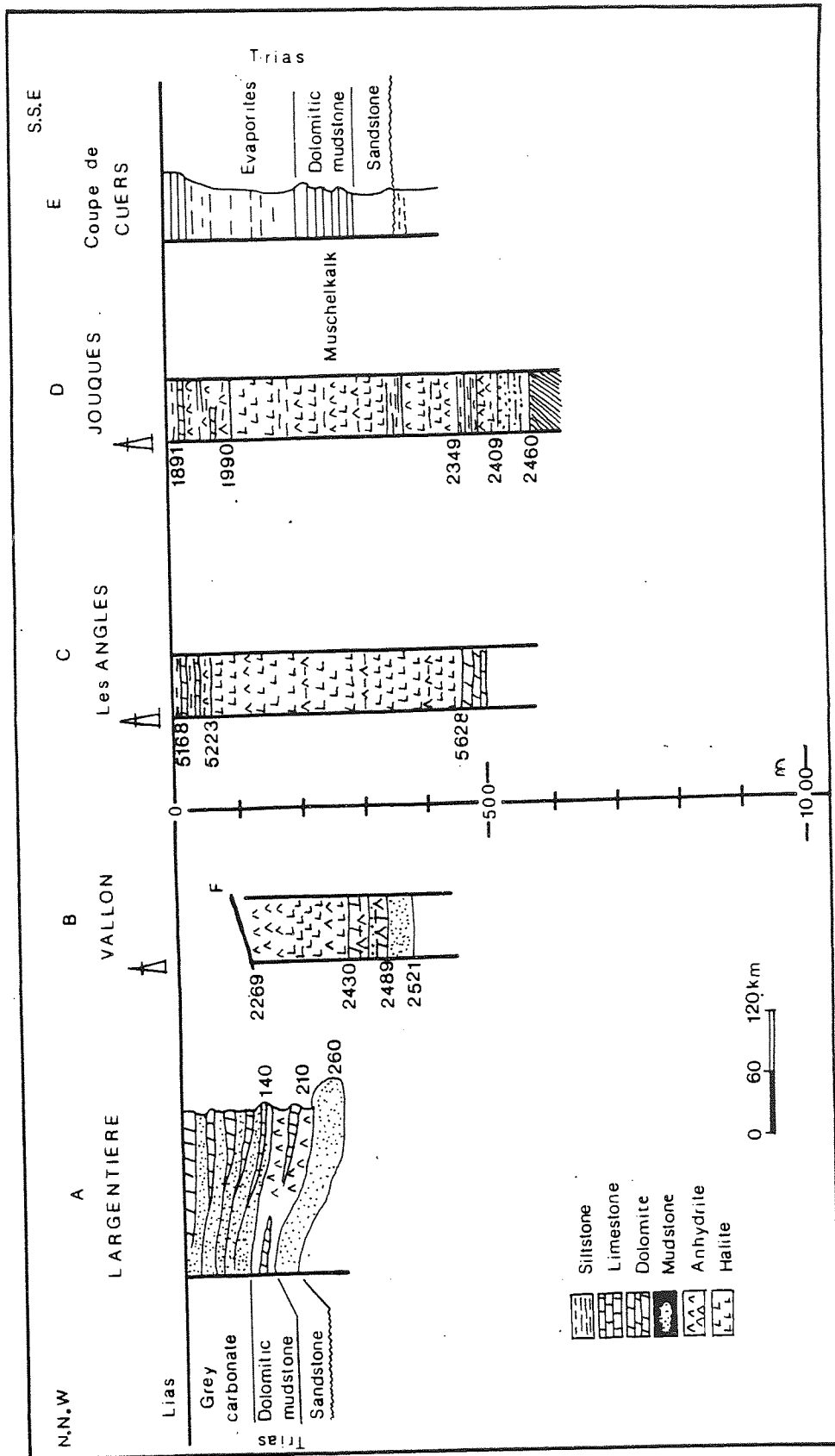


Figure 7.3 Cross section through the Triassic sediments in the southeastern basin of France showing the changes in thickness and facies across the basin. (The section AE corresponds to Figure 7.2). (Modified from Baudrimont & Dubois 1977).

FIGURE 7.3



but the faults themselves are not mineralised (Soulé et al. 1980).

Previous workers on the Largentière deposit have noted the elevated Pb-Zn-Ba contents of the unweathered Hercynian basement rocks to the northwest. This led Samama (1976) to suggest that crystalline rocks of the Massif Central were the source area for the heavy metals in the Largentière orebody. Soulé et al. (1980) noted that ores similar to those in the Mesozoic cover at Morvan, occur in the Hercynian basement nearby; as yet, no genetic relationship has been confirmed between the two types of deposit.

The genetic models proposed for the above deposits fall into two categories; Samama (1968) proposed that precipitation of metals occurred at the contact between continentally-derived groundwaters and marine waters at the edge of a shallow marine basin, followed by diagenetic remobilisation of the ores. Alkaaby et al. (1985) favoured a similar model for the genesis of the mineralisation at Carnoulès involving metal transport by continental meteoric waters, sulphur derived from evaporites and plant debris providing the local reducing environments. Soulé et al. (1980) suggested that basinal brines which leached fluorine and base metals from argillaceous horizons in the Paris basin were responsible for the formation of the deposits at Morvan. These models will be discussed further below.

Isolated occurrences of galena, barite, copper sulphides and oxidised copper minerals are common in the Permo-Triassic rocks of Central England (King 1968), but are seldom found in economic quantities. The mineralisation is similar in character to the Cheshire Basin deposits but the occurrence of sulphides and barite in the sandstones of the Mercia Mudstone Group in Leicestershire and Staffordshire indicate that the mineralisation is not restricted to the Sherwood Sandstone Group. The most significant concentrations of base metals occur in the basal Triassic conglomerates of Leicestershire (King 1968) which lie unconformably on Pre-Cambrian volcanics. Galena, chalcopyrite, sphalerite, bornite and djurleite occur as impregnations in the conglomerates and sandstones of the Mercia Mudstone Group and are accompanied by calcite, dolomite, barite and celestite gangue.

The geological setting of these deposits is poorly known due to the lack of exposures in Central England, however, the close association of hydrocarbons with galena and

barite mineralisation in the Bunter Pebble Beds (Sherwood Sandstone Group) at Swadlincote, Leicestershire suggests that these deposits formed in a similar manner to those in the Cheshire Basin. Theories for the genesis of the deposits in the English Midlands include the hypothesis favoured by Dunham (1934), who suggested that the mineralisation was merely a continuation of the epigenetic Hercynian mineralisation of the Pennine ore fields. An alternative model proposed by King (1968) involves the deposition of sulphides from shallowly circulating groundwaters.

Concentrations of rare elements in Permo-Triassic red beds have been reported from southwest England (Harrison 1975), northern Switzerland and Heligoland (northern Germany) (Hofmann 1986). These rare elements are enriched in the dark-coloured zones of the so-called 'reduction spots' and occur sporadically in bleached zones of red bed sequences. Vanadiferous nodules in red Permian (Zechstein ?) marls of south Devon were first documented by Carter (1931). The same author noted the occurrence of similar nodules in the Keuper Marl (Mercia Mudstone Group) of Sidmouth and in boreholes at Wells and Williton, Somerset. A more recent investigation of reduction spots in the Permian red beds of Devon, southwest England, revealed the presence of native copper and silver, bornite, chalcocite, chalcopyrite, covellite, niccolite, rammelsbergite, coffinite, vanadian mica and malachite (Harrison 1975). Hofmann (1986) reported the enrichment in the elements C, Mg, P, S, K, Ca, V, Cr, Mn, Co, Ni, Cu, Zn, As, Se, Mo, Pb, Ag, Sb, Te, Re, Au, Hg, Bi and U relative to the host red beds in a study of Permian (Oberrotliegendes) marls and sandstones in northern Switzerland. The most important minerals were found to be rammelsbergite, niccolite, coffinite and roscoelite. Harrison (1975) suggested that metalliferous solutions responsible for the ores in Devon were ultimately derived from 'deep-seated sources', whilst Hofmann (1986) proposed that diagenetic processes led to the accumulation of the ores in Switzerland.

7.3 COMPARISON OF THE CHARACTERISTICS OF THE DEPOSITS

7.3.1 ASSOCIATED METALS

Copper is widespread in the Cheshire Basin deposits and in the Permo-Triassic red beds of Devon, southwest England. Oxidised copper minerals such as malachite, azurite and chrysocolla form the bulk of the ores in the Cheshire Basin, whilst native copper,

copper sulphides, and uranium and vanadium oxides are associated with the so-called 'reduction spots' in Permian red mudstones and sandstones of south Devon (Harrison 1975). Minor amounts of Zn, Ag, Co, Ni, V, As, Sb and Mn are associated with the copper mineralisation in the Cheshire Basin. Carlon (1979) estimates that the deposits at Alderley Edge represent no more than 350,000 tons of ore (1.5-2% Cu).

Lead occurs in important concentrations in all the deposits examined; galena is a major constituent of the ores in the Inner Moray Firth Basin, at Maubach and Mechernich, West Germany and at Largentiere, France (Bernard & Samama 1970). The Pb-dominant deposits vary in size from 6 tons of lead ore in the Cherty Rock at Elgin, Inner Moray Firth Basin, to 225 million tons of ore at Mechernich. The ore grades at Mechernich are low (1.7% Pb, 1.3% Zn, 0.05% Cu; Hennecke 1977), and are typical of those in all the red bed-hosted deposits. Sulphides are rare at Freihung, Oberpfalz, where cerussite is the dominant ore mineral. The copper contents of the Pb-rich deposits are extremely variable, ranging from negligible (Inner Moray Firth Basin and Freihung) to 0.04% and 0.05% at Maubach and Mechernich respectively. Zinc is generally less abundant than lead but is present in all the deposits investigated here. Iron is associated with red bed-hosted deposits but pyrite and marcasite tend to be only minor components of the ore assemblage. The cobalt, nickel and arsenic contents are extremely variable, with little systematic variation evident. Data on metal zoning is scarce, but at Largentiere and Mechernich, an upward increase in zinc relative to lead has been noted (Bjørlykke & Sangster 1981).

Barite is commonly associated with red bed Cu-Pb-Zn deposits, particularly in the Cheshire and Inner Moray Firth Basins. Other gangue minerals include fluorite (Inner Moray Firth Basin, Largentiere), and carbonates (Cheshire Basin, Maubach, Mechernich and Largentiere). The precious metal content of all the deposits is low.

7.3.2 HOST LITHOLOGY AND REGIONAL STRATIGRAPHIC SUCCESSION

The mineralisation commonly occurs within, or immediately adjacent to, thick sequences of red coloured sandstones, mudstones and shales deposited in a continental or marginal marine environment. The haematite responsible for the red colouration is generally absent in the mineralised horizons. The age of the host rocks ranges from

Permian (Zechstein ?) in south Devon and Switzerland to Rhaetian in the Inner Moray Firth Basin. The major Pb-rich deposits of Maubach, Mechernich and Largentière are hosted by Buntsandstein sediments (Anisian).

The depositional environments in which the host sandstones accumulated include continental fluvial environments (Cheshire and Inner Moray Firth Basins, Maubach and Mechernich) and marginal marine environments (Oberpfalz and Largentière). This subdivision is somewhat arbitrary and it is perhaps more relevant to discuss the palaeogeographical setting for the deposition of the host rocks on a regional or basinwide scale. The mineralised horizons occur within relatively thin (< 500m) sedimentary sequences dominated by clastics, on the margins of deep sedimentary basins containing thick sequences of red beds, evaporites and minor carbonates. Regional seals for the mineralising fluids are present in several of the basins studied including the Cheshire Basin (Mercia Mudstone Group), Inner Moray Firth Basin (Jurassic shales), Morvan, Paris Basin (Jurassic shales) and at Largentière (clay-rich dolomites and siltstones). The Permo-Triassic basins described in this study vary in size from 25 km² (Nideggen Trough) to 19,200 km² (Southeast Basin, France). The thickness of sediments in these basins also varies considerably ; the Nideggen Trough contains only 300m of sediment, whilst the Permo-Triassic sediments in the Cheshire Basin reach thicknesses of 3.5-4 km. These observations demonstrate that the size of the ore deposit bears no relation to either the present size of the associated sedimentary basin or to the present day thickness of the basin-fill.

Local stratigraphical controls on the distribution of the mineralisation are evident in all the deposits studied. The Cu-Pb-Zn ores in the Cheshire Basin occur within porous sandstones and conglomerates, especially where these are overlain by, or faulted against, mudstone horizons so as to form locally significant stratigraphic traps. This is also observed at Largentière (Fogliérini et al. 1980) and in the Morvan area (Soulé et al. 1980) and is thought to reflect the ponding of mineralising fluids beneath impermeable horizons.

A characteristic feature of these deposits is the occurrence of ores in grey or white horizons within a predominantly red succession. Detrital and authigenic iron oxides are

responsible for the red colouration and textural evidence indicates that the white colour of the mineralised horizons is a secondary feature formed as a result of leaching of iron by reducing groundwaters (Turner 1980). However, the close association between the reduced horizons and the sulphide mineralisation suggests that either the processes responsible for sulphide deposition or the mineralising fluids themselves, caused bleaching of the host sandstones. Sulphate reduction generates weak acidic solutions which are capable of removing iron oxides from sandstones adjacent to the ore-bearing horizons.

Bjørlykke & Sangster (1981) noted the association between sialic basement and the occurrence of 'sandstone lead deposits' such as Largentière, in the overlying quartz-rich sandstones. The Pb-rich deposits in the Oberpfalz and the mineralised horizons at Largentière are located on the borders of Hercynian basement massifs. Furthermore, Samama (1976) showed that the basement rocks at Largentière are enriched in lead (mean Pb content = 45 ppm) relative to the average enrichment (23 ppm) cited by Wedepohl (1978) for granitic rocks. The presence of a crystalline basement with elevated base metal contents is clearly not a prerequisite for the formation of Cu-Pb-Zn red bed-hosted deposits, as the mineralisation in the Cheshire Basin occurs in a thick red bed sequence underlain by Carboniferous Coal Measures. In addition, the deposits in the Inner Moray Firth Basin and in the Eifel Mountains of West Germany show no affinity to crystalline basement rocks.

7.3.3 SULPHIDE PARAGENESIS

The deposition of early sulphides commonly coincides with the precipitation of authigenic quartz overgrowths. Early haematite, pyrite, chalcopyrite and bravoite are often enclosed within euhedral quartz overgrowths in the mineralised sediments of the Cheshire Basin, at Maubach and Mechernich, whilst at Largentière, galena appears to have precipitated contemporaneously with quartz overgrowths.

The main sulphide cements postdate the formation of euhedral quartz and feldspar overgrowths in the red bed-hosted deposits. Bravoite and pyrite are the first sulphides to precipitate, followed by chalcopyrite, sphalerite, bornite and galena. Rarer minerals include tetrahedrite-tennantite, freibergite, jamesonite, bournonite, gersdorffite and Fe, Ni, Co sulpharsenides. This primary assemblage has undergone significant alteration to

secondary copper sulphides (covellite, djurleite etc.) and carbonates and sulphates of copper, lead and zinc.

The timing of gangue phases relative to the timing of sulphide precipitation varies between deposits. At Maubach and Mechernich, the dolomite gangue precedes the deposition of the main sulphide cements, whereas calcite gangue at Bickerton, Cheshire, formed after sulphide cements.

7.3.4 TECTONIC SETTING

The ore occurrences described in this study are to a certain extent, controlled by regional structure. Most of the deposits are located on, or near, the faulted margins of sedimentary basins where compaction-driven updip migration of brines is likely to have occurred. The assignment of the Oberpfalz deposits to this general tectonic setting is problematical because weathering and modern groundwaters have caused a redistribution of the primary sulphides.

Cathles & Smith (1983) pointed out that simple basin dewatering cannot explain the origin of similar basin edge Mississippi Valley-type Pb-Zn deposits which are thought to form at elevated temperatures (100 to 150 °C) and at reasonably shallow depths (Anderson & MacQueen 1982). The model devised by Cathles & Smith (1983) involves episodic expulsion of brines and pore fluids up a steep-sided, tectonically stable basin margin. According to Cathles & Smith (1983), basin characteristics conducive to the formation of lead-zinc deposits include abundant complex shale units, stable, steep-sided margins to allow multiple fluid pulses to deposit metals at the same locality, a thin, highly permeable basal aquifer and finally, structures capable of directing dewatering fluids to restricted sections of the basin margin. This model may be relevant to the European Permo-Triassic basins described here; the Cheshire Basin, for example, meets some of the criteria for the basin brine expulsion model. The Cheshire Basin has thick complex shale and mudstone units in the Mercia Mudstone Group and is bounded by deep fault systems which are thought to have been responsible for channelling ore solutions to sections of the steep-sided basin margins. Both the Inner Moray Firth Basin and the Southeast Basin of France meet the criteria defined by Cathles & Smith (1983). However, neither the Nideggen Trough nor the Oberpfalz Basin appear to be deep enough to develop sufficiently warm basinal brines and also lack steep-sided basin

margins. It is possible that Tertiary inversion in these areas has resulted in the removal of huge volumes of sediment, and that the present-day geological setting of these basins bears no resemblance to the environment in which the ores accumulated.

Bethke (1985) argued that gravity-driven groundwater flow from deep basins is an attractive alternative explanation for the means by which warm/hot basinal fluids were introduced into shallow basin margin sediments without significant heat loss.

7.3.5 ASSOCIATION WITH EVAPORITES

The majority of red bed-hosted Cu-Pb-Zn deposits are closely associated with evaporites. The evaporites of the Zechstein (Inner Moray Firth), Upper Triassic (Cheshire) and Muschelkalk (Eifel, Oberpfalz) are all important potential sources of sulphur and for the high salinities required for metal mobilisation at the relatively low temperatures indicated by fluid inclusion studies.

The mineralised horizons in the Inner Moray Firth Basin and at Largentière occur in clastic sequences which are underlain by, or are laterally equivalent to, thick evaporite sequences in the basin centre. The Zechstein evaporites of the Inner Moray Firth Basin comprise anhydrite, gypsum and dolomite facies and reach thicknesses of 200 m (Taylor 1984), whereas Triassic evaporites in the Southeast Basin of France attain thicknesses in excess of 500m in the basin centre. The Cheshire Basin and Maubach and Mechernich deposits have a more distant association with evaporites. The evaporite-bearing horizons of the Mercia Mudstone Group in the Cheshire Basin are thick (600 m), and are structurally lower than the ore-bearing horizons in the Sherwood Sandstone Group (see Fig. 2.3), as a result of basin inversion in the Tertiary. In contrast, in the Eifel region of West Germany, the mineralised horizons in the Middle Buntsandstein lie below the evaporite-bearing Muschelkalk.

7.3.6 ASSOCIATION WITH ORGANIC MATTER AND HYDROCARBONS

Numerous authors have remarked on the close association between terrestrial organic carbonaceous debris and red bed Cu deposits (Stanton 1972). However, the mineralised horizons in the European deposits are invariably bleached sandstones which contain little or no evidence for the presence of organic terrestrial material or hydrocarbons.

Exceptions include the Oberpfalz deposits in which sulphides have replaced wood cells

and the deposits at Carnoulès where vegetational debris is recorded (Alkaaby et al. 1985). The occurrence of organic matter in the Triassic red bed-hosted deposits of Western Europe has not been documented, but this may simply reflect the fact that any organic material present prior to, and during, the deposition of sulphides has subsequently been destroyed.

The role of hydrocarbons in the genesis of red bed copper deposits remains to be assessed, but hydrocarbons may have played a significant part in the formation of the Cheshire Basin deposits (see Chapter 2). Potential hydrocarbon source rocks are associated with the Cheshire and Inner Moray Firth Basins, as well as the basins of Central and southwest England where isolated deposits of copper are found (Harrison 1975). Methane derived from the Carboniferous Coal Measures, may have been responsible for the reduction of sulphate to form sulphides in the Cheshire Basin. The organic-rich shales of the Kimmeridgian Clay Formation of the Inner Moray Firth Basin may be potential sources of base metals and sulphur for the mineralisation in the Elgin sandstones.

7.3.7 ASSOCIATION WITH VOLCANIC ACTIVITY

The absence of evidence for post-Triassic magmatic activity and obvious feeder vein systems was noted in all the sedimentary basins described here. Gustafson & Williams (1981) used the lack of an association with igneous activity as the principal criterion for distinguishing Pb-Cu-Zn sediment-hosted stratiform deposits from massive stratiform Cu-Pb-Zn deposits associated with volcanic rocks.

7.3.8. TIMING OF THE MINERALISATION

Textural investigations of the ores and their host sediments indicate that the ores were precipitated from mineralising fluids passing through the sediments after the deposition of the detrital sand grains. Paragenetically early sulphides such as pyrite and bravoite were deposited during authigenic quartz and feldspar overgrowth formation. The early diagenetic features in modern red alluvium include the development of overgrowths of authigenic quartz and K-feldspar (Walker et al. 1978), and are closely comparable to the eodiagenetic changes in the Permo-Triassic sandstones of the Cheshire and Inner Moray Firth Basins and Nideggen Trough (see Chapters 3, 4 and 6). Quartz and K-feldspar authigenesis appears to have occurred prior to significant burial

compaction and it therefore seems likely that the sulphides enclosed within the overgrowths were precipitated during shallow burial of the host sediments. Furthermore, the lack of deformation in the wood cells replaced by the sulphides in the Oberpfalz is seen as evidence for the early emplacement of pyrite, sphalerite and galena.

The bulk of the ores were precipitated from mineralising fluids which were introduced into the host sediments at a later stage, during burial diagenesis, as the main sulphide cements clearly postdate the formation of euhedral quartz and feldspar overgrowths.

The precise timing of the mineralisation relative to tectonic events in the Permo-Triassic basins remains conjectural, as the post-Triassic histories of these basins is poorly documented. The ore deposits appear to have formed after, or during, the movement of the basin margin faults. The lack of brecciation in the mineralised faults and fractures in the Cheshire and Inner Moray Firth Basins and at Largentière, suggests that the ^{sulphide} mineralisation postdates most of the faulting in these areas. An alternative explanation favoured by Samama (1969) for the ores at Largentière is that the sulphides in the fractures simply reflect a remobilisation of the primary ores. In the Maubach and Mechernich deposits, faults are seen to displace the orebodies (Behrend 1948) and slickensides were observed on the ore surfaces (see Chapter 6).

A modified version of the model proposed by Cathles (1986) for the genesis of basin-edge shale-hosted massive sulphide deposits may be relevant to this discussion. McKenzie (1978) suggested that sedimentary basin evolution occurs in two stages in which the crust and underlying lithosphere are stretched and thinned and a second thermal stage when the thickness of the lithosphere returns to normal and is accompanied by further subsidence. Cathles (1986) attempted to relate the formation of basin edge shale-hosted massive sulphide deposits to the late tectonic stage of basin development and envisaged listric faults acting as channels for the mineralising fluids flowing towards the basin margin. The European Permo-Triassic basins described in this study are thought to have developed in a similar manner to that described by McKenzie (1978) and it is possible that some of the ores hosted by red beds were formed during the late tectonic stage of sedimentary basin evolution.

The European Permo-Triassic basins were subject to considerable uplift and erosion

as a result of the Alpine orogeny which climaxed in the Mid-Tertiary (Ziegler 1982). The uplift in the Cheshire Basin can be inferred by comparison with the adjacent East Irish Sea Basin where vitrinite reflectance data indicate up to 2 km of uplift (Colter 1978). Reactivation of previously extensional faults accompanied basin inversion in the Cheshire Basin and it seems likely that warm basinal fluids were expelled from the basin and ascended faults during, and after, the Tertiary inversion. Cathles & Smith (1983) note that sudden rupture can result in the rapid expulsion of fluids into near-surface environments without significant heat loss. On the basis of the evidence presented above, it is not possible to determine the exact timing of ore deposition; however, it is interesting to speculate on the importance of the compressional stresses and basin inversion in the genesis of European red bed-hosted Cu-Pb-Zn deposits.

A fundamental question posed by Ohle (1980), in his review of Mississippi Valley-type lead-zinc deposits, concerns the timing of metal mobilisation relative to the diagenetic processes operating in the basin sediments. Were the base metals mobilised early in the basin history when most of the pore waters were expelled? Alternatively, did the fluids released during burial diagenesis (eg. during the illite-smectite transition) play a major part in the genesis of the ores? These possibilities will be discussed further below (see section 7.4.2).

7.3.9 TEMPERATURE OF SULPHIDE DEPOSITION

The lack of direct temperature constraints for sulphide deposition reflects the fact that the deposits are characterised by fine-grained ores and gangue phases which are difficult to study using fluid inclusion and stable isotope techniques. Fluid inclusion studies on the quartz gangue at Elgin, Inner Moray Firth, provide the only information concerning the temperature of sulphide precipitation. Homogenisation temperatures range from 94.8 to 139.0 °C (mean 114.8 °C) and provide minimum estimates of the temperature of trapping and galena precipitation in the Cherty Rock horizon. Calcite-hosted fluid inclusions in the Cheshire Basin yield homogenisation temperatures averaging 69.0°C, but textural studies showed calcite precipitation to have followed the main phase of ore deposition.

Despite the scarcity of fluid inclusion data, generalisations can be made about the temperature of ore deposition from the knowledge of the geological setting of the

orebodies, the sulphide mineral assemblages and the sulphur isotope characteristics of the sulphides and sulphates. The location of the ores in shallowly-buried clastic sequences on the margins of sedimentary basins and the absence of hydrothermal alteration are consistent with the suggestion that the ores were precipitated at reasonably low temperatures ($< 200^{\circ}\text{C}$). This is confirmed by the similarity between the mineralogy of the host rocks and adjacent unmineralised sandstones, with the exception of the ore minerals. Ixer & Vaughan (1982) made tentative estimates for the temperature and sulphur activity at which sulphide deposition took place at Alderley Edge, Cheshire (60°C and 10^{-29} atm respectively). These values were obtained by examining the intersection of sulphidation curves for sphalerite containing 0.1 mol% FeS with that defining the pyrite-pyrrhotite fields (Vaughan & Craig 1978).

The application of sulphur isotope geothermometry to the red bed-hosted deposits is limited by the fact that sulphur isotope equilibrium was not established between coexisting sulphides nor between coexisting sulphides and sulphates. Assuming that the mineral phases were in equilibrium during ore deposition and that no isotopic exchange has taken place after the formation of the minerals, then the sulphur isotope disequilibrium characteristic of these deposits may provide a minimum estimate of the temperature of sulphide deposition. Data on sulphur isotope exchange kinetics (Ohmoto & Lasaga 1982) suggest that at temperatures below $\sim 100^{\circ}\text{C}$ isotopic equilibrium between sulphide and sulphate is unlikely to be established within a geologically reasonable time period. Ohmoto & Lasaga (1982) note that in seawater which contains 2.8×10^{-2} m total sulphur and $\text{pH} = 8.1$, it would take approximately 10^{-19} years to reach equilibrium.

The fluid inclusion measurements, the unaltered nature of the host sediments and the sulphur isotope geothermometry suggest that temperatures during ore deposition ranged from $60\text{-}200^{\circ}\text{C}$, but were most probably between $100\text{-}150^{\circ}\text{C}$.

7.3.9 SULPHUR ISOTOPE CHARACTERISTICS

The principal features of the sulphur isotope data are as follows;

- 1) The $\delta^{34}\text{S}$ values for barite in the Cheshire Basin and in the Oberpfalz correspond closely to those in associated Triassic evaporites (Fig. 7.4). This suggests that the majority of the barite sulphur was sourced from these evaporite horizons. In contrast, δ

^{34}S barite in the Inner Moray Firth Basin are consistently heavier than those expected for Permian or Triassic evaporites.

2) Sulphur isotopic equilibrium was not established by co-existing sulphides in the Cheshire and Inner Moray Firth Basins. The low temperatures of ore formation (100-150°C) are thought to be responsible for this phenomenon.

3) The spread of $\delta^{34}\text{S}_{\text{sulphide}}$ values within individual deposits varies from 18‰ (Cheshire Basin) to 31.8‰ (Inner Moray Firth Basin). In both these areas, the highest value of sulphide $\delta^{34}\text{S}$ corresponds to the lower values obtained for barite (Fig. 7.4). Thus the distribution patterns for the sulphides are compatible with a mechanism whereby sulphide was derived from sulphate by means of sulphate reduction processes (Ohmoto & Rye 1979).

The $\delta^{34}\text{S}$ values for sulphides in the German deposits are strongly negative, with sulphur isotopic compositions ranging from -20 to -40 ‰ in the Oberpfalz (v. Gehlen 1966) and between -12 and -27‰ in the Eifel region (Bayer et al. 1970). These values are suggestive of a bacteriogenic source for the sulphide sulphur (v. Gehlen & Nielsen 1985). Preferred models for the genesis of these Pb-rich deposits involve precipitation of sulphides via bacteriogenic reduction of sulphate-bearing fluids whose initial sulphur isotope composition was approximately +20‰ (see Chapter 6).

4) The substantial variation in $\delta^{34}\text{S}$ between the deposits in Britain and Germany may be related to differences in the isotopic composition of the source and to the fractionation effects during the formation of the minerals, but may also reflect changes in the supply of sulphate to the site of ore deposition.

7.3.10 SUMMARY

The Cu-Pb-Zn mineralisation in the Permo-Triassic sediments of Western Europe shows a distinct association with thick sequences of red beds and evaporites. The spatial distribution of the mineralisation is largely controlled by proximity to basin-edge fault systems and, on a local scale, is dependent on the permeability of the host sediments. The geographical and structural location of the deposits in the Cheshire and Inner Moray Firth Basins (Chapters 2 and 4), on the margins of deep sedimentary basins containing

pore fluids are expelled during shallow burial. However, Boles & Franks (1979) demonstrated that the depth-related conversion of smectite to illite is responsible for the transportation of considerable quantities of dissolved ionic species from mudrocks into adjacent sandstones.

The sulphate-rich evaporites which are present in all the sedimentary basins examined, are the likely source of the barite sulphur. This was confirmed by the sulphur isotope data from the Cheshire Basin and the Obepfalz where the $\delta^{34}\text{S}$ values for barite are closely comparable to the $\delta^{34}\text{S}$ values for the evaporites and Triassic seawater respectively. The barite sulphur in the Inner Moray Firth Basin is somewhat anomalous as it is isotopically heavier than the associated Zechstein evaporites. This inconsistency is thought to result from sulphate reduction processes operating in the evaporite-bearing horizons of the Inner Moray Firth Basin.

It is proposed that red beds, with their high metal contents in associated iron oxides, ferromagnesian grains and feldspars, in conjunction with evaporite sequences, are likely sources of the metals and sulphur found in the basin margin deposits. Other possible contributors of metals, and to a lesser extent, sulphur, include the Carboniferous Coal Measures beneath the Cheshire Basin and the sulphur-rich Jurassic shales of the Inner Moray Firth Basin.

7.4.2 CHARACTERISTICS OF THE ORE FLUIDS

Fluid inclusion analyses have provided important information on the characteristics of the mineralising fluids in the Cheshire and Inner Moray Firth Basins. Microthermometric studies have shown that the mineralising solutions were warm (60-150°C) and fluid inclusion salinities fall in the range 9 to 22 wt% equiv NaCl, with NaCl as the dominant salt. These data and the close association of the deposits with basin margins, provide strong evidence that the red bed-hosted deposits formed from warm, saline brines derived from the associated sedimentary basin. Development of the high salinities is thought to result from the interaction of the ore fluids with evaporites. Genetic hypotheses involving groundwater as the dominant ore solutions can be effectively discounted in the light of fluid inclusion microthermometric data.

The mineralising fluids in the Cheshire Basin are suggested to have been

sulphate-rich chloride brines that were mildly alkaline and in equilibrium with haematite, quartz, feldspar, illite and carbonate. Metals such as Cu, Pb and Zn are thought to have been transported as chloride complexes. Rose (1976) proposed that brines of a similar composition were probably associated with the formation of other red bed copper deposits.

It is not clear whether the deposits in the Inner Moray Firth Basin are products of similar brines. The Pb-rich nature of the mineralisation, the association of the ores with a carbonate horizon and the presence of black shales in the basin suggest that the ore fluids were more similar to those responsible for the formation of Mississippi Valley-type deposits. The mineralising fluids are likely to have been low pH fluids which transported base metals, Ba, F and reduced sulphur to the site of ore deposition. Barrett & Anderson (1982) and Sverjensky (1984) demonstrated that basinal brines, analagous to modern oil field brines are only able to transport sufficient quantities of base metals and sulphur to form an ore deposit if the pH is significantly lower than neutral.

Bjørlykke & Sangster (1981) presented a genetic model for the Triassic sandstone-hosted Pb deposits (eg. Maubach, Mechernich and Largentière) involving metal transport by oxidising groundwaters. The genetic model proposed by Samama (1969) was based largely on his observations at Largentière and involves the release of metals into saline groundwaters during extensive weathering of the basement. These authors envisaged sulphide precipitation occurring when the groundwaters encounter a reducing environment produced by the accumulation of organic matter, or when they come into contact with sulphate-rich pore waters in a marginal marine environment. Unfortunately, no fluid inclusion data are available for these deposits and it has not been possible to establish the exact nature of the mineralising fluids.

The nature of the mineralising fluids in these red bed Cu-Pb-Zn deposits clearly requires further investigation. The experimental studies of Rose (1976) and Sverjensky (1984, 1987) need to be extended if we are to unravel the uncertainties surrounding the characteristics of the ore solutions. At present, the pH, oxidation state and contents of trace metals and sulphur in the mineralising solutions responsible for the red bed-hosted deposits remains uncertain, although the fluids are clearly capable of silicifying the host rock and may have caused the bleaching in the mineralised horizons.

7.4.3 PRECIPITATION MECHANISMS FOR THE ORES

New sulphur isotope data presented in this study have contributed greatly to the understanding of the mechanisms of sulphide formation in red bed-hosted Cu-Pb-Zn deposits. The association of evaporites with the mineralisation lends credence to the idea that evaporite sulphate is the major source of sulphide in the red bed deposits. Potential mechanisms whereby sulphide is produced include bacterial sulphate reduction and thermochemical reduction of sulphate by hydrocarbons. Experimental evidence shows that bacteriogenic sulphate reduction is restricted to temperatures less than 100°C, whilst abiological sulphate reduction by hydrocarbons has only been demonstrated at higher temperatures (200-250°C) (Trudinger et al. 1985). The red bed Cu-Pb-Zn deposits appear to have formed at moderate temperatures (60-200°C), thus the role of each of these mechanisms in the formation of sulphide in these deposits can only be inferred, in view of the limited and controversial experimental data.

The distribution of $\delta^{34}\text{S}$ sulphide values in the Cheshire basin are interpreted as indicating that sulphate reduction is the principal sulphide precipitation mechanism. The $\delta^{34}\text{S}$ sulphide values range from -1.8‰ to +16.2‰, with the highest value similar to the $\delta^{34}\text{S}$ values obtained for barite. The spread of $\delta^{34}\text{S}$ values and the geological setting of the deposits are consistent with closed system reduction of sulphate to form sulphide by hydrocarbons or by bacteriogenic processes. Methane, sourced from the Carboniferous Coal Measures, may have been responsible for sulphate reduction in the Cheshire Basin. Indeed, the pattern of $\delta^{34}\text{S}$ values is more consistent with this suggestion (see Figs. 7.4 and 2.8).

The isotopic differences between the sulphate and sulphide ($\Delta \text{SO}_4\text{-H}_2\text{S} \sim 30$ to 40‰) observed at Mechernich and Maubach and in the Oberpfalz are 'typical' of the distribution of sulphur isotope values generated by closed system reduction of sulphate by bacteria (Ohmoto & Rye 1979). The $\Delta \text{SO}_4\text{-H}_2\text{S}$ reflects the kinetic isotope fractionation associated with bacteriogenic sulphate reduction, which is related to the rate of sulphate reduction, which, in turn is controlled by the rate of supply of nutrient to the sulphate-reducing bacteria.

Interpretation of the sulphur isotope data from the Inner Moray Firth (Chapter 4) has been hampered by the lack of geologic, geochemical and mineralogical data from the basin sediments. If the mineralising fluids were reducing metal-H₂S-bearing brines, possible sulphide depositional mechanisms include a fall in temperature, dilution by groundwaters, or reaction with carbonate. Alternatively, sulphate reduction may have been important if the mineralising fluids were oxidising and sulphate-bearing.

7.5 SUGGESTIONS FOR FURTHER RESEARCH

This study has emphasised the need for an integrated approach to research on sediment-hosted ore deposits. Detailed geological studies are required to establish the sedimentological and structural development of the sedimentary basin in which the ore bodies are situated. A knowledge of the diagenetic history of the host lithology and associated sediments is vital. Geochemical and mineralogical data, such as texture, paragenesis, trace element and phase relations of ore minerals, radiogenic isotope compositions and fluid inclusions must be supplemented by sulphur isotope analyses. Careful application of stable isotopes to the study of sediment-hosted ore deposits can contribute greatly to our understanding of the processes of ore formation. Finally, this programme of research must take place on a basin-wide scale if we are to fully appreciate the importance of sedimentary processes in ore formation.

Suggestions for further research in each of the study areas are outlined in Table 7.1.

TABLE 7.1 Suggestions for further research in the study areas

Study area	Ideas for further research
Cheshire Basin and Central England	<p>1. Detailed structural studies to establish a) the timing of the faulting episodes and their relationship to the mineralisation b) the burial history of the sediments in various parts of the basin.</p> <p>2. More fluid inclusion microthermometric studies on gangue phases supplemented by geochemical analyses to help determine the nature of the mineralising fluids.</p> <p>3. $\delta^{18}\text{O}$ analyses and fluid inclusion microthermometry of sulphide-bearing quartz overgrowths to constrain the characteristics of the fluids from which they precipitated.</p> <p>4. $\delta^{13}\text{C}$ analyses of calcite cements to see whether they formed as a result of methanogenesis.</p>
Inner Moray Firth Basin	<p>1. A basinwide sedimentological study is necessary in order to establish the exact nature of the offshore sediments.</p> <p>2. Textural and geochemical studies of the basin sediments may shed some light on the mechanisms of ore genesis in the basin.</p> <p>3. Sr isotope studies on fluorite and barite may help to resolve the problem of their origin (Ruiz et al. 1988. and references therein).</p> <p>4. Mass balance calculations to determine the scale of K-feldspar dissolution needed to account for the volumes of barite and lead in the basin margin deposits.</p>
Cherty Rock, Lossiemouth	<p>1. Application of carbon and oxygen stable isotopes to other ancient calcretes with emphasis on isotopic variations with depth and cement type.</p>
Triassic basins of West Germany	<p>A more detailed study of the geological setting of the deposits is required to constrain ideas on their genesis and to provide a background for further geochemical studies.</p>
Largentière	<p>A sulphur isotope analysis of gypsum, barite and sulphides to confirm that the evaporites were the principal sulphur source; the distribution of $\delta^{34}\text{S}$ values may help to constrain ideas on the mechanism(s) of sulphide precipitation. Fluid inclusion studies on fluorite and other gangue phases to increase the knowledge of the nature of the mineralising fluids.</p>

REFERENCES

- ALKAABY, A., LEBLANC, M. & PÉRISSOL, M. 1985. Mineralisation diagenétique précoce (Pb-Zn-Ba) dans un environnement détritico continental: cas du Tiras de Carnoulès (Gard, France). *Comptes Rendu Académie Sciences Chimiques Paris*, **18**, 919-922.
- ANDERSON, G.M. & MacQUEEN, R.U. 1982. Ore deposits-models 6, Mississippi Valley lead-zinc deposits. *Geoscience Canada*, **9**, 108-117.
- BARRETT, T.J. & ANDERSON, G.M. 1982. The solubility of sphalerite and galena in NaCl brines. *Economic Geology*, **77**, 1923-1933.
- BAUDRIMONT, A.F. & DUBOIS, P. 1977. Un bassin mésogéen du domaine péri-alpin: le Sud-Est de la France. *Bulletin Centres Recherches Exploration Production, Elf, Aquitaine*, **1**, 261-308.
- BAYER, H., NIELSEN, H. & SCHACHNER, D. 1970. Schwefelisotopenverhältnisse in sulfiden aus Lagerstätten der Nordeifel im Raum Aachen-Stolberg und Maubach-Mechernich. *Neues Jahrbuch für Mineralogie Abhandlungen*, **113**, 251-273.
- BEALES, F.W. & JACKSON, S.A. 1966. Precipitation of lead-zinc ores in carbonate reservoirs as illustrated by Pine Point ore field, Canada. *Transactions of the Institute of Mining and Metallurgy*, **75**, B278-285.
- BERNARD, A. & SAMAMA, J.C. 1970. Essai méthodologique sur la prospection des 'red beds' pombo-zincifères. *Sciences de la Terre*, **15**, 207-264.
- BETHKE, C.M. 1985. A numerical model of compaction-driven groundwater flow and heat transfer and its application to the paleohydrology of intracratonic basins. *Journal of Geophysical Research*, **90**, 6817-6828.
- BJØRLYKKE, A & SANGSTER, D.F. 1981. An overview of sandstone lead deposits and their relation to red-bed copper and carbonate-hosted lead-zinc deposits. *Economic Geology 75th Anniversary Volume*, 179-213.
- BOLES, J.R. & FRANKS, S.G. 1979. Clay diagenesis in Wilcox Sandstones of southwest Texas: implications of smectite diagenesis on sandstone cementation. *Journal of Sedimentary Petrology*, **49**, 55-70.
- CARTER, G.E.L. 1931. An occurrence of vanadiferous nodules in the Permian beds of South Devon. *Mineralogical Magazine*, **22**, 609-613.

- CATHLES, L. M. 1986. A tectonic/hydrodynamic view of basin-related mineral deposits. In: TURNER, R.J.W. & EINUADI, M.T. (eds) *The Genesis of Stratiform Sediment-Hosted Lead Zinc Deposits*. Conference Proceedings. Stanford University Publications in the Geological Sciences vol. XX.
- CATHLES, L.M. & SMITH, A.T. 1983. Thermal constraints on the formation of Mississippi Valley-type Pb-Zn deposits and their implications for episodic basin dewatering and deposit genesis. *Economic Geology*, **78**, 983-1002.
- COLTER, V.S. 1978. Exploration for gas in the Irish Sea. *Geologisch en Mijnbouw*, **57**, 503-516.
- DUNHAM, K.C. 1934. Genesis of the North Pennine ore deposits. *Quarterly Journal of the Geological Society of London*, **90**, 689-720.
- FOGLIÉRINI, F., SAMAMA, J.C. & REY, M. 1980. *Le gisement stratiforme de Largentière (Ardèche)*. Publications du 26^e Congrès Géologique International, Paris.
- GEHLEN, K.von. 1966. Schwefel-Isotope und die Genese von Erzlagestätten. *Geologisches Rundschau*, **55**, 178-197.
- GEHLEN, K. von. & NIELSEN, H. 1985. Sulphur isotopes and the formation of stratabound lead-bearing Triassic sandstones in northeastern Bavaria. *Geologisches Jahrbuch*, **70**, 213-233.
- GUSTAFSON, L.B. & WILLIAMS, N. 1981. Sediment-hosted stratiform deposits of copper, lead and zinc. *Economic Geology 75th Anniversary Volume*, 139-178.
- HARRISON, R.K. 1975. Concretionary concentrations of the rarer elements in Permo-Triassic red beds of south-west England. *Geological Survey of Great Britain Bulletin*, **52**, 1-26.
- HENNECKE, J. 1977. Die bergwirtschaftliche Bedeutung der Blei-Zink-Erzlagerstätte Mechernich. *Gluckauf ForschHft*, **38**, 9-18.
- HOFMANN, B. 1986. Small-scale multi-element accumulations in Permian red beds of northern Switzerland. *Neues Jahrbuch für Mineralogie Monatsch*, **8**, 367-375.
- HOLMES, I., CHAMBERS, A.D., IXER, R.A., TURNER, P. & VAUGHAN, D.J.

1983. Diagenetic processes and the mineralization in the Triassic of Central England. *Mineralium Deposita*, **18**, 365-377.
- IXER, R.A. & VAUGHAN, D.J. 1982. The primary ore mineralogy of the Alderley Edge deposit, Cheshire. *Mineralogical Magazine*, **46**, 485-492.
- KING, R.J. 1968. Mineralization. In: SYLVESTER-BRADLEY, P. C. & FORD, T.D. *The Geology of the East Midlands*, Leicester University Press.
- McKENZIE, D.P. 1978. Some remarks on the development of sedimentary basins. *Earth and Planetary Science Letters*, **40**, 25-32.
- OHLE, E.L. 1980. Some considerations in determining the origin of ore deposits of the Mississippi Valley type. Part II. *Economic Geology*, **75**, 161-172.
- OHMOTO, H. & LASAGA, A.C. 1982. Kinetics of reactions between aqueous sulphates and sulphides in hydrothermal systems. *Geochimica et Cosmochimica Acta*, **46**, 1727-1745.
- OHMOTO, H. & RYE, R.O. 1979. Isotopes of sulphur and carbon. In: BARNES, H. L. (ed.). *Geochemistry of Hydrothermal Ore Deposits*, 2nd edition, Wiley & Sons, New York.
- ROSE, A.W. 1976. The effect of cuprous chloride complexes in the origin of red bed copper and related deposits. *Economic Geology*, **71**, 1036-1048.
- RUIZ, J., RICHARDSON, C.K. & PATCHETT, P.J. 1988. Strontium isotope geochemistry of the fluorite, calcite and barite of the Cave-In-Rock fluorite district, Illinois. *Economic Geology*, **83**, 203-210.
- SAMAMA, J.C. 1968. Contrôle et modèle génétique de minéralisations en galène de type 'Red Beds', Gisement de Largentière, France. *Mineralium Deposita*, **3**, 261-271.
- SAMAMA, J.C. 1969. *Contribution à l'étude des gisements de type Red Beds. Étude et Interprétation de la géochimie et de la métallogénie du plomb en milieu continental. Cas du Trias ardéchois et du gisement de Largentière*. These Nancy.
- SAMAMA, J.C. 1976. Comparative review of the genesis of the copper-lead sandstone-type deposits. In: WOLF, K.H. (ed). *Handbook of stratabound and stratiform ore deposits*, **6**, 1-20. Elsevier, Amsterdam.
- SOULÉ DE LAFONT, D. & LHÉGU, J. 1980. *Les gisements stratiformes de fluorine*

- du Morvan (sud-est du bassin de Paris, France). Publications du 26^e Congrès Géologique International, Paris.
- STANTON, R.L. 1972. *Ore Petrology*. McGraw-Hill, New York.
- SVERJENSKY, D.A. 1984. Oil field brines as ore-forming solutions. *Economic Geology*, **79**, 23-37.
- SVERJENSKY, D.A. 1987. The role of migrating oil field brines in the formation of sediment-hosted Cu-rich deposits. *Economic Geology*, **82**, 1130-1141.
- TAYLOR, J.C.M. 1984. Late Permian-Zechstein. In: GLENNIE, K.(ed) *Introduction to the Petroleum Geology of the North Sea*. Blackwell Scientific Publications, Oxford.
- TRUDINGER, P.A., CHAMBERS, L.A. & SMITH, J.W. 1985. Low temperature sulphate reduction: biological versus abiological. *Canadian Journal of Earth Sciences*, **22**, 1910-1918.
- TURNER, P. *Continental Red Beds*. Developments in Sedimentology, 29, Elsevier, Amsterdam.
- VAUGHAN, D.J. & CRAIG, J.R. 1978. *Mineral Chemistry of Metal Sulfides*. Cambridge University Press, Cambridge, England.
- WALKER, T.R., WAUGH, B. & CRONE, A.J. 1978. Diagenesis in first-cycle desert alluvium of Cenozoic age, southwestern United States and northwestern Mexico. *Bulletin of the Geological Society of America*, **89**, 146-155.
- WEDEPOHL, K.H. 1978. *Handbook of Geochemistry*. Springer-Verlag, Heidelberg.
- ZIEGLER, P.A. 1982. *Geological Atlas of Western and Central Europe*. Elsevier, Amsterdam.

APPENDIX I.

SAMPLE PREPARATION AND ANALYTICAL TECHNIQUES

LX-RAY FLUORESCENCE SPECTROMETRY

1.1 Trace element analysis using pressed powder pellets

22 samples were analysed for a range of trace elements (Zn, Cu, Ni, Ba, Pb, Mn). Samples were prepared by adding 1.5g of Bakelite binding agent to 8.5g of dried sample powder. The samples were shaken for approximately 15 minutes to ensure that the sample powder and bakelite were thoroughly mixed. Disc-shaped pellets were made by applying a load pressure of 20 tons per in² for ten seconds. The pellets were dried in an oven at 120°C for 24 hours before storing in air-tight bags.

Samples were analysed using a Phillips PW System 1400 X-ray spectrometer fitted with a rhodium tube and calibrated using USGS standards.

1.2 Major element analysis of pressed powder pellets

Semi-quantative analysis of major elements was performed on pressed powder pellets by generating regression data for USGS standards incorporating line overlap and matrix corrections using existing Phillips software. The accuracy of the analyses was tested by obtaining semi-quantative data for USGS standards of known ^m composition which were not used in the X-ray fluorescence spectrometer calibration (see Table I.1). The reproducibility of results was checked by running several samples three times (Table I.2).

2. X-RAY DIFFRACTION ANALYSIS

Whole rock samples were disaggregated using a pestle and mortar. The < 2µm clay fraction was separated out by sedimentation and sodium hexametaphosphate was used as a deflocculating agent. Oriented specimens were obtained by suction of suspended material onto a flat, unglazed ceramic tile (Kintner & Diamond 1956).

X-ray diffraction patterns were obtained from samples on air dried tiles using a Phillips PW 2253 goniometer, Co K α radiation with an Fe filter, and with a scanning speed of 1/2° 2 θ per minute. The machine was operated at 30m.A and 30kv. Further patterns were obtained after glycolation and after heating to 550°C for 24 hours. Quartz

was used as an internal standard.

3. ATOMIC ABSORPTION SPECTROPHOTOMETRY

0.1 g of dried sample powder was weighed out accurately and mixed with 0.5 g of lithium metaborate (LiBO_2). The mixture was placed in a furnace at 1000°C for 15 minutes and the ensuing melt was dissolved in dilute nitric acid. The resulting solution was then diluted as required for atomic absorption analysis. This method is suitable for the preparation of a solution from silica-rich rocks whose Fe, CaO, MgO and MnO contents are to be measured using conventional atomic absorption techniques.

Samples were analysed for a range of elements (Al, Ca, Fe, K, Mg, Mn, Na, Si, Ti). Al and Si were analysed using an air-acetylene flame and the remainder of elements were analysed using a nitrous oxide-acetylene flame (McClaughlin 1977).

4. Electron probe microanalysis

Thin sections and blocks were prepared by cutting the samples and mounting them in araldite. The surfaces of the sections to be analysed were ground and polished using 6, 1, and $1/4\ \mu\text{m}$ diamond paste, and were coated with a carbon film (approximately 20 nm thick) prior to analysis.

Microprobe analyses on silicate minerals was carried out using a modified Cambridge Instrument Company Geoscan at Manchester University. The energy dispersive spectrometer (EDS) comprises a Kevex detector, a Harwell 2010 pulse processor and Link Systems 290 Electronics. X-ray spectra were converted to chemical analyses using Link Systems software. Operating conditions were as follows:

15 kV electron beam accelerating voltage

Take off angle 75°

Beam current 3 n.A

Sulphide analyses were undertaken using a C.A.M.E.C.A. microprobe at Manchester University, fitted with two wavelength dispersive spectrometers (W.D.S) and a Link Systems 860-500 EDS system. Link Systems software was used for data reduction and operating conditions were as follows:

15 kV accelerating potential for EDS analysis

20 kV accelerating potential for WDS analysis of sulphides

Take off angle: 40°

3 n.A beam current for EDS analysis

14.5 n.A beam current for EDS+WDS analysis

The standards used are listed below;

Na : Jadeite or Albite

Mg : Periclase

Al : Corundum

Si : Wollastonite or Forsterite

S : Pyrite

K : K-feldspar

Ca : Wollastonite

Fe : Fayalite

Cr, Ni, Cu, Zn : Metals

Ba : Barite

Pb : Galena

Cd : Greenockite

Bi : Matildite

Sb : Chalcostibite

5. Sulphur isotope analysis

Sample preparation techniques involved extraction of the more massive sulphides and sulphates using a dentists drill whereas barite and sulphide-cemented sandstones were crushed and heavy liquids used to separate out the barite and sulphide from the 212-422 μm size fraction. The concentrate was then hand picked under a binocular microscope before final cleaning with organic solvents. The sulphide samples were ground with 200 mg of Cu_2O and heated to 1075°C (after Robinson & Kusakabe 1975) to produce SO_2 . Sulphates were ground with 200 mg of Cu_2O plus 600 mg of SiO_2 before heating to 1120°C (following Coleman & Moore 1978). The resulting SO_2 was analysed using an 'ISOSPEC' 64 spectrometer. Reproducibility of results was 0.27‰ as derived from 20 complete analyses of the internal laboratory standard (including combustion).

REFERENCES

- COLEMAN, M.L. & MOORE, M.P. 1978. Direct reduction of sulphates to sulphur dioxide for isotopic analysis. *Analytical Chemistry*, **50**, 1594-1595.
- KINTNER, E.B. & DIAMOND, S. 1956. A new method for preparation and treatment of oriented aggregate samples of soil clays for X-ray diffraction analysis. *Soil Science*, **81**, 111-120.
- McCLAUGHLIN, R.J.W. 1977. Atomic Absorption Spectrometry. In: ZUSSMAN, J. (ed) *Physical Methods in Determinative Mineralogy*. 2nd edition. Academic Press, New York.
- ROBINSON, B.W. & KUSAKABE, M. 1975. Quantative preparation of sulphur dioxide for $^{34}\text{S}/^{32}\text{S}$ analyses from sulphides by combustion by cuprous oxide. *Analytical Chemistry*, **47**, 1179-1181

TABLE I.1. Accuracy of the semiquantitative X-ray fluorescence data.

Element	Range of standard material (Wt%)	(O - E) (Wt%)	S.D.
Si	63.39 - 80.40	2.766	2.46
Al	13.57 - 17.34	3.318	1.89
Fe	0.54 - 6.85	2.665	0.39
Mg	0.11 - 2.76	0.060	0.02
Ca	0.08 - 2.64	0.060	0.02
K	2.82 - 15.35	0.389	0.26
Mn	< 0.01 - 0.12	0.019	0.03
Ti	0.05 - 1.00	0.080	0.03
P	0.02 - 0.22	0.010	0.01

Where (O - E) = mean difference between observed and expected elemental compositions for six selected standard samples,
and S.D. = standard deviation.

Samples used include NIM-S (syenite), SDC-2 (quartz mica schist), SCO-1 (shale), QMC-I (quartz aplite) and two samples of quartz porphyry of known composition.

TABLE I.2 Reproducibility of results from XRF semi-quantative analysis.

Sample	SiO ₂	Al ₂ O ₃	Fe ₂ O ₃	MgO	CaO	Na ₂ O	K ₂ O	TiO ₂	TOTAL
Hopeman Sandstone	96.69	1.82	0.15	0.05	0.02	0.08	1.02	0.13	99.96
NJ 152702	96.72	1.73	0.16	0.09	0.03	0.10	1.01	0.12	99.96
Hopeman Sandstone	95.54	2.28	0.50	0.06	0.03	0.08	1.39	0.09	99.97
NJ 13656920	95.74	0.07	0.50	0.07	0.03	0.10	1.38	0.08	97.97
Bridgenorth Sandstone,	92.16	4.43	0.08	0.26	0.04	0.22	1.78	0.22	99.19
Shropshire	92.16	4.43	0.84	0.28	0.05	0.23	1.80	0.22	100.01
	92.00	4.54	0.84	0.27	0.05	0.23	1.78	0.22	99.93
Penrith Sandstone,	98.56	0.82	0.21	0.02	0.01	0.00	0.28	0.06	99.96
Cumbria	98.55	0.82	0.22	0.02	0.01	0.00	0.28	0.06	99.96
	98.50	0.84	0.22	0.02	0.01	0.00	0.28	0.06	99.93

APPENDIX II.

FLUID INCLUSION STUDIES; SAMPLE PREPARATION AND CALIBRATION OF THE LINKAM TH600 FLUID INCLUSION STAGE

1. FLUID INCLUSION WAFER PREPARATION

The procedure described by Shepherd et al (1981) for making doubly-polished mineral slices was modified to produce thin ($< 100\mu\text{m}$) wafers, polished on their upper surface and attached to a glass cover slip. The friable and fine-grained material in this study was successfully prepared using the technique outlined below.

A 0.5 cm thick slice was taken from the sample and impregnated with resin (MY 778 Ciba Geigy) and hardener (951-HY). The samples were ground with progressively finer grades of silicon carbide grit (400, 800, 1200) on a glass plate. The sample was ultrasonically cleaned between each grade. A cover slip was then attached to a glass slide ($\sim 1\text{mm}$ thick) with dental wax, and ground further using a logitech machine. The rock slice was attached to the cover slip with epoxy resin (301) and cold cured for 24 hours.

The rock slice was ground to a thickness of $300\mu\text{m}$ using a Jones and Shipman Surface Grinder and finally to $100\mu\text{m}$ on the logitech. The upper surface of the sample was ground manually using the 800 and 1200 grades of silicon carbide grit. Ultrasonic cleaning was necessary between each grade. The surface was then polished using either a tin oxide slurry or diamond paste (6 and $1\mu\text{m}$) on a rotary lapping machine.

The cover slip was removed from the glass slide by gentle heating on a hot plate and the sample cleaned in the ultrasonic bath and with Inhibisol before labelling and storage. The final combined thickness of the cover slip and wafer was approximately $160\text{-}200\mu\text{m}$.

2. CALIBRATION OF THE LINKAM TH600 HEATING-COOLING STAGE

Fluid inclusion measurements were carried out on a Linkam TH600 stage (Shepherd 1981). The calibration of the Linkam TH600 heating-cooling stage at Aston University was undertaken in September 1987 and the procedure outlined below. The main reason

for the calibration was to detect deviations of the temperature response of the measuring device from linearity, and to establish the degree of accuracy obtainable during routine microthermometric measurements.

Calibration was achieved by observing the apparent temperature of melting (T_m obs) of substances whose true melting point is accurately known. Ideally, substances should have a high degree of chemical purity and should melt over a small temperature range. The chemicals used in this study are listed in Table II.1. The standards were sandwiched between two glass cover slips before they were placed on the stage.

Conditions under which measurements were made were standardised as follows;

1. The temperature recorded, T_m (obs) is the final melting temperature of the substance.
2. A brass ring was placed on the cover slips containing the samples to reduce the effects of heat transfer to, or from, the upper glass window.
3. The flow of N_2 through the stage was kept to a minimum.
4. Following a trial run to determine T_m obs, substances were heated rapidly ($50^\circ\text{C}/\text{min}$) to a temperature 1°C below T_m obs. The heating rate was then reduced to $0.5^\circ\text{C}/\text{min}$ and melting recorded.

Six separate samples of each standard were run; the means and standard errors (Table II.2) were calculated by combining the mean values for each sample.

The possibility of the existence of horizontal temperature gradients across the stage was discounted following the observation that the standards melted at the same temperature regardless of their position on the sapphire window. In view of the fact that the thickness of the fluid inclusion wafers approximates that of the two cover slips used during calibration, vertical thermal gradients were considered to be negligible.

Fig. II.1 shows the difference between the true and observed melting temperatures (ΔT) plotted against T_m obs for all of the standards; the bars on each point are estimated 95% confidence intervals for the mean, and this is the final calibration curve.

REFERENCES

SHEPHERD, T.J. 1981. Temperature-programmable heating-freezing stage for microthermometric analysis of fluid inclusions. *Economic Geology*, 76, 1244-1247.

SHEPHERD, T.J., RANKIN, A. & ALDERTON, D. 1985. *A Practical Guide to Fluid Inclusion Studies*. Blackie & Sons, London.

Table II 2. True, observed and corrected melting temperatures for standards used in the calibration of the fluid inclusion stage.

Standard	True T _m (°C)	Mean T _m obs and 95% confidence interval	ΔT(°C) and 95% confidence interval
Chlorobenzene	-46.0	-47.60 ± 0.05	+ 1.6 ± 0.05
CCl ₄	-23.3	-22.61 ± 0.15	-0.69 ± 0.15
Aniline	-6.5	-0.63 ± 0.24	+0.13 ± 0.24
Water	0.0	-0.40 ± 0.18	+0.40 ± 0.18
Calcium Nitrate	42.7	42.60 ± 0.40	-0.18 ± 0.40
Ferric Nitrate	47.2	47.62 ± 0.41	-0.42 ± 0.41
Phenyl benzoate	69.0	68.73 ± 0.27	+0.27 ± 0.27
Benzoic Acid	122.4	122.63 ± 0.53	+0.28 ± 0.53
Tempilar paint	149.0	151.1 ± 0.35	-0.10 ± 0.35
Tempilar paint	204.0	205.0 ± 1.02	-1.00 ± 1.02

FIGURE II.1

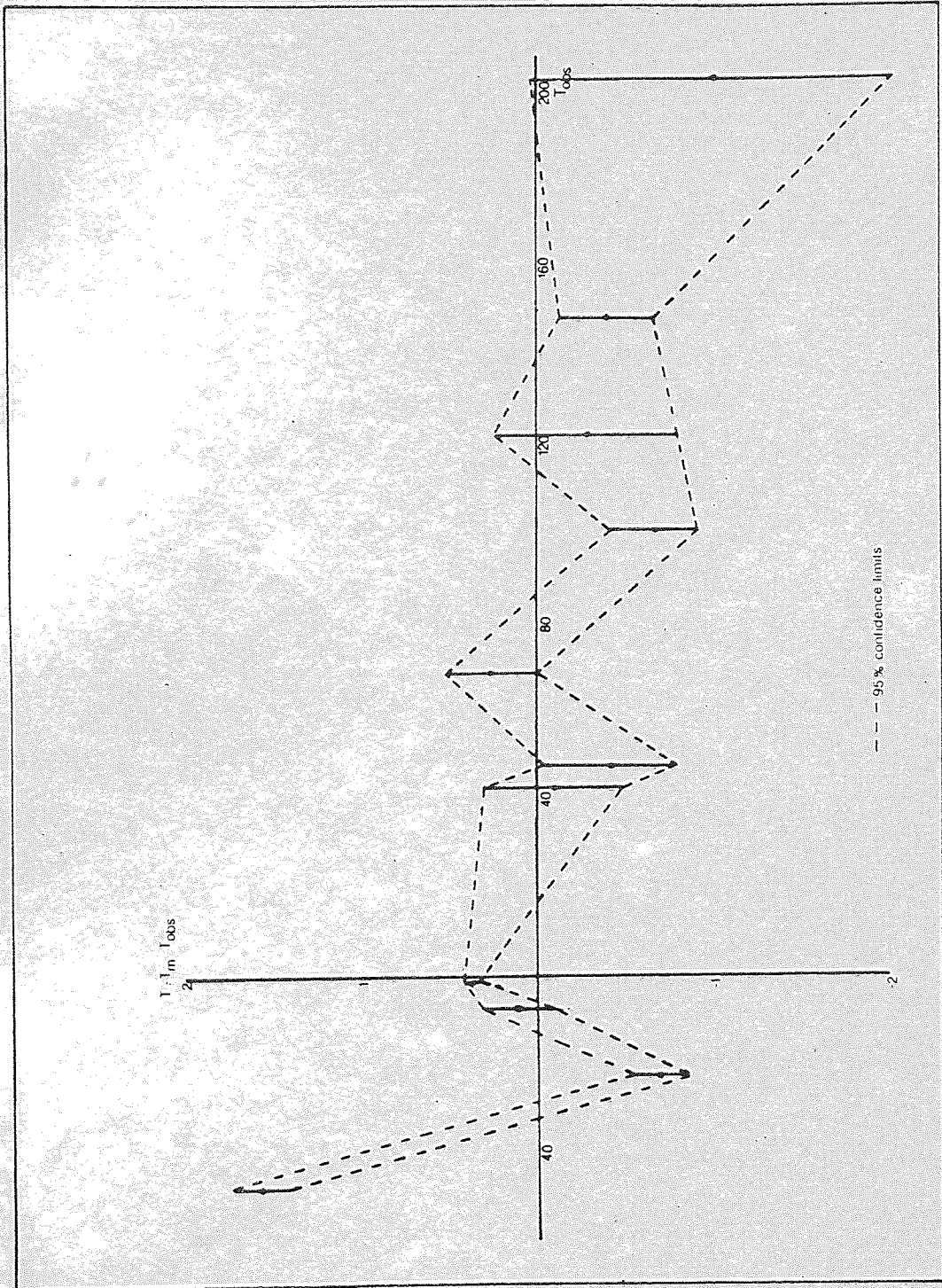


Figure II 1.1 Calibration curve for the Linkam TH600 heating-cooling stage